Role of transportin-1 in the pathogenesis of FTLD-FUS: a pathological, biochemical and cellular study

Jack Brelstaff

A thesis submitted for the degree of Doctor of Philosophy

University College London

Institute of Neurology

Department of Molecular Neuroscience

Institute of Neurology

1 Wakefield Street

London

WC1N 1PJ

Declaration

I, Jack Brelstaff confirm that the work presented in this thesis is my own. Where information has been derived from other sources, I confirm that this has been indicated in the thesis.

Abstract

Frontotemporal lobar degeneration (FTLD) is the second most common form of pre-senile dementia. Recent discoveries have identified the proteins present in the pathological ubiquitinated inclusions of previously undifferentiated subtypes of FTLD. Fused in Sarcoma (FUS) is the primary pathological marker of a subtype now called FTLD-FUS. This normally nuclear protein is seen within the cytoplasmic and intranuclear aggregates of FTLD-FUS. FUS, together with Ewing's Sarcoma (EWS) and TATA box binding associated factor 68kDa (TAF15), forms the FET family. These related proteins are predominately nuclear owing to the action of the nuclear importin Transportin1 (TRN1).

Investigations by other authors have implicated TRN1 in the cytoplasmic aggregation of ALS-associated mutant FUS. Since ALS and FTLD represent different ends of a disease spectrum, the role of TRN1 in the pathology and biochemistry of FTLD-FUS was investigated. Extensive TRN1, TAF15 and EWS cytoplasmic and intranuclear inclusions were seen throughout the frontal cortex, hippocampus and entorhinal cortex, medulla, XIIth cranial nerve nucleus and spinal cord. Double-label immunofluorescence revealed TRN1 and FUS pathology co-localised. Immunoblotting of solubility fractions demonstrated that highly insoluble, likely highly aggregated TRN1 is present in FTLD-FUS, and not in healthy controls.

Stress granules are transient cytoplasmic foci consisting of stalled translation initiation complexes and associated proteins produced by the cell in response to various stressors. Cellular investigations revealed that the same antibodies used to detect TRN1 pathology in FTLD-FUS labelled cytoplasmic stress granules induced after oxidative or osmotic stress. The re-localisation of wild type endogenous FET proteins was investigated under various pharmacological agents as well as TRN1 knockdown and overexpression.

Evidence is presented that the pathology of FTLD-FUS is more complex than previously thought. Cellular studies investigate the implication of stress granules in aggregate formation and find that there is evidence to support oxidative stress in protein re-localisation and aggregation.

Acknowledgments

I would like to acknowledge my supervisors Professor Tamas Revesz and Dr Rina Bandopadhyay and thank them for their guidance and support, particularly in the publication of my first author paper. Additionally, I'd like to thank Adam Mamais and Tammaryn Lashley for putting up with my nagging questions about techniques. Special thanks to Professor Khadija Rantell for advice regarding statistical analysis.

Publications

Original papers related to this thesis

1. **Brelstaff J**, Lashley T, Holton JL, Lees AJ, Rossor MN, Bandopadhyay R, Revesz T.Transportin1: a marker of FTLD-FUS. Acta Neuropathologica. 2011 Nov; 122(5):591-600
2. Lashley T, Rohrer JD, Bandopadhyay R, Fry C, Ahmed Z, Isaacs AM, **Brelstaff JH**, Borroni B, Warren JD, Troakes C, King A, Al-Saraj S, Newcombe J, Quinn N, Ostergaard K, Schrøder HD, Bojsen-Møller M, Braendgaard H, Fox NC, Rossor MN, Lees AJ, Holton JL, Revesz T. A comparative clinical, pathological, biochemical and genetic study of fused in sarcoma proteinopathies. Brain. 2011 Sept; 134(Pt 9):2548-64

Original papers unrelated to this thesis

1. Fricker FR, Antunes-Martins A, Galino J, Paramsothy R, La Russa F, Perkins J, Goldberg R, **Brelstaff J**, Zhu N, McMahon SB, Orengo C, Garratt AN, Birchmeier C, Bennett DL. Axonal neuregulin 1 is a rate limiting but not essential factor for nerve remyelination. Brain. 2013 July; 136(Pt 7):2279-97

Abstracts

1. **J. Brelstaff**, T. Lashley, J.L. Holton, A.J. Lees, M.N. Rossor, R. Bandopadhyay, T. Revesz. The nuclear importin Transportin1 is present in the pathological inclusions of FTLD-FUS. Neuropathology and Applied Neurobiology. 2012 Jan; 38 (Suppl. 1): 7
2. **J. H. BRELSTAFF**, A. MAMIAS, T. LASHLEY, J. L. HOLTON, A. LEES, M. N. ROSSOR, T. REVESZ, R. BANDOPADHYAY. The FTLD-FUS marker Transportin1 is incorporated into stress granules that may act as inclusion precursors. 442.06/E46. 2012 Neuroscience Meeting Planner. New Orleans, LA: Society for Neuroscience, 2012. Online
3. **Jack Brelstaff**, Adamantios Mamais, Tammaryn Lashley, Janice Holton, Tamas Revesz, Rina Bandopadhyay. The aggregate proteins of FTLD-FUS are re-localised to stress granules upon oxidative stress. Neuropathology and Applied Neurobiology. 2013 Jan

Table of Contents

List of Figures

List of Tables

Abbreviations

3R	3 repeat tau
4R	4 repeat tau
aFTLD-U	atypical frontotemporal lobar degeneration with ubiquitinated inclusions
AGD	Argyrophilic grain disease
ALS	Amyotrophic lateral sclerosis
AMPA	2-amino-3-(3-hydroxy-5-methyl-isoxazol-4-yl)propanoic acid
APP	Amyloid precursor protein
ATP	Adenosine triphosphate
Aβ	Amyloid β
BBP	Break point binding protein
BIBD	Basophilic inclusion body disease
BSA	Bovine serum albumin
bvFTD	behavioural varient frontotemporal dementia
c-ABL	Abelson murine leukemia viral oncogene homolog 1
CAS	Cellular apoptosis susceptibility protein
CBD	Corticobasal degeneration
CHOP	CCAAT-enhancer-binding protein homologous protein
CNS	Central nervous system
DCP1a	mRNA decapping enzyme 1a
ECL	enhanced chemiluminescence
eIF2α	eukaryotic initiation factor 2α
ERK	Extracellular regulated kinase
ETS	E-twenty six
EWS	Ewing's Sarcoma
FA	Formic acid
FTD	frontal temporal dementia
FTLD	Frontotemporal lobar degeneration
FTLDP-17	Frontotemporal lobar degeneration with parkinsonism linked to chromosome 17
FUS	Fused in Sarcoma
G3BP	Ras-GAP associated endoribonucelase
GCN2	general control nonrepressed 2
HD	Huntington's Disease
HDAC6	Histone deacetylase 6
HEAT	Huntington Elongation factor 3 A subunit of protein phosphatase 2A lipid kinase Tor1
hFUS	Human FUS
HRI	Heme-Regulated Inhibitor
HuR	Human antigen R
Karb2	Karyopherin β2
LSM 1-7	Sm and Sm-like proteins

MAPT	microtubule associated protein tau
MSTD	multiple system tauopathy with dementia
NES	Nuclear export signal
NIFID	Neuronal intermediate filament inclusion disease
NLS	Nuclear localisation signal
NMDA	N-Methyl-D-aspartic acid
p53	protein 53
PBS	Phosphate buffered saline
PC	Pressure cook
PERK	Protein kinase-like endoplasmic reticulum kinase
PKR	Protein kinase R
PNFA	Primary non-fluent aphasia
PrP^{C}	Prion Protein Common form
PrP^{Sc}	Prion Protein Scrapie form
PSP	Progressive supranuclear palsey
RanGDP	RAs-related nuclear protein guanosine diphosphate
RanGTP	RAs-related nuclear protein guanosine triphosphate
RNA	Ribonucleic acid
ROS	Reactive oxygen species
RRM	RNA recognition motif
SCA	Spinocerebellar Ataxia
SD	Semantic dementia
siRNA	silencing RNA
SNPs	single nucleotide polymorphisms
snRNA	small nuclear RNA
Sup35	Suppresor 35
TAF15	TATA box binding protein associated factor 68 kDa
tBH	tert-butyl-hydroxyperoxide
TFIID	Transcription factor II D
TIA-1	T-Cell-Restricted Intracellular Antigen-1
TLS	Translated in liposarcoma
TRN1	Transportin1
TRN2	Transportin2
TRN3	Transportin3
$tRNA_i^{met}$	translation RNA initiation methionyl
Xrn1p	Exonuclease 1p
YB-1	Y-box binding protein 1

Chapter One: Introduction

1.1 The clinical presentation of frontotemporal lobar degeneration

The term frontotemporal dementia (FTD) is used to describe the clinical presentation of the underlying frontotemporal lobar degeneration (FTLD) pathology, which defines a heterogeneous group of neurodegenerative diseases with varying yet often overlapping clinical presentations. Behavioural variant frontotemporal dementia (bvFTD), progressive non-fluent aphasia (PNFA) and semantic dementia (SD) are the three best-characterised clinical syndromes. An overlap with motor neuron disease or amyotrophic lateral sclerosis (ALS) is very common, to the extent that they are now considered part of a spectrum disorder (Giordana et al., 2011). The behavioural variant is the most common, and diagnosis is made upon presentation of emotional blunting, loss of empathy, apathy, selfishness or neglect of personal hygiene (Bathgate et al., 2001). Given that diagnosis focuses on behavioural changes rather than cognitive decline there is some concern that an erroneous diagnosis of late onset depression or schizophrenia may be made (Kipps et al., 2009, Kipps et al., 2008). The disease progresses insidiously from these initial-onset symptoms, to a more severe and generalised dementia, caused by a preferential atrophy of the frontal and anterior temporal lobes. Clinical signs of bvFTD are associated with a symmetrical frontal and anterior temporal dysfunction, whilst PNFA is typically a left lateralised frontotemporal dysfunction, perhaps relating to the left lateralisation of the arcuate fasciculus (Glasser and Rilling, 2008). SD shows greater left anterior temporal lobe atrophy and is therefore also asymmetrical.

1.2 Proteins and pathology associated with frontotemporal lobar degeneration

Ultimate classification of FTLDs relies on the identification of the main protein component of the neuronal inclusions observed post-mortem. Although there is some

correlation between the clinical and pathological subtypes, the clinical presentation does not always predict the underlying pathology. The proteins responsible for the majority of the cases are tau, the TAR DNA-binding protein-43 (TDP43) and the fused in sarcoma (FUS) protein (Mackenzie et al., 2010a, Mackenzie et al., 2009).

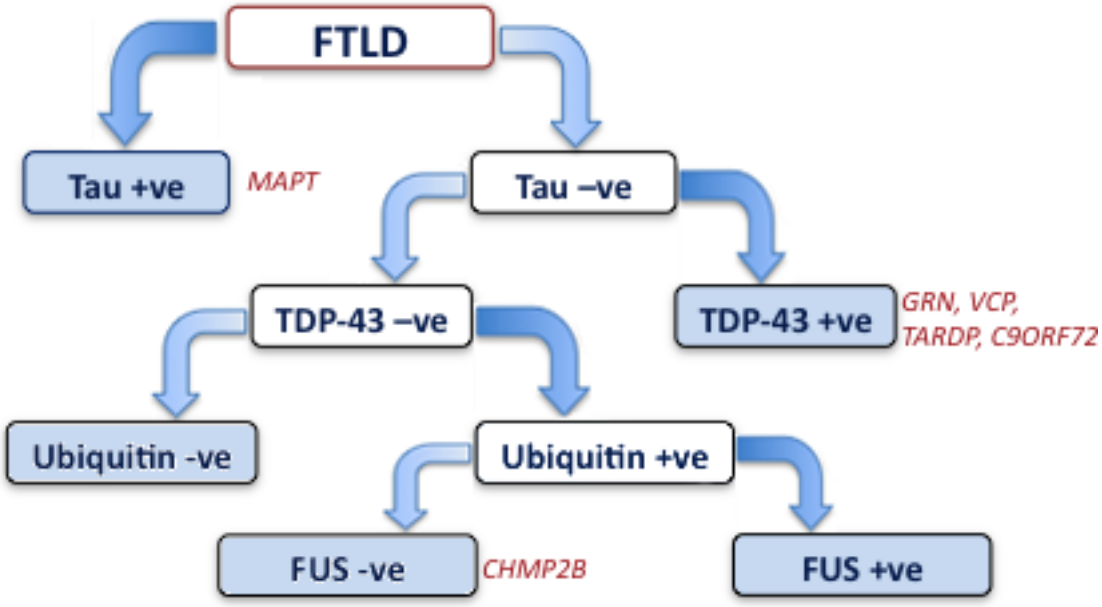

Figure 1.1 Diagnosis flow diagram for the pathological classification of FTLD variants. Variants are in blue; Tau +ve is FTLD-tau, TDP-43 +ve is FTLD-TDP, FUS +ve is FTLD-FUS, the rarer entities include ubiquitin –ve dementia lacking distinctive histology (DLDH), and FUS –ve FTLD- of the ubiquitin proteosome system FTLD-UPS. The associated genetic mutations in red italics.

1.2.1 Tau

Tau is a microtubule associated phosphoprotein that is ubiquitously expressed in the central and peripheral nervous systems. Its primary role is to promote microtubule assembly and thereby aid the axoplasmic transport of proteins and organelles (Cleveland et al., 1977, Weingarten et al., 1975). Aberrant intracellular accumulation of tau is a characteristic of several neurodegenerative diseases that are grouped together as 'tauopathies' (Tolnay and Probst, 2003, Lee et al., 2001). Detailed analysis of the composition of these aggregates reveals differences in the degree of phosphorylation and ratio of tau isoforms between different tauopathies (Delacourte, 2008). The tau gene (MAPT) is located on chromosome 17q21 and is predominantly found as two haplotypes:

H1 and H2. The differences between these two haplotypes are a set of single nucleotide polymorphisms (SNPs), a 238 base pair deletion in intron 9, and an approximately 900kb inversion. Alternative splicing gives rise to 6 possible isoforms expressed in the adult human brain. Exons 9, 10, 11 and 12 encode the microtubule binding domains that are crucial for its function. The alternative splicing of exon 10 can give rise to a predominance of tau containing 3 or 4 microtubule binding domains (3R and 4R-tau). In healthy adult brains the ratio is 1:1, but the ratio is often skewed in one direction or another in tauopathies (Goedert et al., 1989a, Goedert and Spillantini, 2006, Goedert, 2004). Inheritance of the H1 haplotype appears to predispose an individual to sporadic tauopathies such as progressive supranuclear palsy (PSP)and corticobasal degeneration (CBD), both of which present with 4R pathological tau.

FTLD-tau is a term that encompasses several diseases that could be described as individual disease entities. Moreover, these definitions and descriptions have been modified and adjusted many times since Arnold Pick first described them over a 100 years ago (Pick, 1892). The term Pick's disease is now retained for cases of FTLD with intraneuronal agyrophilic inclusions (Pick bodies) that can be identified with 3R tau immunohistochemistry. Broadly speaking FTLD-tau includes Pick's disease, PSP, CBD, argyrophilic grain disease, (AGD), tangle predominant dementia, and frontotemporal dementia with parkinsonism linked to chromosome 17 (FTLDP-17 *T*). Each of these presents with a predominance of 3R or 4R –tau (or both) in the pathological inclusions.

There are four characteristic histopathological findings of Pick's disease, which are Pick bodies, Pick cells, neuronal loss in particular layers, and gliosis. Pick bodies are rounded globose cytoplasmic inclusion bodies approximately 10-15μm in diameter that stain strongly with anti-tau AT8 immunohistchemistry. These can also be seen on a standard haematoxylin eosin stain and are intensely argyrophilic with silver impregnations such as the Bielschowsky method. They can be easily found in the CA1 region of the

hippocampus, the subiculum, the dentate fascia neurons and, cerebral cortex, deep grey and brainstem nuclei (Munoz-Garcia and Ludwin, 1984). Pick cells are swollen, ballooned neurons in which the nucleus is often displaced from the centre of the cell body, and the cytoplasm does not retain Nissl substance. These cells are easiest to find in areas of the cortex that isn't drastically affected by neuron loss. The neuronal loss can be so extreme that the cortical laminar architecture is severely disrupted due to the loss of the neuropil and proliferation of glial cells. Layer III pyramindal neurons are thought to be the most vulnerable followed closely by layers II and V (Arnold et al., 1994). The resulting spongiosis leaves a network of glial fibres and vessels behind.

Mutations in *MAPT* that give rise to tauopathies can be separated into missense mutations in exons 9 to 13 that affect the normal function of tau, intronic, and coding mutations affecting the splicing of exon 10 at the mRNA level (Goedert et al., 1989b). In the later part of the 20th century genetic linkage between a familial form of FTLD with parkinsonism and chromosome 17q21-22 was made (FTLDP-17) (Wilhelmsen et al., 1994). Later, approximately half of the original kindreds were found to have *MAPT* mutations (Hutton et al., 1998, Poorkaj et al., 1998, Spillantini et al., 1998b), and the remainder had progranulin (*GRN*) mutations (Cruts et al., 2006, Baker et al., 2006). However, those individuals processing *GRN* mutations present with TDP43 pathology.

1.2.2 TDP43

TDP43 is a ubiquitously expressed, 414 amino acid long protein with a molecular weight of 43kDa. TDP43 is encoded by the *TADBP* gene, which has 6 exons encoding a glycine-rich region, two RNA recognition motifs and a nuclear export, and import signal (NES and NLS respectively), all of which are crucial to its numerous functions (Ou et al., 1995). Whilst it was originally studied as one member of a splicing complex affecting the cystic fibrosis transmembrane conductance regulator gene (Buratti et al., 2001), more recent investigations attribute a multitude of functions to TDP43, including; micro RNA

biogenesis, apoptosis, cell division, mRNA stabilisation and neuronal plasticity (Strong et al., 2007, Wang et al., 2008). After languishing in relative obscurity for years, TDP43 was identified as the primary pathological protein of a proportion of sporadic ALS and FTLD cases in 2006 (Neumann et al., 2006, Arai et al., 2006). Thirty-eight TDP43 mutations have so far been identified in ALS patients, which explain approximately 4% of the familial, and <1% of the sporadic disease burden. Far fewer reports of TDP43 mutations in FTLD exist in the literature (Gitcho et al., 2009), and fewer still produce a clinically pure FTD (Benajiba et al., 2009). However, as larger disease cohorts are assembled, more probable pathogenic variants are being discovered (Borroni et al., 2010).

1.2.2.1 GRN, VCP and C9ORF72

As previously discussed the genetic linkage was identified in patients with FTLD with Parkinson's and many of them had a *MAPT* mutation and tau pathology. However, there remained a subset of cases, which remained negative for tau pathology and *MAPT* mutations. These individuals were found to be harbouring *GRN* mutations, and presenting with TDP43 pathology. The gene *GRN* is 1.7Mb centromeric to *MAPT* and encodes the progranulin protein. Families bearing *GRN* mutations exhibit an autosomal dominant inheritance of FTLD-TDP with 66 identified mutations causing a haploinsufficiency of progranulin through production of premature stop codons, one disrupting the splice donor site of intron 0 leading to loss of transcript through nuclear degradation, and one lies within the initiation Met leading to a failure to initiate translation (Baker et al., 2006, Cruts et al., 2006, Finch et al., 2009). Very little was known about this protein at the time of the genetic discovery, but research pointed towards a secreted growth factor role (Van Damme et al., 2008). The cell surface receptor sortilin has now been identified as a key binding partner of progranulin. Whilst an exact theory of pathogenesis is still outstanding, it has been shown that under stress activated microglia will release progranulin and sortilin bearing neurones will rapidly endocytose it (Hu et al., 2010). Mutations in *VCP* cause a rare familial syndrome in which

a triad of conditions show variable penetrance, namely; inclusion body myopathy, Paget disease of the bone, and frontotemporal dementia (FTD) (Watts et al., 2004, Kimonis et al., 2008). Twelve different missense *VCP* mutations in 29 families have been identified and correlated with a specific TDP43 pathology that is characterised by numerous neuronal intranuclear inclusions, few neuronal cytoplasmic inclusions and abundant dystrophic neurites. Several kindreds in the literature presented with a particular TDP43 pathology genetically linked to chromosome 9p21. This linkage has now been resolved to an expansion of a noncoding GGGGCC hexanucleotide repeat in the gene *C9ORF72* (Dejesus-Hernandez et al., 2011, Renton et al., 2011). This discovery is of particular significance because the expansion is the most common cause of familial and sporadic forms of FTLD and ALS.

1.2.2.2 TDP43 pathology

Under normal conditions TDP43 is localised to the nucleus, but as part of its normal functioning it is able to shuttle between the cytoplasmic and nuclear compartments. Under pathological conditions such as ALS and FTLD abnormal TDP43 redistribution to the cytoplasm is considered to be a crucial early step in pathogenesis (Giordana et al., 2010). Sequestering the protein into cytoplasmic and or intranuclear aggregates is thought to further retard TDP43's normal function and give rise to malignant effects (Neumann et al., 2006, Davidson et al., 2007, Igaz et al., 2008, Van Deerlin et al., 2008). Sequential solubility extraction and immunoblotting of detergent insoluble protein from affected brains reveals a signature pattern of hyperphosphorylated and ubiquitinated TDP43 as well as 25kDa fragments from the C-terminal region of TDP43 (Neumann et al., 2006, Arai et al., 2006).

TDP43 immunohistochemistry has provided a wealth of knowledge regarding the detailed pathology of FTLD-TDP. Previously this FTLD variant was only described in terms of routine histological stains and ubiquitin immunohistochemistry. TDP43

immunohistochemistry revealed previously unrecognised ubiquitin negative pathology such as; glial cytoplasmic inclusions (Neumann et al., 2007), diffuse cytoplasmic pre-inclusions (Brandmeir et al., 2008, Geser et al., 2009), and CA1 neurites (Hatanpaa et al., 2008). Further development of antibody technology has produced phosphorylation dependant antibodies that label only the aberrantly hyperphosphorylated TDP43 and not the normal TDP43 (Hasegawa et al., 2008, Inukai et al., 2008). The level of detail revealed with TDP43 immunohistochemistry has allowed FTLD-TDP to be further subdivided into four pathological subtypes. Two authors identified these four subtypes independently and concurrently leading to the publication of two labelling systems that identified the correct subtypes but labelled them differently, leading to confusion in the field (Mackenzie et al., 2006, Sampathu et al., 2006). More recently a harmonized classification system was suggested using letters instead of numbers and listing the most common first. Type A is characterised by numerous short dystrophic neuritis, and crescent shaped or oval neuronal cytoplasmic inclusions occurring mainly in neocortical layer 2. Intranuclear lentiform inclusions are common in some but not all cases. Type B has more moderate numbers of neuronal cytoplasmic inclusions throughout all cortical layers, but few dystrophic neuritis. Type C is characterised by a predominance of elongated dystrophic neuritis in upper cortical layers with very few neuronal cytoplasmic inclusions. Finally and rarest, Type D includes pathology associated with inclusion body myopathy with early-onset Paget disease and frontotemporal dementia caused by *VCP* mutations, namely numerous short dystrophic neurites and frequent intranuclear inclusions. Subdividing the pathological characteristics of FTLD-TDP in this manner may appear to be a purely academic exercise but support for this practice comes from the specific correlations that can be drawn between pathological type and clinical phenotype or genetic cause (Mackenzie et al., 2006, Davidson et al., 2007).

1.2.3 FUS

Fused in Sarcoma (FUS), also known as Translocated in liposarcoma (TLS) is one member of the FET (**F**used in sarcoma, **E**wing's sarcoma, **T**AF15 RNA polymerase II TATA box binding associated factor 68kDa) protein family. All members of this family are infamous thanks to their role in particularly malignant tumours often affecting children. At the time of writing 20 years have passed since FUS was identified as one half of a chimeric protein resulting from a translocation and the driving force of cancerous proliferation (Crozat et al., 1993). The chimeric protein harboured by these tumours consists of the N-terminus of FUS fused to a transcription factor such as CHOP.

The full length wild type FUS protein (Figure 1.2) has been shown to preferentially bind to GGUG motif mRNA (Lerga et al., 2001), utilizing each of its RNA binding domains thus suggesting a complex protein-RNA structure. In the same vein, FUS has also been shown to bind telomerase primer RNA signifying a possible role in the maintenance of telomeres and senescence (Lerga et al., 2001). FUS and the entire FET family have been shown to associate with the RNA polymerase II and TFIID transcription complex suggestive of a core role of these proteins in transcription (Schwartz et al., 2012, Bertolotti et al., 1996, Bertolotti et al., 1998). However, recent findings have described FUS as a repressor of RNA polymerase III dependent transcription of small untranslated RNAs, perhaps suggesting a more general role in the orchestration of transcription apparatus (Tan and Manley, 2010). What is clear is that the normal role of FUS is intimately entwined with RNA.

Figure 1.2. Domain structure of the FUS protein. SYGQ-rich: Serine Tyrosine Glycine Glutamine-rich domain. RGG: Arginine Glycine Glycine-rich domain. RRM: RNA recognition motif. Zn: putative zinc finger. NLS: Nuclear localisation signal.

Members of the multifunctional FET protein family, including FUS, are all linked to malignantly proliferative diseases. Their normal roles support the correct expression of protein, but the expression of the FET proteins themselves can be regulated by trans

elements surrounding proliferation. Specifically, the proliferating neuroblastoma line SH-SY5Y can be differentiated into a more quiescent, neuronal cell type with the addition of 1μM all-trans retinoic acid to the culture medium. Over 9days this will reduce cell proliferation and induce neurite formation, as well as reducing the detectable protein levels of all three FET proteins (Andersson et al., 2008a).

The significance of FUS in neurodegeneration was recognised with the discovery that mutations in the *FUS* gene are responsible for familial amyotrophic lateral sclerosis (ALS) type 6 (ALS-FUS) (Kwiatkowski et al., 2009a, Vance et al., 2009b). At the time of writing there are 60 reported mutations in FUS that give rise to familial and sporadic disease, 58% of which cluster in the NLS (Appendix 1.1). Subsequently FUS has also emerged as a significant disease protein in a subgroup of FTLDs, previously characterized by immunoreactivity of the neuronal inclusions for ubiquitin, but not for TDP43 or tau with a proportion of the inclusions also containing α-internexin in a further subgroup known as neuronal intermediate filament inclusion disease (NIFID). The disease entities which are now considered subtypes of FTLD-FUS are atypical frontotemporal lobar degeneration with ubiquitinated inclusions (aFTLD-U), NIFID (otherwise known as neurofilament inclusion body disease (Josephs et al., 2003b) and basophilic inclusion body disease (BIBD), which together with ALS-FUS comprise the FUS-opathies (Munoz et al., 2009, Neumann et al., 2009b, Mackenzie et al., 2010b, Neumann et al., 2009d).

The cause and pathomechanism of inclusion formation in the FUS-opathies is only partially understood. In keeping with its important functions in transcription regulation, FUS protein is present in considerably larger amounts in the nucleus than in the cytoplasm of neurons while it is restricted to the nuclei and not found in the cytoplasm of glial cells (Andersson et al., 2008b). Under normal physiological conditions the FUS protein shuttles between the nucleus and cytoplasm through the nuclear pore (Zinszner et al., 1997, Lagier-Tourenne et al., 2010). Transport of FUS from the cytoplasm to the

nucleus takes place with the aid of transportin1 (TRN1), also known as M9-interacting protein or karyopherinβ2 (Karb2), which is an 890-amino acid-long protein (OMIM; http://omim.org/entry/602901). Karyopherinβ-s (Karbs), also known as importins and exportins are responsible for the majority of the cellular nucleocytoplasmic transport. In humans ten Karbs have been shown to carry diverse macromolecular substrates into the nucleus and in one of these import pathways Karb2 is responsible for the import of a significant group of RNA processing proteins, including FUS (Macara, 2001, Bonifaci et al., 1997, Weis, 2003, Xu and Massague, 2004, Lee et al., 2006, Dormann et al., 2010). Binding of substrates to import and export Karbs is dependent on the nuclear localisation signal and nuclear export signal, which are predicted to be located at the C-terminal end and the beginning of the RNA recognition motif of FUS, respectively (Lee et al., 2006, Lagier-Tourenne et al., 2010). The NLS of FUS can be described as a PY motif very similar to previously described M9 signals and a likely target of the TRN1 nuclear import system (Dormann et al., 2010, Lee et al., 2006). During nuclear import of proteins, the Karb-protein cargo complex translocates into the nucleus through its association with the nuclear pore complex. Once inside the nucleus the Karb-protein complex dissociates, which is dependent on RanGTP binding to the import Karbs**.** The free Karbs are then recycled into the cytoplasm to be available for a new cycle of cargo import (Weis, 2003).

In 2010, Dormann et al showed that mutations in the nuclear localisation signal of FUS, that had been previously linked to ALS, cause a redistribution of FUS to the cytoplasm (Dormann et al., 2010). In a similar manner to TDP43, re-localisation of FUS to the cytoplasm is thought to be a crucial early event in pathogenesis. The cell system used to model these ALS-FUS mutations also showed that this re-localised FUS began to accumulate into punctuate structures that were positive for stress-granule markers. Furthermore, this group were able to show that the nuclear importin TRN1 was responsible for the primary mode of import. The most convincing finding was that the

degree of FUS re-localisation correlated strongly with the severity of clinical symptoms in carriers of that mutation.

1.2.4 EWS

Ewing's Sarcoma protein (EWS) is named after the family of highly malignant cancers that includes Askin tumours, and primitive neuroectodermal tumours. These tumours occur most frequently in the long bones and sometimes in the soft tissues (Kauer et al., 2009). Ewing's sarcoma is associated with specific chromosomal translocations and the resulting chimeric transcripts and proteins. Ewing's sarcoma is the second most common bone cancer and is considered highly malignant (Rodriguez-Galindo et al., 2003). They harbour translocations of the *EWS* gene on chromosome 22 and any one of the *ETS* family genes, the most common of which is the *FLI1* gene on chromosome 11 (Downing et al., 1993). The resulting chimeric product drives pathological proliferation through transcriptional activation of *IGF1, NKX2, TOPK, SOX2* and *EZH2* all of which are proliferative, involved in cell differentiation, or cell survival, but also repression of apoptotic and cell cycle arrest genes including *IGFBP3, p57kip, p21* and *TGFβ2* (Lin et al., 2011, Cironi et al., 2008, Sollazzo et al., 1999, Herrero-Martin et al., 2009, Smith et al., 2006, Fukuma et al., 2003, Garcia-Aragoncillo et al., 2008, Zwerner et al., 2008, Richter et al., 2009, Siligan et al., 2005, Kikuchi et al., 2007, Hahm et al., 1999, Nakatani et al., 2003, Dauphinot et al., 2001, Prieur et al., 2004, Riggi et al., 2010).

The normal function of EWS appears to be heavy related to its ability to bind RNA and DNA (Janknecht, 2005). The protein also interacts with the TFIID pre-initiation complex and with subunits of the RNA polymerase II implicating a role in transcriptional regulation (Bertolotti et al., 1998). EWS has also been shown to interact with splicing apparatus proteins like Y box binding protein 1 (YB-1), and branch point binding protein (BBP/SF1) (Dutertre et al., 2010, Zhang et al., 1998). Perhaps most conclusively, EWS was shown to regulate alternative splicing of mouse double minute 2 homolog (MDM2),

which is an important repressor of p53 (Dutertre et al., 2010). Depletion of EWS results in alterations in alternative splicing of genes involved in DNA repair and geneotoxic stress signalling including *ABL2, CHERK2* and *MAP4k2* (Paronetto et al., 2011). The same effect can be seen under ultra violet light (U.V.) irradiation whereupon EWS refocuses from a diffuse nuclear distribution to nucleoli presumably away from the splicing machinery, with a concomitant reduction in c-ABL protein expression. Given the role of c-ABL in cell division and stress response this would appear to be an adaptive response to DNA damage elicited by U.V. radiation. Knockout mice survive for only a few days and show defects in pre-B cell development, a hypotrophic thymus, defects in spermatocytes, premature cellular senescence and hypersensitivity to ionizing radiation (Li et al., 2007). Such a wide array of defects suggests EWS has roles in normal immune cell differentiation, homologous DNA pairing between XY bivalents (Guipaud et al., 2006), and telomere independent senescence.

Since many of the roles attributed to EWS surround RNA and DNA it is unsurprising that its domain structure comprises a transcriptional activation domain, a zinc-finger motif, three RGG boxes, one RRM and nuclear localisation signal (NLS) (Zakaryan and Gehring, 2006) (Figure1.3).

Figure 1.3. Domain structure of the EWS protein. SYGQ-rich: Serine Tyrosine Glycine Glutamine-rich domain. RGG: Arginine Glycine Glycine-rich domain. RRM: RNA recognition motif. Zn: putative zinc finger. NLS: Nuclear localisation signal.

The NLS of EWS consists of 18 amino acid residues (PGKMDKGEHRQERRDRPY) and is very well conserved across the FET family. Three arginine residues (R648, R652 and R654), a proline (P655) and a tyrosine (Y656) represent a pattern conserved across this region in all FET proteins. Replacement of any of these residues with alanine will abolish the nuclear localisation of EWS (Zakaryan and Gehring, 2006). Interestingly, replacement

of the arginine residues with lysine, another positively charged amino acid, will not ablate nuclear import (Zakaryan and Gehring, 2006). This may demonstrate that the electrostatic interaction between this region and the importin TRN1 mediates nuclear import.

Relatively little is known about the role EWS might play in neurodegeneration. It was first implicated when IHC studies discovered the inclusions of FTLD-FUS, but not those of ALS-FUS, were visible with anti-EWS antibodies (Neumann et al., 2011). This was accompanied by a relative (but not significant) shift of EWS towards the insoluble fraction, which is an important biochemical marker of disease. Genetic screening of the *EWS* gene in these cases revealed no mutations, however the exon screen was not able to investigate possible duplications. This lack of apparent genetic cause is repeated in all FET proteins and TRN1 despite these proteins apparently aggregating in tandem. Cell culture models that block TRN1 driven import by substrate competition have shown that EWS will re-localise to the cytoplasm and rapidly amalgamate with stress granules upon heat shock (Neumann et al., 2011). The same is true even if TRN1 import is not artificially blocked, oxidative and non-oxidative stress can re-localise EWS to varying degrees (Andersson et al., 2008a). Given the extensive similarities between EWS and FUS the hypothesises of aberrant cytoplasmic re-localisation being key to pathology could be extended to EWS.

1.2.5 TAF15

'TAF15 RNA polymerase II TATA box binding associated factor 68kDa' (TAF15) is also known as TAFII68, TAF2N, RBP56 or Npl3 (OMIM; http://omim.org/entry/601574). As with all the FET proteins, TAF15 is a nuclear protein that shuttles back and forth from the cytoplasm (Bertolotti et al., 1996). However, less is known about TAF15 and its role within the cell possibly due to the relative rarity of genetic translocations involving this gene (Nyquist et al., 2011). The fusion of TAF15 and the zinc finger containing ZNF384

results in acute lymphoblastic leukemia which is one of the most common malignancies in children accounting for 20% of pediatric cancer. What is known regarding TAF15's normal function is that during the initiation of transcription the general RNA polymerase II transcription factor IID (TFIID) recognizes the core promoter sequence and initiates the assembly of the preinitiation complex. TFIID is an extremely heterogeneous complex of various proteins, including TAT-binding protein and a series of associated proteins of which TAF15 is one (Bertolotti et al., 1996). In addition to this transcriptional activation domain, TAF15 also possesses RRM and RGG motifs (Figure 1.4) much like FUS (Figure 1.2) and EWS (Figure 1.3). Cross linking and immunoprecipitation experiments have shown that one of the mRNA targets of TAF15 is U1A small nuclear RNA (snRNA) and that this U1-TAF15 snRNP associates with chromatin (Jobert et al., 2009b). Interestingly, this association increases 2.5 fold upon transcription arrest stress (Jobert et al., 2009b), this sequestration may indicate a role for TAF15 in altering the spliceosomal function of U1-SM snRNP or transcriptional activation via U1-TFDIIH (Kwek et al., 2002). High throughput analysis of TAF15 targets revealed enrichment for neuronal function, including mRNA for NMDA receptor subunits, potassium voltage-gated channels, AMPA receptors, neurexin 1 & 3, neuroligin 1 and protocadherin-9. This may be pertinent for theories of FTLD-FUS pathogenesis particularly because approximately 89% of TAF15 targets are also targeted by FUS (Ibrahim et al., 2013). Complete clearance of all the FET proteins from the nucleus to aggregate bodies would circumvent this possible functional redundancy and likely have a dramatic impact on cell function and viability.

The NLS of TAF15 is only marginally different to that of FUS and EWS with 6 previously conserved residues replaced with similar amino acids. Crucially the PY motif remains unchanged and it is therefore a target of TRN1 driven import (Figure 1.5). Contrary to results from FUS studies no putative nuclear export signal has been found within TAF15 (Kino et al., 2011, Marko et al., 2012). Despite being a target of TRN1 its nuclear localisation can be partially disrupted by treatment with actinomycin D which inhibits

transcription (Marko et al., 2012). Similar results have been shown for FUS suggesting both TAF15 and FUS are RNA polymerase II activity sensing (Pinol-Roma and Dreyfuss, 1993).

Figure 1.4. Domain structure of the TAF15 protein. SYGQ-rich: Serine Tyrosine Glycine Glutamine-rich domain. RGG: Arginine Glycine Glycine-rich domain. RRM: RNA recognition motif. Zn: putative zinc finger. NLS: Nuclear localisation signal.

Recently identified variants in TAF15 have been suggested to be causative in familial and sporadic ALS (Ticozzi et al., 2011, Couthouis et al., 2011). These disease associated variants formed cytoplasmic foci when expressed in primary neuron cultures and induced neurodegeneration in Drosophia models. These authors also investigated spinal cord neurons of sporadic ALS patients and found TAF15 to be accumulating in the cytoplasm within small punctate inclusions which contradicts findings of other authors who state TAF15 aggregation is unique to FTLD-FUS (Neumann et al., 2011). It remains to be seen if the cytoplasmic foci formed in primary neurons and the punctate inclusions in ALS co-localise with stress granule markers. Briefly, stress granules are transient foci of triaged mRNA and proteins brought about by cellular stress known to harbour mutant FUS and wild type TAF15 (Dormann et al., 2010, Blechingberg et al., 2012b)(Discussed further in 1.4.2). Notably there have been no reports of mutations in TAF15, putative or otherwise, in cases of FTLD-FUS.

1.2.6 TRN1

Transportin1 is a key component of the non-classical nuclear import pathway. In contrast the classical import pathway TRN1 binds its cargos directly rather than through an adaptor protein like karyopherin α (Suzuki et al., 2005). Binding of TRN1 to target cargos depends on the NLS motif present in said cargo. Typically, this motif conforms to very well conserved patterns and is referred to as the M9 signal or a PY-motif (Figure

1.5). Although only three cargos of TRN1 are discussed in detail here there are many more reflecting the importance of TRN1 in nuclear import (Appendix 1.2).

Figure 1.5. The M9 signal or PY-motif in each of the FET proteins. Blue cells indicate identical residues vital for the PY-motif.

TRN1 has a super helical structure created by the helical stacking of 20 HEAT (Huntington, Elongation factor 3 A subunit of protein phosphatase 2A lipid kinase Tor1) repeats (Andrade and Bork, 1995, Lee et al., 2006, Imasaki et al., 2007). Considerable flexibility is afforded to this 3D structure which is crucial to its function as a cargo and co-factor binding transport protein. Within the eighth HEAT repeat there is an insertion termed the 'acidic-loop' (residues 311-373) that plays a fundamental role in cargo dissociation within the nucleus. In its unbound state the acidic-loop of TRN1 assumes a random coil structure which allows a cargo protein to bind. This binding takes place within the C-terminal arch of the super helix at 2 distinct sites through a series of H-bonds (Wang et al., 2011). At this point the TRN1-cargo complex translocates through the nuclear pore and into the nucleoplasm. Once in the nucleus the high concentration of RanGTP ensures binding of this co-factor to TRN1. This causes the acidic-loop to adopt a partially unfolded α-helix conformation, which moves to sterically dislodge the cargo (Wang et al., 2011). TRN1 is then recycled back into the cytoplasm where GTP hydrolases convert RanGTP to RanGDP. This reduces the affinity of TRN1 for Ran by 4 orders of magnitude. However, TRN1 remains bound to RanGDP in the cytoplasm because of its high concentration until a sufficiently strong interaction between TRN1 and a possible cargo occurs (Figure 1.6).

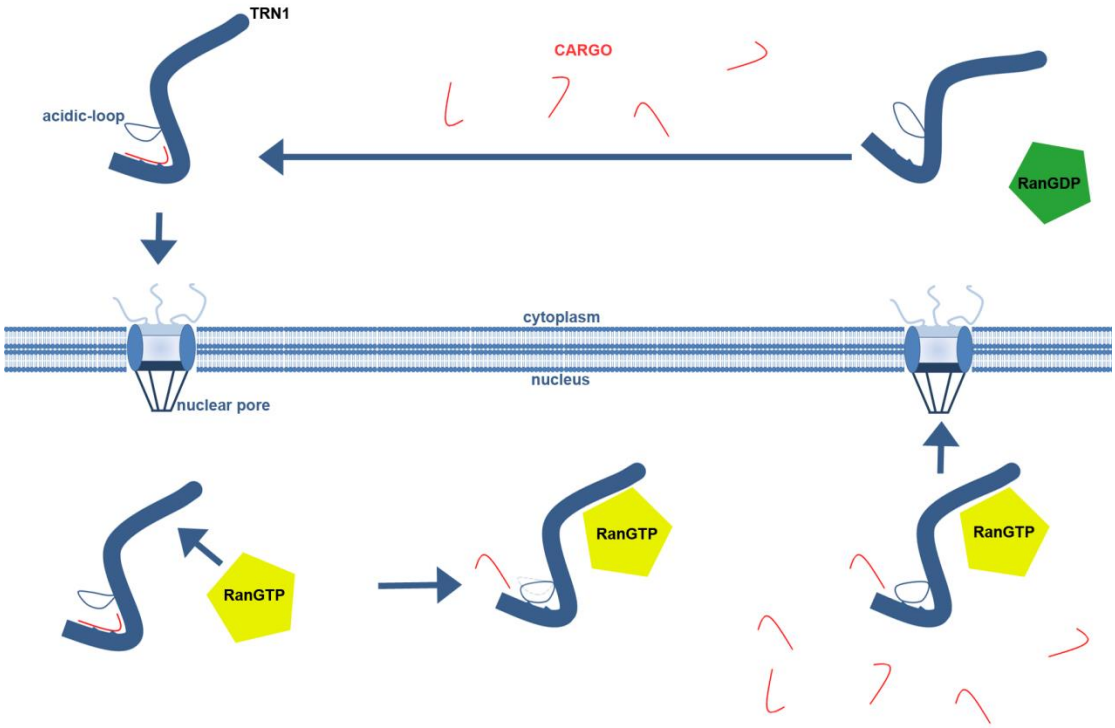

Figure 1.6. Functional cycle of TRN1. CARGO could be any of the described TRN1 targets includes FUS, EWS or TAF15. Changes in the tertiary structure of TRN1 brought about by RanGTP binding force the acidic-loop to displace the cargo within the nucleus.

Exactly how this TRN1-cargo complex is attracted to, and moves through, the nuclear pore remains unclear. One model suggests that the movement through the pore occurs by facilitated diffusion. In this model, one-way directionality would be conferred by Ran-dependant steps on either side of the pore. A second model suggests that the direction of transport is due to a ratcheted mechanism of gradually increasing affinity between the importin and nucleoporins as the TRN1-cargo complex moves through the nuclear pore. A more favoured model is based on the observation that the pore is lined with many hydrophobic phenylalanine and glycine containing nucleoporins. In this selective phase model the hyrophobic attraction of the phenylalanine-glycine rich regions for each other creates a hydrophobic phase blocking the passage of most proteins. Essentially this model proposes that there is a selective affinity of importins for this environment, which would link the ability of the nuclear pore to exclude many proteins from passage and facilitate diffusion of TRN1 complexes. Support for the latter model comes from the rapid transmission kinetics associated with nuclear import, as well as the observations that

importins interact with the phenylalanine-glycine repeats of nucleoporins (Denning et al., 2003).

Before the discovery of TRN1 in the pathology of FTLD-FUS, there was no association of TRN1 with any human disease. However, transportin3 (TRN3) was the subject of a spate of research papers after genome wide siRNA screens identified it as an important factor for efficient HIV infection (Brass et al., 2008, Konig et al., 2008, Zhou et al., 2008, Ocwieja et al., 2011). Recent research into nuclear shuttling proteins and FTLD-TDP has identified several members of the exportin family as being connected to the disease. Expression analysis of 82 nuclear factors in post-mortem brain samples from patients with FTLD-TDP revealed a considerable reduction in expression of cellular apoptosis susceptibility protein (CAS) (Nishimura et al., 2010). In nuclear export pathways protein cargo and RanGTP bind co-operatively to an exportin such as CAS, and it is the hydrolysis of RanGTP to RanGDP in the cytoplasm that releases the protein cargo.

Further exploration of the importin-exportin proteins may reveal greater insights into the pathology of FTLD.

1.3 Pathology of FTLD-FUS

FTLD-FUS can be further subdivided into aFTLD-U, NIFID and BIBD. These subtypes were originally classified in this manner because a proportion of the intracellular inclusions of NIFID were also positive for α-internexin and neurofilaments (Josephs et al., 2003a, Cairns et al., 2007). Before the discovery of TRN1 and the other FET proteins within the inclusions of FTLD-FUS, FUS was the primary pathological marker alongside more general markers of pathology such as ubiquitin and p62. Detailed histological analysis of pathology revealed superficial spongiosis affecting the frontal and temporal cortices (Lashley et al., 2011), which can be seen macroscopically as shrunken lobes, widened sulci and reduced gyri. Both subtypes possess the characteristic neuronal cytoplasmic inclusions but they are more frequent in the NIFID subtype (Lashley et al.,

2011). These can be found most readily within the superficial cortical layers and include a variety of morphologically distinct types. The NIFID subtype shows crescent-shaped cytoplasmic inclusions that rap around the nucleus, large globus Pick body-like inclusions that stain evenly throughout the structure, flame or tangle-like inclusions that extend into the apical dendrites of pyramidal neurons, as well as rare lentiform or vermiform shaped intranuclear inclusions. The aFTLD-U subtype presents with the same cresent-shaped cytoplasmic inclusions, but also smaller bean-like rather than Pick body-like inclusions, intranuclear inclusions are absent from the cortex of aFTLD-U cases but not the hippocampal formation. Cases of aFTLD-U typically show some degree of hippocampal sclerosis which can extend into the subiculum (Lashley et al., 2011). However, the degree of inclusion pathology can vary significantly between cases. Some cases show frequent intranuclear inclusions throughout the granule cell layer, sometimes accompanied by bean-shaped cytoplasmic inclusions, others contain only occasional inclusions. The same variability can be seen in NIFID cases where instances of intranuclear inclusions occurring alongside cytoplasmic inclusions in the same cell pepper the granule cell layer in some cases but not others. In contrast, BIBD pathology demonstrates a predilection for pyramidal and extrapyramidal motor regions with relative sparing of the cerebral cortex. Neuronal cytoplasmic inclusions affect the dorsal midbrain, locus ceruleus, substantia nigra, globus pallidus, and spinal cord. These vary in morphology ranging from compact and rounded, tangle-like, and crescent shaped. Neuronal intranuclear inclusions are also present as well as dystrophic neurites and swollen axons.

In light of the spectrum disorder hypothesis that argues FTLD-FUS and ALS-FUS represent cortical and motor ends of a disease spectrum, it is not unsurprising that motor neurons are affected in FTLD-FUS. The XIIth cranial nerve nucleus appears to maintain its neuronal population but also harbours either compact or filamentous skein-like cytoplasmic inclusions in both subtypes (Lashley et al., 2011). The spinal cord of

FTLD-FUS patients is also notably affected, filamentous skein-like inclusions, punctate dot-like inclusions, or more compact cytoplasmic inclusions are common in the cervical segments. Beyond typical FTLD-FUS pathology markers such as FUS, the spinal cord has also been reported to show increased microglia and macrophages by CD68 immunohistochemistry indicating degeneration of these tracts (Lashley et al., 2011).

Biochemical markers of pathology in FTLD-FUS focus of the detection of highly insoluble proteins also seen in characteristic immunohistopathology. Despite a predicted molecular weight of 53kDa FUS has been shown to run at 2 distinct bands, one at 53kDa and another at approximately 75kDa (Lashley et al., 2011). Neuron cell lysate runs at 75kDa whilst brain homogenate produces two bands which has led to debate about which band or bands represent FUS. Sequential solubility extractions reveal the FUS biochemical signature of this disease is quite complicated. Sequential solubility fractionation separates proteins via ultracentrifugation and buffers of increasing detergent strength. Those proteins found in the final urea buffer fraction are considered to be highly insoluble and likely highly aggregated. Detecting proteins present in the inclusions of FTLD-FUS in the urea fraction is an important confirmatory step before including them in the pathology of disease. However, depending on the exact technique used to separate the fractions, FUS is either present or completely absent from the urea fraction of healthy controls (Page et al., 2011, Lashley et al., 2011). Generally speaking a shift towards the insoluble fraction is seen with FUS immunoblots and this is considered pathologically relevant in terms of protein aggregation.

A similar shift in protein insolubility can be seen with TAF15 immunoblotting in both aFTLD-U and NIFID (Neumann et al., 2011). Notably, this shift can be far more pronounced than that seen for FUS, which when coupled with the fact that TAF15 antibodies give a simpler banding pattern suggests TAF15 is a more clear-cut biochemical marker. Whilst EWS displays a similar tendency for higher insoluble levels, this does not reach significance (Neumann et al., 2011).

It is important to note that neither FUS, TAF15 nor EWS display abnormal molecular weight species associated with ubiquitination which presents a quandary given that ubiquitin is abundant within FUS TAF15 EWS inclusions.

1.4 Putative mechanisms of pathogenesis

1.4.1Protein mis-folding and prionoid proteins

The conversion from soluble predominantly α-helix secondary structure to insoluble β-sheet-rich aggregates is a common phenomenon in neurodegenerative disease. Alzheimer's disease is the best known example of a mis-folded protein aggregating and causing disease. The usually soluble products of amyloid precursor protein (APP) have their metabolism altered in some manner, which results in greater production of the Amyloid-β $_{1\text{-}42}$ fragment (Aβ). This peptide is intrinsically aggregate prone and will self-aggregate in aqueous solution under conditions of high peptide concentration by taking on a β-sheet form (Barrow et al., 1992). The residues 17-21 and 32-42 have a higher hydrophobicity and are therefore more likely to assume a β-sheet conformation. Additionally, the residues 9-21 can transition between α-helix and β-sheet forms and replacement of any residue between amino acids 17-23 with proline will increase solubility, reduce β-sheet formation and also prevent fibrilisation (De Strooper et al., 1995). This fribrilisation is seen in disease, ultrastructural analysis of Aβ aggregates reveals anti-parallel β-sheet structure organized into unbranching fibrils (Fraser et al., 1991, Serpell et al., 1995). Thus fibrillogenesis is linked to the conversion from α-helix to β-sheet structure.

Parkinson's disease is the classic example of Lewy body disease, but many neurodegenerative diseases have also been found to harbour some degree of Lewy body burden (Jensen et al., 1995, Spillantini et al., 1998a). Lewy bodies are intracellular aggregates composed of aggregated α-synuclein, a very small (14kDa) presynaptic molecule found throughout various regions of the brain (Jakes et al., 1994). Circular

dichromism predicts a largely unstructured random coil protein but residues 1-60 have at least the ability to form α-helices, 61-95 are predicted to be highly amyloidogenic, and the remainder is an acidic proline rich region (Kim, 1997, Davidson et al., 1998, George et al., 1995, Manning-Bog et al., 2002). Similarly to Aβ this protein's α-helical content will increase if it is in a lipid environment (Shen and Murphy, 1995, Davidson et al., 1998). This maintenance of α-helical structure in these conditions is logical given its likely synaptic role, from which it takes its name. Highly malignant mutations in *SNCA* that give rise to familial Parkinson's disease (PARK1/4) have been shown to increase the rate of β-sheet adoption and fibrilisation (Serpell et al., 2000), and that these fribils are formed through a nucleation step (Conway et al., 2000, Wood et al., 1999). Injection of mice with mis-folded insoluble α-synuclein produces a prionoid spreading of α-synuclein pathology as soluble protein is templated into insoluble β-sheet conformations (Masuda-Suzukake et al., 2013, Li et al., 2008). Therefore, Parkinson's disease is another protein folding prionoid neurodegenerative disease.

FTLD-TDP and cases of sporadic ALS demonstrate thioflavin-S staining within the intranuclear and cytoplasmic aggregates suggesting a strong β-sheet content (Bigio et al., 2013). The density of FTLD-TDP thioflavin-S positive inclusions is similar to that seen under ubiquitin immunohistochemistry but fewer compared with TDP43 immunohistochemistry, suggesting that there may be 2 stages of inclusion formation and aggregation. First TDP43 re-localises and coalesces in the cytoplasm (TDP43 positive inclusion), then over time it becomes mis-folded, thiofavin-S positive, and ubiquitinated (TDP43 positive aggregate). FTLD-FUS inclusions were typically negative for thioflavin-S, however there were some positive granular cytoplasmic inclusions in the hippocampal dentate gyrus neurons (Bigio et al., 2013). Bacterial expression systems of both TDP43 and FUS have shown these proteins do spontaneously form fibrils visible under electron microscopy, but the lack of thioflavin-S staining in FTLD-FUS may suggest a divergent pathogenesis between these two highly related proteins and diseases.

This theory of mis-folded protein being a convergent moment in the pathogeneisis of multiple diseases comes hand in hand with the theory of prionoid spread and the phenomenon of permissive-templating (Hardy, 2005). Well described permissive-templating diseases include transmissible spongiform encephalopathies like Creutzfeldt–Jakob disease, and inheritable prion diseases caused by mutations in the *PRNP* gene. In these cases normally folded PrP^{C} changes to a β-sheet-rich conformation (PrP^{Sc}) that is protease resistant and insoluble. The key property of PrP^{Sc} that makes this disease so devastating is its ability to template this change onto the reservoir of normally folded PrP, not just within the cell but adjoining brain regions. Interestingly, this self-templating prion behavior is rooted in survival not disease. Yeast cells use prion proteins as genetic elements which confer survival benefits under certain conditions. For example, yeast Sup35 protein is normally required for stop-codon recognition and translational termination; however, under certain stressful conditions it can form a self-propagating fibrillar β-sheet conformation that is inheritable to daughter cells (Liebman and Sherman, 1979, Patino et al., 1996). This self-templating β-sheet conformation seems to be dependent on the N-terminal region, which is rich in Q/N residues. Because this glutamine/asparagine rich region is characteristic to prion-like propagation, it is referred to as the 'prion domain' (Masison and Wickner, 1995). Conversion of the yeast Sup35 protein to the prion state leads to loss of function and as a consequence widespread read through of stop codons. This radical change in gene expression allows the rapid emergence of novel survival phenotypes. This represents a molecular adaptive strategy for yeast survival under stressful conditions based on the phenomena of conformational change.

The mammalian proteome, and particularly those proteins capable of binding RNA, contain several glutamine/asparagine rich prionoid domains that may use self-aggregation to modulate their activity. A well-known example is the RNA binding protein T-Cell-Restricted Intracellular Antigen-1 (TIA-1), which is a vital component of stress

granules (Gilks et al., 2004). Briefly, these cytoplasmic RNA-protein complexes form under conditions of cellular stress, and mediate adaptive mRNA translational suppression. The prion-related glutamine/asparagine domain of TIA1 is essential for self-aggregation and stress granule formation. Thus, one consistent theme for proteins containing prion-related glutamine/asparagine rich domains from yeast to mammals is stress-induced conformational change leading to self-aggregation, which then alters protein function to orchestrate an adaptive response in gene expression or translation. Several predictive algorithms have been used to identify proteins containing prion-like domains in both yeast and human proteomes, many of which bind to DNA/RNA based on their amino acid sequence (King et al., 2012). Where particular proteins rank in terms of prionogenicity depends on the design and sensitivity of the algorithm as well as how it was trained. However, in all published analyses FUS, EWS, and TAF15 rank exceptionally high in terms of prionoid properties, often higher than TIA1 (Alberti et al., 2009, Toombs et al., 2010, Couthouis et al., 2011).

1.4.2 Stress Granules and P-bodies

The aggregation of proteins in neurodegenerative disease contrasts with the functional aggregation of Sup35 in yeast, but also TIA1 in mammalian stress granules. These cytoplasmic foci are heavily involved in the processing and turn-over of mRNA. RNA binding proteins such as those we see aggregating in FTLD-FUS have both nuclear and cytoplasmic functions related to mRNA. Nuclear functions encompass regulating mRNA maturation including; RNA helicase activity, RNA polymerase elongation, splicing, and nuclear export (Heyd and Lynch, 2011). In the cytoplasm these proteins can regulate RNA transport, translation or silencing, as well as degradation (Liu-Yesucevitz et al., 2011). Much of this cytoplasmic regulative activity occurs at distinct macromolecular sites assembled by protein-protein interactions through glycine rich domains and Q/N rich regions, and protein-mRNA interactions through RNA recognition motifs (RRM) (Krichevsky and Kosik, 2001). Importantly, different macromolecular granules are

assembled to undertake different functions. Visualizing proteins associated with these different functions allows microscopic delineation of these separate granules.

Stress granules can be visualized with antibodies directed to TIA-1, whose RRM will recognize uracil rich 30-37 nucleotide bipartite motifs (Lopez de Silanes et al., 2005), or TIA1 cytotoxic granule-associated RNA binding protein-like 1 (TIAR) that will recognize mRNA with 28-32 long stem loops (Kim et al., 2007). The HuR proteins will bind mRNA uracil rich 17-20 nucleotide long sequences (Lopez de Silanes et al., 2004), and Ras-GAP associated endoribonucelase (G3BP), which is important in the formation of stress granules, cleaves mRNA between CA dinucleotides (Tourriere et al., 2001). The reaction cascade that leads to stress granule formation is complex but can be best interpreted through the phosphorylation of eukaryotic translation initiation factor 2α (eIF2α). Cellular stress prompts the phosphorylation of eIF2α at serine 51 by stress kinases (PKR, HRI, PERK or GCN2), which inhibits the translation complex containing $tRNA_i^{met}$.(Kedersha et al., 1999). Capped mRNA remains bound to the pre-initiation complex and forms a nucleus for aggregation through TIA-1 and other protein-protein interactions. Stress granules are initially small and punctate but will increase in size as the RNA binding proteins listed above begin to coalesce and aggregate through their glycine-rich domains and Q/N rich regions. The vital nature of stress granules in the survival response is highlighted by increase apoptosis upon stress after knockdown of TIA-1 or inhibition of eIF2α phosphorylation (Phillips et al., 2004, Jiang et al., 2003). However, this response has evolved to cope with acute transient stress, and the consequence of long term persistence of stress granules has not been explored. Stress granules dissociate relatively rapidly (1-3 hours) once the stress has been removed (Kedersha et al., 1999), once again through the phosphorylation status of eIF2α (Moreno et al., 2012). Pharmacological agents allow the manipulation of stress granules by altering the processes outlined here. Cycloheximide and emetine inhibit their formation by interrupting protein elongation whilst maintaining polysomes, thus preventing free

mRNA accumulating in the cytoplasm and therefore stress granule nucleation (Kedersha and Anderson, 2007). Conversely, puromycin causes premature chain termination within the ribosome, and therefore disassembly of the polysome.

Whilst sequestration of basal mRNA is the remit of stress granules, their subsequent degradation is mediated by a separate but related granule called P-bodies. These can be visualized by a separate group of markers including; mRNA-decapping enzyme 1a (DCP1a), the Sm and SM-like (LSm 1-7) proteins (Ingelfinger et al., 2002). Given their highly related function it is not unexpected that some components of one can be found within the other and moreover they are often found adjacent to one another (Parker and Sheth, 2007). The vast majority of P-body constituents are geared towards mRNA repression, interference and non-sense mediated decay. Examples include, mRNA decapping machinery, activators of decapping and the 5' to 3' exonuclease Xrn1p (Cougot et al., 2004, Ingelfinger et al., 2002).

Both stress granules and P-bodies are not free floating entities but rather they are closely associated to the cytoskeleton and require microtubule alteration to function properly (Kwon et al., 2007). Histone deacetylase 6 (HDAC6) deacetylates tubulin to reduce cellular motility and is vital to the formation of stress granules. This enzyme also provides an interesting link with tau, because low activity is associated with tau accumulation, a hallmark of neurodegeneration (Cook et al., 2012). Furthermore, the dynein motor has been shown to tether stress granules to the cytoskeleton and aid the coalescence of small granules (Tsai et al., 2009).

The discovery that the cytoplasmic inclusions of FTLD-FUS contain stress granule markers (Dormann et al., 2010) has led to a flurry of research around this theme (Bosco et al., 2010, Gal et al., 2011). Some authors hypothesized that stress granule formation may be a precursor to the more sinister cytoplasmic aggregates (Dormann et al., 2010). Yet these proteins are known to easily disperse and return to solution (Kedersha et al.,

2000). Despite this, stress granule markers such as TIA-1 co-localize with the characteristic neuronal aggregates of Alzheimers disease, ALS, FTLDP-17, FTLD-TDP, and FTLD-FUS (Liu-Yesucevitz et al., 2010) suggesting there may be a link between the two phenomena. However, when considering human pathological tissue it is worth remembering that any observation is of the absolute final time point of death. It is possible that as the aggregate grew it absorbed other non-membranous structures like stress granules as it dominated the cytoplasm. Evidence to the contrary comes from animal models which aim to emulate decades of disease in a matter of weeks. These animals also show stress granule markers within their induced pathology (Vanderweyde et al., 2012).

All of the widely accepted pathological markers of FTLD-FUS have been found to re-localise to stress granules or P-bodies when subjected to cellular stress (Liu-Yesucevitz et al., 2010, Blechingberg et al., 2012b, Chang and Tarn, 2009). However, re-localisation to the cytoplasm and arrangement into foci does not cause these proteins to become highly insoluble. This is crucial since highly insoluble protein is a core feature of aggregated disease protein.

1.4.3 Oxidative and non-oxidative stress

The term 'reactive oxygen species' (ROS) is widely used in conjunction with neurodegeneration, particularly in the field of Alzheimer's disease (Hardy and Allsop, 1991, Selkoe, 1996). It refers to the generation of the superoxide anion $[O_2]^-$, this species is highly reactive and widely described as damaging to DNA and proteins alike. ROS are included in the pathogenesis hypothesis of Alzheimers' disease because of several observations. Firstly, the alteration of mitochondrial function in this disease is likely to lead to electron leakage in the respiratory chain and the consequent formation of superoxide radicals. The unbalanced high activity of superoxide dismutase and monoamine oxidase B causes the production of more H_2O_2. The increase of lipid

peroxidation and other cell membrane changes indicative of ROS attack. However, many of these changes can be found in otherwise healthy aged brains. The milieu of an aging brain is therefore considered a more oxidizing environment than its younger counterpart.

Early evidence implicating oxidative stress in ALS was gleaned from identifying clues such as lipid peroxidation in the spinal cord and cortex of patients (Shibata et al., 2001, Ferrante et al., 1997). As the disease progresses products of peroxidation like malondialdehyde and 8-hydroxy-2'-deoxyguanosine from DNA damage can be detected in the cerebrospinal fluid and even the blood sera (Oteiza et al., 1997). Strong evidence for the deleterious role of oxidative stress comes from patients harbouring SOD1 mutations. These mutations are causative in ALS can affect the function of superoxide dismutase 1, an enzyme responsible for eliminating superoxide free radicals. Since ALS and FTLD are now thought to be two ends of a disease spectrum it is not unexpected that they share signs of oxidative stress. Increases in 4-hydroxynonenal adducts are found in all subtypes of FTLD (tau/TDP43/FUS) as a product of lipid peroxidation (Martinez et al., 2008). These unstable nucleophiles react with nucleophilic side chains of cysteine, histidine, and lysine residues generating covalent bonds between aldehyde carobonyl groups and peptide chains, often resulting in a loss of protein function and eventual apoptosis (Kruman et al., 1997, Uchida, 2003, Zarkovic, 2003). Lipid peroxidation damage is associated with changes in membrane unsaturation and fatty acid profile, which in a highly membrane dependent cell type such as neurons could have profound implications for proper function. Similarly to ALS the clearest evidence of oxidative stress in the pathogenesis of FTLD comes from patients with progranulin null or missense mutations. It has been shown that progranulin protein stimulates phosphorylation activation of the neuronal extracellular regulated kinase ERK/p90 ribosomal S6 kinase and phosphatidylinositol-3 kinase cell survival pathways (He et al., 2002, Lu and Serrero, 2001, Monami et al., 2006, Zanocco-Marani et al., 1999). These are

capable of neuroprotection from apoptosis induced by glutamate hyperexcitotoxicity and oxidative stress. The progranulin haploinsufficiency associated with FTLD-TDP has yet to be fully explored but in the context of what is known about progranulin function it would seem that oxidative stress is paramount to pathogenesis. The use of oxidizing agents on cell models attempts to mimic the environment of the aged brain and has produced some interesting results.

Sodium arsenite ($NaAsO_2$) is a well-characterized oxidative stressor widely used in cell culture experiments to model oxidative stress and stress granules (Vahter et al., 1995, Wang et al., 1997, Lynn et al., 1998). It is known to inhibit pyruvate dehydrogenase and thereby reduce the adenosine-5'-triphosphate (ATP) energy production of the cell, but also produce ROS as is interferes with basal metabolic oxidation-reduction reactions. It is this property that drives lipid peroxidation (Schlenk et al., 1997), protein/enzyme oxidation and glutathione depletion, poly ADP-ribosylation, and apoptosis (Abernathy et al., 1999). Tert-butyl hydroperoxide (tBH) a relatively stable alkyl hydroperoxide that is metabolized by cytochrome P450, haemoproteins, and other systems to produce free radical intermediates that initiate lipid peroxidation and glutathione depletion, resulting in cellular damage (Barr and Mason, 1995, Schnellmann, 1988, Van Duuren et al., 1966, Younes and Wess, 1990). Sorbitol is a relatively less well-characterized stressor that is generally not grouped together with the oxidative stressors since its metabolism produces only low levels of ROS through the polyol pathway and the sorbitol dehydrogenase reaction. It is more commonly dissolved in the liquid media at high enough concentrations to produce an osmotic imbalance between the cell and its environment. In this regard it is referred to as an osmotic stressor (Dewey et al., 2011).

1.4.4 Cell and animal models of FTLD-FUS

The ability to effectively model neurodegenerative diseases in cellular systems has been a long sort-after boon to research. However, developing accurate and malleable models

takes time and requires a detailed understanding of the pathway being modified. For instance, one issue that has confounded attempts to effectively model neurodegenerative disease is the uncertain nature of the cytoplasmic and intranuclear inclusions that are almost ubiquitous to all forms of neurodegeneration. Theories range from; they are themselves composed of a toxic species that are harmful to the cell, or that they are epiphenomena brought about by a toxic event and are not responsible for disease, or that they are in fact the result of protective efforts by the cell and should be encouraged. Attempts to model the various forms of FTLD have produced varying levels of success. Pure TDP43 synthesized from bacteria is highly prone to aggregation, thanks to the intrinsic properties of its C-terminal region (Johnson et al., 2009). Furthermore, these aggregates formed amorphous non-amyloid structures strikingly similar in properties to those found in TDP43 positive ALS and FTLD. Yeast models have compounded this finding by demonstrating TDP43 aggregation when over expressed (Johnson et al., 2009, Johnson et al., 2008). These studies were also able to show that over expression of TDP43 was toxic to the cell. However, attempts to recapitulate these finding in mammalian cells have struggled. Over expression of full length TDP43 in mammalian cells produced predominantly soluble and nuclear TDP43 (Wang et al., 2004, Ayala et al., 2008, Winton et al., 2008). Instead it was the expression of the C-terminal fragment implicated earlier that produced cytoplasmic insoluble TDP43. FUS research has produced similar findings, namely that bacterially expressed FUS spontaneously aggregates into filamentous structures (Sun et al., 2011). However, over expression of FUS in mammalian cells produced a soluble and normally localised phenotype. To reproduce the pathological findings of insoluble FUS aggregating in cytoplasmic and intranuclear inclusions in a cellular system will require more than just over expression.

Given that one of the prominent hypotheses of FTLD-FUS and ALS-FUS hinges on the loss of FUS function, discussing the phenotypes of knockout mice is worthwhile. Heterozygous knockouts are slightly smaller at birth, a characteristic that is exacerbated

during weaning resulting in an animal 30% smaller than wild type (Kuroda et al., 2000). Interestingly, other than their reduced size they appear developmentally normal, and outbred strains survive for just as long. However, animals on an inbred background do not survive beyond weaning (Kuroda et al., 2000). No clear reason for this difference is forthcoming. Homozygotes are severely infertile with males showing complete sterility and females reduced fertility. This male sterility was not androgen related because animals showed normal mounting behaviour and internal sexual organs (Kuroda et al., 2000). However, these mice did show deficits in homologous pairing of chromosomes leading to defects in spermatogenesis. Unfortunately, these authors were not specifically interesting in possible neurological deficits associated with ALS and FTLD and therefore did not perform in-depth immunohistochemical examination of the CNS. However, since normal mounting behaviour was noted it could be surmised that normal motor function remains. Knockin mice overexpressing tagged human FUS (hFUS) show highest expression in the brain, spinal cord and testis (Mitchell et al., 2013). It is tempting to take this finding as indicative of anatomical areas reliant on FUS for proper function, but this pattern is typical of human PrP promoter driven expression (Borchelt et al., 1996). Overexpression was accompanied by a concomitant down regulation of murine FUS, suggesting an expression feedback loop. At 4 weeks these mice develop tremor and a stilted gait, then rapidly progressing motor neuron deficits exemplified by poor rotor-rod and open field performance (Mitchell et al., 2013). At 7-8 weeks the hind limbs are paralyzed, which contrasts with heterozygotes that show normal growth and motor performance. Immunohistochemical examination of the CNS reveals cytoplasmic accumulation of hFUS but this is not accompanied by the ubiquitination so characteristic of FTLD-FUS (Mitchell et al., 2013). In rat models overexpressing mutant (R521C) but not wild type hFUS causes progressive paralysis in transgenic rats. This motor neuron degeneration is similar to that seen in mice, but it was also accompanied by significant neuron loss in the frontal cortex and dentate gyrus, two areas predominantly affected in

FTLD-FUS. Interestingly, unlike paralysis this was evident under both mutant and wild type hFUS (Huang et al., 2011). Ubiquitinated inclusions were evident in mutant expressing animals at the same time point of paralysis, and present in wild type expressing animals at advanced stages of cortical degeneration (Huang et al., 2011). These inclusions were not FUS positive regardless of genotype and furthermore FUS remained mainly nuclear despite the R521C mutation producing strong cytoplasmic staining in cell culture (Dormann et al., 2010). How this relates to the pathogenesis of human disease is unclear. Clearly aberrantly high levels of FUS are neurotoxic but the protein is not as aggregation prone as previously thought, at least in rats.

Due to the relatively new discoveries of EWS, TAF15 and not least TRN1 in the pathology of FTLD-FUS, no animal models have been created to investigate these proteins. It will be interesting to see if simultaneous overexpression of the FET proteins or TRN1 will produce the most accurate pathology and behavioural measures.

1.5 Aims of this study

Due to the similarities in pathology between ALS-FUS and FTLD-FUS, TRN1 and nuclear import in the context of oxidative stress could have an important role to play in FTLD-FUS.

This study aimed to investigate the role of TRN1 in FTLD-FUS in terms of:

- Pathology and biochemistry of TRN1 in FTLD-FUS
- Characterizing the response of TRN1 and the FET proteins in SH-SY5Y cells subjected to various stressors.
- Characterizing the response of TRN1 and the FET proteins in rat primary hippocampal neurons subjected to oxidative stress

Chapter Two: Materials and Methods

2.1 Tissue procurement

Human tissue for these studies was partly obtained from the archive at the Queen Square Brain Bank for Neurological Disorders, UCL Institute of Neurology where tissue is collected with the ethical approval of the London Multicentre Research Ethics Committee and with the informed consent of next-of-kin. Tissue were also obtained from the MRC London Brain Bank for Neurodegenerative Diseases, Institute of Psychiatry, King's College, London, UK ; Neuropathology Department, Århus Kommunehospital, Århus, Denmark and NeuroResource, UCL Institute of Neurology, University College London. All patients had details of a standard clinical history and had undergone both neurological examination and cognitive assessment. Details of FTLD-FUS cases including age of onset and post-mortem delay are available in the next chapter.

2.2 Tissue Processing: Paraffin embedded tissue

Representative areas of formalin fixed brain and spinal cord tissue were processed as shown in table 1.

Step	Reagent	Time (hrs)
1	70% alcohol	6:00
2	90% alcohol	6:00
3	90% alcohol	6:00
4	Absolute alcohol	6:00
5	Absolute alcohol	6:00
6	Absolute alcohol	6:00
7	Absolute alcohol	6:00
8	Chloroform	6:00
9	Chloroform	6:00
10	Wax	6:00
11	Wax	6:00
12	Wax	6:00

Table 2.1 Processing of paraffin tissue. Reagents and times used

After processing tissue was embedded in paraffin wax and stored until required. Paraffin sections were cut using a Shandon Finesse (Thermo) rotary microtombe at 8µm and floated out onto warm water. The sections were picked up on HistoBond (Marienfield) slides, and left to dry at 37°C for several hours followed by an overnight incubation at 60°C.

2.3 Immunohistochemistry on paraffin embedded sections

Sections were de-waxed in three changes of xylene for 5 minutes, followed by rehydration using graded alcohols (100%, 90% and 70%). For all immunohistochemical staining the endogenous peroxidase activity was blocked using 0.3% H_2O_2 in methanol for 10 minutes followed by washes in tap water for at least 5 minutes. Sections were pre-treated for antigen retrieval in pH 6 citrate buffer and pressure cooked at over 120°C and 100 kPa. Non-specific protein binding was blocked using 10% non-fat milk in PBS (0.05M pH 7.2) by incubating the sections for 30 minutes at room temperature. The milk was then replaced with the required primary antibody and incubated for 1 hour at room temperature or overnight at 4°C (Table 2.2) depending on the primary antibody used (e.g. mouse monoclonal 1hr at room temperature, rabbit polyclonal over night at 4˚C), followed by two washes in PBS. Incubation with the relevant secondary antibody (Table

2.3) was carried out for 30 minutes at room temperature, followed by washing in PBS. Sections were incubated in avidin-biotin complex (ABC, Dako) for 30 minutes at room temperature, followed by washes in PBS. The antigen-antibody reaction was visualized using di-aminobenzidine (DAB, Sigma) as the chromogen by using 500µg/100ml DAB in PBS solution that was activated with 32µl H_20_2 (30% solution, VWR chemicals) for 2 minutes before the colour intensity checked. Sections were replaced into the DAB solution if darker colour intensity was required. Sections were counterstained with Mayers haematoxylin (VWR chemicals) for 15 seconds, washed in warm tap water and finally dehydrated through 70%, 90% and absolute alcohol before being cleared in three changes of xylene and permanently mounted with DPX (VWR chemicals).

2.4 Immunohistochemistry on frozen sections

Frozen sections were cut at 10µm from either flash frozen or slow frozen material, using a cryostat (Bright), and mounted onto either superfrost slides (VWR) or vectabond coated slides (Vector), depending on the size of the sections collected. Sections were air dried for 30 minutes, frozen at –80°C and stored until needed. Sections were removed from the freezer and placed on foil and air dried for 10 minutes, post-fixed in 4% paraformaldehyde, for 30 minutes at room temperature. This was followed by washes in distilled water and two washes in PBS. The endogenous peroxidase activity was blocked using 0.3% H_2O_2 in methanol for 10 minutes followed by washes in distilled water and two changes of PBS. The non-specific protein was blocked using 10% non-fat milk for 30 minutes at room temperature. The sections were incubated with the primary antibody for 1 hour at room temperature and the remaining protocol was followed as previously described.

2.5 Double immunofluorescence on paraffin embedded sections

Sections were de-waxed in three changes of xylene for 5 minutes, followed by rehydration using graded alcohols (100%, 90% and 70%). For all immunohistochemical

staining the endogenous peroxidase activity was blocked using 0.3% H_2O_2 in methanol for 10 minutes followed by washes in tap water for at least 5 minutes. Sections were pre-treated for antigen retrieval in pH 6 citrate buffer pressure cooked at over 120°C and 100 kPa. Non-specific protein binding was blocked using 10% non-fat milk in PBS (0.05M pH 7.2) by incubating the sections for 30 minutes at room temperature. The milk was then replaced with the required primary antibody and incubated for 1 hour at room temperature or overnight at 4^0C depending on the primary antibody used, followed by two washes in PBS. Anti-mouse fluorescent secondary antibody was incubated with the tissue for 1 hour followed by two washes in PBS. Anti-rabbit biotinylated secondary antibody was then incubated with the tissue for 30 minutes followed by washing in PBS. Incubation with avidin-biotin complex for 30 minutes and washing was followed by visualization with tyramide signal amplification (PerkinElmer). Sections were washed in PBS and mounted with vectashield DAPI containing media (Vector) and sealed with nail varnish for long term storage.

To establish the proportion of FUS-positive inclusions also labelled with the anti-TRN1 antibody double-labelled sections of the hippocampus were chosen from 3 NIFID and 3 FTLD-U cases, the granule cell layer was identified using the Leica DM5500B fluorescence microscope and ten sequential visual fields of this structure using an X63 objective were captured. Subsequently z-stack of images through the full depth of the tissue section were taken and a non-blind deconvolution algorithm was applied. A maximum projection of the z-stack provided the final image for analysis. TRN1 or FUS-positive NCIs and NIIs were visually identified on the appropriate channels and the co-localisation was confirmed on the combined images.

2.6 Bacterial cell culture protocols

The lysogeny broth (LB) media used in the bacterial procedures was 10% w/v Bacto Tryptone (Beckon Dickinson), 5% Bacto Yeast Extract (Beckon Dickinson) and 10% NaCl

dissolved in distilled de-ionised water which was subsequently autoclaved. Agar (Invitrogen) was added at 15% w/v before sterilization to make agar plates. Kanamycin (sigma Aldrich) was added to a final concentration of 50µg/ml when making colony selection plates.

Plasmid DNA was obtained from OriGene (RC218884). The vector was pCMV6-Entry and drove expression of human TNPO1 transcript variant 1. Bacterial antibiotic resistance was against kanamycin.

Lab stocks of previously made competent XL1-Blue *E.coli* from the CaCl method were thawed on ice and 1µg of plasmid DNA was added and gently mixed, the tubes were incubated on ice for 30 minutes. The tubes were then pulse heated in a 42°C heating block for 45 seconds and subsequently quenched on ice for 2 minutes. Pre-warmed LB was added (1ml) and the tubes were incubated at 37°C for 1 hour while shaking. The cells were then pelleted by pulse-centrifugation and 800µl of the supernatant was discarded. The pellet was re-suspended in the remaining 200µl and streaked on ampicillin-containing agar plates then incubated at 37°C over night.

A single colony was picked with the aid of a sterile plastic loop and used to inoculate 5ml of ampicillin containing LB media. This was then incubated at 37°C for 6 hours whilst shaking at 250 rpm. This starter culture was then used to inoculate a total of 500ml of ampicillin containing LB that was incubated at 37°C over night with 250 rpm shaking.

Stocks of transformed bacteria were made by transferring 700µl of an over night culture to a 1.5ml eppendorf tube and adding 300µl of 50% sterile glycerol solution to obtain a final 15% v/v glycerol content. This was gently mixed and frozen to -80°C for long term storage.

Plasmid purification was achieved using the mega prep kit from Qiagen and following the manufacturer's instructions. Briefly, the over night bacterial culture was pelleted by centrifugation and resuspended in a tris-based buffer. Subsequent alkaline lysis of the

cells followed neutralization of the lysate by the addition of a low salt and low pH buffer. An anion-exchange resin was used to bind the DNA while RNA, proteins and low molecular weight impurities were removed by washing with a medium salt buffer. The plasmid DNA was purified in a high salt buffer and subsequently concentrated and desalted by isopropanol precipitation. The purified DNA was finally resuspended in 500µl of 10mM tris-HCl pH 8.

A single microliter of purified plasmid was assessed by spectrophotometry to determine its DNA concentration and purity. The absorbance was measured with the aid of a nano-drop spectrophotometer at wavelengths of 260nm and 280nm, against a blank sample of tris buffer. DNA absorbs ultraviolet light with an absorption peak of 260nm, and protein shows an absorption peak at 280nm. A ratio of the absorptions at two wavelengths gives an indication of purity with respect to protein contamination, a result of 1.8 is considered 'pure'. The concentration of DNA is assessed using the following equation;

Concentration (mg/ml)=[(total volume/DNA volume) x A_{260} x 50] / 1000

To increase the purity of DNA the method of Phenol-Chloroform extraction was used. An equal volume of phenol/chloroform/isoamyl alcohol (at a ratio of 25:24:1) was added to the DNA sample and mixed by brief vortexing. The mixture was then centrifuged in a microcentrifuge at 14,000 rpm for 5 minutes. The upper aqueous phase was carefully transferred to a fresh tube, avoiding the white interphase region containing the protein impurities. The phenol extraction process was repeated and the final aqueous phase was transferred to a fresh tube. Sample was extracted two times with equal volumes of chloroform:isoamyl alcohol to remove traces of phenol. Two volumes of pure ethanol were added to the sample and sodium acetate pH 5.2 was added to a final concentration of 0.3M. The solution was mixed and incubated on dry-ice for 10 minutes. The tube was centrifuged at 14,000 rpm for 10 minutes. The supernatant was carefully discarded and the DNA pellet was washed with 200µl of 70% ethanol. The tube was centrifuged again

for 2 minutes at 14,000 rpm and the supernatant was again discarded. The pellet was dried in a vacuum centrifuge for 5 minutes and the DNA was finally resuspended in 10mM tris pH 8.

2.7 Mammalian cell culture protocols

The immortalised neuroblastoma cell line SH-SY5Y is derived from a neuronal population, and was chosen because such a line would allow investigation of events that could prime neurons for pathogenesis.

Cells were initially recovered from frozen stocks stored in liquid nitrogen. Cells were thawed in 37°C and re-suspended in pre-warmed media before being centrifuged at 150g for 5 minutes. The medium was decanted and the cell pellet re-suspended in fresh media then plated onto cell culture dishes. Frozen stock was replenished once new cells had reached adequate confluence levels by removing cells from plate via trypsinisation (0.5mg/ml in PBS) and centrifugation at 150g for 5 minutes. The supernatant was decanted and the cell pellet was re-suspended in 1.5ml of freezing stock solution (10% DMSO in complete media) and placed into a Cryovial. Cells were frozen gradually to -80°C over night in an isopropanol-insulated container, before being moved to liquid nitrogen for long term storage.

Mammalian cells were grown and maintained in 6cm Petri dishes with Dulbecco's Modified Eagle Medium (DMEM)(Life Technologies) with 10% foetal bovine serum (Life Technologies) and 1% antibiotics (Life Technologies) in incubators maintained at 37°C and 5% CO_2.

Glass coverslips (24 x 24mm^2 thickness 1) were treated with 40% HCL for 10 minutes with shaking, and then washed thoroughly with water. Coverslips were dried on blotting paper and baked overnight at 80°C wrapped in foil. In plating primary neurons the coverslips were treated with 30µg/ml ply-D-lysine for 30 minutes before being washed with distilled water and dried.

Transfection for siRNA mediated knockdown was achieved by plating cells at approximately 70% confluency on coverslips or 6-well plates in antibiotic free DMEM. The transfection mix was 90µl room temperature DMEM, 4µl lipofectamine RNAimax and an appropriate volume of siRNA solution depending on the desired concentration. This was left to complex at room temperature for 20 minutes. The mix was added dropwise to the cells and media for a total volume of 1ml per well. This was repeated three days later and left for another three days before lysis or fixation. Effect of this siRNA transfection on detectable protein levels is shown in Figure 2.1.

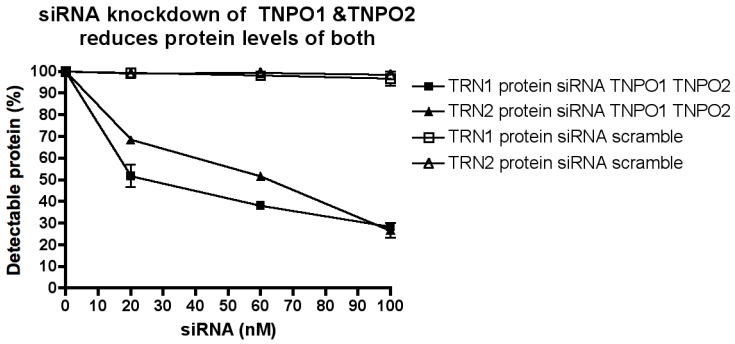

Figure 2.1. Reduction of TRN1 and TRN2 protein levels by siRNA knockdown. Densitiometric quantification is expressed at percent of protein detected compared to untreated cells (0nM). Scramble siRNA has no effect on either TRN1 or TRN2 protein levels at any concentration. Pool of anti TNPO1 and TNPO2 siRNA reduced TRN1 protein levels by 71.7% and TRN2 by 73.4% at 100nM each. Error bars SEM, n=3.

Transient transfection for over expression was achieved by plating cells at approximately 70% confluency on coverslips or Petri dishes. Cells were serum starved in DMEM for 1hr 45 minutes before the transfection mix was added. The transfection mix was 190µl room temperature DMEM, 4µl lipofectamine2000 (Invitrogen) and 5µg DNA. This was added to cells dropwise and left for 4 hours and 30 minutes, then replaced with complete media. Harvesting or fixation occurred 24 hours later to allow sufficient expression of the plasmid.

Compounds (drugs or toxins) were added to pre-warmed complete media from stock solutions. The following were kept in either de-ionized distilled autoclaved water or DMSO; arsenite (Sigma Aldrich) at 0.5M in distilled water, tBOOH (Sigma Aldrich) at

7.3M in distilled water, puromycin dihydrochloride (Sigma Aldrich) at 18.4mM in distilled water, emetine dihydrochloride (Sigma Aldrich) at 180mM in DMSO. Sorbitol was kept in dry stock until needed whereupon it was dissolved in warm media.

2.8 Preparation of dissociated e18 rat hippocampal neurons

Embryonic day 18 rats were obtained from the Biological Services Unit at University College London. Individual embryos were separated from the amniotic sack and the heads removed and placed in dissection solution (Hank's Balanced Salt Solution (HBSS) containing sodium pyruvate at 10mM and HEPES pH7.4 at 100mM (Sigma-aldrich). Two pairs of forceps were used to steady the head and peel away the skull and meninges. The brain was then scooped out of the skull and any remaining membrane or blood vessels were removed. The brain naturally opens along the hemispheres exposing the deep structures, the hippocampus is the most obvious structure and can be removed with a snipping action from the forceps. The excised hippocampi were held in a separate dish containing chilled dissection solution. Once all the hippocampi had been harvested they were placed into pre-warmed papain solution (neurobasal media (Invitrogen) and 15U/ml papain (Sigma-aldrich) for 25 minutes at 37°C. The papain solution is then replaced with papain inhibitor solution (neurobasal media and DNase 1 0.2mg/ml (ROCHE) and the tissue physically dissociated using flame narrowed Pasteur pipettes. The cells are then spun down at 75g for 5 minutes and the supernatant aspirated. The pellet is then resuspended in plating media (neurobasal media containing glutamine (Sigma-aldrich) and B27 (Gibco) supplements and penicillin/streptomycin) and counted on a haemocytometer using 1% trypan blue. Cells were plated at 200,000 cells per coverslip , and allowed to settle in plating media. The coverslips had been treated with poly-D-lysine at 0.1mg/ml for 30 minutes with shaking to ensure cell adherence. Three days later the media was replenished by removing $^1/_3$ of the volume and replacing it with $^1/_2$ the volume of replenishing media (neurobasal media containing glutamine and B27).

Differentiation was followed morphologically over 5 days using phase contrast microscopy.

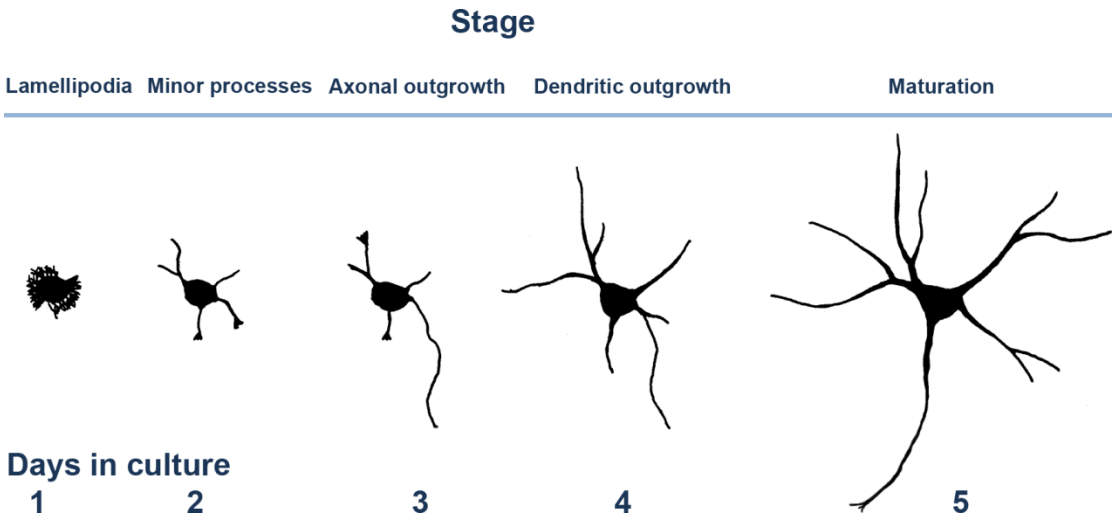

Figure 2.2. Stages of differentiation in rat hippocampal neurons. By day 5 neurons are fully differentiated.

2.9 Cell immunocytochemistry

Cells on coverslips were fixed in 4% paraformaldehyde (in PBS) for 15 minutes on ice and subsequently washed three times in PBS for 10 minutes each. Cells were permeabilised in 0.2% triton (in PBS) for 7 minutes and blocked in 3% bovine serum albumen (BSA) at room temperature. Primary antibodies were added at the appropriate dilution in 1% BSA in PBS and incubated at 37°C for 2 hours. The cells were then washed three times in PBS for 10 minutes. Secondary antibodies were added at a 1:200 dilution and the cells were left at room temperature in the dark for 1 hour. After three washes in PBS for 10 minutes each the coverslips were mounted using vectashield DAPI containing media (Vector) and sealed with nail varnish for long term storage. Fluorescence microscopy was conducted with a Leica DM5500B widefield in most cases, or LSM 710 confocal in the case of Figure 5.3.

2.10 Quantification of stress granule counts

Microscope slides were blinded for treatment (e.g. arsenite, tBH, or sorbitol) and stain (e.g. TRN1+G3BP or TRN1+FUS), coverslips were then divided into a grid of 30 19.2mm^2 squares. A random number generator produced values between 1 and 30 and the cells

visible in one visual field from that grid-square were analysed under the 63X objective. The number of cells was counted via nuclear DAPI staining; the number of cytoplasmic TRN1 foci were counted and compared to either G3BP, FET protein or ubiquitin staining for co-localisation. This was repeated for 10 non-duplicated grid squares. Graphing of co-localisation with TRN1 foci was done as percentage of total TRN1 foci for ease of interpretation. An analysis of variance adjusted for multiple testing with Bonferroni was performed on the raw data to determine the proportion of co-localisation between TRN1 and the counter stain (e.g. G3BP), and compare this under different conditions. Statistical analysis was done with the aid of Stata™ and graphing with the aid of GraphPadPrism™.

2.11 Thioflavin S staining in cells

Cells grown on coverslips were fixed with 4% paraformaldehyde (in PBS) for 15 minutes on ice and washed three times in PBS for 10 minutes each. Cells were then permeabilized with 0.2% triton (in PBS) for 7 minutes and washed three times in PBS for 10 minutes, before being stained with 0.01% thioflavin S (in distilled water) for 5 minutes. Cells were then washed in 70% ethanol (in distilled water) twice for 7 minutes each, then twice in distilled water for 5 minutes. After a final wash in PBS the cells were blocked in 3% BSA for 30 minutes ready for incubation with primary and secondary antibodies as described previously.

2.12 BCA protein assay

The concentration from cell lysates or brain fractions was determined with a bicinchoninic acid assay (Pierce). The protocol was followed according to the manufacturer's guide lines. The assay follows the principle that peptide bonds from the sample to be assessed reduce Cu^{2+} ions in cupric sulphate to Cu^{+}. The amount of Cu^{+} produced is proportional to the amount of protein present in the solution and the temperature the reaction occurs at (37°C). Two molecules of bicinchoninic acid chelate

with each Cu^{+} ion forming a purple product that absorbs light at 562nm. The concentration of protein in sampled solutions can be quantified by measuring the absorption spectra and comparing it to that of known concentrations.

2.13 Sequential solubility extractions and western blotting: Tissue

Tissue samples from frontal cortex (grey matter) from 4 controls, 3 NIFID and 4 aFTLD-U cases were homogenised at a ratio of 1:2 (wt/vol) in high-salt (HS) buffer (50mM Tris-HCl, 750mM NaCl, 10mM NaF, 5mM EDTA) containing 1% Triton-X and protease and phosphatase inhibitors (Roche). Tissue homogenate was spun at 1000g to remove nuclear and membrane debris. The resulting supernatant was subjected to ultracentrifugation at 120,000g for 30 min at 4^{0}C, following which the supernatant was retained (HS fraction). Using this HS fraction we performed immunoblotting with both the monoclonal (Abcam ab10303, 1:500) and the polyclonal antibodies (Abcam ab67352, 1:500) to test antibody specificity. Antibody specificity was confirmed by omission of the primary antibody. The results of these preliminary experiments indicated that the monoclonal antibody identified a strong band at ~100 kDa representing the expected molecular weight of TRN1. In addition to this band the polyclonal antibody also labeled additional low molecular weight bands. Therefore the monoclonal antibody was regarded as more specific and was chosen for the full biochemical analysis.

The pellet, retained after harvesting the HS fraction, was subjected to further extractions with RIPA buffer (50mM Tris-HCl, 150mM NaCl, 1% NP-40, 0.5% deoxycholate) containing 2% SDS and protease and phosphatase inhibitors as before, which was subjected to ultracentrifugation at 120,000g for 30 min at 15°C to avoid SDS precipitation, with the resulting supernatant being termed RIPA-SDS fraction. The final pellet was resuspended in 8M urea containing 8% SDS (urea-soluble) fraction. Protein concentration was determined by the BCA protein assay (Pierce) and 20µg of protein from the HS and RIPA-SDS fraction, and 5 µg of protein from the urea fraction, of each

case was loaded onto 10% Bis-Tris polyacrylamide gels (Invitrogen) and run at 200V with MES buffer (Invitrogen) under reducing conditions. Following electrophoresis, the proteins were transferred onto Hybond P membrane (GE Healthcare), blocked with 5% non-fat dried milk in PBS containing 0.1% Tween (PBS-T) and probed overnight with the monoclonal anti-TRN1 (Abcam ab10303, 1:500) antibody at 4˚C. Following washes in PBS-T, the blot was treated with HRP-conjugated secondary antibody (Santa Cruz). Blots were visualised by enhanced chemiluminesence (Pierce) and the image captured onto Kodak, X-Omat (Sigma) films.

2.14 Sequential solubility extractions and western blotting: Cells

Stressor containing media was aspirated from the cells, which were then washed three times in ice cold phosphate buffered saline (PBS). Ice-cold RIPA buffer containing phosphotase and protease inhibitor was then used to lyses the cells. Cell lysates were then agitated for 30 minutes at 4°C. Lysates were then subjected to ultracentrifugation at 120,000g for 30 min at 4°C with the resulting supernatant being termed RIPA fraction. The pellet was resuspended in 7M urea containing 4% 3-[(3-Cholamidopropyl)dimethylammonio]-1-propanesulfonate (CHAPS) 30mM TRIS-HCl pH8 and termed the urea-soluble fraction. Protein concentration was determined by the BCA protein assay and 5µg of protein from the RIPA fraction and the urea-soluble fraction, of each time point was loaded onto 12% Bis-Tris polyacrylamide gels and run at 200V with MES buffer under reducing conditions. Following electrophoresis, the proteins were transferred onto Hybond P membrane (GE Healthcare Life Sciences), blocked with 5% non-fat dried milk in PBS-T and probed overnight with the monoclonal anti-TRN1 (1:500) antibody at 4˚C. Following washes in PBS-T, the blots were treated with HRP-conjugated secondary antibody. Blots were visualised by enhanced chemiluminesence and the image captured onto Kodak, X-Omat films (Sigma Aldrich).

2.15 Densitometric quantification of Western blotting

Computer scanning of X-Omat films with CanoScanLiDE700F digitised them to an 8-bit TIFF image. Briefly, to quantify the bands obtained via Western blot analysis, we applied ImageJ software based analysis (http://rsb.info.nih.gov/ij/). The area under curve (AUC) of the specific signal was corrected for the AUC of the loading control (β-actin). If β-actin normalisation was not possible because of the erratic distribution of actin in RIPA and urea fractions as in the case of insolubility extractions this is noted in the legend. The fraction of protein in question over actin load was plotted (arbitrary values) and analysed with either one-way ANOVA followed by a Dunett's post-test or Mann-Whitney U statistical test depending on the experimental design, to determine any statistical

difference between conditions. Statistically significant differences are noted with asterisks symbols as follows: * p<0.05, ** p<0.01, *** p<0.001, **** p<0.0001.

2.16 Co-immunoprecipiation

Cells were lysed in co-immunoprecipiation (Co-IP) buffer (1% NP-40, 25mM tris pH8, 150mM NaCl, 100mM EDTA, 5% glycerol), clarified at 30,000g for 30 minutes at 4°C, the supernatant was added to 50µl of IgG conjugated beads (TrueBlot) and pre-cleared for 1 hour by rotation at 40rpm. The mixture was spun down at 1000g for 10 minutes and the supernatant recovered for protein assay. A sample of 10µg was removed and held as input. The remaining sample was rotated with the appropriate antibody at 1:500 (or not if sample was IP negative control) overnight at 4°C. Another 50µl of species specific beads (same as pre-clear) was added and rotated with sample for 2 hours at 4°C. The mixture was spun down at 1000g for 5 minutes and the supernatant discarded. The pellet was washed six times with 1ml of Co-IP buffer and centrifugation. The pellet was finally resuspended in Co-IP buffer and laemmli buffer with reducing agent ready for western blotting. To avoid detection of non-specific immunoglobulin heavy and light chains specialist TrueBlot® HRP-conjugates secondary antibodies (eBioscienec) were used (Table 1.3).

2.17 FTLD-FUS and other cases of neurodegenerative disease

Brains were donated to the Queen Square Brain Bank for Neurological Disorders, UCL Institute of Neurology, University College London; the MRC London Brain Bank for Neurodegenerative Diseases, Institute of Psychiatry, King's College, London, UK ; Neuropathology Department, Århus Kommunehospital, Århus, Denmark and NeuroResource, UCL Institute of Neurology, University College London. All FTLD-FUS cases had previously been diagnosed as NIFID (7 cases) or aFTLD-U (7 cases) (Table 3.1). Two aFTLD-U (case 13 was the mother of case 9) cases are from the same family, although no mutations in the FUS gene have been found (Lashley et al., 2011). In

addition, 3 normal control cases and 3 cases each with multiple system atrophy, corticobasal degeneration, motor neuron disease, Alzheimer's disease, Parkinson's disease, progressive supranuclear palsy, Pick's disease and FTLD-TDP types 1 and 3 were selected from the archives of the Queen Square Brain Bank. Three cases with FTLD-TDP type 2 pathology, which included one of the motor neuron disease cases with extensive cortical TDP43 pathology and also used as motor neuron disease control, were also used for the TRN1 in FTLD-FUS study. In addition to frontal and hippocampal regions, the cervical or thoracic spinal cord from each motor neurone disease cases was also stained for TRN1. No BIBD cases were available for this study in our archives. The investigation into TRN1 and FUS in polyglutamine diseases used 6 cases of spinocerebellar ataxia (two of type 3, and one of types 1, 2, 6 & 7), 2 cases of Huntington's disease, and one case of neuronal intranuclear inclusion body disease. Regions investigated included; frontal cortex, hippocampus, medulla, pons, basal ganglia, cerebellum, and spinal cord.

2.18 Primary antibodies used for this thesis

Antibody Table				
Antibody	**Species**	**Dilution for IHC**	**Dilution for Western blot**	**Company**
DCP1a	rabbit	1:200	NA	sigma aldrich
DDX3	rabbit	1:100	NA	abcam
eIF2α	goat	1:2000	1:500	Santa Cruz
eIF2α(phospho)	goat	1:2000	1:500	Stanta Cruz
eIF4G	rabbit	1:200	NA	Cell Signalling
EWS (G-5)	mouse	1:50	NA	Santa Cruz
FUS	mouse	1:200	1:1000	sigma aldrich
FUS	rabbit	1:200	NA	sigma aldrich
FUS (565)	rabbit	1:200	1:10,000	Novus Biologicals
G3BP	rabbit	1:100	1:1000	abcam
G3BP	mouse	1:200	1:1000	abcam
hnRNP A1	mouse	1:200	NA	abcam
Importin β1	rabbit	1:50	NA	abcam
karyopherin β3	mouse	1:200	NA	abcam
myc-tag	mouse	1:200	NA	abcam
myc-tag	rabbit	1:200	1:500	abcam
NUP98	rat	1:200	NA	abcam
NXF1	mouse	1:50	NA	abcam
PABP1	mouse	1:100	NA	sigma aldrich
TAF15	rabbit	1:200	NA	Novus Biologicals
TAF15	mouse	1:200	1:1000	sigma aldrich
TIA-1	mouse	1:200	1:500	sigma aldrich
TRN1	rabbit	1:200	1:500	abcam
TRN1 (D45)	mouse	1:200	1:500	abcam
TRN2	rabbit	1:200	1:500	abcam
Ubiquitin	rabbit	1:200	1:500	Dako
Ubiquitin	mouse	1:200	1:500	sigma aldrich
YB1	rabbit	1:100	NA	abcam

Table 2.2. The primary antibodies used, their species and dilution for experiments in this thesis.

2.19 Secondary antibodies used for this thesis

Secondary Antibody Table				
Antibody	**Species**	**Target species**	**Dilution**	**Company**
AlexaFluor 488	goat	mouse	1:200	Life Techologies
AlexaFluor 488	donkey	rabbit	1:200	Life Techologies
AlexaFluor 568	goat	mouse	1:200	Life Techologies
AlexaFluor 568	donkey	rabbit	1:200	Life Techologies
AlexaFluor 657	goat	mouse	1:200	Life Techologies
Biotinylated	goat	rabbit	1:200	Dako
Biotinylated	rabbit	mouse	1:200	Dako
HRP-conjugate	goat	rabbit	1:2000	abcam
HRP-conjugate	goat	mouse	1:2000	abcam
Trueblot	-	rabbit	1:2000	eBioscience
Trueblot	-	mouse	1:2000	eBioscience

Table 2.3. The secondary antibodies used, their species and dilution for experiments in this thesis.

Chapter Three: New proteins in the pathology of FTLD-FUS and other neurodegenerative diseases (Results I)

3.1 Introduction

The neuropathological hallmark of FTLD-FUS and familial ALS-FUS is extensive FUS pathology. The discovery of FUS inclusions in both ALS and FTLD has further confirmed the spectrum disorder hypothesis that argues these disease entities represent cortical and motor ends of a disease continuum (Neumann et al., 2009a). This is further supported by reports of up to 50% of ALS patients show some degree of cognitive impairment and a substantial number of FTLD patients develop motor neuron disease (Talbot and Ansorge, 2006). The FUS protein is a DNA and RNA binding protein that continuously shuttles back and forth between the cytoplasm and the nucleus where it is at a much higher concentration in healthy cells (Zinszner et al., 1997). However, in FTLD and ALS FUS inclusions form predominately in the cytoplasm implying that defects in nuclear shuttling may lead to cytoplasmic miss-localisation and subsequent aggregation. This may sequester the protein away from its normal nuclear localisation and therefore represent a loss of nuclear function, or cause a toxic gain of function due to excessively high concentrations in the cytosol. The mutations that cause familial ALS-FUS cluster in the C-terminus of the protein, within the NLS (Belzil et al., 2009, Chio et al., 2009, Kwiatkowski et al., 2009b, Ticozzi et al., 2009, Vance et al., 2009a, Corrado et al., 2010). It has been shown that the NLS of FUS is necessary and sufficient to import FUS into the nucleus, and that ALS associated mutations in the NLS disrupt this import (Dormann et

al., 2010). Crucially, it has also been shown that it is the interaction with TRN1 that is retarded when the NLS of FUS is mutated. Given what is known about the close relationship between ALS-FUS and FTLD-FUS and the emerging importance of TRN1 in the miss-localisation of FUS in familial ALS-FUS, it is possible TRN1 may have a role to play in FTLD-FUS.

3.2 Hypothesis

TRN1 plays an important role in the pathogenesis of FTLD-FUS and aggregates alongside FUS in the inclusions of this, but not other, neurodegenerative diseases.

3.3 Cases

Brains were donated to the Queen Square Brain Bank for Neurological Disorders, UCL Institute of Neurology, University College London; the MRC London Brain Bank for Neurodegenerative Diseases, Institute of Psychiatry, King's College, London, UK ; Neuropathology Department, Århus Kommunehospital, Århus, Denmark and NeuroResource, UCL Institute of Neurology, University College London. All patients had details of a standard clinical history and had undergone both neurological examination and cognitive assessment. All cases had previously been diagnosed as NIFID (6 cases) or aFTLD-U (7 cases).

3.4 Clinical summary

Our NIFID group consisted of six women and one man whilst the aFTLD-U group consisted of three women and four men. The mean age of onset was similar in both groups; mean 45.6 (standard deviation 15.3) years old in the NIFID group and 47.0 (standard deviation 5.1) years old in the aFTLD-U group. However, the variability of age of onset was greater in the NIFID group with a range of 28 to 69 years, with a much smaller range of 40 to 55 years in the aFTLD-U group. There was a notable difference between the disease duration from symptom onset to death between the groups with a shorter relatively rapid disease course in the NIFID group; mean 3.0 (standard deviation 1.1) years compared to a longer disease duration in aFTLD of 7.3 (standard deviation 2.9) years. The most common clinical diagnosis was the behavioural variant of frontotemporal dementia and all of the aFTLD-U patients had initial behavioural features with a combination of dis-inhibition, apathy, obsessive/compulsive behaviour and change in appetite, which usually took the form of sugar craving. Patients later developed cognitive impairment, most prominently executive dysfunction, but often episodic memory impairment as well. Post mortem (PM) delay is recorded in table 3.1 because it is a significant factor in the preservation of antigens and therefore histological characteristics. Those cases with longer PM delay have weaker normal nuclear

TRN1/FUS/EWS/TAF15 immuno-reactivity, but retained pathological staining (inclusions). The short disease duration and younger onset reported here is typical of the FTLD-FUS subtype.

Case No.	Clinical Diagnosis	Previous pathological diagnosis	Sex	Age of onset (years)	Age at Death (years)	PM delay (hrs)	Disease duration (years)
1	bvFTD	NIFID	F	27	n/a	n/a	n/a
2	CBS	NIFID	F	41	43	55	2
3	bvFTD with CBS like syndrome	NIFID	F	43	46	30	3
4	MND with PSP like syndrome	NIFID	M	44	46	96	2
5	MND	NIFID	F	63	68	2	5
6	MND	NIFID	F	69	72	90	3
7	CBS	NIFID	M	32	35	n/a	3
8	bvFTD	aFTLD-U	M	40	51	12	11
9	bvFTD	aFTLD-U	F	43	53	96	10
10*	bvFTD	aFTLD-U	M	44	51	24	7
11	bvFTD	aFTLD-U	M	47	52	72	5
12	PSP	aFTLD-U	F	49	55	3.5	6
13	bvFTD	aFTLD-U	M	51	60	48	9
14*	bvFTD	aFTLD-U	F	55	58	n/a	3

Table 3.1. Clinical and case summaries of FTLD-FUS cases available for this study. Where information is not available this is indicated with n/a. Cases 10 and 14 are marked with a * to indicate 14 is the mother of 10.

3.5 The immunohistochemical profile of TRN1 in healthy controls and other neurodegenerative diseases

The cellular localization of TRN1, examined in normal control cases using formalin fixed tissue and TRN1 immunohistochemistry showed that immunoreactivity was localized to the nuclei of both neurons and glial cells (Figure 3.1 M). A similar staining pattern was seen in unaffected neurons in the FTLD-FUS cases and cases with other

neurodegenerative diseases such as Alzheimer's disease, Parkinson's disease, FTLD-TDP types A B and C, Pick's disease (FTLD-tau), multiple system atrophy (MSA), corticobasal degeneration (CBD), motor neuron disease (NMD), progressive supranuclear palsy (PSP), Huntington's disease (HD), and spinocerebellar ataxia (SCA).

3.6 Cerebral cortex pathology and TRN1 immunohistochemistry in FLTD-FUS

In contrast to healthy controls and the other neurodegenerative diseases listed above, FTLD-FUS cases presented with abundant TRN1 inclusion pathology, which also demonstrated subtle differences between the NIFID and aFTLD-U subgroups. All the cases listed in table 3.1 showed some degree of superficial spongiosis affecting the frontal and temporal cortices, with subpial and white matter gliosis also evident. The characteristic crescent shaped neuronal cytoplasmic inclusions were TRN1 positive in all cases, but were notably more numerous in the NIFID subtype than in the aFTLD-U group (Figure 3.1). However, this difference may be the result of severe cell loss found in the cortex in the aFTLD-U subgroup. The superficial cortical layers were more severely affected by inclusion load than the deeper cortical layers in both NIFID and aFTLD-U.

The NIFID subgroup presented with a variety of TRN1 positive neuronal cytoplasmic inclusion morphologies including; Pick body-like homogenously stained inclusions and flame shaped tangle-like inclusions, which could be seen extending into the apical dendrites of pyramidal neurons (Figure 3.1 A, B and D). Additionally, smaller bean-like, crescent and annular-shaped TRN1 positive cytoplasmic inclusions were present in the aFTLD-U subgroup. Rarer vermiform neuronal intranuclear inclusions were found in the cortex of NIFID cases (Figure 3.1 C and E), but not in aFTLD-U cases. TRN1 positive neurites were found in the white matter of the aFTLD-U subgroup, but not the NIFID subgroup (Figure 3.1 L).

3.7 Hippocampal pathology and TRN1 immunohistochemistry in FTLD-FUS

The severity of pathology and strength of staining varied notably between subtypes and even between cases of the same subtype. Whilst both intranuclear and cytoplasmic inclusions were evident in all cases within this structure, neuronal loss affecting the CA1 subregion and subiculum was obvious in NIFID cases 2 and 3, but unremarkable in the remaining NIFID cases. Perhaps related to this, TRN1-positive bean-shaped or Pick body-like neuronal cytoplasmic inclusions and neuronal intranuclear inclusions were present in the granule cell layer of the dentate fascia and neurons of the subiculum in both NIFID cases 2 and 3. TRN1 immunoreactive intranuclear inclusions were also frequent in the granule cell layer of these cases, and remarkably some neurons contained both a neuronal cytoplasmic inclusion and a neuronal intranuclear inclusion (Figure 3.3 D). Compounding the unique nature of these two cases, TRN1-positive oligodendroglial coiled bodies were also seen in the white matter of cases 2 and 3.

The rest of the NIFID cases possessed an occasional crescent shaped TRN1 positive neuronal cytoplasmic inclusion in the granule cell layer of the dentate fascia. In contrast to NIFID cases 2 and 3, no neuronal intranuclear inclusions were observed in the granule cell layer in these cases.

All aFTLD-U cases showed some degree of hippocampal sclerosis (Figure 3.2). Intense cell loss was seen in the CA1 hippocampal subregion extending into the subiculim in aFTLD-U cases 10, 13 and 14. TRN1 immunoreactive neuronal intranuclear inclusions were numerous in the granule cell layer of the dentate fascia. Unusually, these intranuclear inclusions outnumbered the bean-shaped neuronal cytoplasmic inclusions found in the same anatomical region in cases; 9 10 and 11. However this was not the trend overall, the remaining cases only contained an occasional neuronal cytoplasmic inclusion in this structure.

The CA1 subregion was affected by neuronal loss to different degrees in all cases. A proportion of the remaining neurons contained a cytoplasmic inclusion, an intranuclear inclusion or both.

Abnormal neurites were also present in the entorhinal cortex and fusiform gyrus of all aFTLD-U cases.

3.8 Pathology of TRN1 in the motor cells of FTLD-FUS

Motor cells of the XIIth nerve nucleus and spinal cord contained either granular, globular or filamentous Skein-like inclusions as previously seen with FUS immunohistochemistry. No difference was observed the in the inclusion types between the NIFID and aFTLD-U subgroups (Figure 3.4).

3.9 Co-localisation of TRN1 and FUS pathology through double-label immunofluorescence

All cases of FTLD-FUS the cortex, medulla and hippocampal formation were double stained for TRN1 and FUS. Qualitative assessment clearly showed overall very good co-localisation of TRN1 and FUS within the neuronal cytoplasmic and neuronal intranuclear inclusions in both NIFID and aFTLD-U (Figure 3.5). Furthermore, quantitative analysis of three NIFID and aFTLD-U cases also demonstrated that the vast majority of FUS positive inclusions in the granule cell layer of the dentate fascia were also positive for TRN1 (99.4% NIFID 100% aFTLD-U). Interestingly, it was noted that TRN1 labelling of some neuronal intranuclear inclusions was weaker than that seen with FUS antibodies. Additionally, while some nuclear FUS remained in cells baring cytoplasmic inclusions, TRN1 staining was often absent entirely.

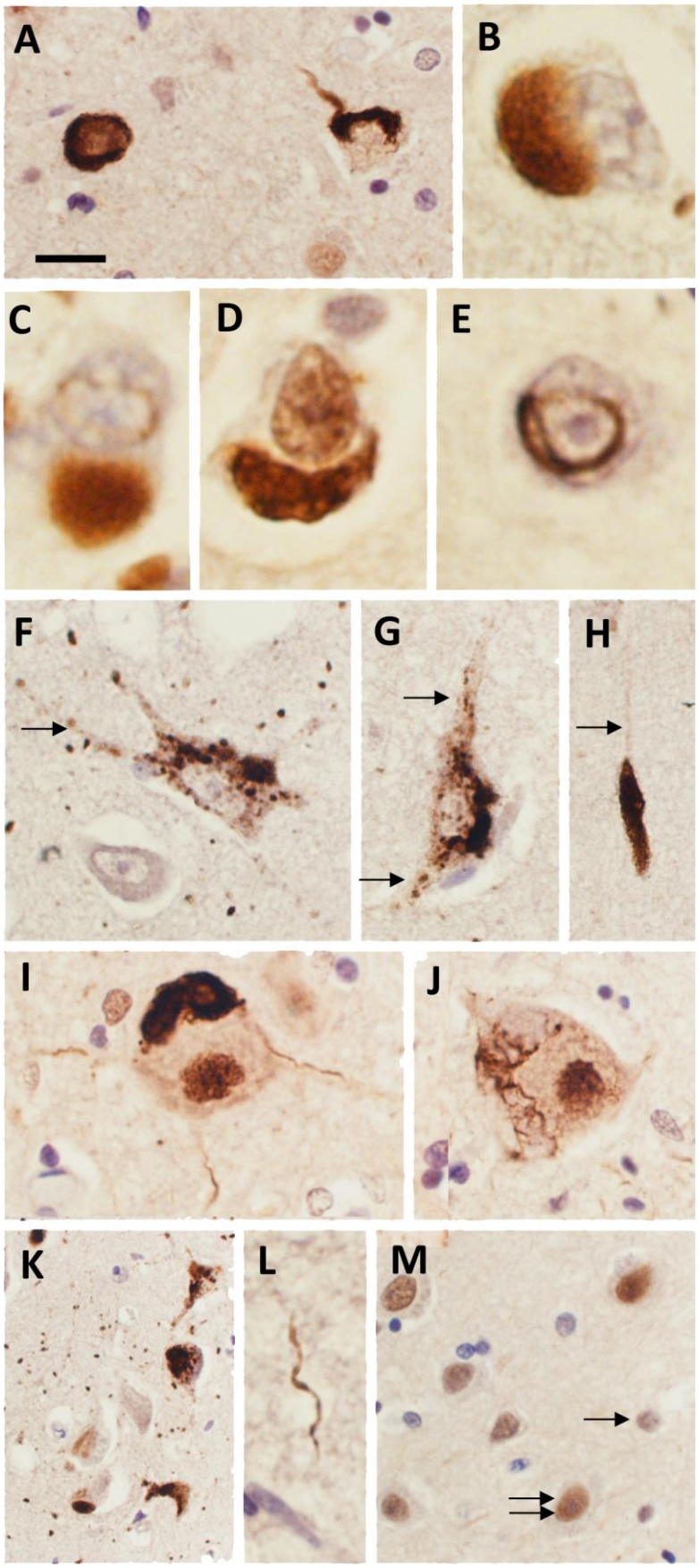

Figure 3.1. TRN1 inclusion morphology in NIFID and FTLD-U. Representative neurons containing classical crescent shaped neuronal cytoplasmic inclusions a NIFID and aFTLD-U (A and D). Pick body-like inclusions were found in the NIFID cases (B) whereas smaller rounded 'bean' shaped inclusions were found in aFTLD-U (C). Neuronal intranuclear veriform inclusions (C and E) were also seen in both NIFID and aFTLD-U respectively. Granular cytoplasmic inclusions were prominent in NIFID case2 (F and G), extending into the dendrites (arrows). Swollen axons were visible with positivity extending into the axon (H arrow). In NIFID case6 Betz cells showed globular and skein-like inclusions (I and J). Argyrophilic grain-like structures were observed in the entorhinal cortex in NIFID case2 (K). Neuritic threads were seen in aFTLD-U case 8 (L). Normal neuronal nuclear (double arrow) and glial nuclear staining (arrow) in frontal cortex of normal controls. Scale bar on A represents 5μm on A-E and L; 10 μm on F-J and 40 μm on K and M.

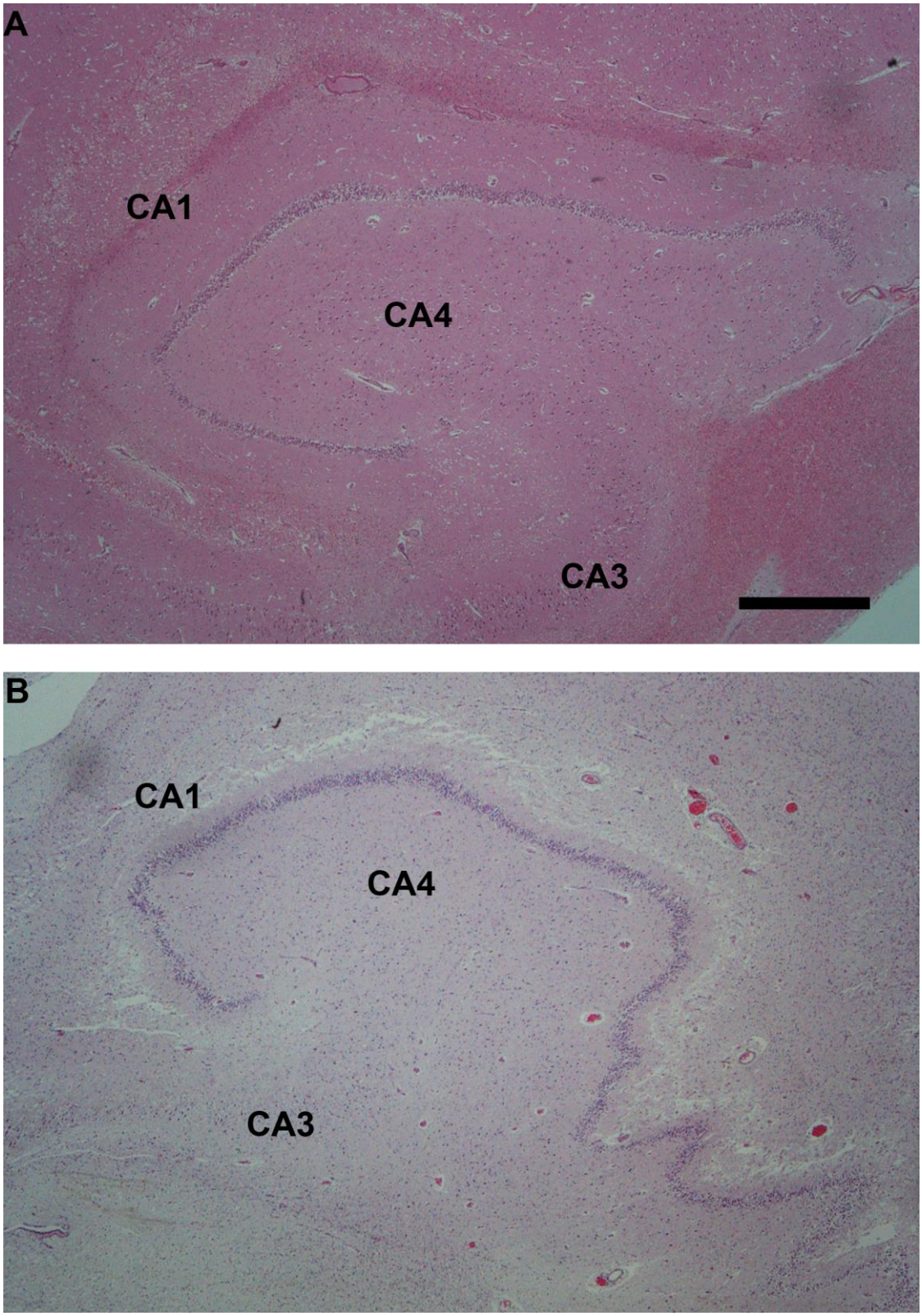

Figure 3.2. Hippocampal sclerosis in FTLD-FUS. Healthy control hippocampal formation shows clearly defined structures and regions CA4, CA3, and CA1 (A). Typical FTLD-FUS hippocampal formation showing cell loss, particularly pronounced in the CA1 region (B). Scale bar in A represents 0.5mm.

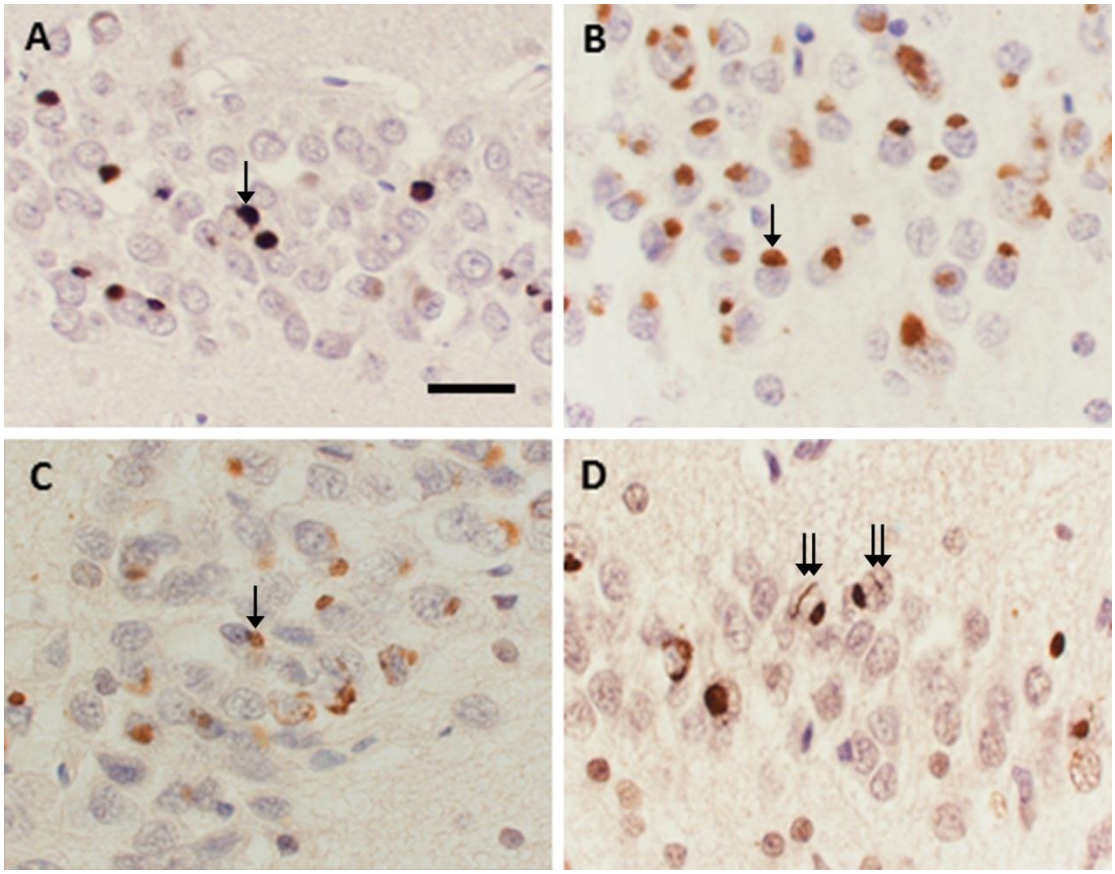

Figure 3.3. TRN1 pathology in the hippocampal granule cell layer. NIFID (A and B) and aFTLD-U (C and D). TRN1 staining in the hippocampal granule cell layer shows both neuronal cytoplasmic inclusions (arrow) and neuronal intranuclear inclusions (double arrow). Scale bar in A represents 50 μm.

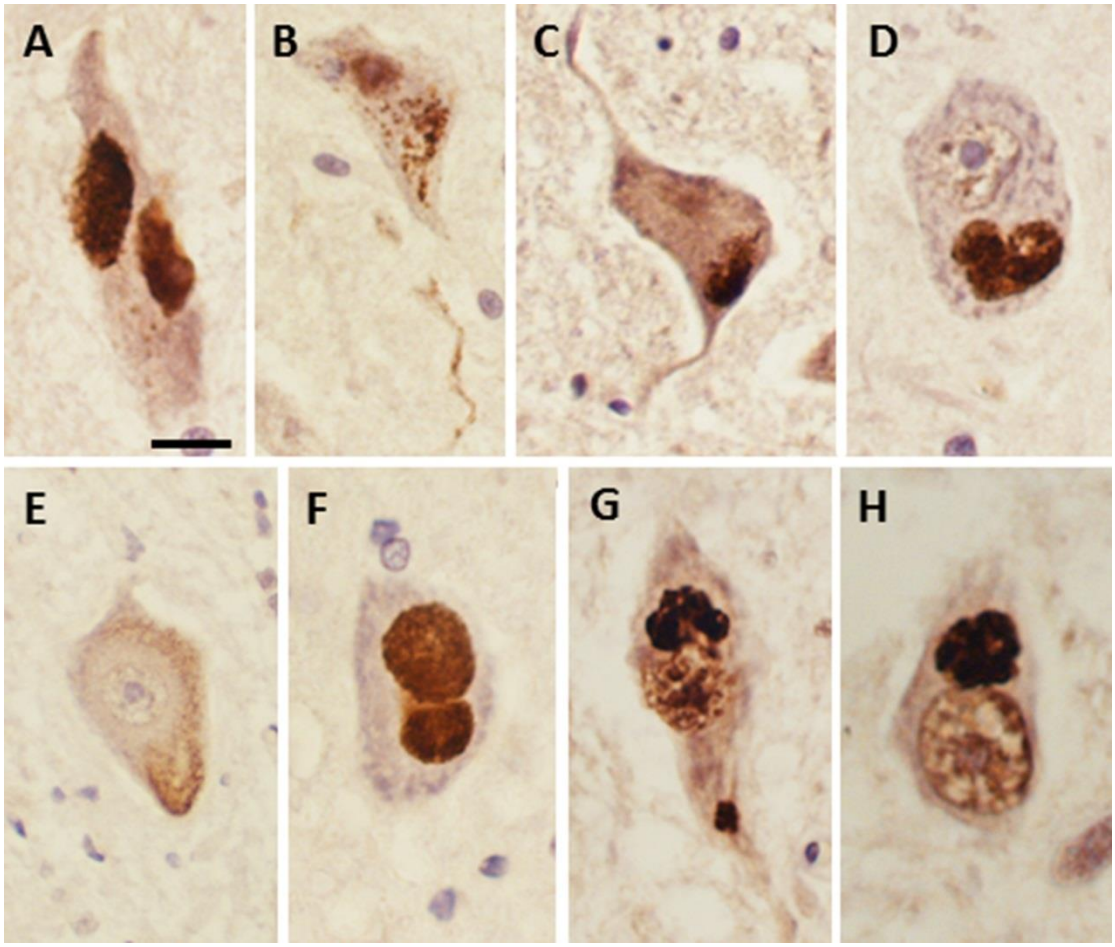

Figure 3.4. TRN1 pathology in the spinal cord and XIIth cranial nerve nucleus in NIFID (A-D) and aFTLD-U (E-H). TRN1 pathology in motor neurons of the XIIth cranial nerve nucleus (A,B,E and F) and spinal cord (C,D,G and H) demonstrated a number of cytoplasmic inclusion types including large globular (A, D and G, F), diffuse granular (B), compacted granular (C and F), filamentous (E). TRN1 clearance from the nucleus is evident in most cases in both NIFID (D) and aFTLD-U (H). Bar in A represents 5µm.

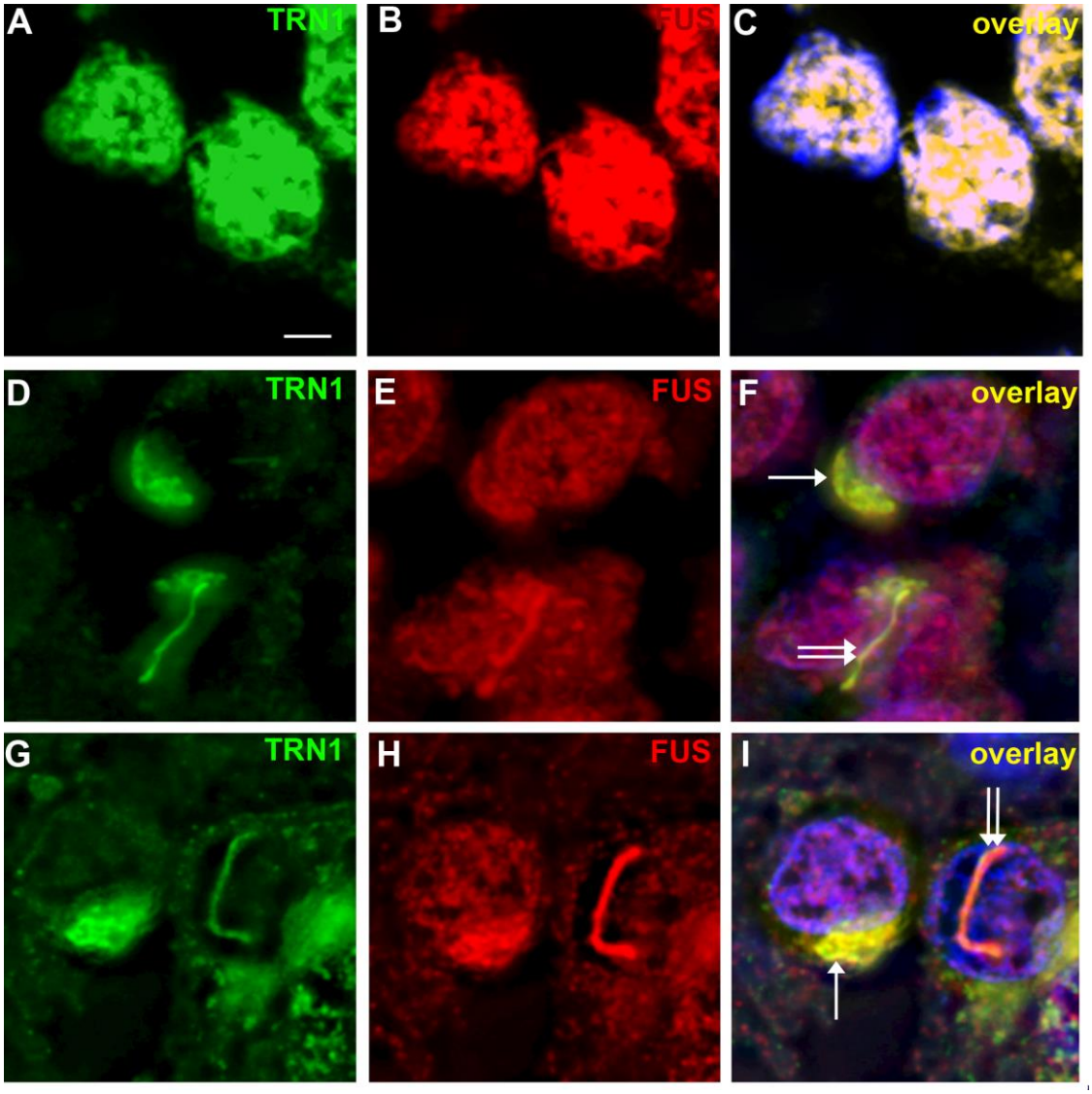

Figure 3.5. Both neuronal cytoplasmic and neuronal intranuclear inclusions are positive for FUS and TRN1. Granule cell layer neurons from representative healthy control (A-C) aFTLD(D-F) and NIFID -U (G-I). Both NIFID and aFTLD-U harbour neuronal cytoplasmic (arrow) and intranuclear (double arrow) inclusions positive for TRN1 and FUS, the intranuclear inclusions of aFTLD-U stain weaker with TRN1 than FUS. Overlay panels include blue nuclear DAPI staining Scale bar on A 5μm.

3.10 Sequential solubility extraction and immunoblot of TRN1 in FTLD-FUS and healthy controls

To investigate the solubility of TRN1 in FTLD-FUS compared to healthy control brain tissue, a sequential solubility extraction was undertaken. Three NIFID and four aFTLD-U cases were processed alongside three healthy controls. Frontal cortex grey matter from flash frozen brains was homogenized and clarified in a high salt buffer. The whole homogenate was first clarified by centrifugation (at 1000g) to pellet out myelin and membranous debris. Ultracentrifugation resolved the clarified supernatant into a solubility fraction of proteins soluble in high salt buffer and a pellet of insoluble species. This pellet was then resuspended in a stronger RIPA based buffer containing 2% SDS and the supernatant retained as the soluble high salt fraction. This was repeated and another pellet of insoluble protein species was resolved. The supernatant was retained as the RIPA soluble fraction and the pellet was dissolved in a urea based buffer containing 8% SDS. This final fraction was termed the urea fraction and contained only the highly insoluble protein species. Size separation of proteins by SDS-polyacrylamide gel electrophoresis and immunoblotting on polyvinylidene fluoride membrane revealed firstly that the antibody used to detect TRN1 pathology immunohistochemically recognised a band at the predicted molecular weight of TRN1. Secondly, TRN1 was present in only the high salt and RIPA fractions in healthy controls, but in NIFID and aFTLD-U TRN1 is present in the urea fraction as well (Figure 3.6). This indicates TRN1 has become highly insoluble in both subtypes of FTLD-FUS, and therefore likely highly aggregated. Interestingly, no abnormally high molecular weight species were observed suggesting TRN1 is not poly-ubiquitinated.

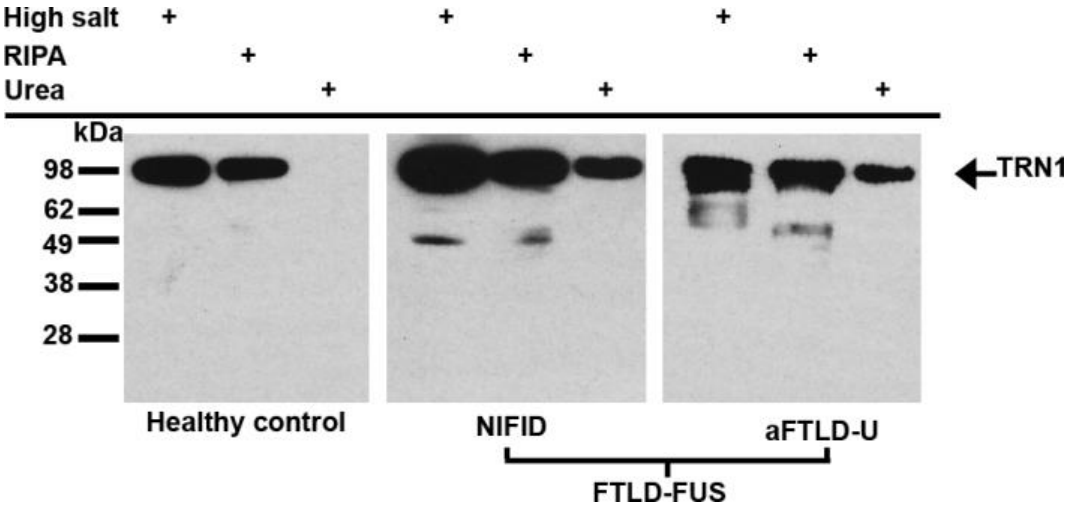

Figure 3.6. Sequential solubility extraction and immunoblotting of three representative cases. Highly insoluble TRN1 is present in the urea fraction of both FTLD-FUS subtypes but absent from healthy controls. Molecular weight of TRN1 102kDa.

3.11 Other importins in FTLD and neurodegenerative diseases

To investigate the possibility that other importins or nuclear import factors may be aggregating in FTLD-FUS frontal cortex tissue was immunohistochemically screened against several proteins related to TRN1. Karyopherin β2b (also known as Transportin2 (TRN2)), karopherin β3 (also known as importin β3), importin β1, and nucleophorin 98kDa (NUP98) were chosen to be screen against FTLD-FUS and healthy control tissue. Immunohistochemical analysis demonstrates that TRN2, karyopherin β3 and NUP98 are present in the nucleus of neurons, whilst importin β1 stains only the nuclear membrane (Figure 3.7 A C E and G). This pattern is repeated in FTLD-FUS with the one exception of NUP98 (Figure 3.7 H), which appears to label occasional cytoplasmic inclusions. NUP98 pathology was visible in NIFID cases but even then labelling appeared to be confined to cytoplasmic inclusions because no additional pathology such as threads, intranuclear inclusions or dot/grain pathology was visible.

3.12 Co-localisation of FUS and NUP98 pathology through immunofluorescence

To confirm that the apparent staining of a cytoplasmic inclusion by NUP98 the frontal cortex of three representative NIFID and three aFTLD-U cases were double stained for FUS and NUP98. Examples of co-localisation were seen in cytoplasmic inclusions between FUS and NUP98 in NIFID cases but not in the aFTLD-U investigated (Figure 3.8). Unfortunately hippocampal tissue was unavailable for this investigation and it was therefore not possible to investigate intranuclear inclusions since these are most abundant in the granule cell layer.

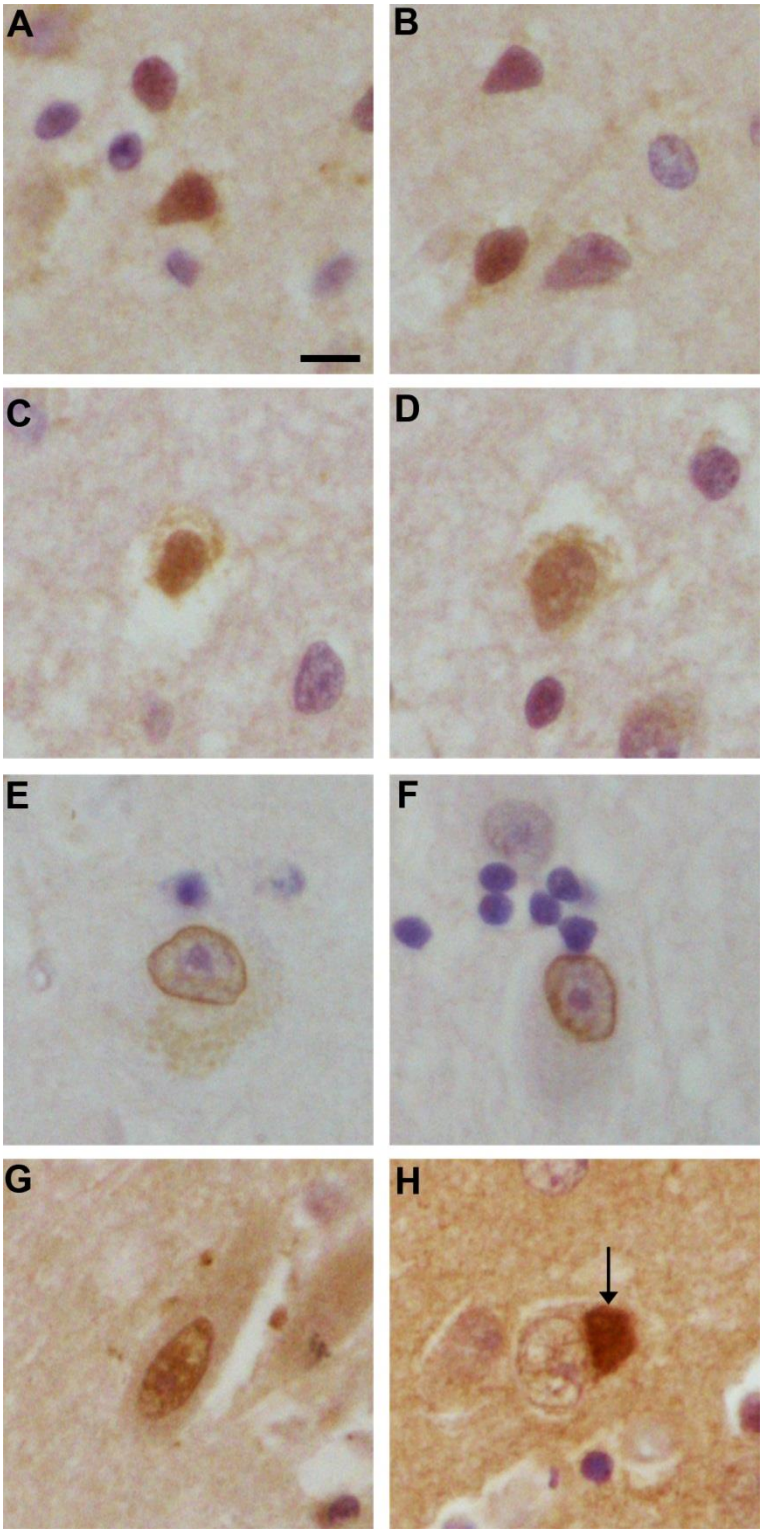

Figure 3.7. Immunohistochemical screen of importins and nuclear pore factors reveals NUP98 as staining cytoplasmic inclusions. Healthy control frontal cortex (A, C, E and G) and FTLD-FUS frontal cortex (B, D, F and H) stained for TRN2 (A and B), karyopherin β3 (C and D), Importin β1 (E and F), and NUP98 (G and H). Normal staining is seen in all except H where the NUP98 antibody stained occasional cytoplasmic inclusions (arrow). Scale bar on A represents 25μm.

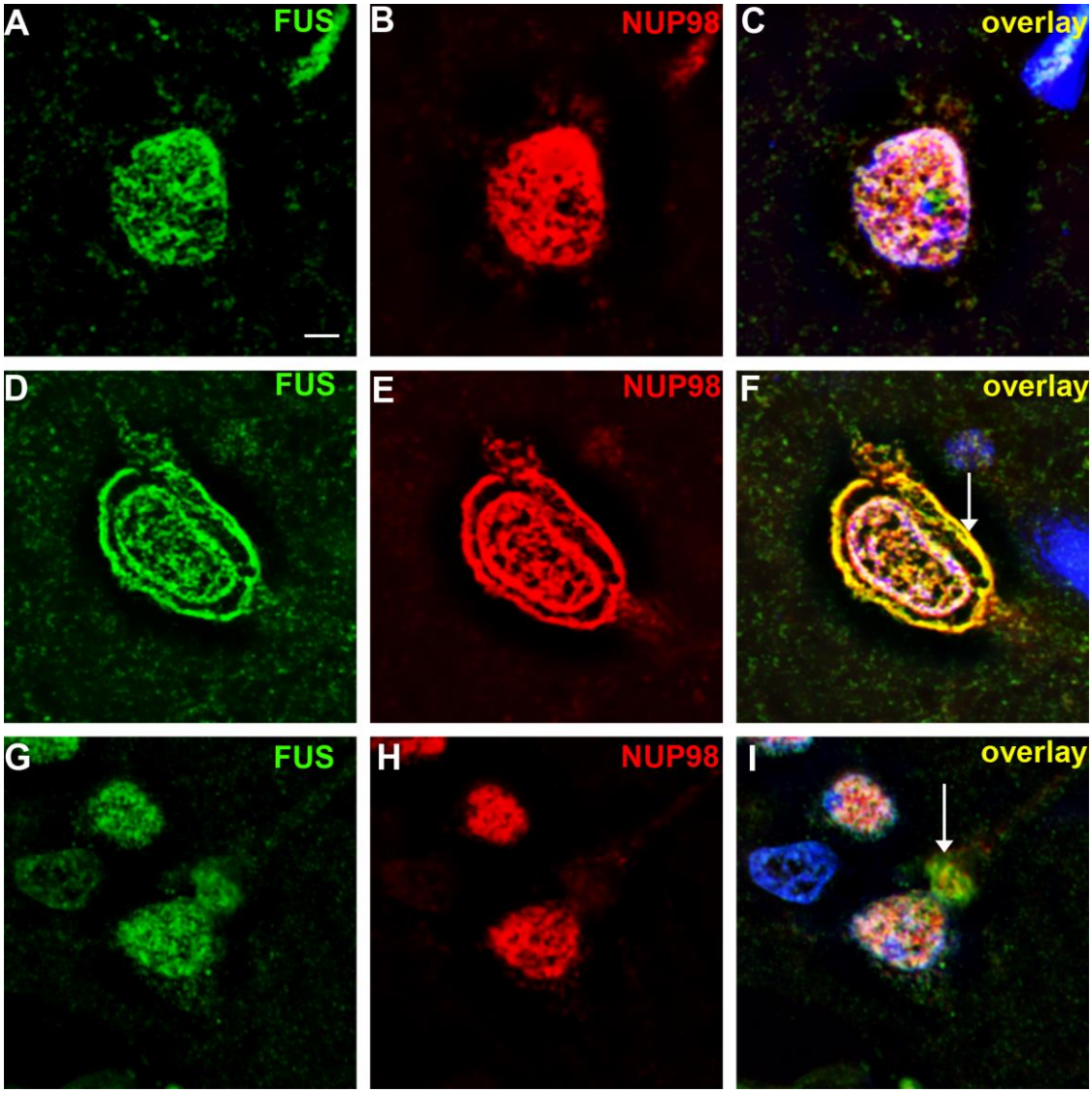

Figure 3.8. Cortical cytoplasmic inclusions of NIFID but not aFTLD-U are positive for both FUS and NUP98. Healthy control neurons from the frontal cortex (A-C). A typical crescent shaped inclusion from a NIFID case (D-F arrow), and a typical bean-like inclusion from an aFTLD-U case (G-I arrow). Overlay panels include blue nuclear DAPI staining Scale bar on A represents 5µm.

3.13 TRN1 immunohistochemistry in other neurodegenerative diseases

Given that the expanded polyglutamine inclusions of Huntington's disease, and spinocerebellar ataxia demonstrate FUS immunoreactivity (Doi et al., 2010)(Figure 3.9 B, D and F), and the FUS-opathy FTLD-FUS demonstrates TRN1 pathology, this might implicate TRN1 in the polyglutamine expansion disorders. Therefore the immunoreactivity of TRN1 was investigated in the polyglutamine expansion disorders to determine if TRN1 inclusion body pathology was unique to FTLD-FUS. The pons, basal ganglia, cerebellum, medulla, and hippocampus were investigated in two Huntington's disease, six spinocerebellar ataxias (two of type 3, and one of types 1, 2, 6 & 7) with immunohistochemistry which revealed no TRN1 reactivity in the characteristic intranuclear inclusions (Figure 3.9 C and E). However, the extremely rare entity neuronal intranuclear inclusion body disease (NIIBD) (one case available) has characteristic hyaline intranuclear inclusions which are visible in both TRN1 and FUS immunohistochemistry (Figure 3.9 A double arrow). Whilst this disease does not possess an expanded polyglutamine tract, the characteristic hyaline intranuclear inclusions are sometimes visible with antibodies raised against polyglutamine (Liu et al., 2008).

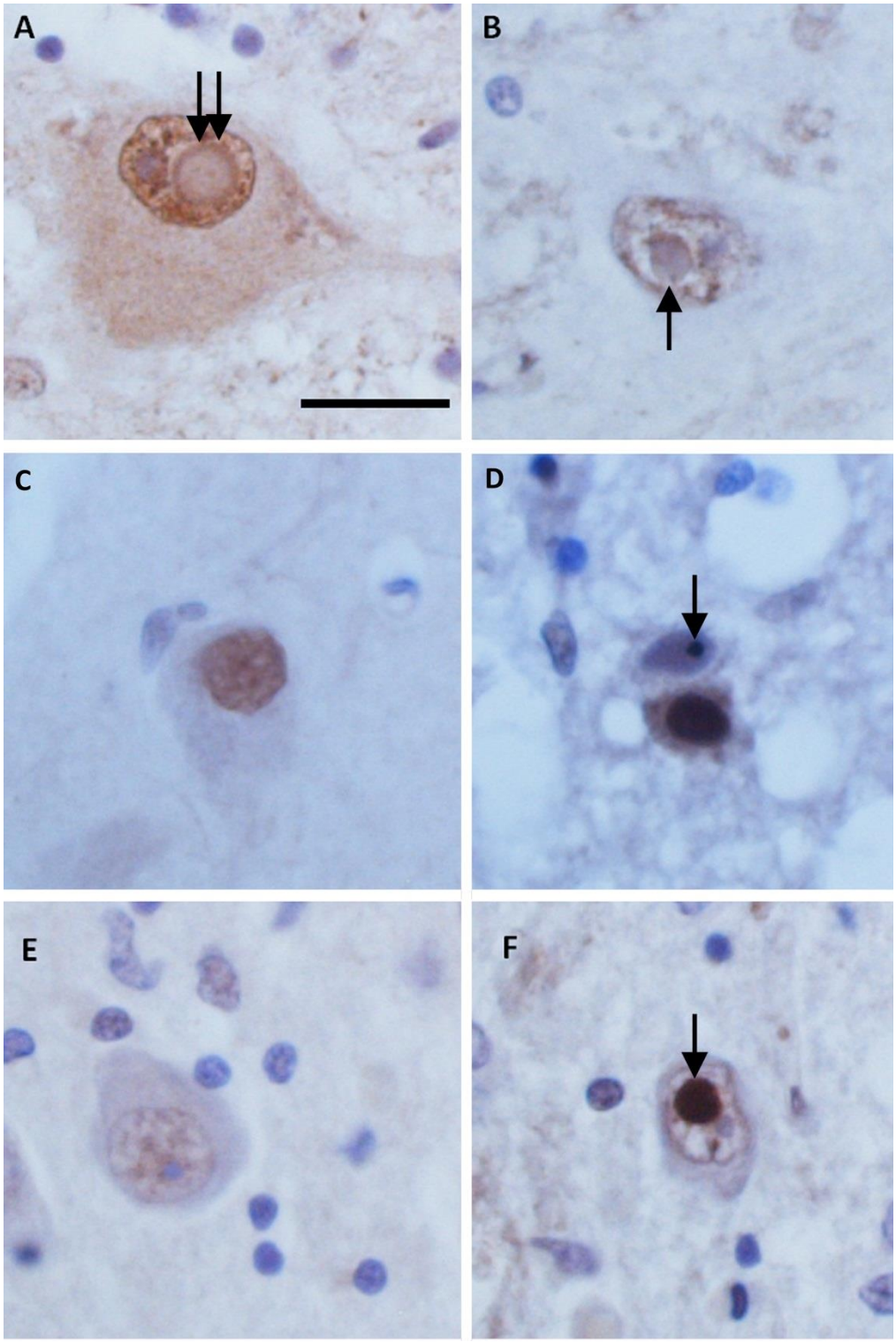

Figure 3.9. The intranuclear inclusions of Huntington's disease, spinocerebellar ataxia, and neuronal intranuclear inclusion body disease are immunoreactive for FUS but only neuronal intranuclear inclusion body disease is positive for TRN1 pathology. The hyaline inclusions of neuronal intranuclear inclusion body disease are visible with FUS (B arrow) and TRN1 (A double arrow) immunohistochemistry. Huntinton's disease (C and D) and spinocerebellar ataxia (E and F) are only positive for FUS (arrows). Sections taken from Pons. Scale bar on A represents 25μm.

3.14 Other TRN1 cargos aggregating alongside the FET proteins

The aggregation of TRN1 in cytoplasmic and intranuclear inclusions and a partial or complete loss of normal nuclear TRN1 staining (Figure 3.5) may lead to sequestration of TRN1 targets beyond the FET proteins. Additionally, the TRN1 cargos EWS and TAF15 have been shown to be aggregating alongside TRN1 and FUS in collections of FTLD-FUS from other brain banks (Neumann et al., 2011). Therefore a similar investigation was mounted on the QSBB collection.

Firstly, the presence of EWS and TAF15 within the inclusions of the QSBB collection of FTLD-FUS was confirmed with immunohistochemistry (Figure 3.10). All cases were stained using previously published and characterized antibodies and compared to healthy controls. A variety of morphologically different inclusions could be seen and these mirrored those observed under FUS and TRN1 immunohistochemistry (Figure 3.1 and Figure3.10). It is of note that the EWS antibody was not as robust as those raised against FUS, TAF15 or TRN1 but a significant amount of pathology was still visible (Figure 3.10 H-M). Both EWS and TAF15 were found in the nucleus of neurons and some glial cells in healthy control tissue (Figure 3.10 O and P). The anatomical locations of EWS and TAF15 pathology mirrored those previously described for FUS and TRN1 and included; frontal cortex, hippocampal formation, and the motor cells of the medulla and spinal cord. Co-localisation of TRN1 and FET protein pathology has been confirmed via double immunofluorescence by other authors (Neumann et al., 2012).

Given the pronounced loss of TRN1 from the nucleus of cells displaying cytoplasmic or intranuclear inclusions (Figure 3.5) the apparent loss of nuclear function this would presumably imbue should disrupt the transport of dozens of cargo proteins. To investigate whether the pathology of FTLD-FUS extends beyond TRN1 and the FET proteins, several targets of TRN1 were screened against FTLD-FUS frontal cortex tissue. A full list of TRN1 cargos investigated by this thesis and other authors is attached in

appendix 1.2. Four targets of TRN1 driven import were investigated in this thesis; heterogeneous nuclear ribonucleoprotein A1 (hnRNP A1), dead box 3 (DDX3), nuclear RNA export factor 1 (NXF1), and Y box-binding protein 1 (YB1). Characterization in healthy control tissue revealed hnRNP A1 (Figure 3.11 G), DDX3 (Figure 3.11 A) and NXF1 (Figure 3.11 C) to be predominantly nuclear in the neurons of frontal cortex tissue. Only YB1 showed marked presence in the cytoplasm as well as the nucleus (Figure 3.11 E). Only hnRNP A1 appeared to label some of the morphologically characteristic inclusions of FTLD-FUS. Crescent shaped neuronal cytoplasmic inclusions were visible in NIFID case 6 and case 3 scattered throughout the superficial layer of the frontal cortex. Larger Pick-body like inclusions were also relatively common in NIFID cases. The aFTLD-U subtype had considerably less hnRNP A1 pathology but those inclusions that were visible were typically bean shaped (Figure 3.11 K). It is of note that no intranuclear inclusions were visible under hnRNP A1 immunohistochemistry even in those areas previously shown to harbour considerable intranuclear pathology such as the granule cell layer of the hippocampus. Double label immunofluorescence showed strong co-localisation between cortical FUS and hnRNP A1 pathology in both NIFID and aFTLD-U (Figure 3.12). This would seem to suggest that hnRNP A1 is incorporated into a subset of inclusions in FTLD-FUS much like NUP98.

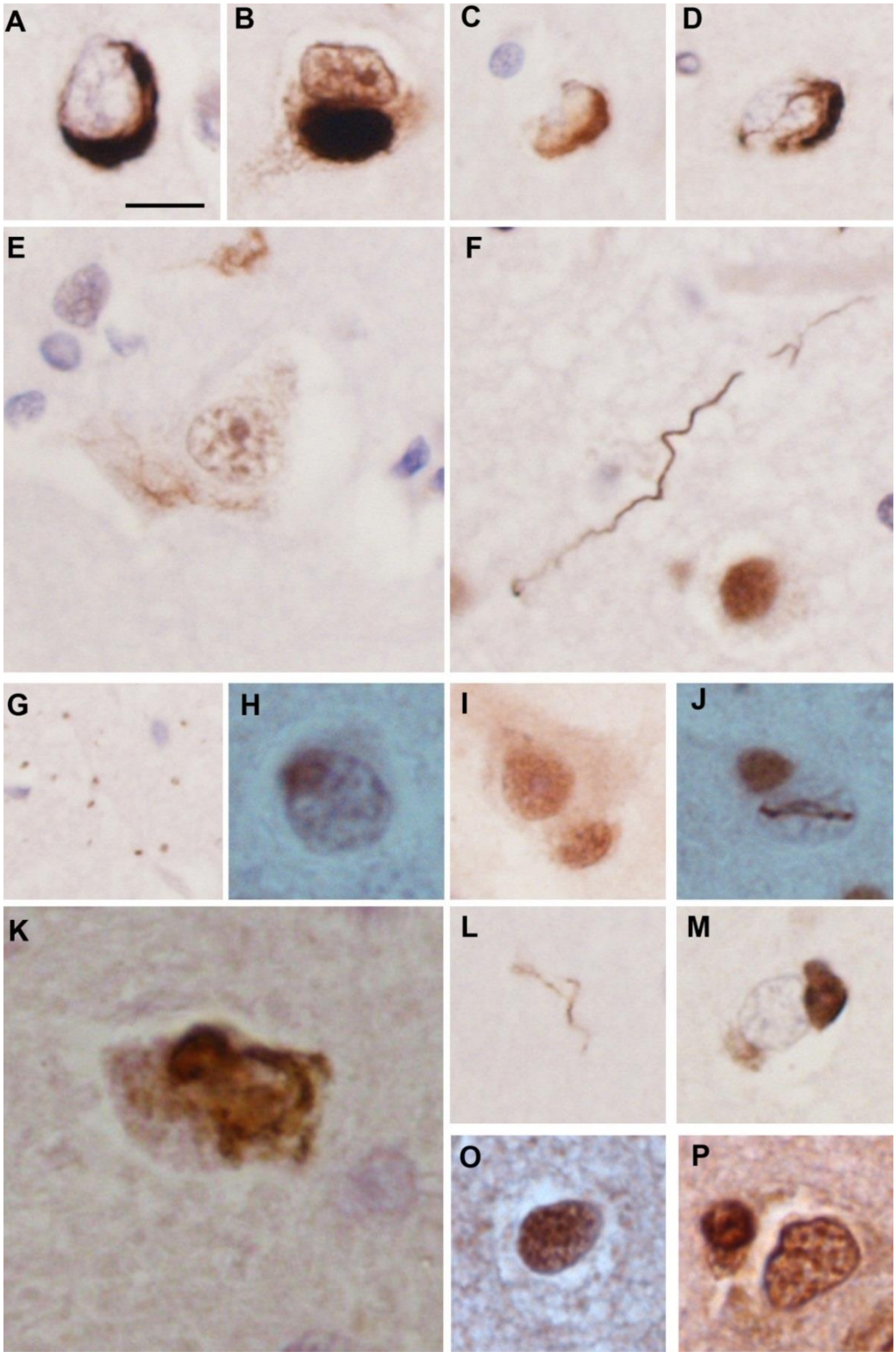

Figure 3.10. TAF15 and EWS immunohistochemistry shows a variety of inclusion morphology in FTLD-FUS. TAF15 labelled cytoplasmic crescent (A), Pick body-like (B), granular (C), Skein-like (E), neuritic threads (F), intranuclear lentiform (D), and dot/grain pathology in the neuropil (G) in NIFID and aFTLD-U. EWS labeled the same pathology but often less strongly, such as bean-like (H), granular (I), Skein-like (K), threads (L), and intranuclear inclusions (J). Normal nuclear TAF15 (O) and EWS (P) in healthy controls. Scale bar on A represents 25μm.

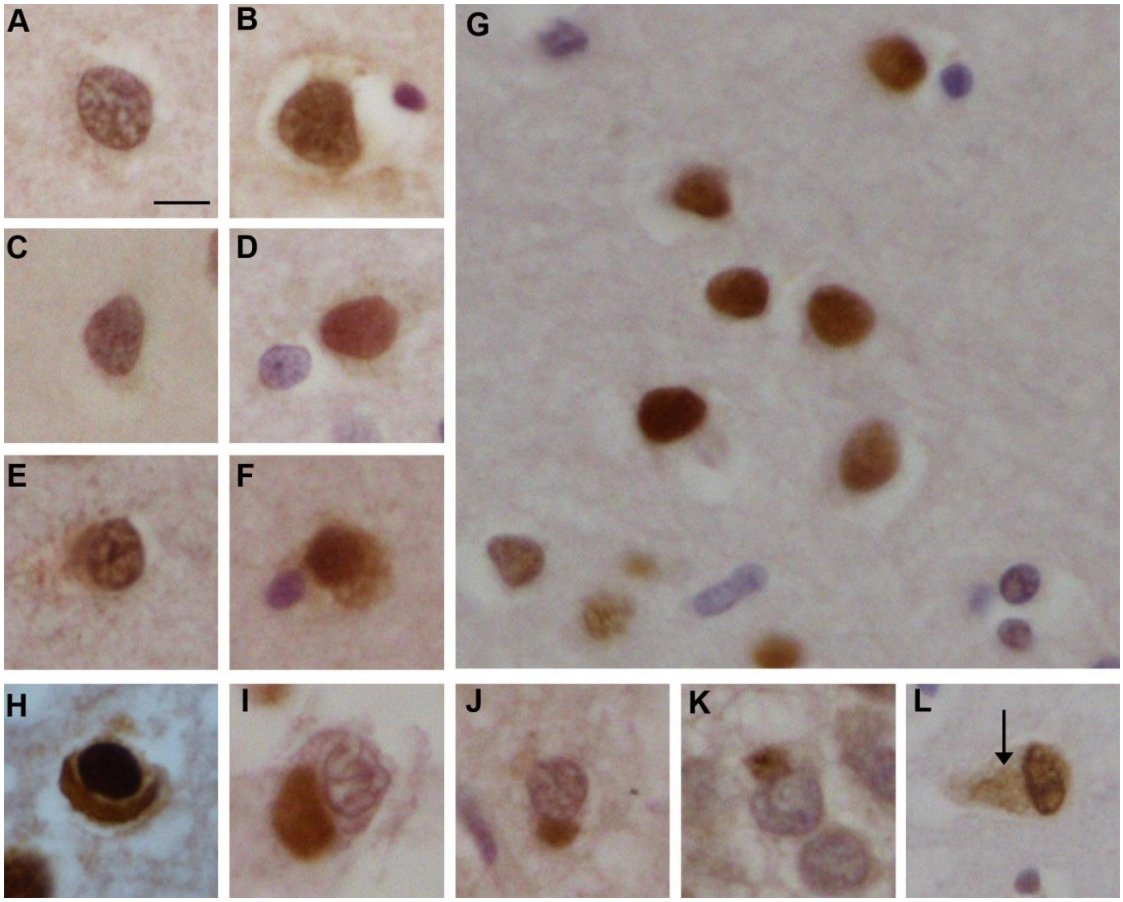

Figure 3.11. Only hnRNP A1 immunohistochemistry shows labelling of some inclusion types. The TRN1 cargos DDX3 and NXF1 are localised to the nucleus in healthy control (A and C) and FTLD-FUS (B and D) frontal cortical neurons. YB1 is predominately nuclear with some cytoplasmic staining in healthy control (E) and FTLD-FUS (F). Similarly hnRNP A1 is strongly nuclear in healthy control neurons (G), but a proportion of FTLD-FUS inclusions are also labelled. Compact crescent shaped (H), large Pick body-like (I), small bean shaped (J and K), and possible flame shaped neuronal cytoplasmic inclusions (L arrow) are visible with hnRNP A1 immunohistochemistry. Nuclear clearing of hnRNP A1 is visible in NIFID (I and J) and aFTLD-U (K), but not in all cases (H). Scale bar in A represents 25μm.

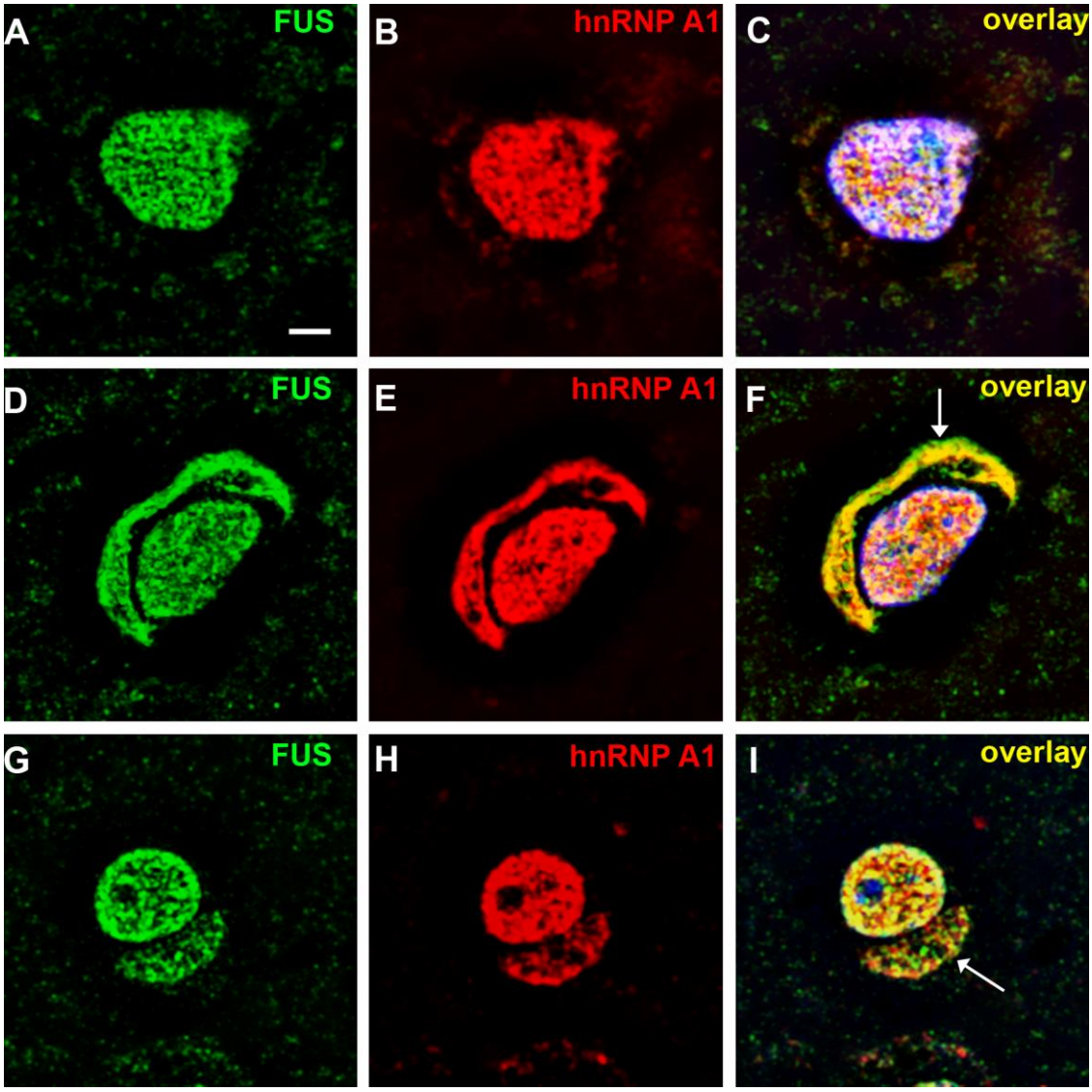

Figure 3.12. hnRNP A1 co-localises with FUS in the inclusions of FTLD-FUS. Frontal cortical neurons from healthy control (A-C) NIFID (D-F) and aFTLD-U (G-I). Both NIFID and aFTLD-U neurons bare cytoplasmic (arrow) inclusions immunoreactive for hnRNP A1 and FUS. Overlay panels include blue nuclear DAPI staining. Scale bar on A represents 5µm.

3.15 Stress granule markers in FTLD-FUS pathology

It has been previously shown by other authors that the inclusions of FTLD-FUS but not FTLD-TDP contain stress granule markers. The QSBB collection of FTLD-FUS was investigated immunohistochemically with antibodies raised against poly-(A) binding protein (PABP1) and GAP SH3 domain-binding protein (G3BP), two widely used markers of stress granules. As has been shown by other authors, antibodies raised against stress granule components label the cytoplasmic inclusions of FTLD-FUS (Figure 3.13). Interestingly, these antibodies did not stain intranuclear inclusions in either NIFID or aFTLD-U cases. This may yield clues to inclusion formation on either side of the nuclear membrane due to the cytoplasmic nature of stress granules.

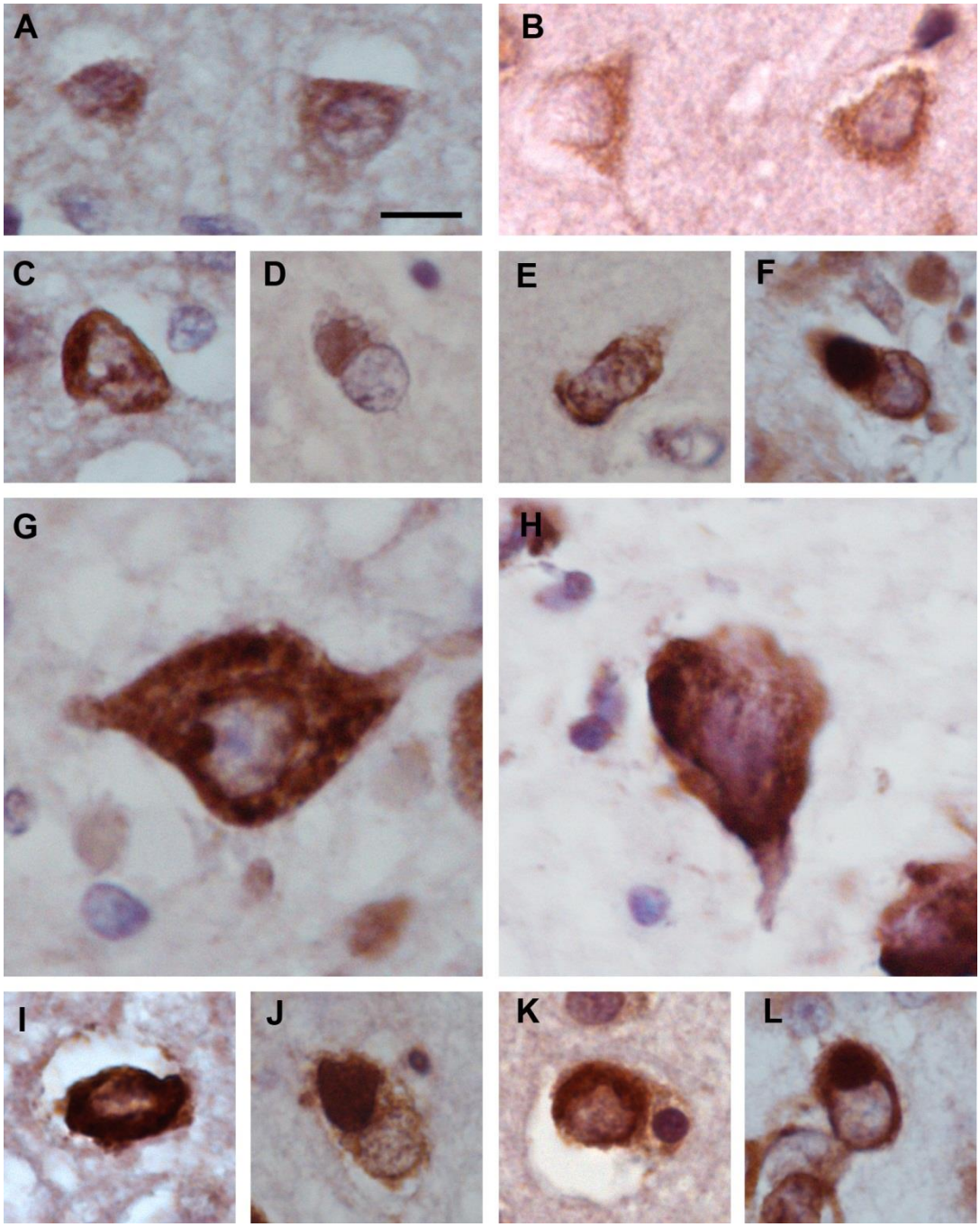

Figure 3.13. The stress granule markers PABP1 and G3BP label the cytoplasmic inclusions of FTLD-FUS. Normal cytoplasmic granular staining of PABP1 (A) and G3BP (B) in healthy control frontal cortex contrasts with the inclusion pathology seen in FTLD-FUS. PAPB1 labels a variety of cytoplasmic inclusions including; crescent shaped (C), bean-like (D), loose filamentous (E), Pick body-like (F) and granular (G). G3BP also labels a variety of inclusions including; granular (H), crescent shaped (I), Pick body-like (J and L) and more filamentous (K). Affected elements include frontal cortex (C D E I J K), granule cell layer of the hippocampus (F and L), and the motor cells of the medulla (G and H). Scale bar in A represents 25μm.

3.16 Total and phosphorylated eIF2α may be increasing in FTLD-FUS

Under normal conditions eukaryotic initiation factor 2α (eIF2α) initiates protein translation in a GTP dependant manner with $_{t}RNA^{met}$. However, phosphorylation of eIF2α prevents GDP-GTP exchange by eIF2B, which lowers the effective concentration of eIF2-GTP-$_{t}RNA^{Met}$. Under these conditions, the stress granule marker TIA-1 is incorporated into a now translationally silent pre-initiation complex. TIA-1 self-aggregation then promotes the accumulation of these complexes into stress granules. In this way the phosphorylation of eIF2α acts as a molecular trigger for stress granule assembly. Given the implication of stress granules in inclusion formation the eIF2α status of FTLD-FUS tissue was investigated. Frontal cortex homogenates from three healthy controls, three aFTLD-U and three NIFID subtypes were cleared and immunoblotted for total and phosphorylated forms of eIF2α (Figure 3.14 A). Densitometric quantification reveals a trend of increased total eIF2α in aFTLD-U and NIFID compared with controls (Figure 3.14 B), and an apparently significant increase in phosphorylated-eIF2α in NIFID cases (Figure 3.14 C). However the significance is lost when readings are expressed as a proportion of total eIF2α (Figure 3.14 D). This trend may become significant if more cases were available for investigation because there was considerable variation in the samples.

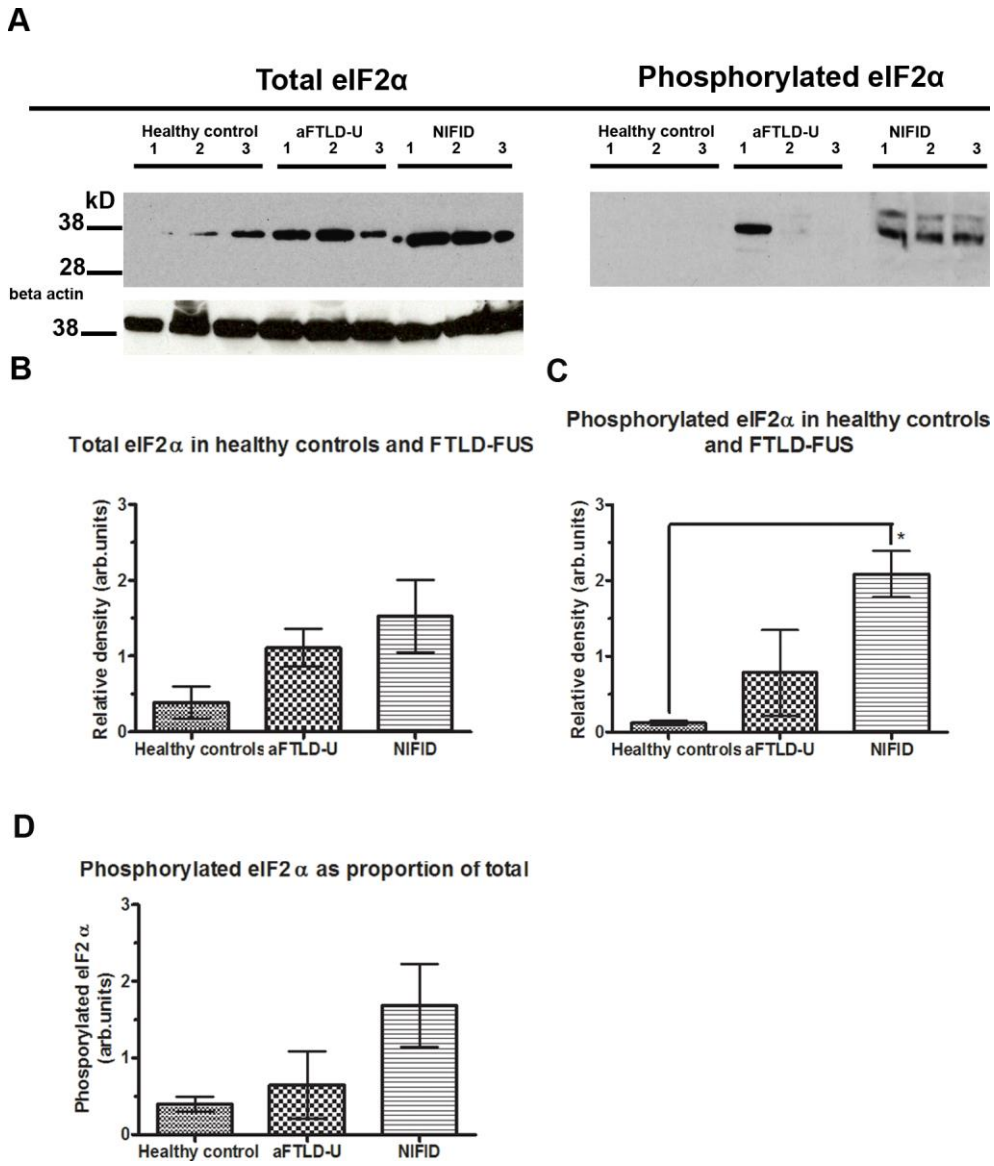

Figure 3.14. Increasing total and phosphorylated eIF2α in FTLD-FUS compared with healthy controls**.** Representative immunoblots of three healthy control, three aFTLD-U and three NIFID frontal cortex homogenates probed for either total eIF2α or phospho-eIF2α (A). Blots were stripped and re-probed for phospho-eIF2α or beta actin. Densitometric quantification and analysis with ANOVA followed by Dunnett's correction shows there is an upward trend of total eIF2α in aFTLD-U and NIFID (B), and a significant increase in phosphor-eIF2α detected (*$p<0.05$) (C), but this significance is lost when expressed as a proportion of total eIF2α (D). Error bars SEM. Molecular weight of eIF2α 36kD.

3.17 Discussion

These data strongly suggest a role for TRN1 in the pathogenesis of FTLD-FUS. The results have shown that TRN1 is deposited within the FUS positive inclusions of FTLD-FUS, and becomes insoluble and therefore likely highly aggregated in this disease. Several other targets of TRN1 import have also been discovered within the inclusions of this disease including all members of the FET family and the hnRNP A1 protein. Additionally, the TRN1 nuclear pore interacting protein NUP98 is present in a proportion of neuronal cytoplasmic inclusions. TRN1 does not co-localise with FUS in Huntington's disease and spinocerebellar ataxia, despite these diseases possessing FUS as a secondary pathological marker. This may suggest that TRN1 is a more specific disease marker for FTLD-FUS than the current primary pathological marker FUS. However, it remains to be seen if the other members of the FET family (TAF15 and EWS) are present in the polyglutamine inclusions of Huntington's disease and spinocerebellar ataxia. No other importins or karyopherins are mis-localised or sequestered into the inclusions of FTLD-FUS suggesting there is something unique about the TRN1-cargo functionality in FTLD-FUS compared with healthy controls and other neurodegenerative diseases. The stress granule markers PABP1 and G3BP stained the neuronal cytoplasmic inclusions of FTLD-FUS suggesting a relationship between these cytoplasmic proteins and the formation of inclusion bodies.

Immunohistochemical investigation of 14 cases of FTLD-FUS (7 NIFID, 7aFTLD-U) revealed TRN1 is deposited in the inclusions of FTLD-FUS and recapitulates other pathological findings such as fine neuropil threads, coarse neurites, swollen axons, dots, and 'grains' that were previously described with FUS antibodies (Lashley et al., 2011). The dots and 'grains' are likely to originate from dentritic processes cut in cross-section because they were clearly seen in the dendritic processes of larger neurons that had been sectioned in such a way so that the cell body and dentritic tree were in one plane. These neurons were typically of the cellular islands of the pre-α layer of the entorhinal

cortex. This may be functionally relevant in view of the fact that FUS has a role in mRNA export and transport to dendritic spines (Fujii et al., 2005, Fujii and Takumi, 2005). The qualitative assessment of the anatomical distribution of TRN1 pathology mirrors that shown by FUS immunohistochemistry. This is exemplified by the double immunofluorescence of TRN1 and FUS within the intranuclear and cytoplasmic neuronal inclusions of the hippocampal granule cell layer. Whilst some variation was observed between the intensity of TRN1 and FUS staining supplementary morphometry indicated a good degree of co-localisation. Differences in the immunolabeling between cases and even between different regions of the same case are not unexpected, and could be due to the length of formalin fixation (Holund et al., 1981, Puchtler and Meloan, 1985). Since the publication of these immunohistochemical findings several independent authors have verified the TRN1 profile in FTLD-FUS (Neumann et al., 2012, Davidson et al., 2012). The discovery of TRN1 in FTLD-FUS moved the focus of pathogenic theories away from the singular protein FUS and put them in context of a functional nuclear import cycle. Consequently, shortly after the publication of the TRN1 investigations, other TRN1 cargos (TAF15 and EWS) were found to recapitulate the pathology of FTLD-FUS (Neumann et al., 2011, Neumann et al., 2012). Whilst these authors attempted to investigate other TRN1 cargos beyond the FET proteins in a similar manner to the data presented here, their antibody selection may have prevented them from detecting hnRNP A1 (Neumann et al., 2012). However such differences are not uncommon between different laboratories and brain banks. For example, the QSBB collection of healthy control and FTLD-FUS tissue demonstrates a clear cut biochemical TRN1 signature of highly insoluble TRN1 in only FTLD-FUS tissue. Meanwhile other authors have failed to reproduce this pattern (Neumann et al., 2012), although this could be due to differences in the extraction protocol.

FUS immunoreactive inclusions are not unique to FTLD-FUS and ALS-FUS. The polyglutamine expansion disorders, including Huntington's disease and some

spinocerebellar ataxias, display FUS immunoreactivity in the intranuclear inclusions (Nukina, 2010a). It has become clear that truncated N-terminal huntingtin aggregates can bind FUS and sequester the protein away from its normal diffuse nuclear pattern (Nukina, 2010b). In the QSBB and UCL Institute of Neurology sample of Huntington's and spinocerebellar ataxia cases TRN1 does not appear to mimic these findings and remains nuclear. However, neuronal intranuclear inclusion body disease has shown positivity for both FUS and TRN1. Neuronal intranuclear inclusion disease is an extremely rare entity with fewer than 40 cases described in the literature (Josephs, 2011). Normally diagnosed post-mortem, the characteristic hyaline inclusions are eosinophilic and positive for ubiqutin, small ubiquitin-related modifier 1 (SUMO1), and occasionally 1C2 (anti-polyglutamine expansion). It is possible that FUS is recruited to the inclusions in a similar manner to Huntington's disease, but small differences in the incorporation of FUS allow TRN1 to bind FUS as well. At this point it is purely conjecture and will likely remain so because the instances of neuronal inclusion body disease are so rare and its pathogenesis so poorly understood.

The lack of other importin or karyopherin proteins aggregating in tandem with TRN1 and a selection of its cargos implies there is something unique about TRN1 and its interaction with these proteins that leads to aggregation in the diseased brain. Highly malignant ALS associated FUS mutations like P525L produce an abnormal cytoplasmic phenotype which is thought to be crucial for cytoplasmic aggregation and disease pathogenesis. In this vein, investigations into ALS associated mutations in the M9 NLS of FUS have revealed that the aberrant re-localisation of FUS seen in cell models can be rescued by treatment with methylation inhibitors (Dormann et al., 2012). Periodate oxidised adenosine (AdOx) is an inhibitor of all S-adenosyl-$_{L}$-methionine (SAM) dependant methylation by protein N-arginine methyltransferase (PRMT). By either inhibiting this enzyme or silencing it through siRNA knockdown the normal methylation of FUS can be reduced, specifically within the RGG domain closest to the NLS. It is this

hypomethlation that rescues the interaction with TRN1 and returns the mutant FUS to its normal nuclear localisation. The authors of this work extend their hypothesis further to explain the TRN1-cargo protein inclusions of FTLD-FUS by arguing that a specific subset of proteins have their methylation status altered, which creates an overly strong interaction with TRN1 resulting in a failure to release its cargo. Support for this comes from immunohistochemistry using methylated-FUS specific antibodies which shows ALS but not FTLD-FUS inclusions are hypermethylated. However, the theory does not satisfactorily explain why inclusions form on both sides of the nuclear membrane. For instance, if the binding of TRN1 and cargo was overly strong this should not retard the movement through the nuclear pore meaning that inclusions should form only within the nucleus.

Since 2009 our knowledge of FTLD-FUS inclusions as increased dramatically. Yet new theories of pathogenesis continue to use FUS as the main protagonist in inclusion formation. Any new theory of inclusion formation centred around the properties of FUS must be satisfactorily extended to include not only the published EWS and TAF15 aggregation but also hnRNP A1 and NUP98.

Aggregation in the cytoplasmic compartment might be explained with the phenomenon of stress granules. These temporary aggregates of mRNA and associated proteins are produced by a cell in response to various stressors to suspend and sequester away non-essential transcripts. It has been shown by other authors that the inclusions characteristic of ALS-FUS and FTLD-FUS are positive for stress granule markers (Fujita et al., 2008, Dormann et al., 2010), and now the QSBB collection of FTLD-FUS can be included in this. Additionally, there appears to be an upward trend in the total and phosphorylated form of eIF2α found in the cases available for biochemistry. Since phosphorylated eIF2α is the molecular trigger for stress granule formation in response to numerous stressors, this could be highly relevant. However, these results are only preliminary and require comparison with other neurodegenerative diseases. For

instance eIF2α phosphorylation has been linked to the neurodegeneration seen in prion disease (Moreno et al., 2012). Combined with the observation that cytoplasmically mis-localised FUS will quickly amalgamate into the stress granules in cell models, stress granules have been proposed as precursors to the ubiquitinated inclusions seen post-mortem. To test this hypothesis, further investigations into the nature of stress granules in the context of FTLD-FUS are carried out in the next chapter.

Chapter Four: Endogenous TRN1 and the FET proteins are recruited to stress granules under conditions of oxidative and osmotic stress (Results II)

4.1 Introduction

As previously mentioned the FET proteins (FUS, EWS and TAF15) are all RNA binding proteins with a plethora of functions not least of which is the binding of pre-mRNA in the splicosomal complex (Orozco et al., 2012), leading many to believe that loss of nuclear function associated with aberrant cytoplasmic localisation is a key feature of pathogenesis (Orozco and Edbauer, 2013).

Stress granules are cytoplasmic foci formed rapidly when the cell is subjected to stress. This stress can be from a variety of stressors affecting a variety of organelles. These foci are temporary aggregates designed to store mRNA encoding basal translation proteins sequestering them away from the translation apparatus. This allows the cell to refocus translation towards survival factors like heat shock proteins. Aside from mRNA stress granules also contain proteins both directly associated with said mRNA, and proteins not directly involved in RNA binding. Some of these include G3BP, TIA-1, PABP1, and TIAR which can be used as reliable markers of stress granules due to the rapid and clear change in staining pattern when stress granules are induced. This induction can take the form of heat-shock, hypoxia, polysome destabilization, oxidative and osmotic stress (Matsuki et al., 2013, Zurla et al., 2011, Shih et al., 2012) to name a few.

From the data presented in the last chapter coupled with previously published description of stress granule markers in the cytoplasmic inclusions of FTLD-FUS (Dormann et al., 2010), a theory of stress granule nucleated inclusion formation has emerged (Bosco et al., 2010, Gal et al., 2011). Some authors hypothesized that stress granule formation may be a precursor to the more sinister cytoplasmic aggregates in both ALS-FUS and FTLD-FUS (Dormann et al., 2010). One major hurdle to this hypothesis is that these stress granule proteins are known to easily disperse and return to solution once the stress has been removed (Kedersha et al., 2000). Despite this, stress granule markers such as TIA-1 co-localize with the characteristic neuronal aggregates of numerous neurodegenerative diseases including FTLD-FUS (Liu-Yesucevitz et al., 2010) suggesting there may be a link between the two phenomena. Stress granules are easily inducible in cell models which allows characterisation after just 15 minutes, but relatively little is known about these foci under prolonged stressful conditions. Furthermore, whilst the list of stress granule components continues to grow with new proteins published regularly little is known about the possible inclusion of the newly discovered FTLD-FUS proteins TRN1, TAF15, and EWS.

4.2 Hypothesis

In SH-SY5Y cells oxidative stress can induce translocation of TRN1 and FET proteins to cytoplasmic stress granules that can prime aggregate formation seen in FTLD-FUS. This re-localisation is due to TRN1 and its ability to bind the FET proteins through their M9 motif. Overexpression of TRN1 will exaggerate the phenotype seen in endogenous cells.

4.3 TRN1 is a good surrogate marker of G3BP positive stress granules, and also labels post-stress G3BP negative foci

The widely accepted best markers of pathology in FTLD-FUS are all functionally related to TRN1, and its role as a nuclear importer might be important to the malignant cytoplasmic aggregation. To investigate the response of TRN1 in the context of FET proteins and aggregation to conditions thought to mimic the aged demented brain, the neuroblastoma cell line SH-SY5Y was subjected to oxidative or osmotic stress over acute (2 hours) or prolonged (24 hours) incubation periods.

In unstressed SH-SY5Y cells TRN1 appeared mainly nuclear, whilst G3BP staining was weak and diffuse throughout the cell. Upon acute treatment with oxidative stress (0.5mM arsenite or 50mM tBH for 2hrs) a radical re-localisation of TRN1 to cytoplasmic foci was evident. These foci very strongly co-localised with G3BP and were therefore stress granules (Figure 4.1 and 4.2). Prolonged exposure to oxidative stress (10μM arsenite or 190μM tBH over 24hrs) produces foci, consisting of TRN1 and G3BP that appeared larger but were far less common. However, when the cells were allowed to recover in fresh media for 6hrs, the staining pattern changed to reflect stress granule dissolution. The majority of what remained were TRN1-positive, G3BP-negative cytoplasmic foci (Figure 4.1 and 4.2).

To compare TRN1 response between oxidative and non-oxidative stressors the osmotic stressor sorbitol was also employed. Osmotic stress was chosen over other possibilities like heat-shock because temperature changes are less physiologically relevant to a central organ like the brain. Under acute stress (600mM for 2hrs) nuclear TRN1 re-localised to numerous, punctate cytoplasmic foci that were strongly positive for G3BP (Figure 4.3). These foci were notably smaller (~1-2μm in diameter) than those produced by 2hrs 0.5mM arsenite stress. Prolonged exposure to sorbitol (400mM for 24hrs) produced fewer TRN1 foci per cell but these remained strongly positive for G3BP.

Recovery in fresh media recapitulated the TRN1 positive, G3BP negative foci seen after oxidative stress (Figure 4.3).

TRN1 was chosen as the primary marker of foci to investigate co-localisation with FET proteins in the following experiments because these experiments aimed to investigate re-localisation of FET proteins to stress granules through a possible TRN1 interaction, furthermore TRN1 consistently labeled stress granules but also labeled post-stress granule foci (Figure 4.1 4.2 and 4.3).

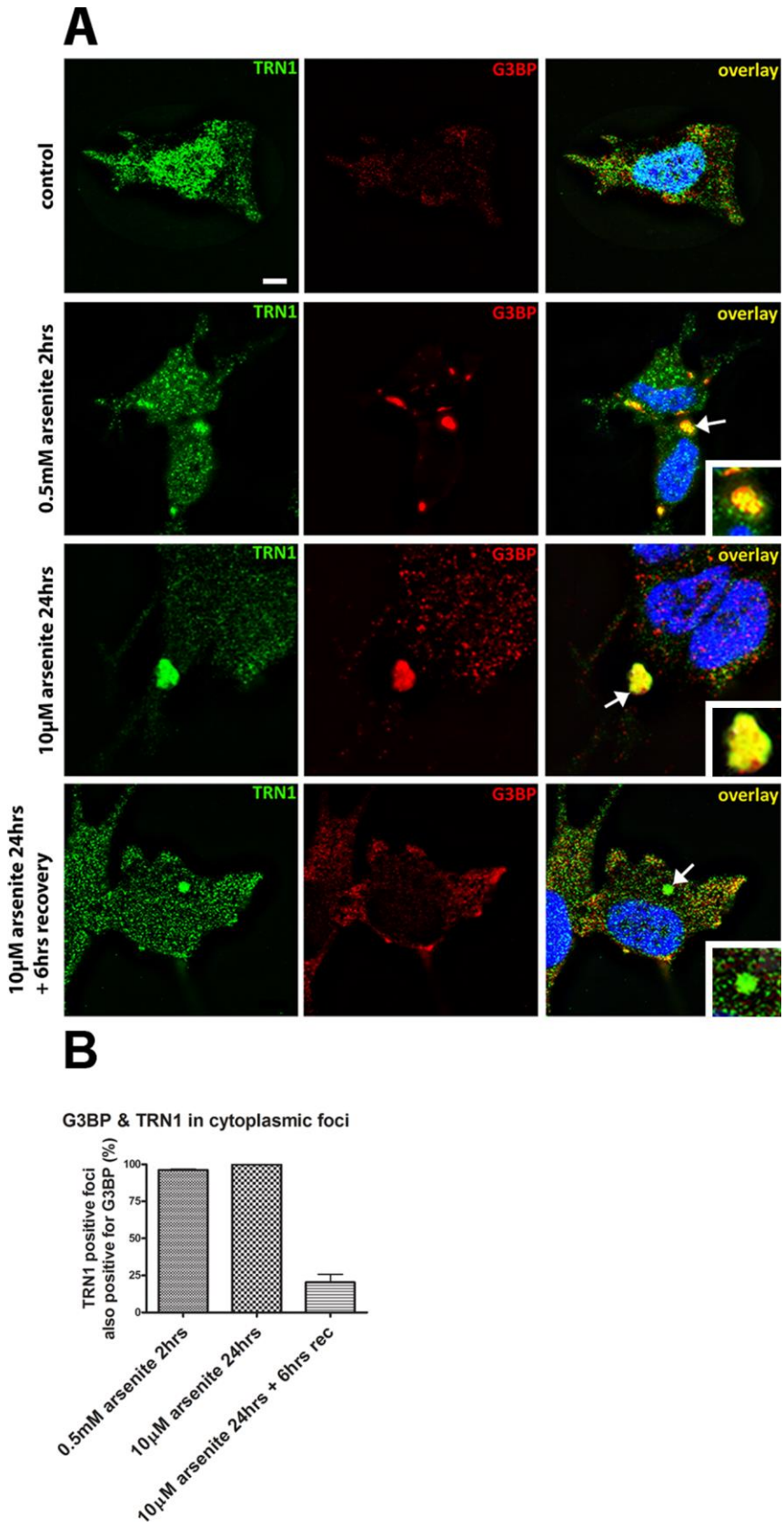

Figure 4.1. Arsenite stress induces translocation of nuclear TRN1 to the cytoplasmic compartment partially co-localising with stress granules. Recovery in fresh media leaves TRN1 positive, G3BP negative foci. TRN1 positive foci (A arrows). Co-localisation quantification of foci counts shows 96.11% co-localisation in TRN1 foci at 2hrs and

100% at 24hrs, but a 20.33% co-localisation after 6hrs recovery (B). Counts graphed as percentage of TRN1 foci also positive for G3BP for ease of interpretation. Error bars SEM. Overlay panels include blue nuclear DAPI stain. Scale bar in A represents 5μm and 2.5μm within insets. N=3.

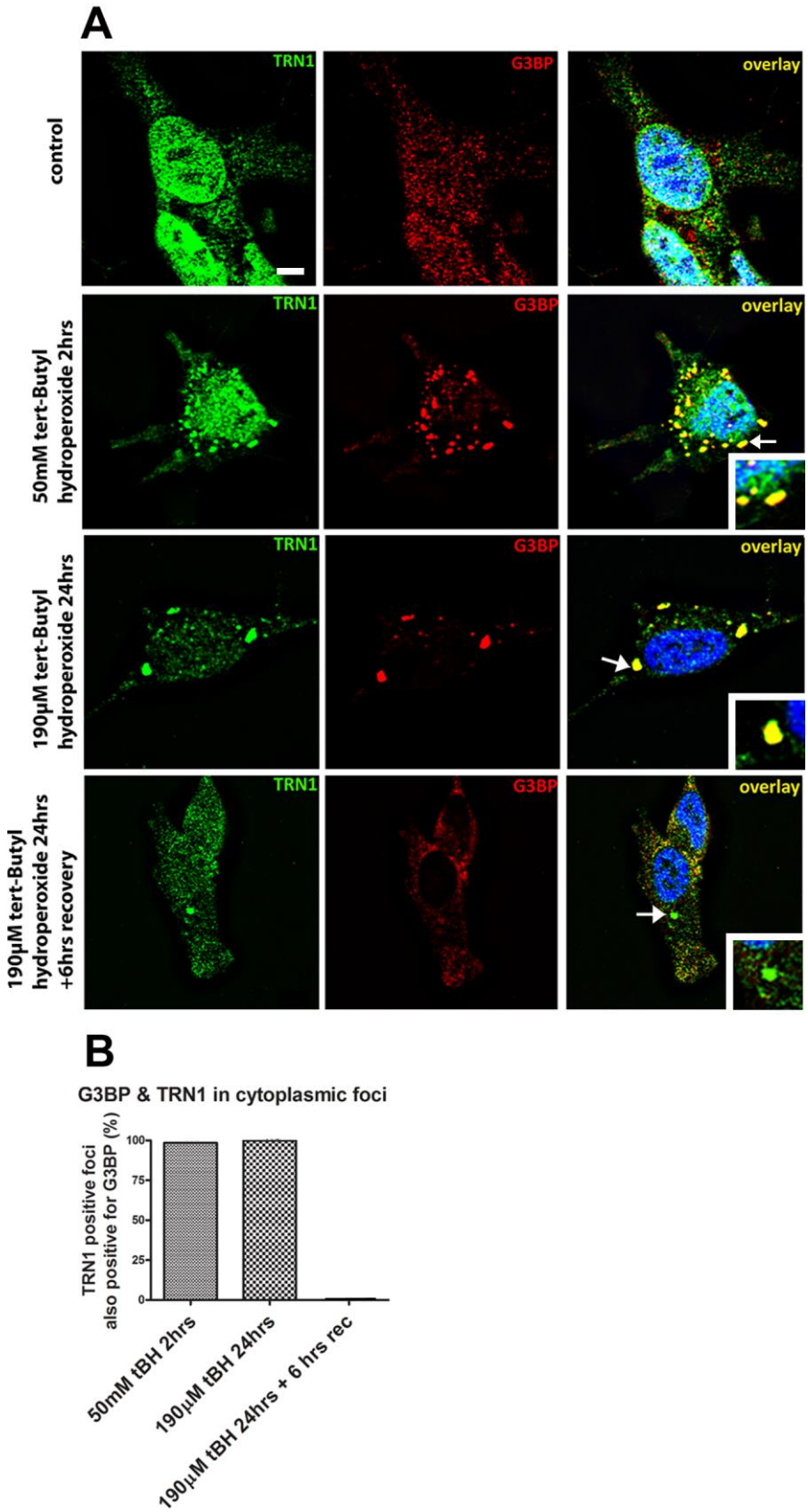

Figure 4.2. tBH stress induces translocation of nuclear TRN1 to the cytoplasmic compartment partially co-localising with stress granules. Recovery in fresh media leaves TRN1 positive, G3BP negative foci. TRN1 positive foci (A arrows). Co-localisation quantification of foci counts shows 98.48% co-localisation in TRN1 foci at 2hrs and 100% at 24hrs, but a 0.03% co-localisation after 6hrs recovery (B). Counts graphed as

percentage of TRN1 foci also positive for G3BP for ease of interpretation. Error bars SEM. Overlay panels include blue nuclear DAPI stain. Scale bar in A represents 5µm and 2.5µm within insets. N=3

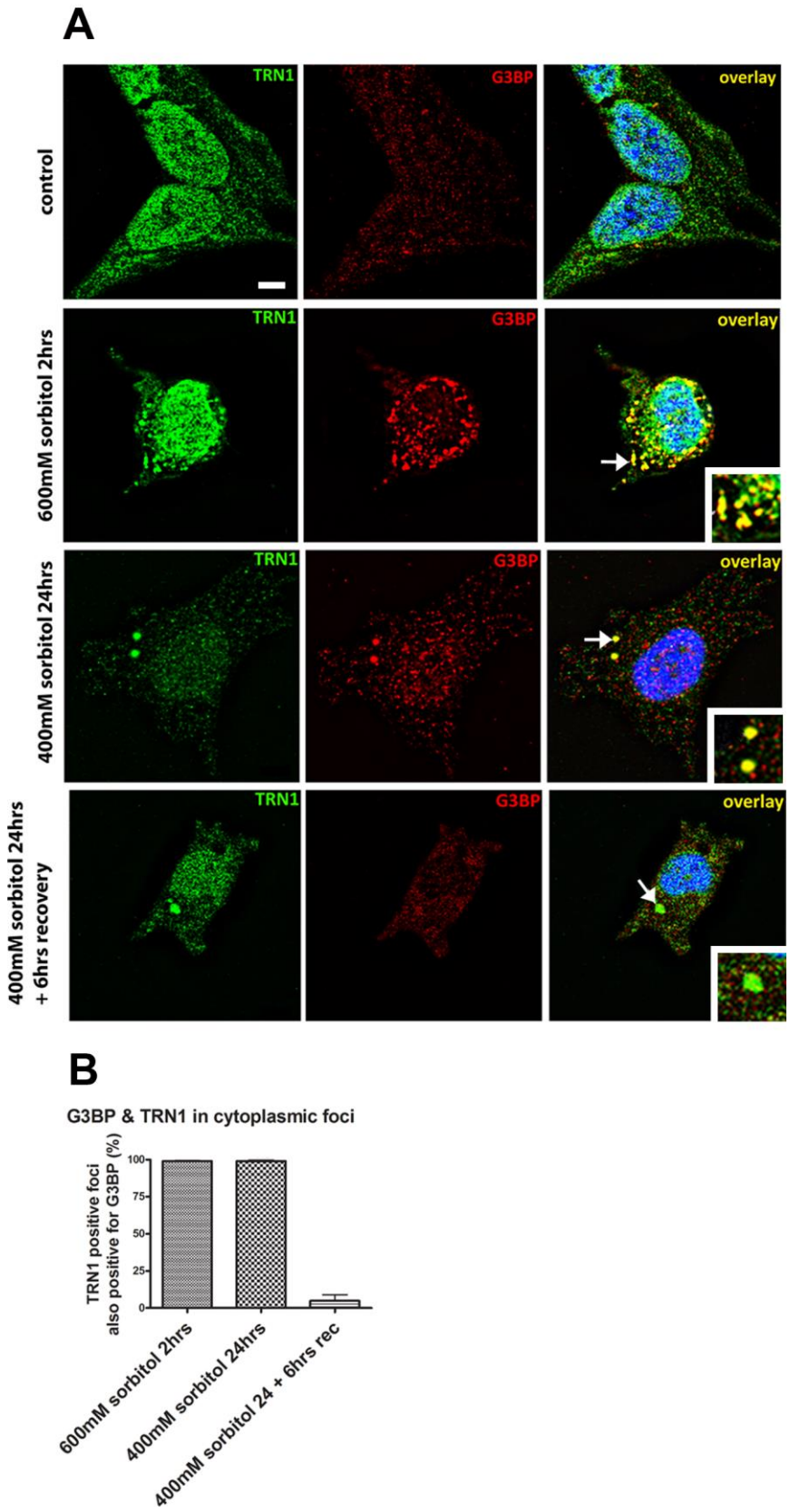

Figure 4.3. Sorbitol stress induces translocation of nuclear TRN1 to the cytoplasmic compartment partially co-localising with stress granules. Recovery in fresh media leaves TRN1 positive, G3BP negative foci. TRN1 positive foci (A arrows). Co-localisation quantification of foci counts shows 99.07% co-localisation in TRN1 foci at 2hrs and 99% at 24hrs, but a 4.86% co-localisation after 6hrs recovery (B). Counts graphed as

percentage of TRN1 foci also positive for G3BP for ease of interpretation. Error bars SEM. Overlay panels include blue nuclear DAPI stain. Scale bar in A represents 5µm and 2.5µm within insets. N=3

4.4 TRN1 and the FET proteins co-localise in stress granules and post-stress foci to varying degrees

Given the potential role of TRN1 in the pathology of FTLD-FUS, it was used as the primary marker of cytoplasmic foci when investigating the FET proteins and ubiquitin. In unstressed control cells, TRN1 staining always appeared in the nucleus together with the FET proteins (Figure 4.4 Figure 4.7 Figure 4.10). Here the extent of co-localisation between TRN1 positive cytoplasmic stress granules, with the three FET proteins and ubiquitin is described.

4.5 Co-localisation with FUS

Acute treatment with arsenite stress produced occasional FUS immunoreactivity in the TRN1 positive stress granule (7.07%) foci whilst the majority remained negative for FUS (Figure 4.4 A and B). Similarly, under prolonged arsenite stress the vast majority of TRN1 foci observed were not FUS positive (96.52% negative 3.48% positive). The same was true of the post-stress TRN1 foci observed after recovery in fresh media (4.70% positive).

Acute tBH stress produced the expected numerous punctate TRN1 stress granules (Figure 4.5 A). Despite a notable increase in the positivity for FUS (29.19% up by 22.12%), the majority were negative (Figure 4.5 B). This pattern continued in the prolonged tBH stress condition (only 15.27% positive), however these foci were less numerous. Recovery in fresh media appeared to show a slight increase in the number of FUS positive TRN1 foci (38.26%) but again a substantial number remained negative (Figure 4.5 B).

Acute osmotic stress produced the most FUS immunoreactive TRN1 stress granules (65.64%), however co-localisation could not be considered complete because there was

still a considerable number of TRN1 positive, FUS negative foci (Figure 4.6 A and B). After prolonged sorbitol stress there were fewer TRN1 foci in a similar fashion to oxidative stress, and under the reduced concentration and 24 hour incubation only a small proportion were FUS positive (9.08%). Interestingly, a slight increase in FUS positivity was observed after recovery in fresh media (31.05%) (Figure 4.6 B).

4.6 Co-localisation with EWS

Acute arsenite stress produced TRN1 stress granule foci that were also strongly immunoreactive for EWS (Figure 4.7 A). The degree of this co-localisation was 94.93%, therefore there was only a small minority of TRN1 foci not positive for EWS. The same was true of those TRN1 stress granule foci produced by prolonged arsenite stress (88.27%), and those foci that were present even after recovery (92.98%) (Figure 4.7 B).

Acute tBH stress produced numerous punctate TRN1 stress granule foci as seen previously with this treatment (Figure. 4.8 A). Despite a difference in morphology between those TRN1 foci produced by arsenite and tBH the degree of co-positivity between TRN1 and EWS was equally almost complete (93.81%) (Figure 4.8 B). Prolonged stress with tBH showed similar findings with no substantial difference between TRN1 and EWS foci (95.86%), and after recovery TRN1 and EWS foci still co-localised (95.38%) (Figure 4.8 A and B).

In contrast to the oxidative stressors, acute osmotic stress produced numerous punctate TRN1 stress granule foci but a substantial number were EWS negative (39.19% negative 60.81% positive) (Figure 4.9 B). After prolonged sorbitol stress drastically fewer TRN1 foci co-localised with EWS (2.62%) whilst after the recovery period no co-localising cytoplasmic foci were observed (Figure 4.9 B).

4.7 Co-localisation with TAF15

Acute stress induced by all three stressors produced TRN1 stress granules that were only minimally positive for TAF15 (arsenite 5.93%, tBH 10.46%, sorbitol 1.48%) (Figure 4.10 B 4.11 B and 4.12 B). However, prolonged stress induced robust TAF15 re-

localisation to TRN1 stress granules and recovery in fresh media maintained the same staining pattern across all stressors (asenite 24hrs 98.39% after recovery 96.03%, tBH 24hrs 100% after recovery 100%, sorbitol 24hrs 98.93% after recovery 100%)(Figure 4.10 4.11 and 4.12).

4.8 Co-localisation with Ubiquitin

Given that the aggregates of FTLD-FUS are post-transcriptionally modified with ubiqitin, we investigated the TRN1 foci seen here with an ubiquitin antibody. Acute or prolonged oxidative stress (arsenite or tBuOOH) did not produce ubiquitin co-localisation with TRN1 foci (2hrs arsenite 0.56% 24hrs 10.12%, 2hrs tBH 0.86% 24hrs 8.24%). However, after a recovery period this changed, revealing good co-localisation between TRN1 and ubiquitin in these TRN1 foci (recovery after arsenite 97.22%, recovery after tBH 91.34%) (Figure 4.13 and 4.14).

Osmotic stress produced a slightly different staining pattern, with acute sorbitol stress producing TRN1 stress granule foci that are not positive for ubiquitin (only 0.21% positive), but after prolonged stress and prolonged stress followed by a recovery period, good co-localisation between TRN1 and ubiquitin could be seen within TRN1 foci (24hrs sorbitol 75.86%, and after recovery 97.82%) (Figure 4.15 A and B).

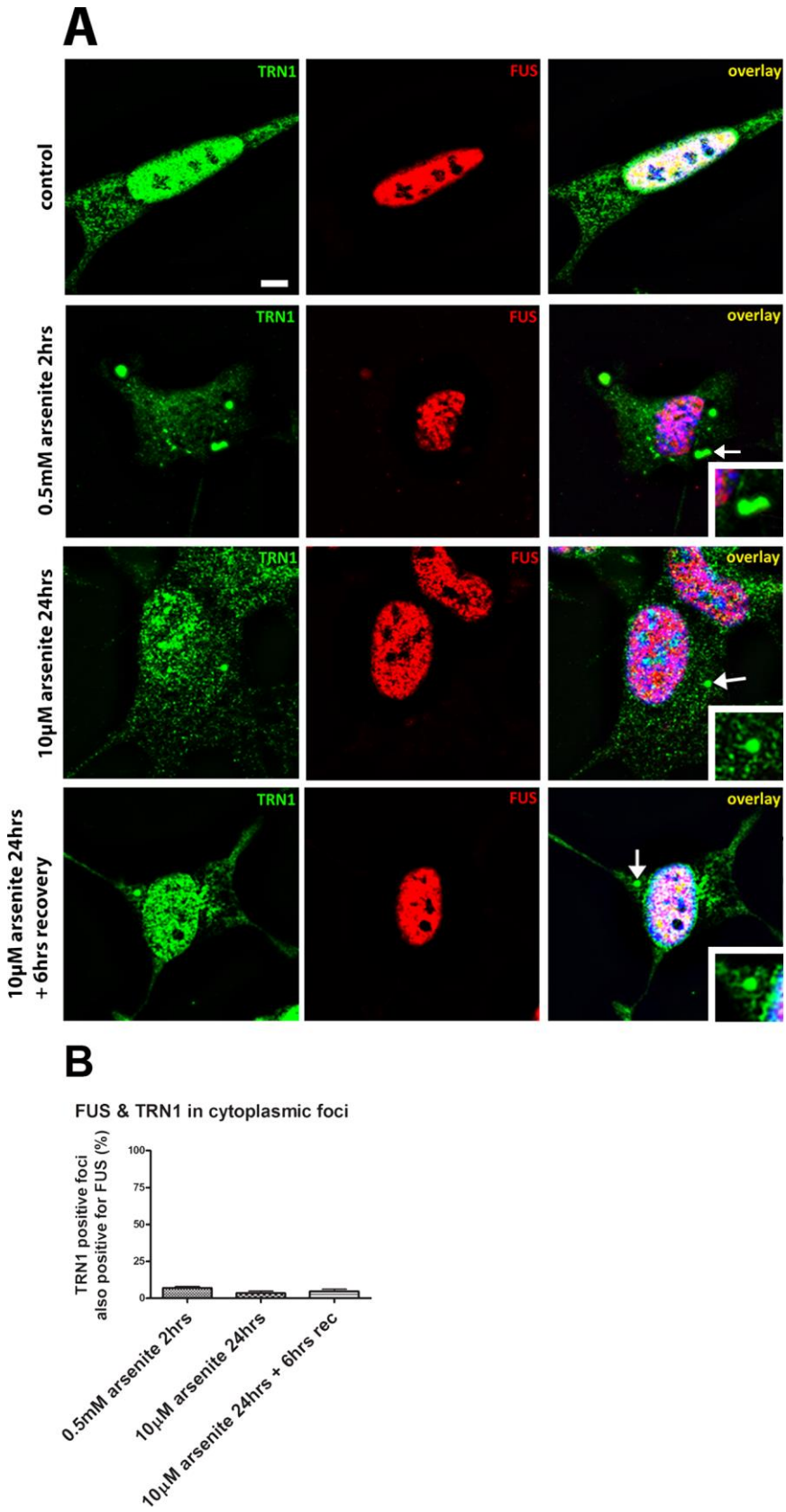

Figure 4.4. Arsenite stress induces translocation of nuclear FUS to the cytoplasmic compartment showing minimal co-positivity with TRN1 stress granules. Recovery in fresh media leaves TRN1 positive, FUS negative foci. TRN1 positive foci (A arrows). Co-localisation quantification of foci counts shows 7.07% co-localisation in TRN1 foci at

2hrs and 3.48% at 24hrs, and 4.70% co-localisation after 6hrs recovery (B). Counts graphed as percentage of TRN1 foci also positive for FUS for ease of interpretation. Error bars SEM. Overlay panels include blue nuclear DAPI stain. Scale bar in A represents 5μm and 2.5μm within insets. N=3

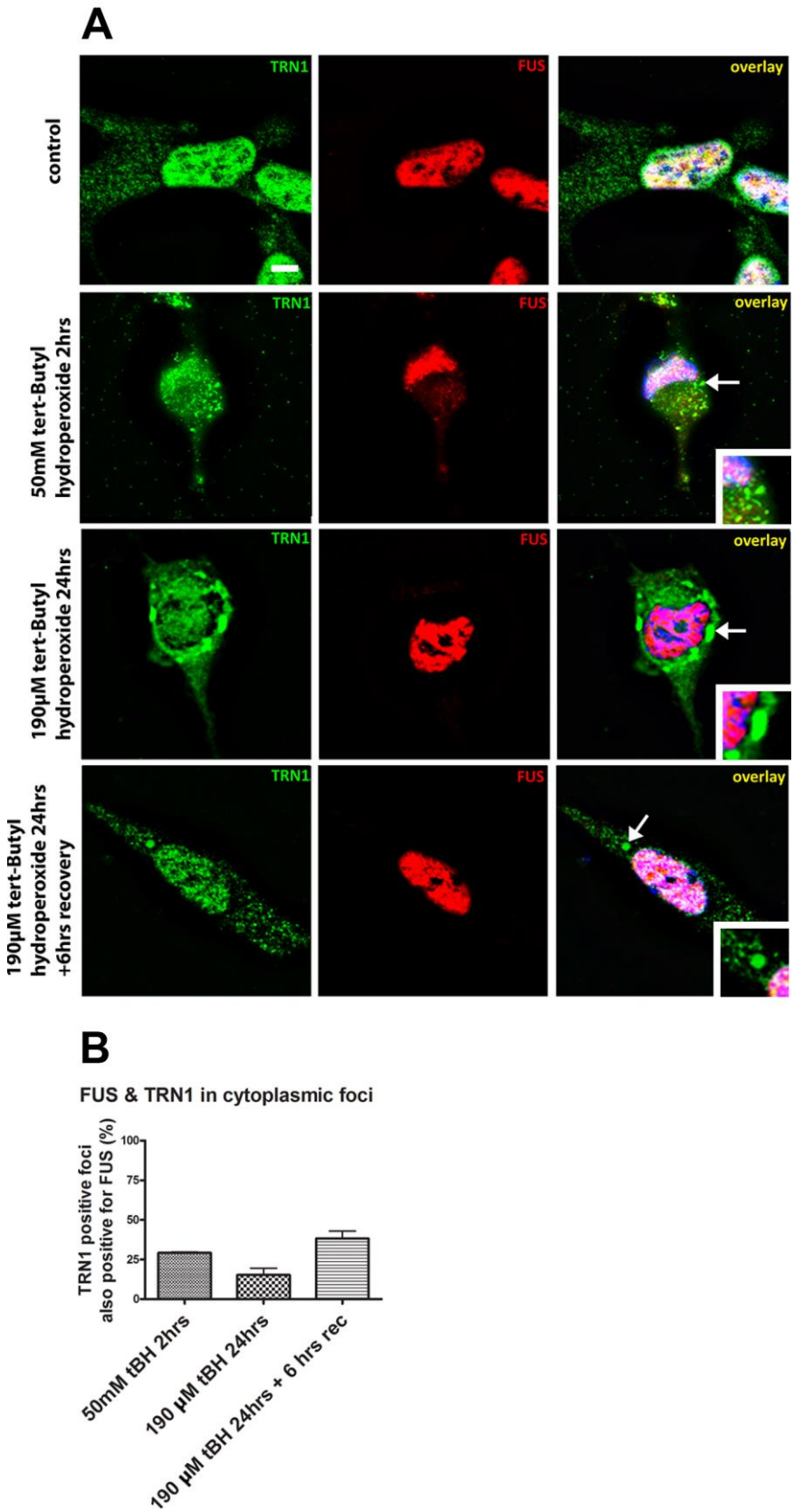

Figure 4.5. tBH stress induces translocation of nuclear FUS to the cytoplasmic compartment showing minimal co-positivity with TRN1 stress granules. Recovery in fresh media leaves TRN1 positive, FUS negative foci. TRN1 positive foci (A arrows). Co-

localisation quantification of foci counts shows 29.19% co-localisation in TRN1 foci at 2hrs and 15.27% at 24hrs, but a 38.26% co-localisation after 6hrs recovery (B). Counts graphed as percentage of TRN1 foci also positive for FUS for ease of interpretation. Error bars SEM. Overlay panels include blue nuclear DAPI stain. Scale bar in A represents 5μm and 2.5μm within insets. N=3

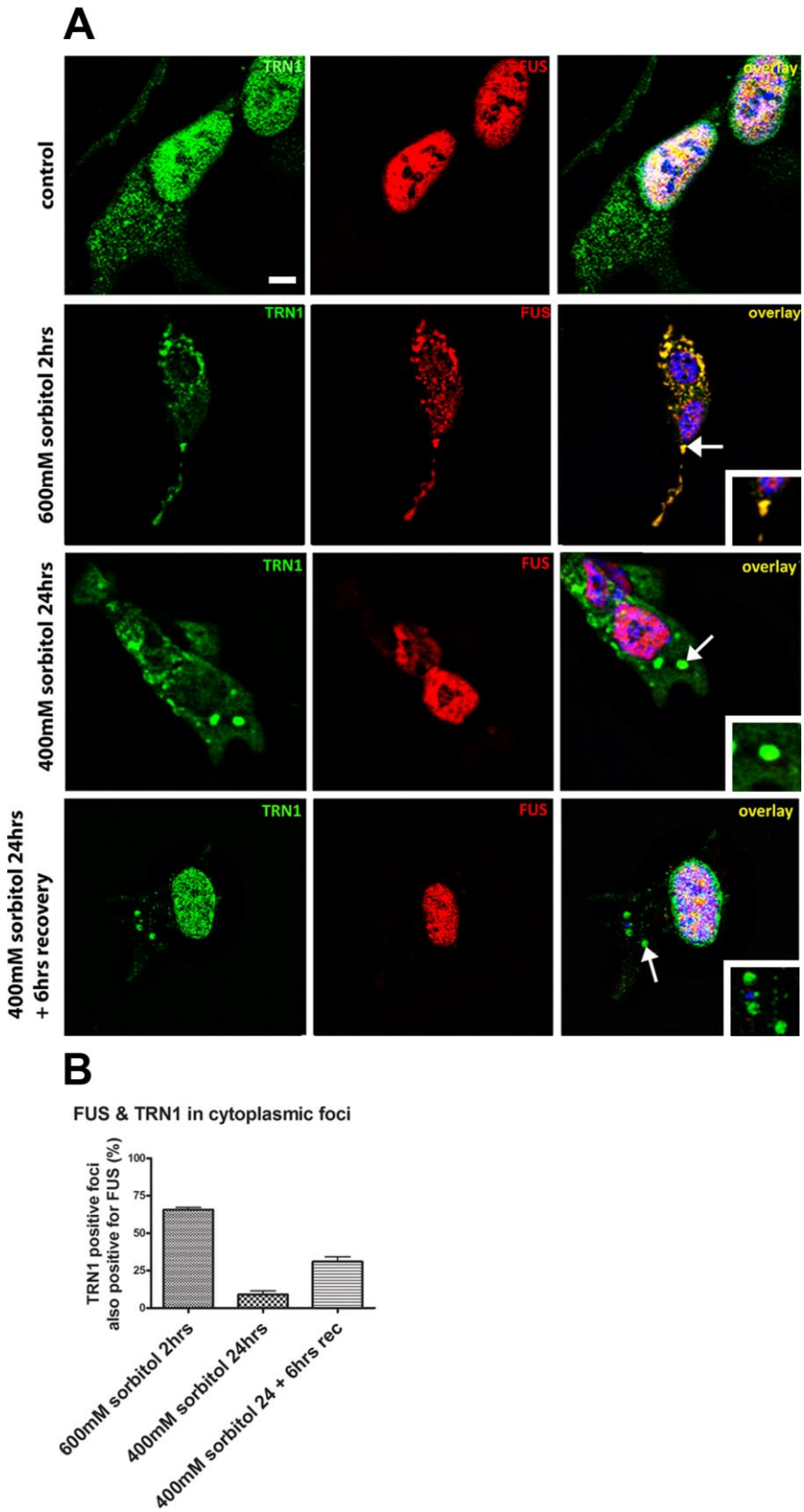

Figure 4.6. . Sorbitol stress induces translocation of nuclear FUS to the cytoplasmic compartment showing partial co-positivity with TRN1 stress granules. Recovery in fresh media leaves TRN1 positive, FUS negative foci. TRN1 positive foci (A arrows). Co-localisation quantification of foci counts shows 65.64% co-localisation in TRN1 foci at

2hrs and 9.08% at 24hrs, but a 31.05% co-localisation after 6hrs recovery (B). Counts graphed as percentage of TRN1 foci also positive for FUS for ease of interpretation. Error bars SEM. Overlay panels include blue nuclear DAPI stain. Scale bar in A represents 5μm and 2.5μm within insets. N=3

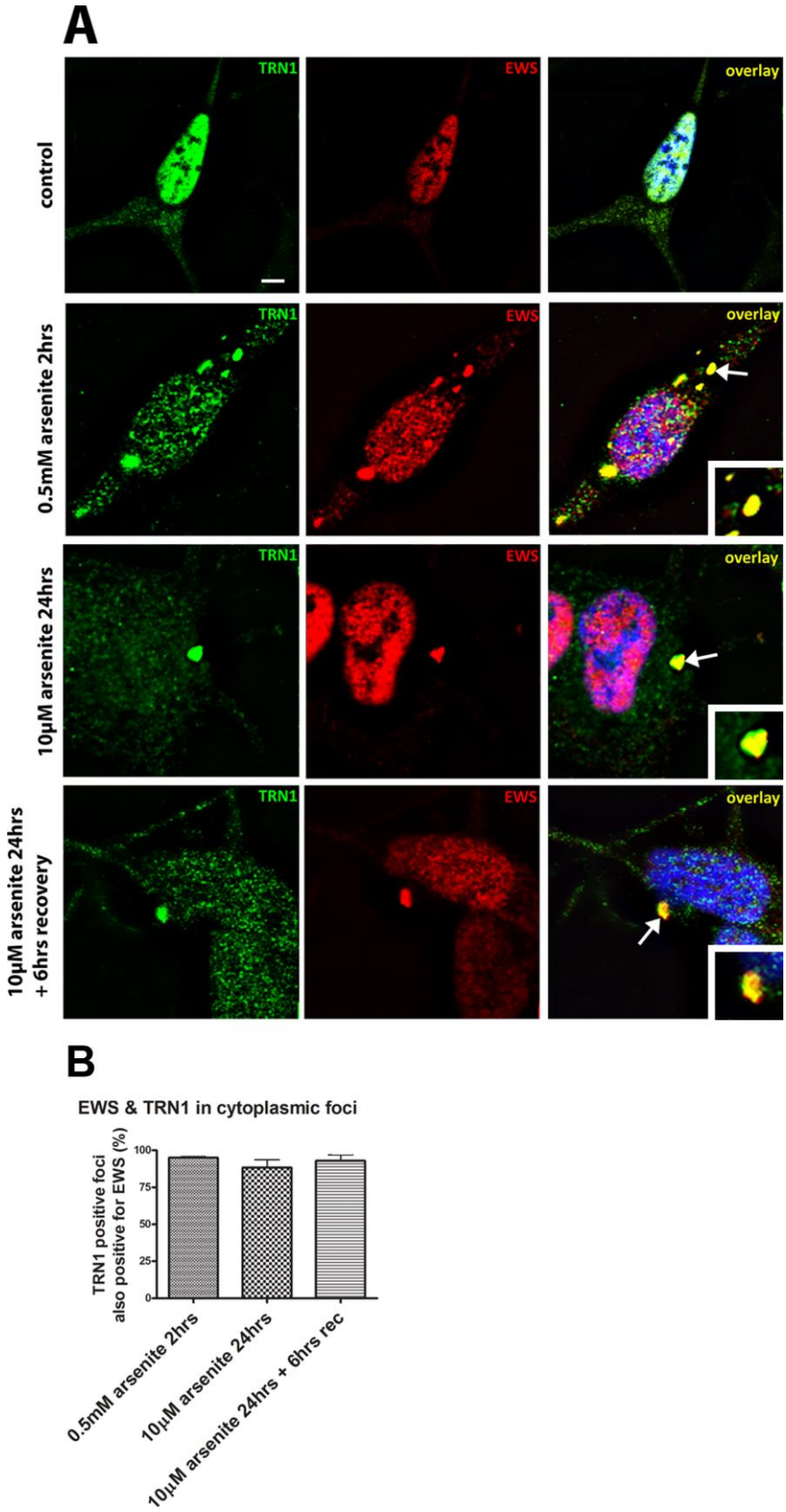

Figure 4.7. Arsenite stress induces translocation of nuclear EWS to the cytoplasmic compartment showing co-positivity with TRN1 stress granules. Recovery in fresh media leaves TRN1 and EWS positive foci. TRN1 positive foci (A arrows). Co-localisation quantification of foci counts shows 94.93% co-localisation in TRN1 foci at 2hrs and

88.27% at 24hrs, and 92.98% co-localisation after 6hrs recovery (B). Counts graphed as percentage of TRN1 foci also positive for EWS for ease of interpretation. Error bars SEM. Overlay panels include blue nuclear DAPI stain. Scale bar in A represents 5μm and 2.5μm within insets. N=3

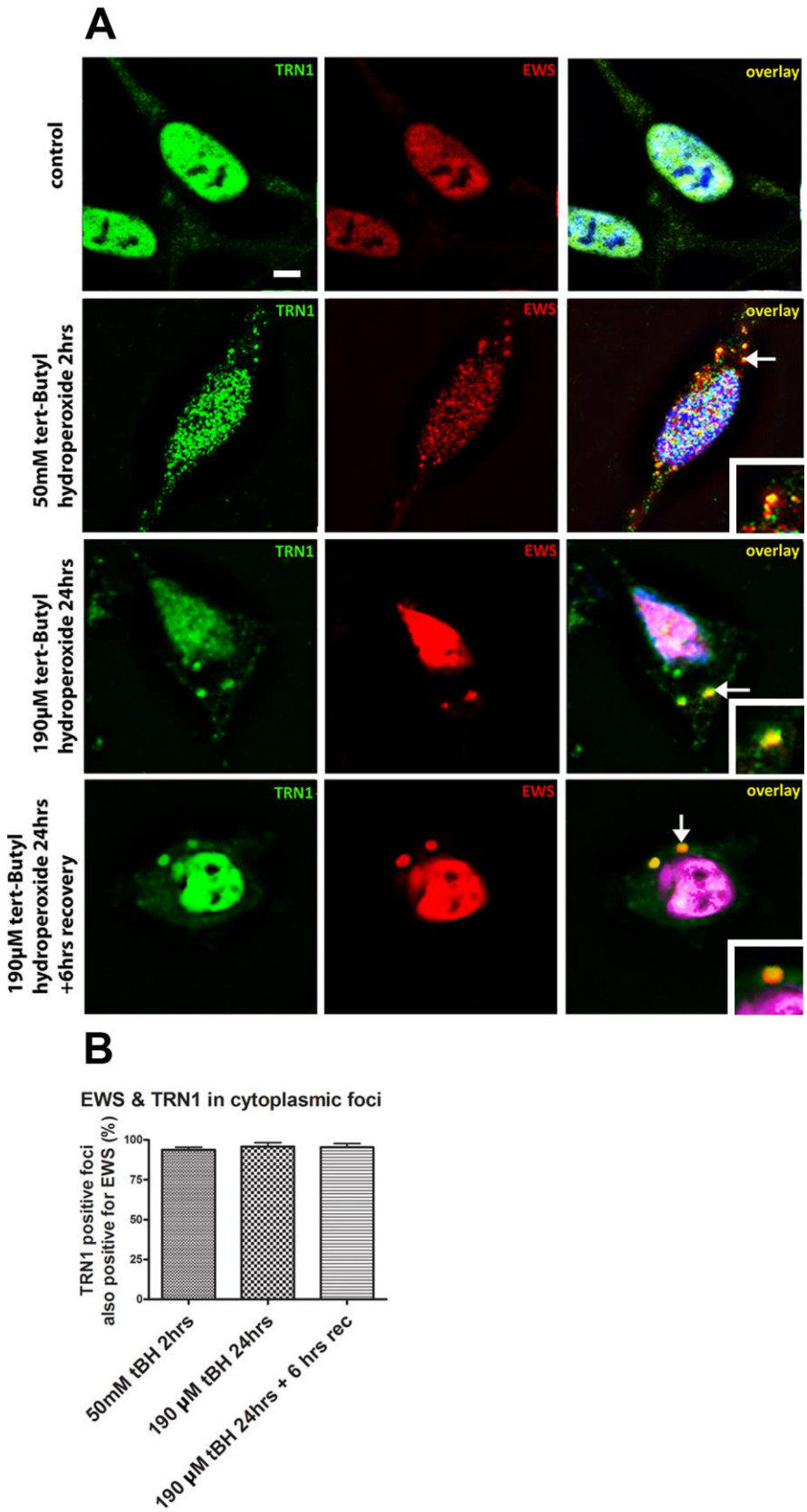

Figure 4.8. tBH stress induces translocation of nuclear EWS to the cytoplasmic compartment showing co-positivity with TRN1 stress granules. Recovery in fresh media leaves TRN1 and EWS positive foci. TRN1 positive foci (A arrows). Co-localisation quantification of foci counts shows 93.81% co-localisation in TRN1 foci at 2hrs and 95.86% at 24hrs, and 95.38% co-localisation after 6hrs recovery (B). Counts graphed as

percentage of TRN1 foci also positive for EWS for ease of interpretation. Error bars SEM. Overlay panels include blue nuclear DAPI stain. Scale bar in A represents 5μm and 2.5μm within insets. N=3

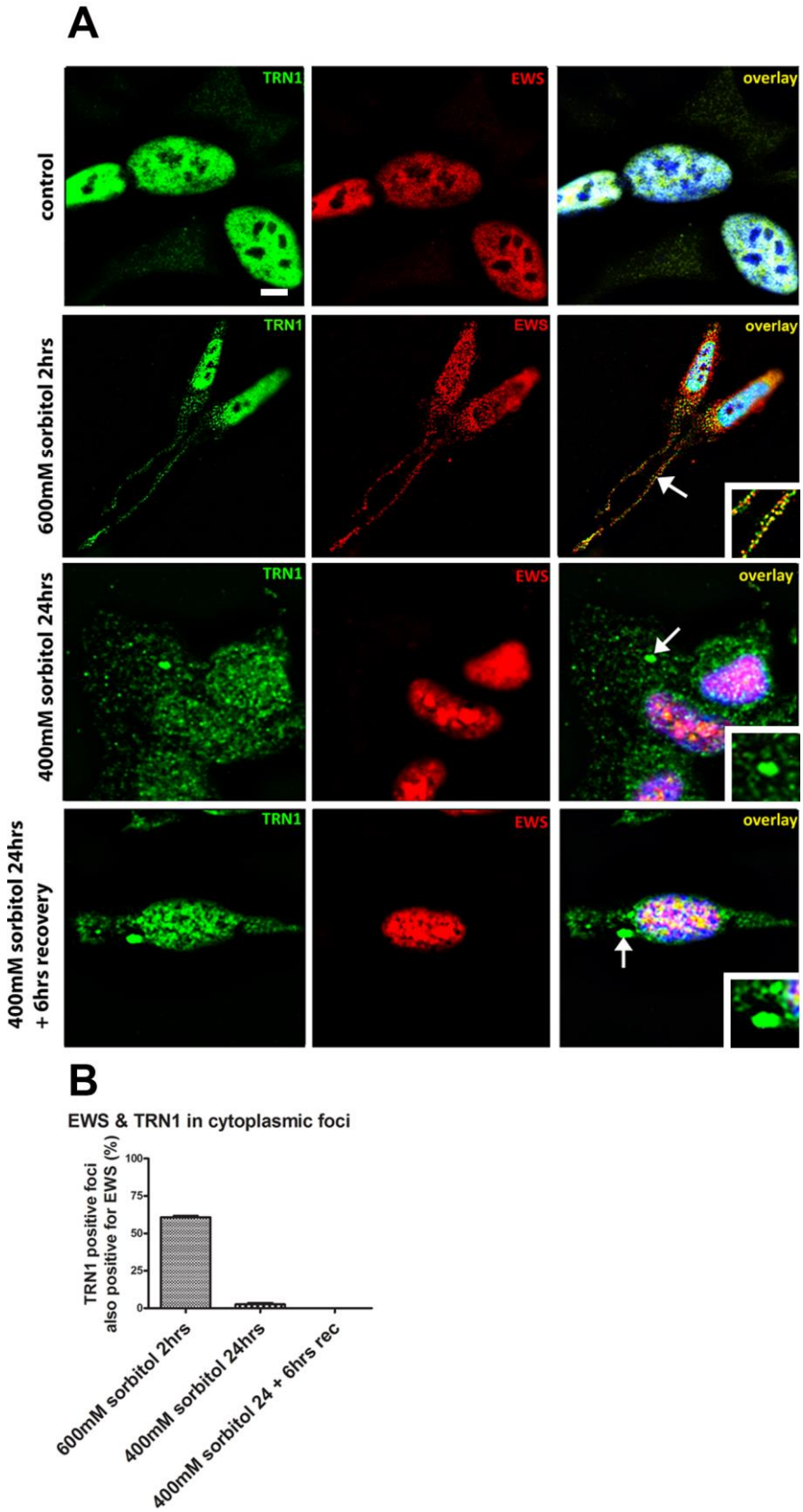

Figure 4.9. Sorbitol stress induces translocation of nuclear EWS to the cytoplasmic compartment showing partial co-positivity with TRN1 stress granules. Recovery in fresh media leaves TRN1 positive, EWS negative foci. TRN1 positive foci (A arrows). Co-localisation quantification of foci counts shows 60.81% co-localisation in TRN1 foci at 2hrs but 2.62% at 24hrs, and no co-localisation after 6hrs recovery (B). Counts graphed

as percentage of TRN1 foci also positive for EWS for ease of interpretation. Error bars SEM. Overlay panels include blue nuclear DAPI stain. Scale bar in A represents 5μm and 2.5μm within insets. N=3

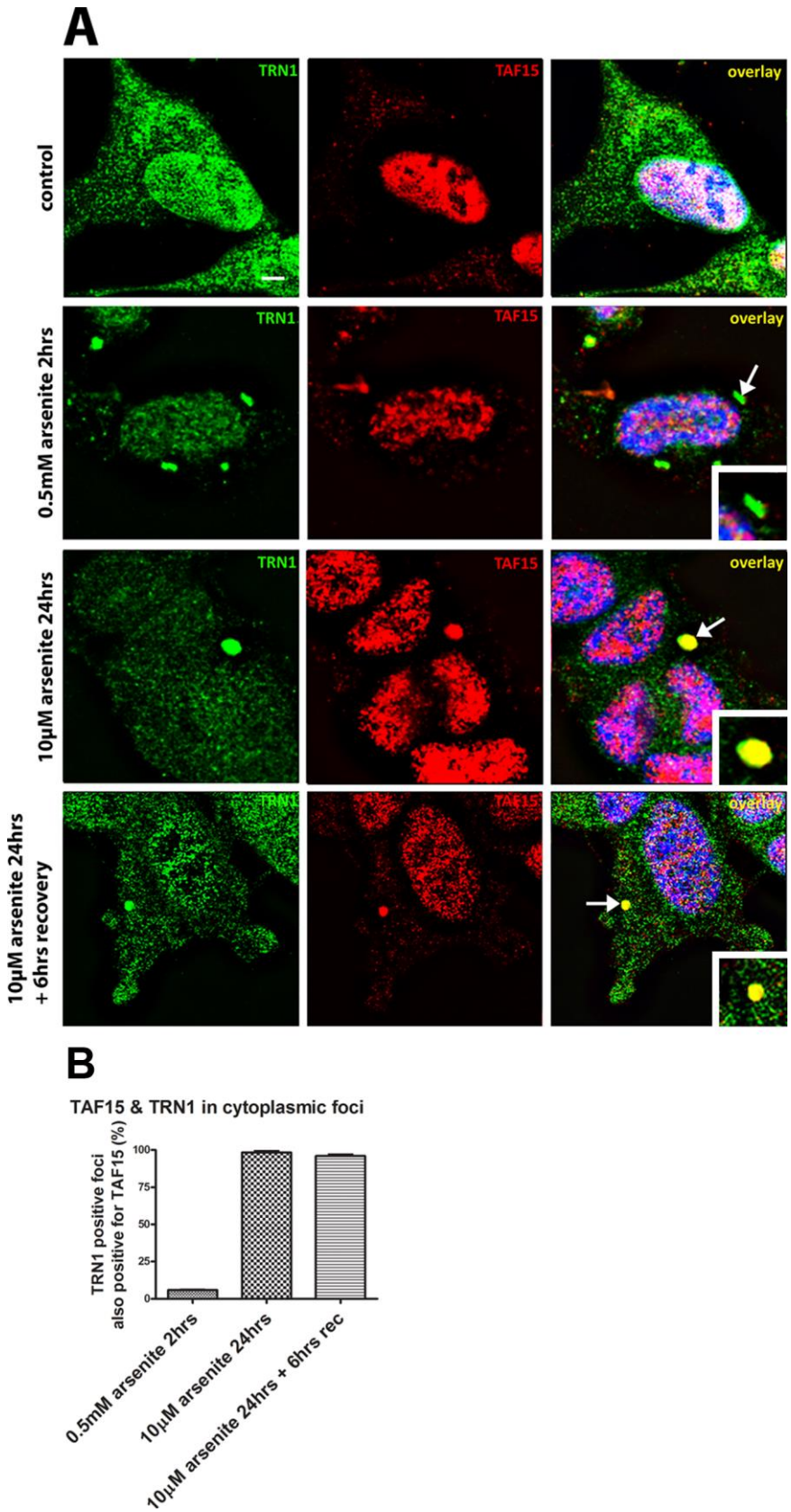

Figure 4.10. Arsenite stress induces translocation of nuclear TAF15 to cytoplasmic pools showing co-positivity with TRN1 stress granules after prolonged stress. Recovery in fresh media leaves TRN1 and TAF15 positive foci. TRN1 positive foci (A arrows). Co-localisation quantification of foci counts shows 5.93% co-localisation in TRN1 foci at 2hrs but 98.39% at 24hrs, and 96.03% co-localisation after 6hrs recovery (B). Counts

graphed as percentage of TRN1 foci also positive for TAF15 for ease of interpretation. Error bars SEM. Overlay panels include blue nuclear DAPI stain. Scale bar in A represents 5μm and 2.5μm within insets. N=3

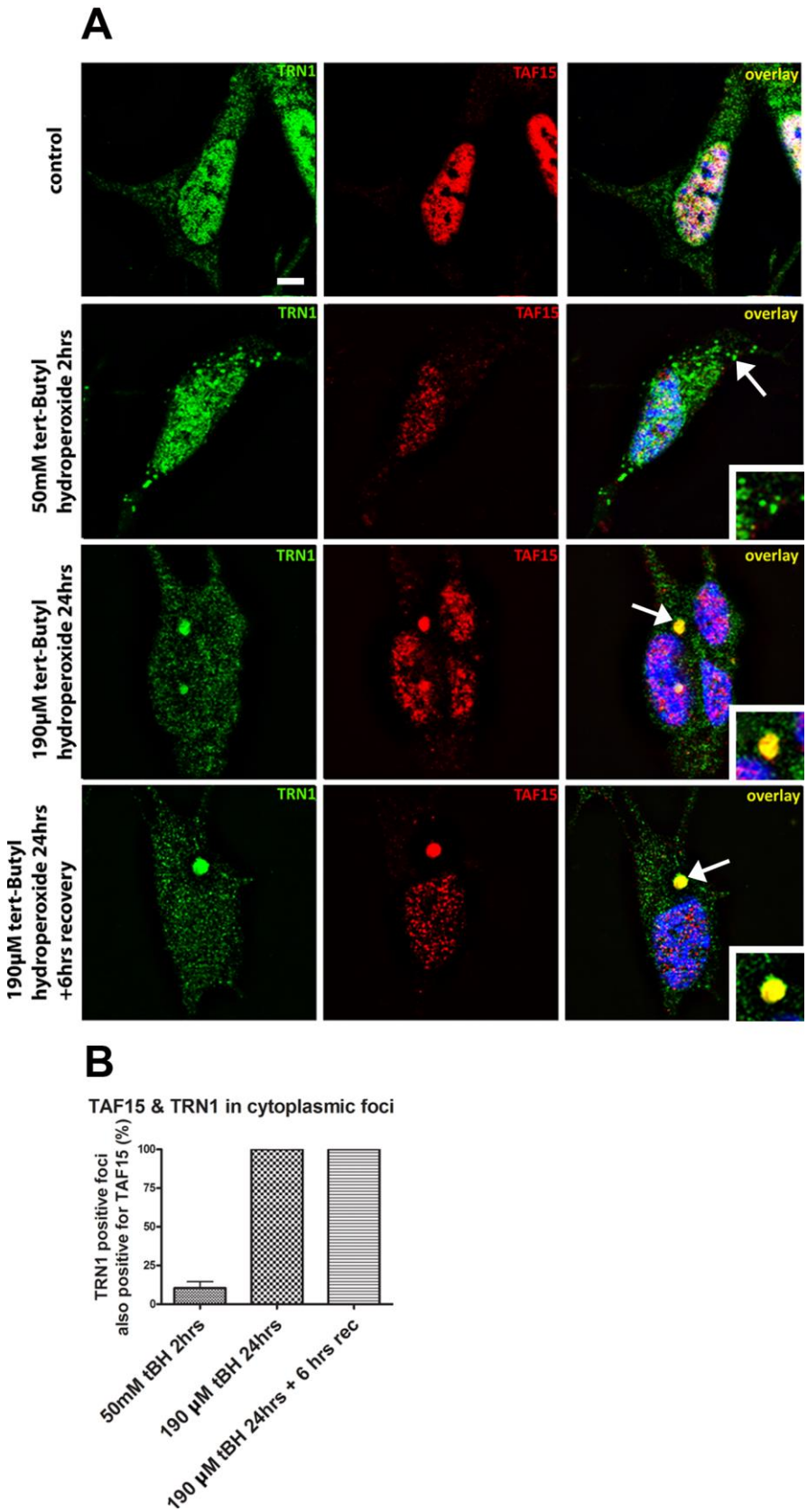

Figure 4.11. tBH stress induces translocation of nuclear TAF15 to the cytoplasmic compartment s showing co-positivity with TRN1 stress granules after prolonged stress. Recovery in fresh media leaves TRN1 and TAF15 positive foci. TRN1 positive foci (A arrows). Co-localisation quantification of foci counts shows 10.46% co-localisation in TRN1 foci at 2hrs but 100% at 24hrs, and 100% co-localisation after 6hrs recovery (B).

Counts graphed as percentage of TRN1 foci also positive for TAF15 for ease of interpretation. Error bars SEM. Overlay panels include blue nuclear DAPI stain. Scale bar in A represents 5µm and 2.5µm within insets. N=3

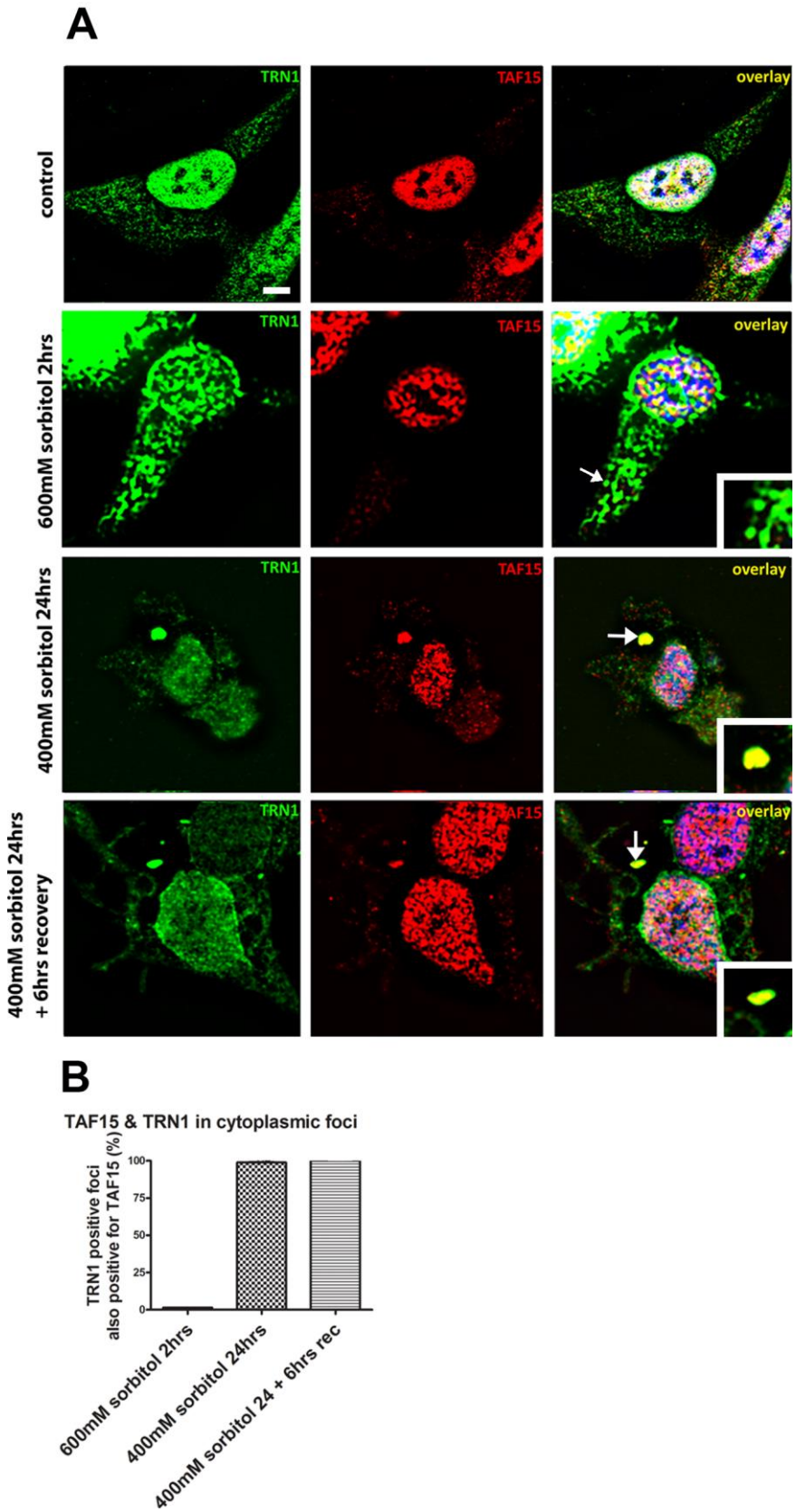

Figure 4.12. Sorbitol stress induces translocation of nuclear TAF15 to cytoplasmic pools showing co-positivity with TRN1 stress granules after prolonged stress. Recovery in fresh media leaves TRN1 and TAF15 positive foci. TRN1 positive foci (A arrows). Co-localisation quantification of foci counts shows 1.48% co-localisation in TRN1 foci at 2hrs but 98.93% at 24hrs, and 100% co-localisation after 6hrs recovery (B). Counts

graphed as percentage of TRN1 foci also positive for TAF15 for ease of interpretation. Error bars SEM. Overlay panels include blue nuclear DAPI stain. Scale bar in A represents 5μm and 2.5μm within insets. N=3

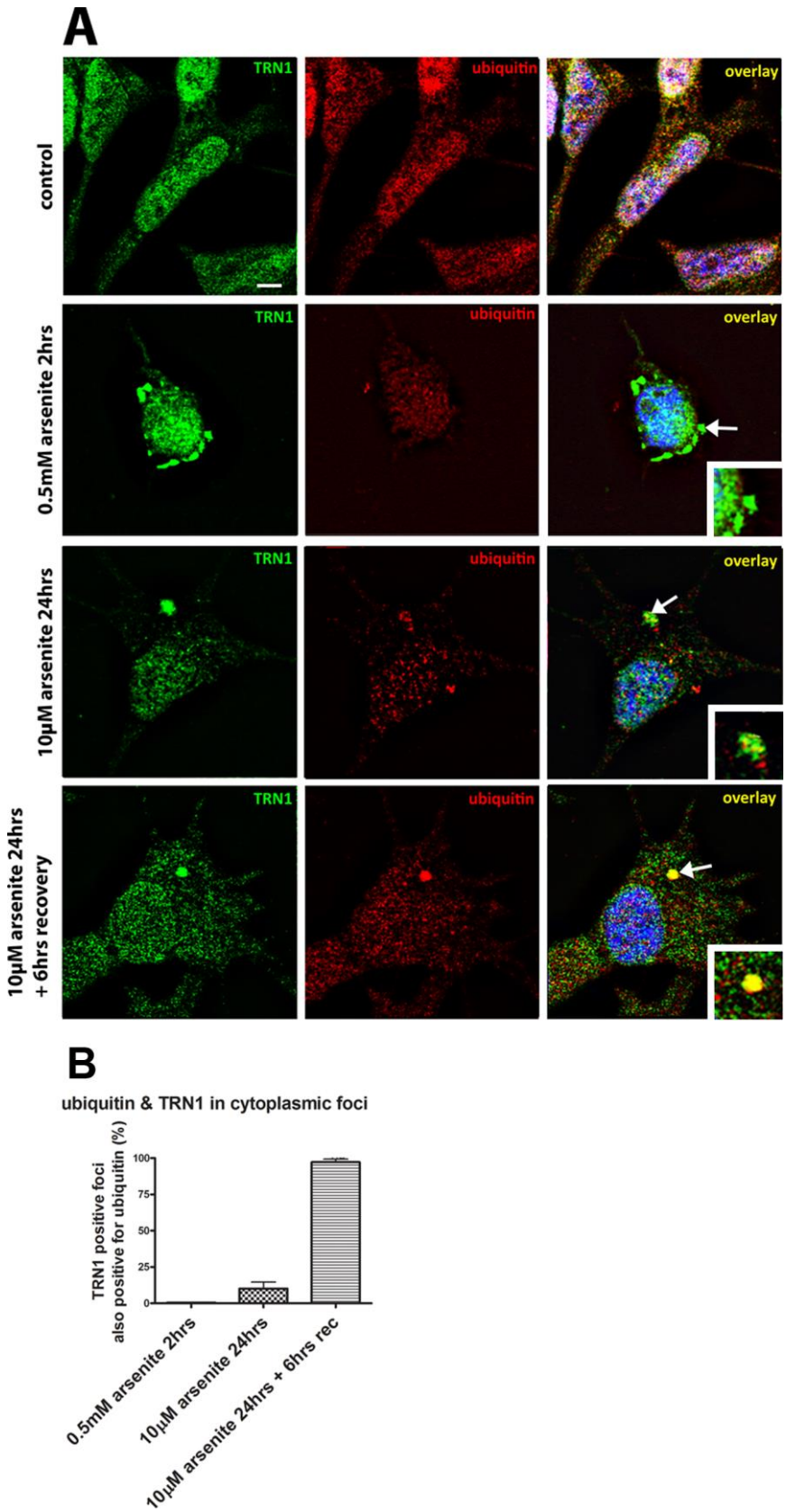

Figure 4.13. Ubiquitin is found within TRN1 foci only after recovery in fresh media from arsenite stress. TRN1 positive foci (A arrows). Co-localisation quantification of foci counts shows 0.56% co-localisation in TRN1 foci at 2hrs and 10.12% at 24hrs, but 97.22% co-localisation after 6hrs recovery (B). Counts graphed as percentage of TRN1 foci also positive for ubiquitin for ease of interpretation. Error bars SEM. Overlay panels

include blue nuclear DAPI stain. Scale bar in A represents 5μm and 2.5μm within insets. N=3

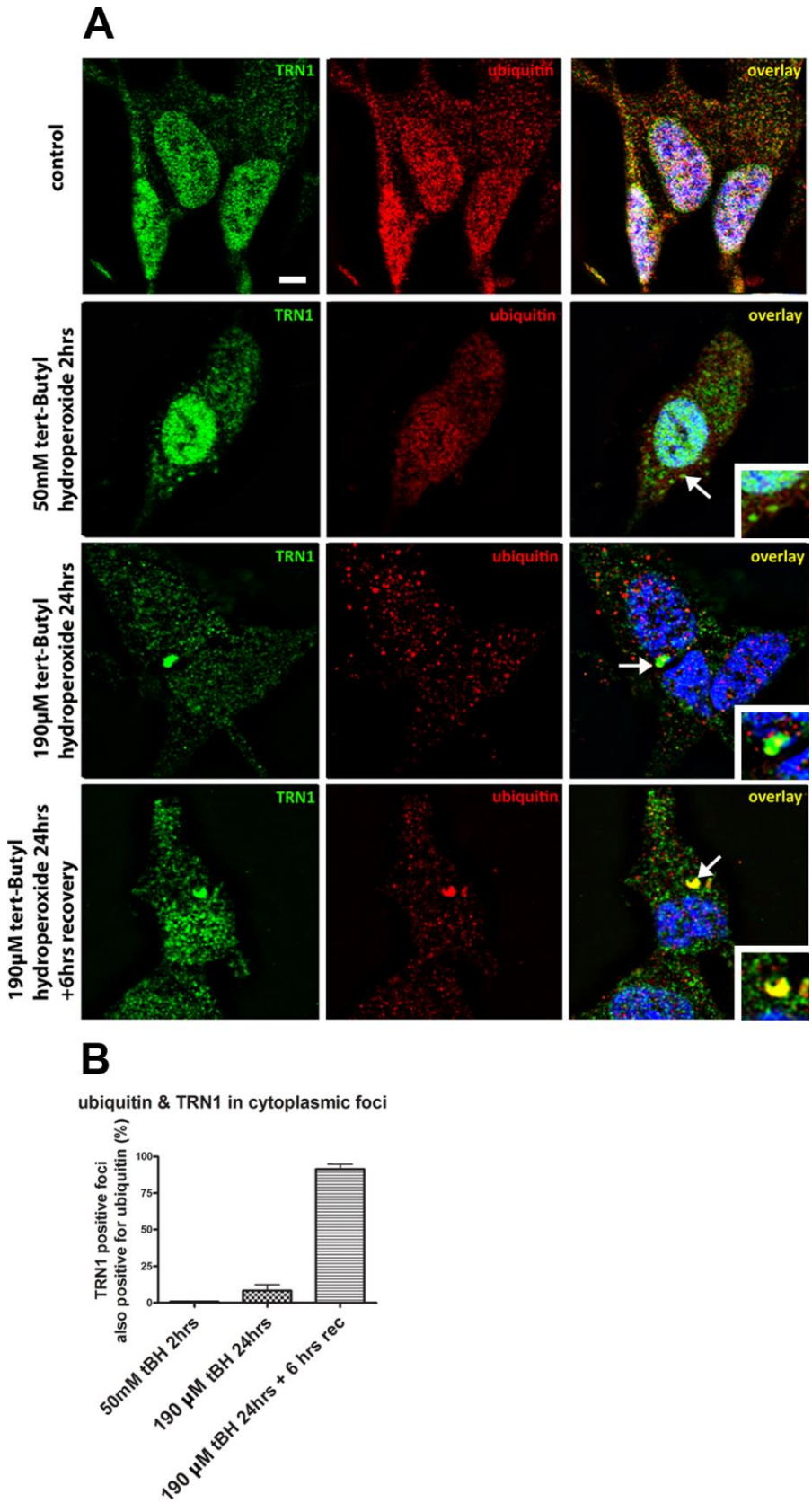

Figure 4.14. Ubiquitin is found within TRN1 foci only after recovery in fresh media from tBH stress. TRN1 positive foci (A arrows). Co-localisation quantification of foci counts shows 0.86% co-localisation in TRN1 foci at 2hrs and 8.34% at 24hrs, but 91.34% co-localisation after 6hrs recovery (B). Counts graphed as percentage of TRN1 foci also

positive for ubiquitin for ease of interpretation. Error bars SEM. Overlay panels include blue nuclear DAPI stain. Scale bar in A represents 5μm and 2.5μm within insets. N=3

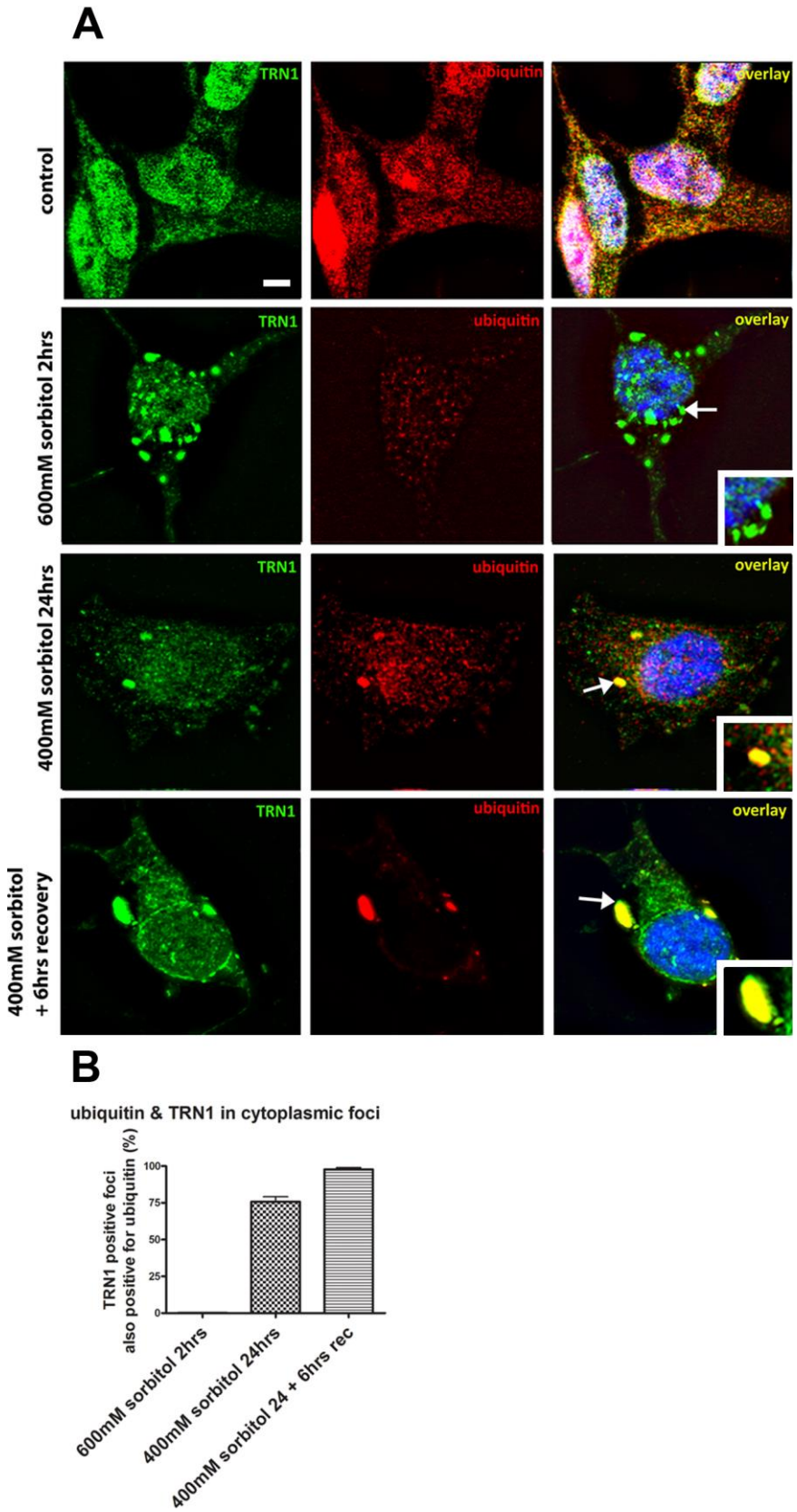

Figure 4.15. Ubiquitin is found within TRN1 foci after prolonged sorbitol stress and recovery in fresh media. TRN1 positive foci (A arrows). Co-localisation quantification of foci counts shows 0.21% co-localisation in TRN1 foci at 2hrs but 75.86% at 24hrs, and 97.82% co-localisation after 6hrs recovery (B). Counts graphed as percentage of TRN1 foci also positive for ubiquitin for ease of interpretation. Error bars SEM. Overlay panels

include blue nuclear DAPI stain. Scale bar in A represents 5μm and 2.5μm within insets. N=3

4.9 Statistical analysis of TRN1 foci reveals significant changes

To illustrate the core findings of this immunocytochemical study, statistical analysis was undertaken by one-way ANOVA and Bonferroni post-test. To summarise the significant findings, the loss of G3BP in TRN1 foci after recovery from stress (arsenite, tBH or sorbitol) is significant. The gain of ubiquitin positivity in TRN1 foci after recovery is also significant. Maximal FUS positivity in TRN1 foci is achieved by acute sorbitol stress. Maximal EWS positivity in TRN1 foci is achieved by oxidative stress (arsenite or tBH). Maximal TAF15 positivity in TRN1 foci is achieved by prolonged stress (arsenite, tBH or sorbitol), and there is no significant difference between stressors. Maximal ubiquitin positivity in TRN1 foci is achieved after recovery from stress (arsenite, tBH, or sorbitol), and there is no significant difference between stressors.

Statistical analysis of G3BP co-localisation with TRN1 foci shows the reduction seen after 6 hours recovery in fresh media is significant for 24 hours 10μM arsenite ($p<0.001$), and 24 hours 400mM sorbitol ($p<0.001$) (Figure 4.16 A). Unfortunately not enough data points were recorded for meaningful analysis of 24 hours 190μM tBH (i.e. too few foci were seen to allow the analysis to run).

Additionally, the increase in ubiquitin positive TRN1 foci seen after recovery is also significant for arsenite ($p<0.001$), tBH ($p<0.001$), and sorbitol ($p<0.05$) (Figure 4.16 B).

Comparing FUS co-localisation with TRN1 foci under acute (2 hours) arsenite 0.5mM, tBH 50mM and sorbitol 600mM treatment shows there is statistically more FUS positive TRN1 foci when cells are subjected to sorbitol stress compared to arsenite ($p<0.001$) or tBH ($p<0.001$). Repeating this analysis for the EWS protein shows there are significantly fewer EWS positive TRN1 foci when the cells are subjected to sorbitol stress compared to arsenite ($p<0.001$), and tBH ($p<0.001$). No difference in TAF15 or ubiquitin positive TRN1 foci is seen across the three treatments in the acute stress condition (Figure 4.16 C).

Comparing FUS co-localisation with TRN1 foci under prolonged (24 hours) arsenite 10μM, tBH 190μM, and 400mM sorbitol treatment shows there was no significant differences in FUS positive TRN1 foci between arsenite and sorbitol or tBH and sorbitol treated cells. Repeating the analysis for EWS shows there is significantly fewer EWS positive TRN1 foci when the cells are subjected to sorbitol stress, compared with arsenite ($p<0.001$), or tBH ($p<0.001$). There are no significant differences in the number of TAF15 positive TRN1 foci between arsenite, tBH or sorbitol treated cells in the prolonged stress condition. Additionally, the number of ubiquitin positive TRN1 foci after sorbitol treatment was significantly higher compared to arsenite ($p<0.001$), or tBH ($p<0.001$) (Figure 4.16 D). No significant difference between arsenite and tBH conditions was noted.

Comparing FUS co-localisation with TRN1 foci after 6 hours of recovery from prolonged (24 hours) arsenite 10μM, tBH 190μM, and 400mM sorbitol treatment shows there are significantly more FUS positive TRN1 foci after recovery from tBH compared to arsenite ($p<0.001$) or sorbitol ($p<0.001$). No significant differences in FUS positive TRN1 foci were apparent between arsenite and sorbitol treated cells. Repeating the analysis for EWS shows significantly fewer EWS positive TRN1 foci in cells recovering from sorbitol stress compared to arsenite ($p<0.001$), or tBH ($p<0.001$). No significant difference in EWS positive TRN1 foci was noted after recovery from arsenite compared to tBH stress. Finally, no significant differences were noted in TAF15 or ubiquitin positive TRN1 foci produced after recovery from arsenite, tBH or sorbitol stress (Figure 4.16 E).

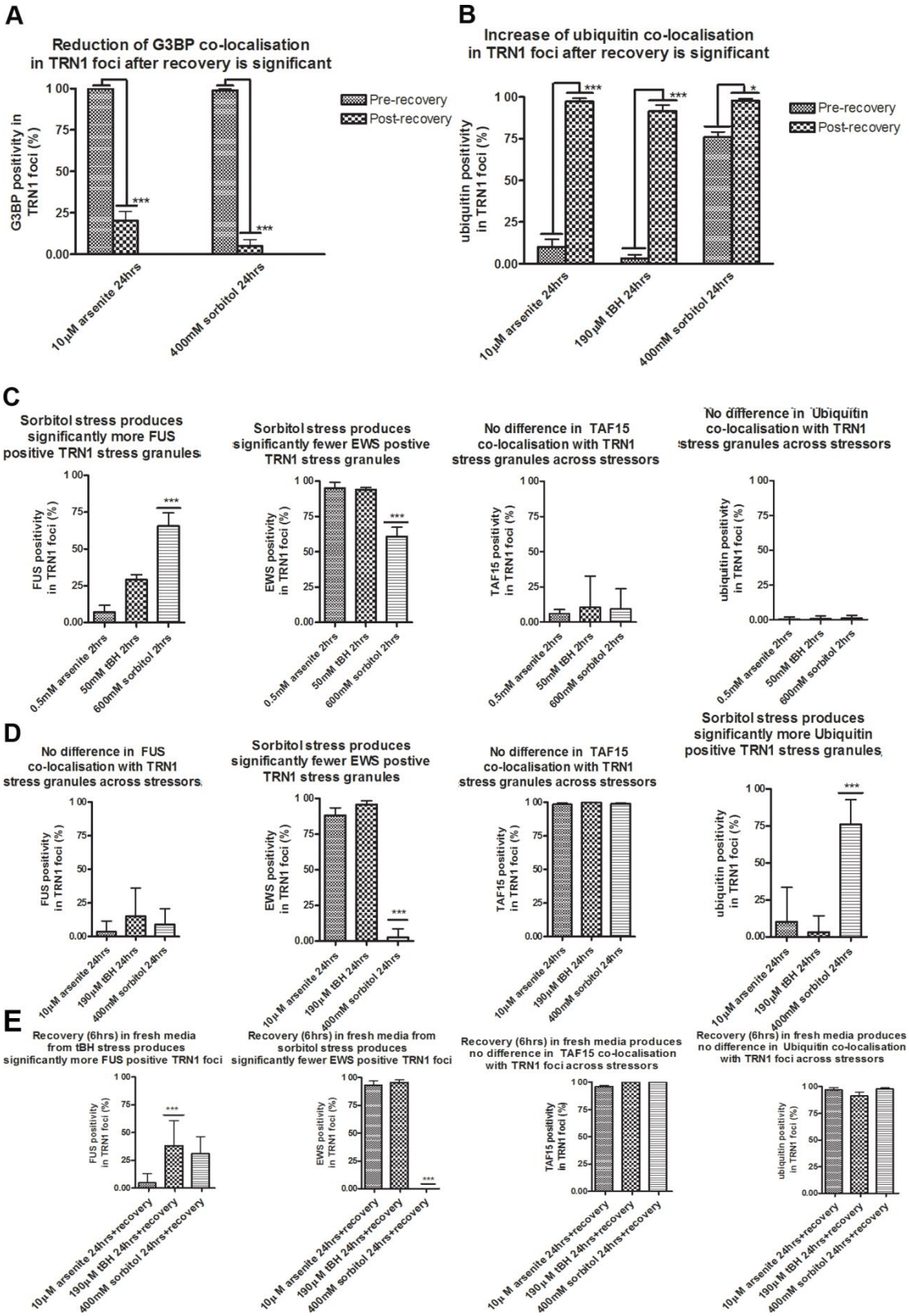

Figure 4.16. Statistical analysis of TRN1 stress granule foci positivity for the FET proteins G3BP and ubiquitin. One-way ANOVA with bonferroni correction identifies significant difference under different conditions (* $p<0.05$ *** $p<0.001$). Changes in G3BP and ubiquitin positivity pre and post 6hrs recovery in fresh media (A & B). Differences in FUS, EWS, TAF15 and ubiquitin positivity of TRN1 stress granule foci at 2hrs (C). Differences in FUS, EWS, TAF15 and ubiquitin positivity of TRN1 stress granule foci at

24hrs (D). Differences in FUS, EWS, TAF15 and ubiquitin positivity of TRN1 foci after 24hrs of stress and 6hrs of recovery in fresh media. Error bars SD.

4.10 Emetine pre-treatment prevented the formation of SGs and post-stress foci.

Emetine is a well-characterized pharmacological agent known to stabiles the polysome thereby preventing the formation of stress granules. To further confirm that the structures observed were indeed stress granules, and to investigate whether the TRN1 foci seen after recovery were post-stress granule foci, SH-SY5Ycells were pre-treated with 6µg/ml emetine for two hours before repeating all the stress conditions. In all of the stress conditions investigated here, emetine pretreatment prevented the formation of stress granules. Moreover, the TRN1 positive 'post-stress foci' were absent from the 24 hour stress followed by 6 hour recovery conditions (Figure 4.16). However, emetine pretreatment produced a much more pronounced TRN1 re-localisation to the cytoplasm when the cells were subjected to stress, compared to stress alone. Interestingly, even after 6 hours of recovery in fresh media, TRN1 had not returned to the nucleus.

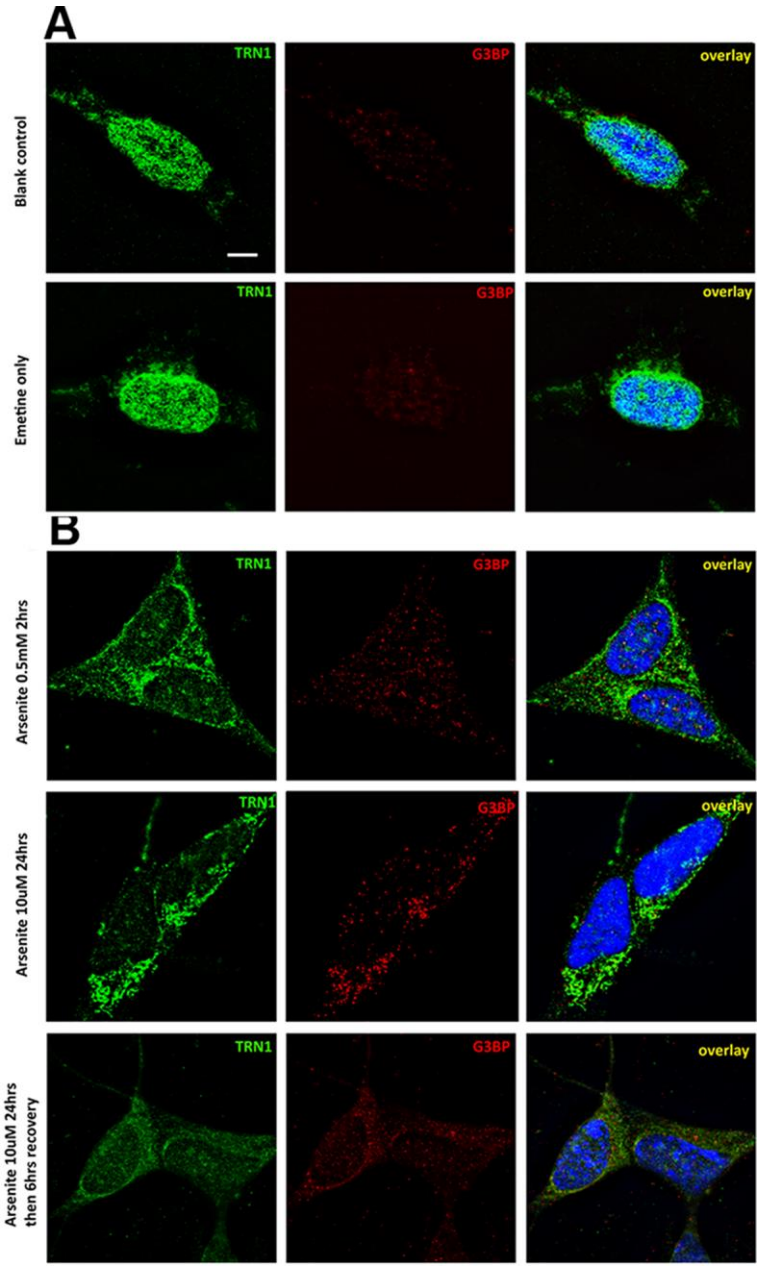
A
TRN1
G3BP
overlay
Blank control
TRN1
G3BP
overlay
Emetine only
B
TRN1
G3BP
overlay
Arsenite 0.5mM 2hrs
TRN1
G3BP
overlay
Arsenite 10uM 24hrs
TRN1
G3BP
overlay
Arsenite 10uM 24hrs
then 6hrs recovery

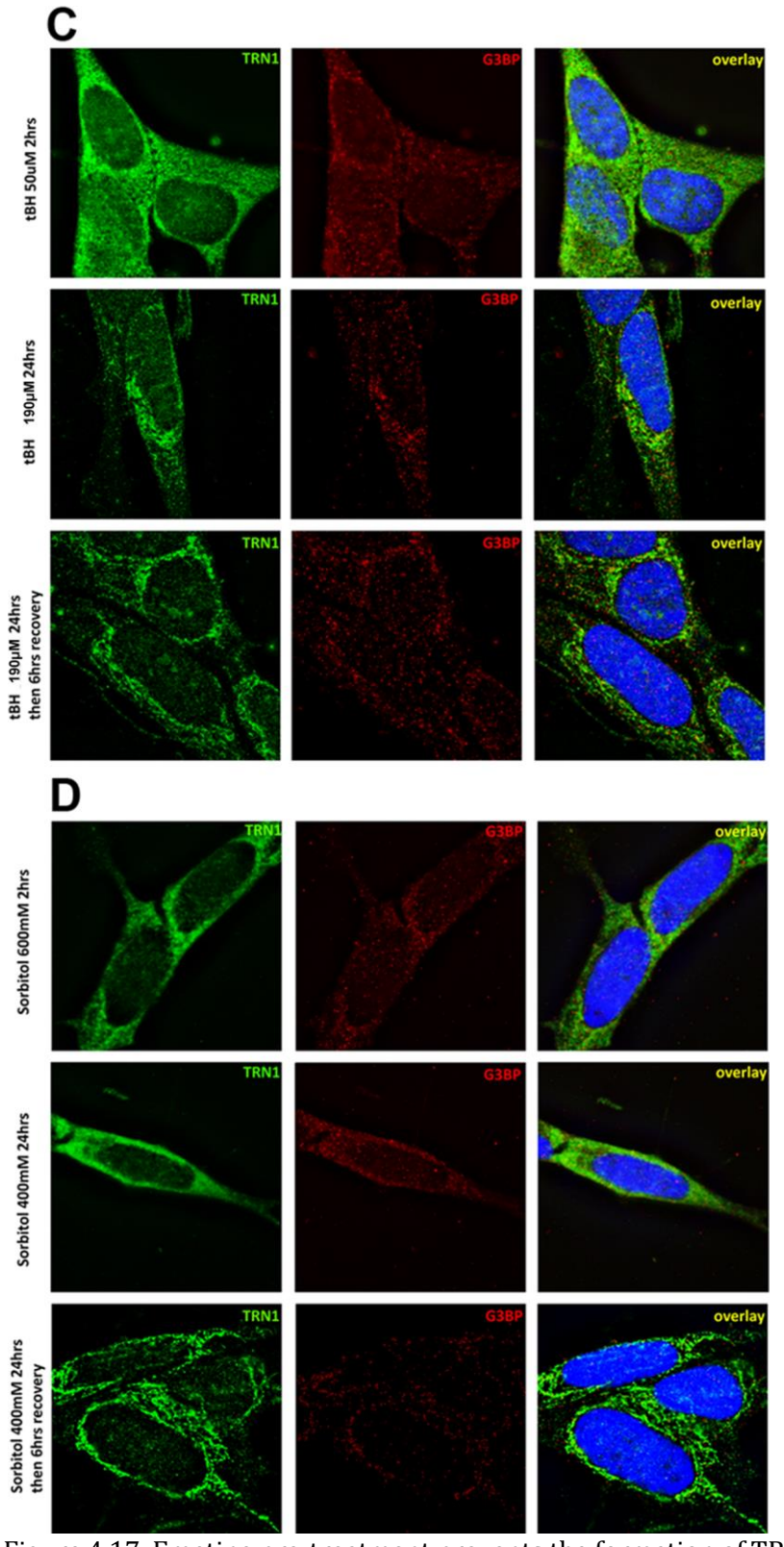

Figure 4.17. Emetine pre-treatment prevents the formation of TRN1 positive stress granules but not the re-localisation to the cytoplasm. In blank untreatred control and emetine treated, TRN1 is nuclear and G3BP is weak and diffuse (A). Arsenite, tBH, or sorbitol stress does not form G3BP positive stress granules but does result in TRN1 cytoplasmic re-localisation (B, C and D). Post-stress granule TRN1 foci are not present in emetine pre-treated stress-and-recovery cells. Scale bar in A represents 5µm. N=3

4.11 The TRN1 positive post-stress granule foci are P-bodies

To further investigate the nature of the TRN1 positive G3BP negative foci found after 6 hours of recovery in fresh media, these cells were stained for the P-body marker, mRNA decapping enzyme 1a (DCP1a). P-bodies are functionally related to stress granules because whilst stress granules collate the non-essential mRNA, the degradation of the mRNA takes place in P-bodies. Much like stress granules they are non-membranous aggregates that form and dissociate as required, and they are often found immediately adjacent to stress granules. However, unlike stress granules they are always present within the cell, even in the absence of stressors. Immunocytochemistry reveals that the TRN1 foci formed after arsenite, tBH or sorbitol stress followed by recovery in fresh media are strongly positive for DCP1a (Figure 4.17 B C and D arrows). Furthermore, whilst the TRN1 foci are P-bodies, not all P-bodies are TRN1 positive (Figure 4.17 A).

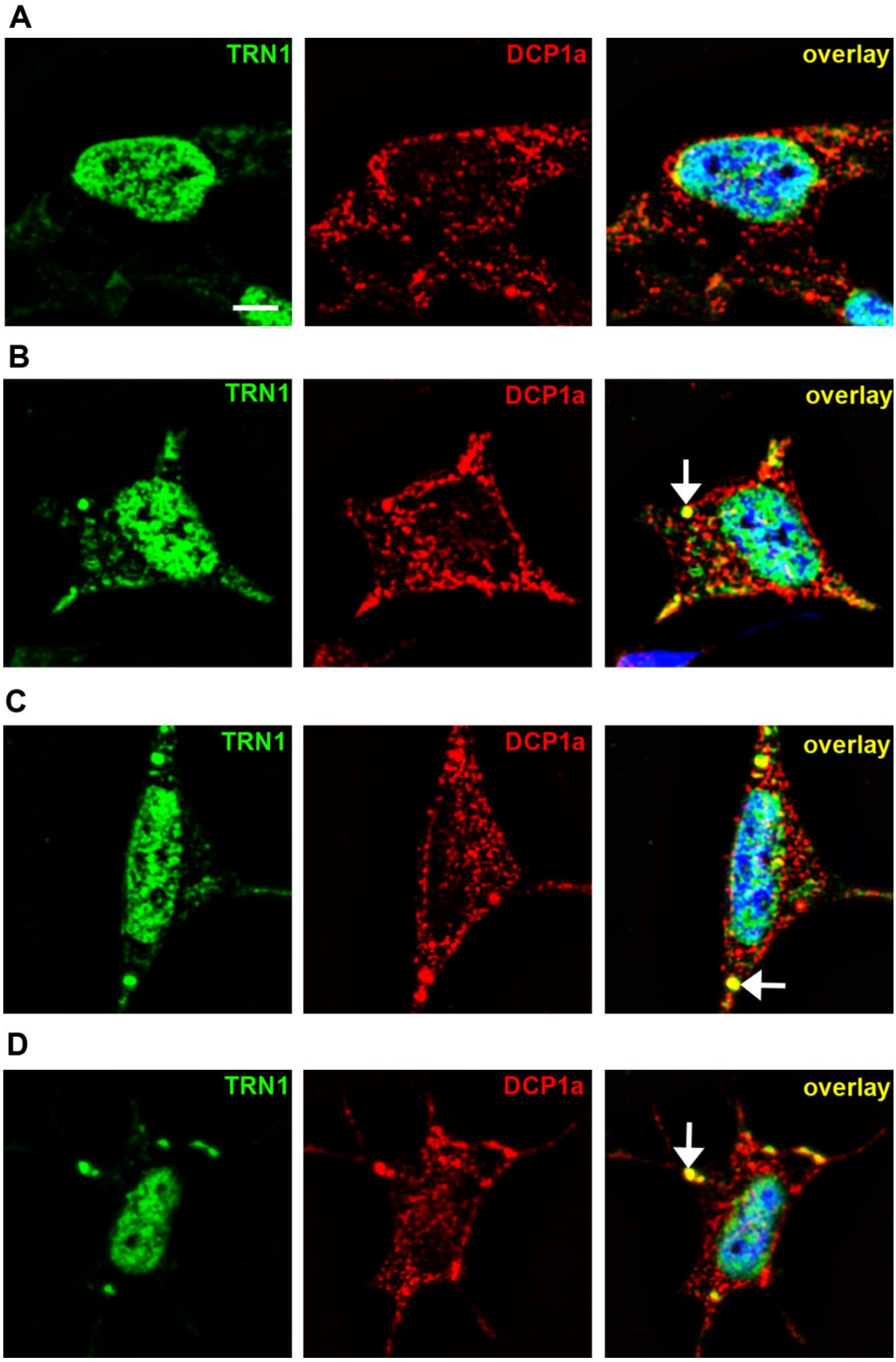

Figure 4.18. The TRN1 positive foci observed after recovery are P-bodies. Unstressed control cells shown normal nuclear TRN1 staining and numerous P-bodies (A). 10µM arsenite (B), 190µM tBH (C), or 400mM sorbitol (D) for 24 hours followed by 6 hours recovery in fresh media produces TRN1 positive foci that co-localise with the P-body marker DCP1a (arrow). Scale bar in A represents 5µm. N=3

4.12 Oxidative stress, not osmotic stress increases the TRN1 found in the urea fraction

Given that highly insoluble TRN1 is associated with FTLD-FUS (Brelstaff et al., 2011), the solubility status of TRN1 was investigated with a similar technique to those investigations in brain tissue. Cells were lysed in RIPA buffer and untracentrifuged to reveal the RIPA insoluble pellet. This was then resuspended in urea buffer to give the highly insoluble fraction. Immunoblotting and densiometric quantification shows that, in a time dependent manner, the oxidative stressors arsenite and tBuOOH increase the amount of TRN1 found in the highly insoluble fraction (0.5mM arsenite for 2 hours $p<0.01$, 50mM tBH for 2 hours $p<0.01$) (Figure 4.18 A and B). This pattern was not seen with sorbitol stress (Figure 4.18 C). No change was seen in the TRN1 detected in the RIPA soluble fraction (Figure 4.18 A, B and C). No change was seen in either the RIPA or urea fractions of TRN1 when treated with any 24hr or 24hr plus recovery paradigm (Figure 4.18 D, E and F). To confirm that the method of solubility fractionation was robust and did not permit carry-over of proteins from the RIPA to the urea fractions blots were probed for the soluble enzyme glyceraldehyde 3-phosphate dehydrogenase (GAPDH). None of the acute stress conditions revealed any detectable urea soluble GAPDH (Figure 4.18 G). This presence of GAPDH solely in the RIPA fraction has been reported elsewhere (Igaz et al., 2011).

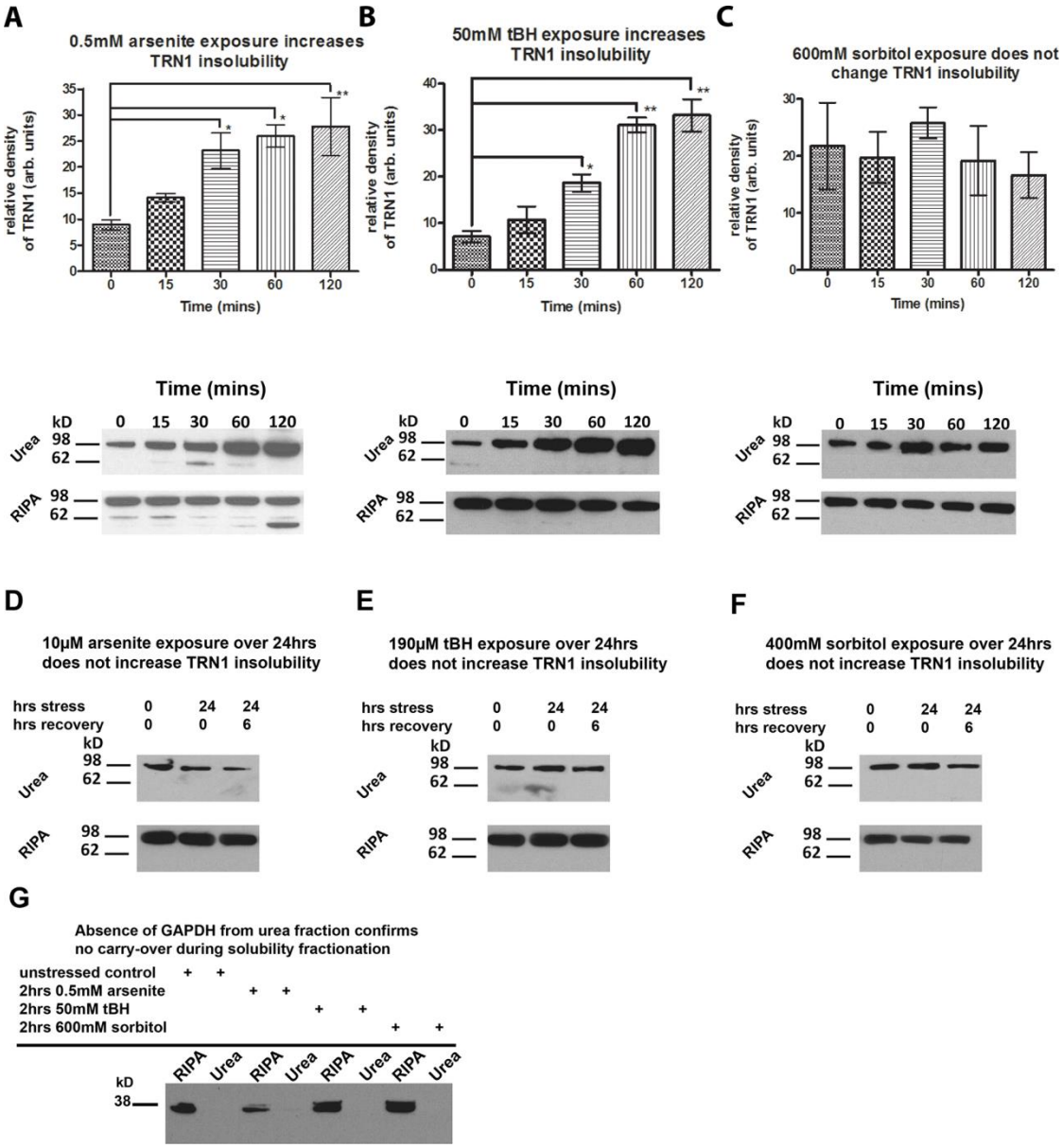

Figure 4.19. Acute oxidative stress increases the levels of insoluble TRN1. Densitometric quantification of immunoblots and analysis with one-way ANOVA followed by Dunnett's post-test reveals 0.5mM arsenite increases detectable urea soluble TRN1 at 30 (*p<0.05), 60 (*p<0.05) and 120 minutes (**p<0.01), and 50mM tBH over 30 (*p<0.05) 60 (**p<0.01) and 120 (*p<0.01) hours increases the detectable urea soluble TRN1, but does not decrease the RIPA soluble TRN1 (A and B). No significant change in urea or RIPA soluble TRN1 levels is noted after 600mM sorbitol stress for 2 hours (C). Exposure to lower concentrations off stress over 24 hours does not affect urea or RIPA soluble TRN1 levels (D, E and F). No carry-over of proteins from the RIPA to urea fraction is seen with this technique (G). Representative immunoblots of three independent experiments. TRN1 molecular weight approximately 102kDa. 5μg of protein was loaded in each lane. Normalisation to loading control was not possible due to extraction method. N=3

4.13 The prevention of stress granule formation does not affect oxidative stress induced increase of TRN1 found in the urea fraction

TRN1 undergoes a dramatic compartmental re-localisation to stress granules which is accompanied by an increase in urea soluble TRN1 upon oxidative stress. To investigate whether these two phenomena are related SH-SY5Y cells were pre-treated with 16.3μM emetine dihydrochloride. The resulting stabilisation of polysomes and suspension of protein elongation prevents the formation of stress granules in response to 2 hours 0.5mM arsenite stress. The cells were then lysed and fractionated as previously described. Comparison of urea soluble TRN1 levels from emetine pre-treated, non-pre-treated, and unstressed control cells reveals the formation of stress granules is not the cause of increased urea soluble TRN1 levels (Figure 4.19).

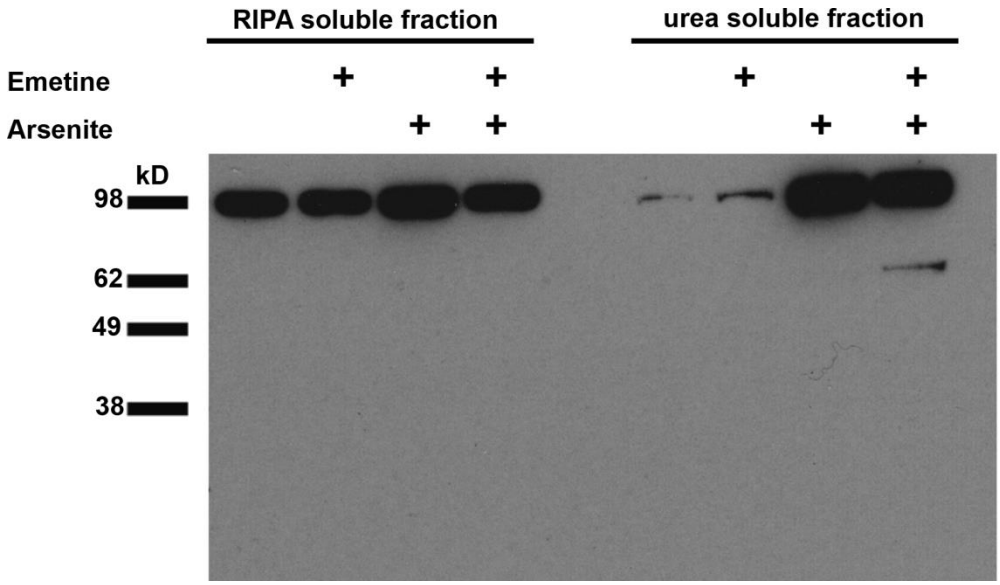

Figure 4.20. Emetine pre-treatment does not prevent arsenite induced increase of insoluble TRN1. Immunoblotting of the urea soluble fraction shows a dramatic increase of insoluble TRN1 levels under 0.5mM arsenite for 2 hours compared with control cells. This is not prevented by blocking stress granule formation via 16.3μM emetine pre-treatment. No loss of RIPA soluble TRN1 is seen under any treatment condition. Representative immunoblot of three independent experiments. Molecular weight of TRN1 approximately 102kDa. 5μg of protein was loaded in each lane.

4.14 Oxidative nor osmotic stress change the levels of RIPA or urea soluble FUS

Given that oxidative stress dramatically increases the levels of urea soluble TRN1 in a manner akin to the biochemistry of FTLD-FUS, the solubility of FUS was investigated to see if this pattern repeated. Neither oxidative (0.5mM arsenite or 50mM tBH) nor osmotic (600mM sorbitol) induced a shift in insolubility similar to that seen in FTLD-FUS (Figure 4.20). This suggests that the cellular mechanisms that drive FUS insolubility may be distinct to those of TRN1. For instance FUS may have a divergent set of interacting partners that drive its increasing insolubility under specific conditions that are not replicated in vitro by oxidative or osmotic stressors.

4.15 Oxidative or osmotic stress shift TDP43 to the insoluble fraction

TDP43 is an important protein in the cause and pathology of FTLD-TDP. It also shares a good deal of similarity with FUS both in terms of structure and function. To investigate whether an RNA DNA binding protein similar to FUS is unaffected by cellular stressors, membranes were stripped and re-probed for TDP43. In contrast to FUS biochemistry, qualitative assessment shows both oxidative and osmotic stress shift TDP43 towards the insoluble fraction by reducing the RIPA soluble and increasing the urea soluble levels (Figure 4.22). This appeared to occur in a time-dependant fashion with the most pronounced loss of RIPA soluble TDP43 at 2 hours. However, this is only a qualitative assessment since the urea fraction contained several higher molecular weight bands that did not resolve sufficiently to allow clear delineation of the correct band for quantification. These may be higher molecular weight species formed by ubiquitination, or other modifications such as phosphorylation.

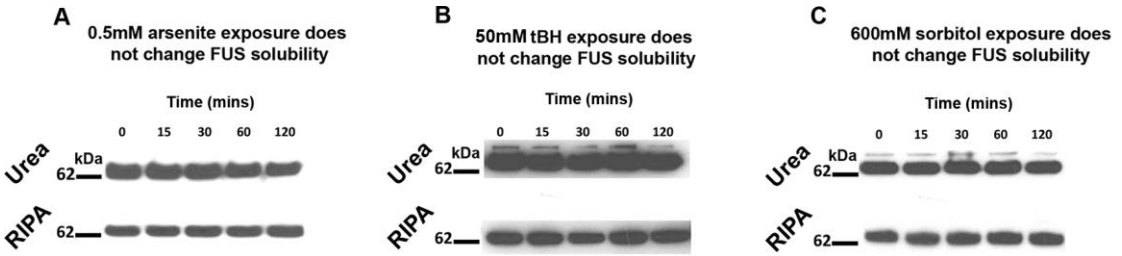

Figure 4.21. Oxidative (0.5mM arsenite or 50mM tBH) nor osmotic stress (sorbitol 600mM) affects the solubility of FUS. No change is evident in RIPA or urea soluble levels of FUS upon arsenite (A), tBH (B) or sorbitol (C) exposure. Representative immunoblot of three independent experiments. Molecular weight of FUS in SDS PAGE approximately 73kDa. 5µg of protein was loaded in each lane.

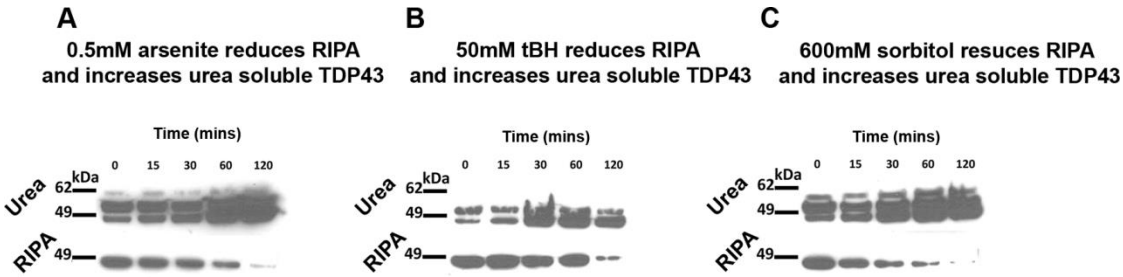

Figure 4.22. Oxidative (0.5mM arsenite or 50mM tBH) and osmotic (600mM sorbitol) stress shifts TDP43 to the insoluble fraction. Arsenite (A), tBH (B) and sorbitol (C) reduce the levels of RIPA soluble TDP43 whilst increasing the urea soluble levels. Representative immunoblot of three independent experiments. Molecular weight of TDP43 approximately 43kDa. 5µg of protein was loaded in each lane.

4.16 TRN2b can bind TRN1 cargos and may act as a redundant nuclear importer

In spite of a pronounced nuclear clearance of TRN1 in FTLD-FUS neurons (Figure 3.4) and a dramatic cytoplasmic re-localisation in stressed cells, there is often discernible nuclear FET protein (Figure 4.1-4.15). If their nuclear localisation was entirely dependent on the function of TRN1 any loss through aggregate sequestration or re-localisation should result in profound FET protein re-localisation. TRN2 has two isoforms TRN2a and TRN2b, it has been suggested that due to high homology between TRN2b and TRN1 it may act as a redundant importer of some TRN1 cargos (Rebane et al., 2004). To investigate this possibility SH-SY5Y TRN2b was immunoprecipitated using an antibody specifically targeted to TRN2b. Co-immunoprecpitation reveals detectable FUS, EWS, TAF15 and hnRNP A1 (Figure 4.22). This suggests that TRN2b could bind and possibly import these cargos which may have consequences in FTLD-FUS.

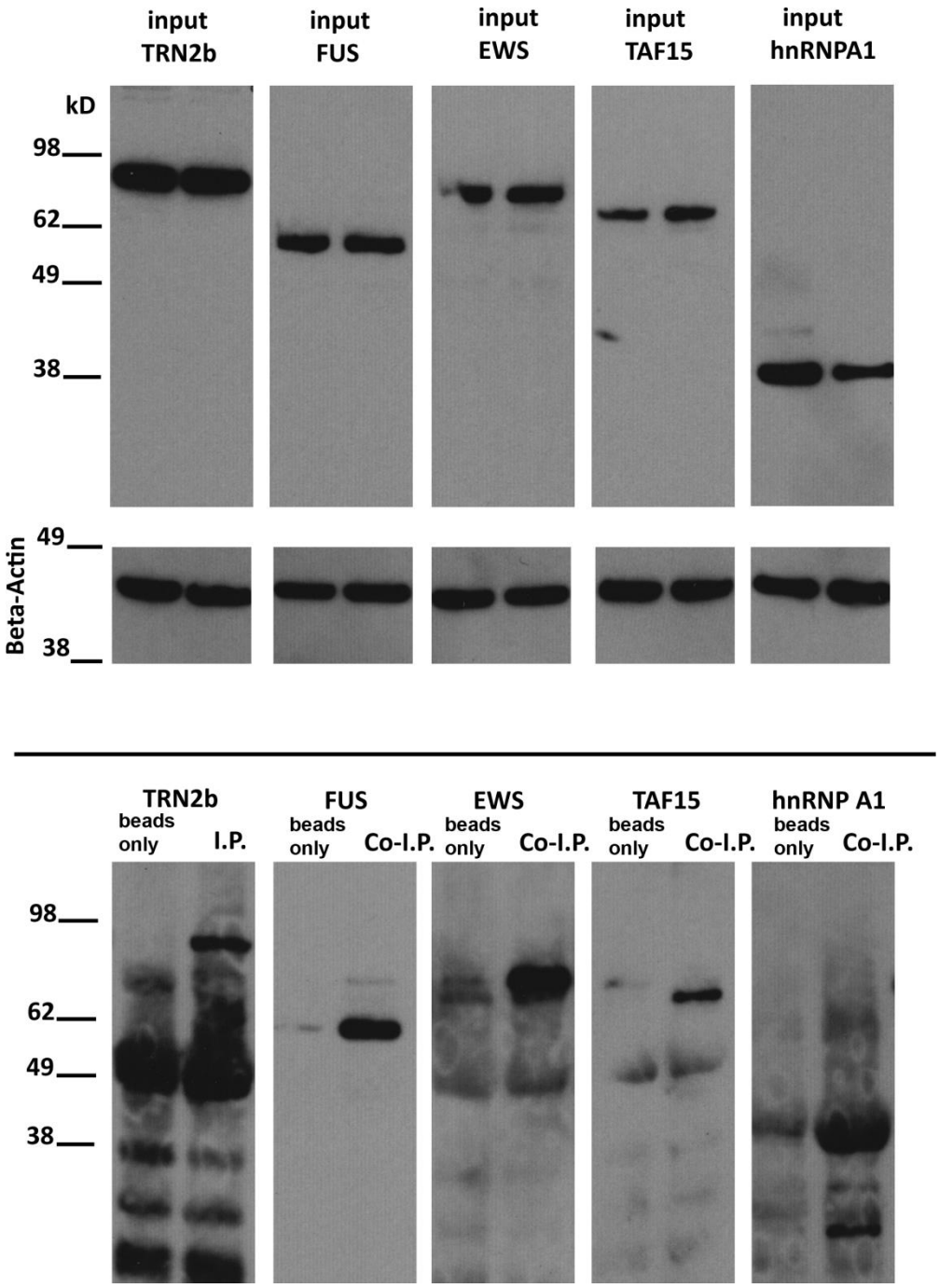

Figure 4.23. The TRN2b isoform can bind the FET proteins and the classical TRN1 cargo hnRNP A1. Co-immunoprecipitation demonstrates the TRN2b isoform of TRN2 can bind TRN1 cargos and may act as a redundant importer. Upper panel demonstrates equal input and loading by beta-actin. Lower panel beads only control lanes shows proteins only minimally bind to beads in the absence of the TRN2b antibody. I.P and Co-I.P. lanes show successful precipitation of TRN2b interacting proteins. Representative immunoblots of three independent experiments. Molecular weight of TRN2b in SDS PAGE approximately 95kD, FUS 73kD, EWS 90kD, TAF15 62kD, hnRNP A1 41kD.

4.17 TNPO1 and TNPO2 siRNA knockdown re-localises TRN1 targets to the cytoplasm

To demonstrate that the FET proteins and hnRNP A1 are targets of TRN1 import in SH-SY5Y cells TRN1 and TRN2 protein levels were knocked down by siRNA targeting of their respective mRNA. TRN2 was included in the knockdown siRNA pool because the isoform TRN2b may act as a redundant importer for these cargoes (Figure 4.23). Maximum knockdown of TRN1 and TRN2 was achieved with 100nM siRNA over 6 days (knock down transfection repeated on days 3)(Figure 4.24 A quantified in B) before toxicity induced large scale apoptosis. Immunocytochemistry reveals non-targeting scramble siRNA does not affect the normal nuclear staining of the FET proteins, hnRNP A1 or TDP43 (Figure 4.24 C). However, the FET proteins and hnRNP A1 lose their nuclear definition and re-localise to a diffuse distribution throughout the cell upon TNPO1 and TNPO2 knockdown (Figure 4.24 C). Since TDP43 is known to be imported through a separate import pathway it is unsurprising that it is unaffected by TNPO1 and TNPO2 knockdown.

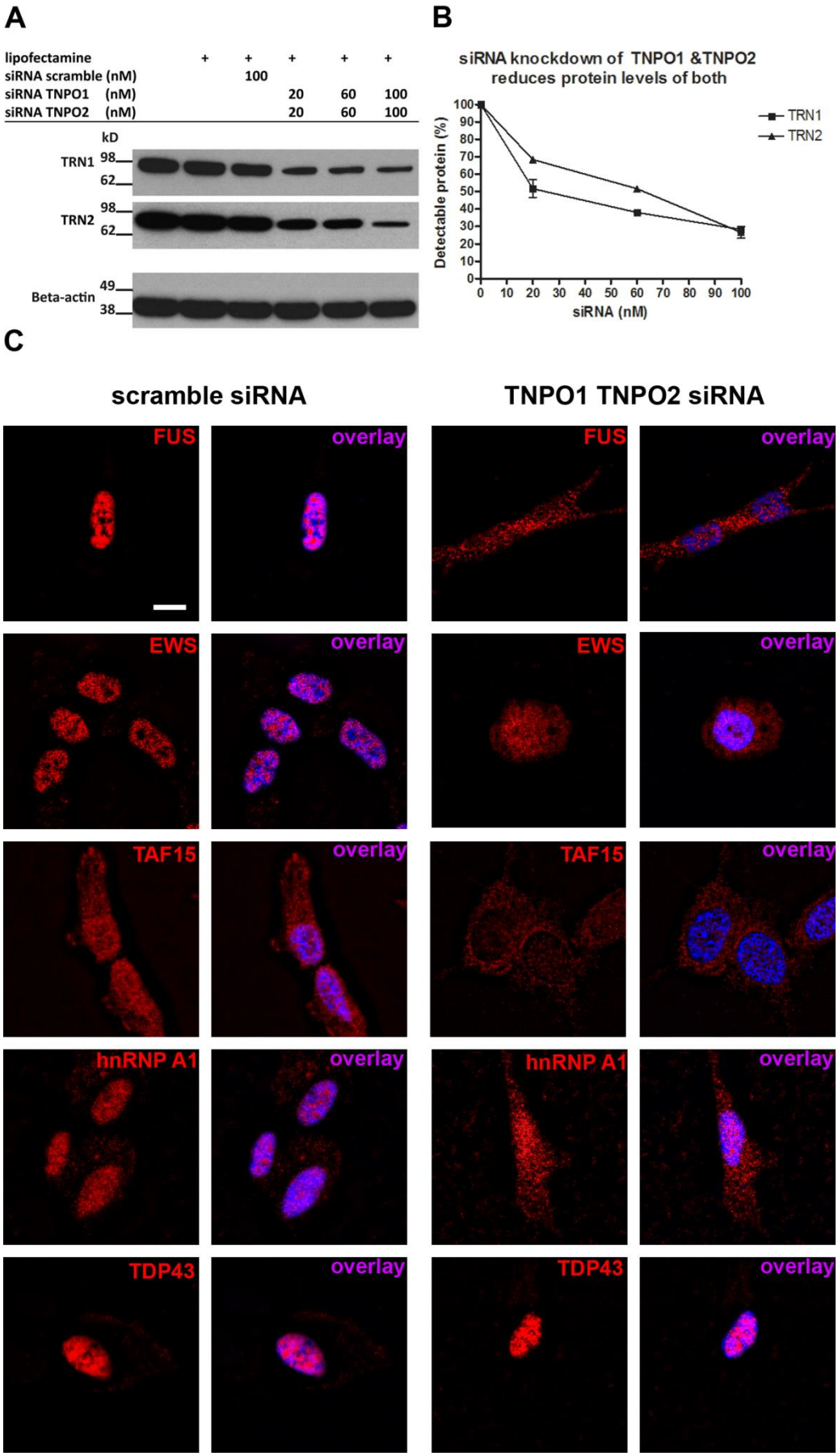
A
lipofectamine + + + + +
siRNA scramble (nM) 100
siRNA TNPO1 (nM) 20 60 100
siRNA TNPO2 (nM) 20 60 100
kD
TRN1
98
62
TRN2
98
62
Beta-actin
49
38
B
siRNA knockdown of TNPO1 &TNPO2 reduces protein levels of both
TRN1
TRN2
Detectable protein (%)
siRNA (nM)
C
scramble siRNA
TNPO1 TNPO2 siRNA
FUS
overlay
EWS
TAF15
hnRNP A1
TDP43

Figure 4.24. siRNA mediated knockdown of TRN1 and TRN2 results in approximately 70% reduction in protein levels which re-localises the FET proteins, and hnRNP A1 but not TDP43 to the cytoplasm. Maximal reduction of TRN1 and TRN2 is achieved with 100nM siRNA (A), which reaches 72.4% and 74% respectively (B). Scrambled siRNA does not affect normal nuclear staining of the FET proteins, hnRNP A1 or TDP43. Knockdown of TNPO1 and TNPO2 re-localises the FET proteins and hnRNP A1 to the cytoplasm but TDP43 remains nuclear. Representative immunoblot (A) of three independent experiments analysed for densiometric quantification (B). Molecular weight TRN1 approximately 102kD, TRN2 95kD. Scale bar 5µm.

4.18 Knockdown of TNPO1 and TNPO2 significantly increases the recruitment of FET proteins to stress granules

To further investigate the role of TRN1 in the recruitment of its cargos to stress granules, knockdown cells were subsequently subjected to 0.5mM arsenite for 2 hours. Knockdown of TNPO1 and TNPO2 resulted in a significant increase of FUS and TAF15 positive stress granules ($p<0.001$) compared with scrambled control siRNA (Figure 4.24 A quantified in B). Unlike FUS and TAF15, EWS strongly localised to stress granules even in untransfected control cells (Figure 4.7 4.8 and 4.9), this pattern holds true in scramble and TNPO1 TNPO2 siRNA transfected cells (Figure 4.24 B). No change in ubiquitin staining was observed. This suggests that cytoplasmicaly re-localised FET proteins are sequestered into stress granules to a greater degree under conditions of TRN1 and TRN2 knockdown. Perhaps most importantly, these results suggest that TRN1 and TRN2 are not required for stress granule incorporation of the FET proteins, despite being functional binding partners of those importins.

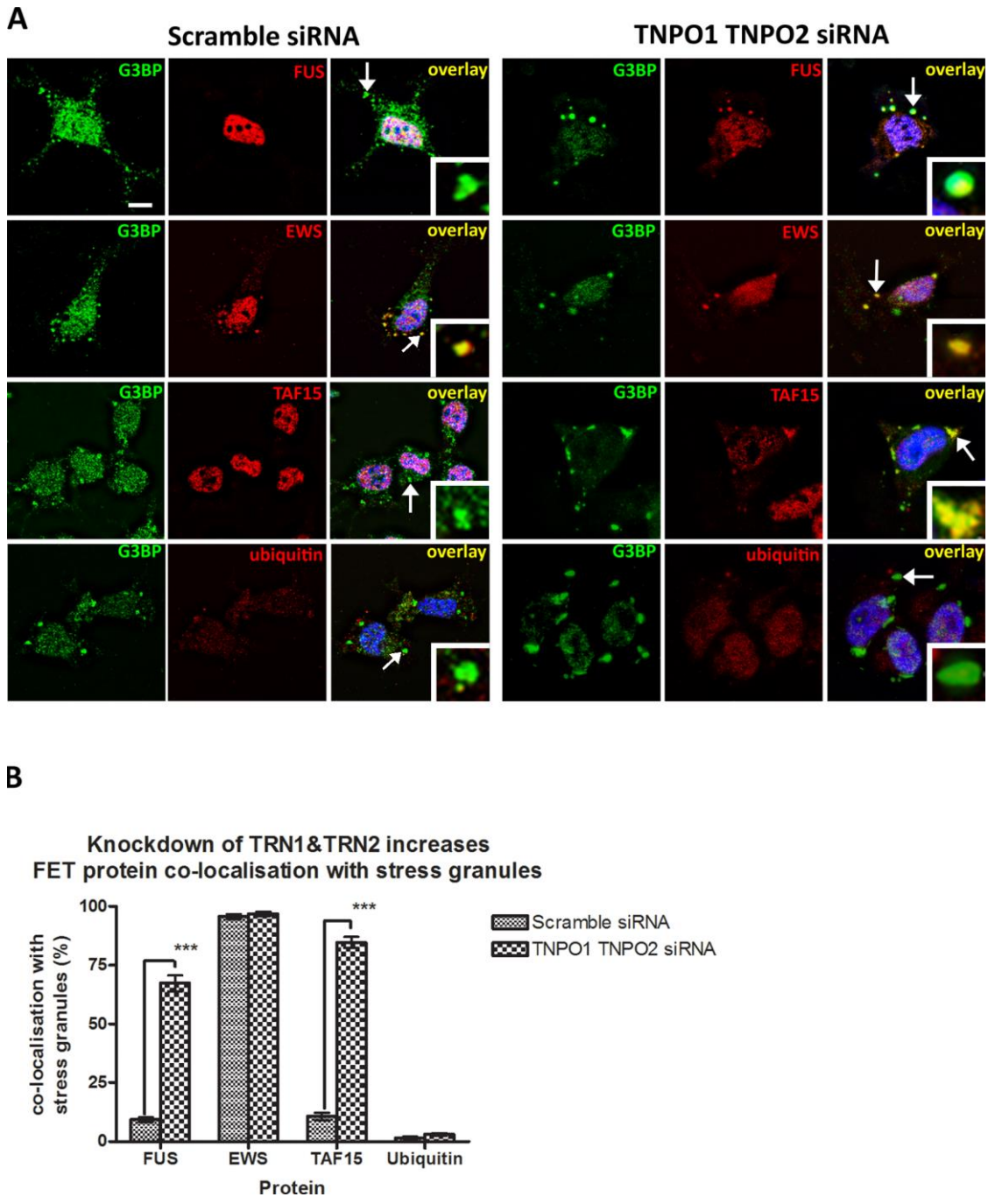

Figure 4.25. siRNA knockdown of TNPO1 and TNPO2 significantly increase FUS and TAF15 recruitment to stress granules. SH-SY5Y cells were transfected with either scramble or TNPO1 and TNPO2 siRNA before 0.5mM arsenite stress for 2 hours. Non-targetting siRNA does not perturb the formation of stress granules (A arrow) or disturb the normal nuclear localisation of the FET proteins nor affect ubiquitin staining. Knockdown of TNPO1 and TNPO2 re-localises the FET proteins to the cytoplasm and into stress granules (A arrows) upon 0.5mM arsenite stress for 2 hours. Quantification of G3BP stress granule counts also positive for FUS, EWS, TAF15 or ubiquitin in scramble or knockdown conditions via Mann-Whitney U test reveals a significant (***$p<0.001$) increase in FUS and TAF15 positive stress granules upon TNPO1 and TNPO2 knockdown (B). Scale bar in A represents 5µm and 2.5µm within insets. N=3

4.19 Over expression of TRN1 produces cytoplasmic staining that does not co-localise with FET proteins or stress granules and may be artifactual

The inclusions of FTLD-FUS have a unique immunohistochemical profile that includes TRN1 and many of its cargo proteins alongside generalised markers of aggregation like ubiquitin and p62. Stress granule based hypotheses of cytoplasmic inclusion formation appear muddied by the action of TRN1. In untransfected cell lines endogenous TRN1 strongly re-localises to stress granules, which is accompanied by incomplete FET protein incorporation. Depletion of TRN1 via siRNA increases the sequestration of FUS and TAF15 in these foci, but they now lack the key TRN1 pathology. A more accurate situation would include TRN1 and all three FET proteins cytoplasmically mis-localised and aggregating. Several models of neurodegeneration employ over expression of a key protein to accentuate a phenotype that leads to aggregate formation and or degeneration. To this end, wild-type TRN1 plasmids were transiently transfected into SH-SY5Y cells. Western blotting demonstrates that TRN1 can be successfully expressed in SHSY5Y by transient transfection and anti-myc tag antibodies can detect the TRN1-myc tagged protein. (Figure 4.25 A and B). Immunocytochemistry was performed using the myc antibody to stain for transiently expressed myc-tagged TRN1. Control untransfected cells showed minimal background staining (Figure 4.26 A). Transfection with wild type TRN1-myc produces unrefined cytoplasmic staining additional to the expected nuclear stain (Figure 4.26 C double arrows). Cytoplasmic TRN1-mycstaining does not co-localise with any of the FET proteins (Figure 4.26 C). Oxidative stress with 0.5mM arsenite for 2 hours induced stress granules (Figure 4.26 D arrows) but these did not co-localise with the TRN1-myc staining (double arrows). Cytoplasmic myc staining weakly co-localised with ubiquitin in both unstressed (Figure 4.26 C) and stressed cells (Figure 4.26 D). Despite a passing resemblance to the cytoplasmic aggregates of FTLD-FUS, the cytoplasmic staining observed here is likely an artefact of overexpression.

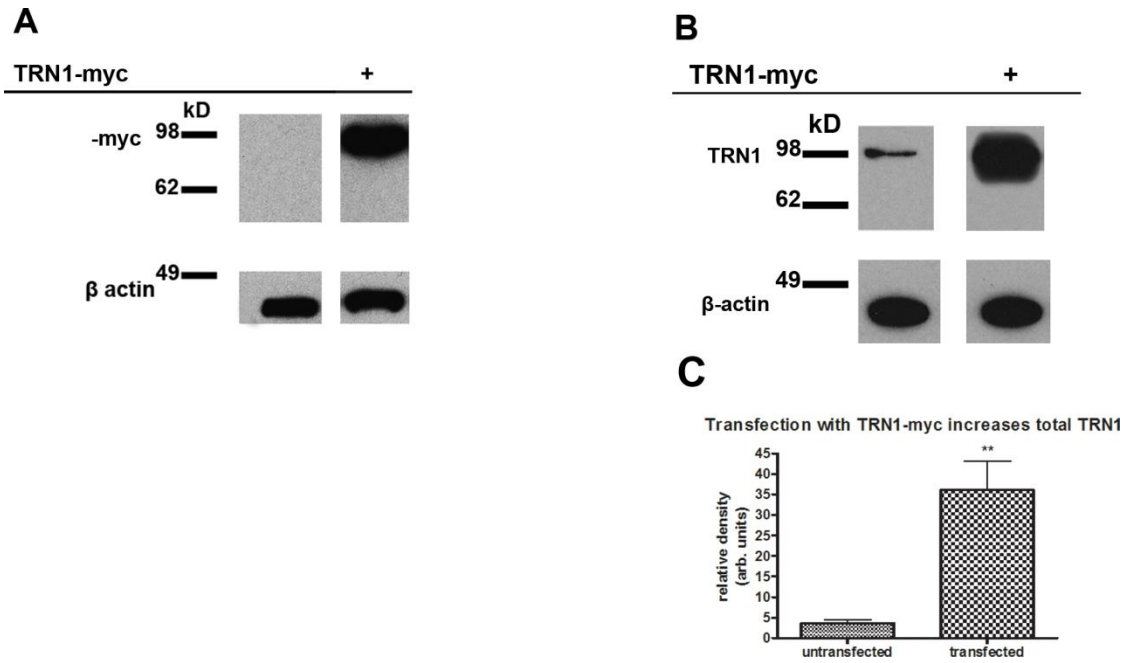

Figure 4.26. Immunoblotting of TRN1-myc transfected SH-SY5Y cells shows –myc tag antibody detects TRN1-myc at 103kD, and probing for total TRN1shows increase in TRN1 from transfected cells. Transfection with 5µg of TRN1-myc plasmid DNA produces detectable levels of protein via –myc antibody (A). Probing with anti-TRN1 antibody reveals vast increase over endogenous levels of TRN1 when quantified with densitometry and analysed with Mann-Whitney U test (** $P<0.01$) (B). Representative immunoblots of three independent experiments. Protein load was 2µg in all lanes, and equal loading confirmed by β actin probe. Molecular weight of TRN1 102kD, TRN1-myc 103kD.

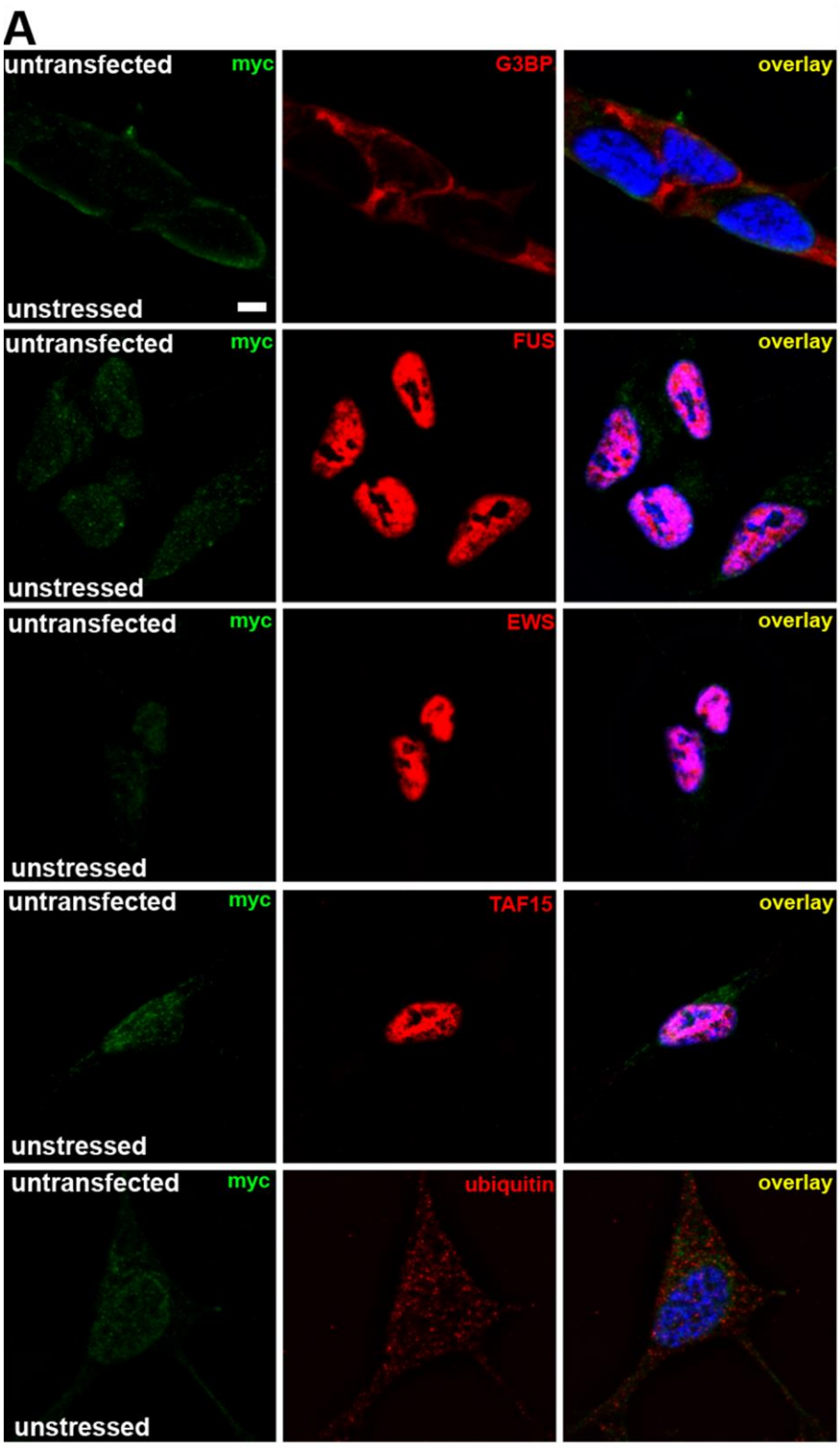
A
untransfected
myc
G3BP
overlay
unstressed
untransfected
myc
FUS
overlay
unstressed
untransfected
myc
EWS
overlay
unstressed
untransfected
myc
TAF15
overlay
unstressed
untransfected
myc
ubiquitin
overlay
unstressed

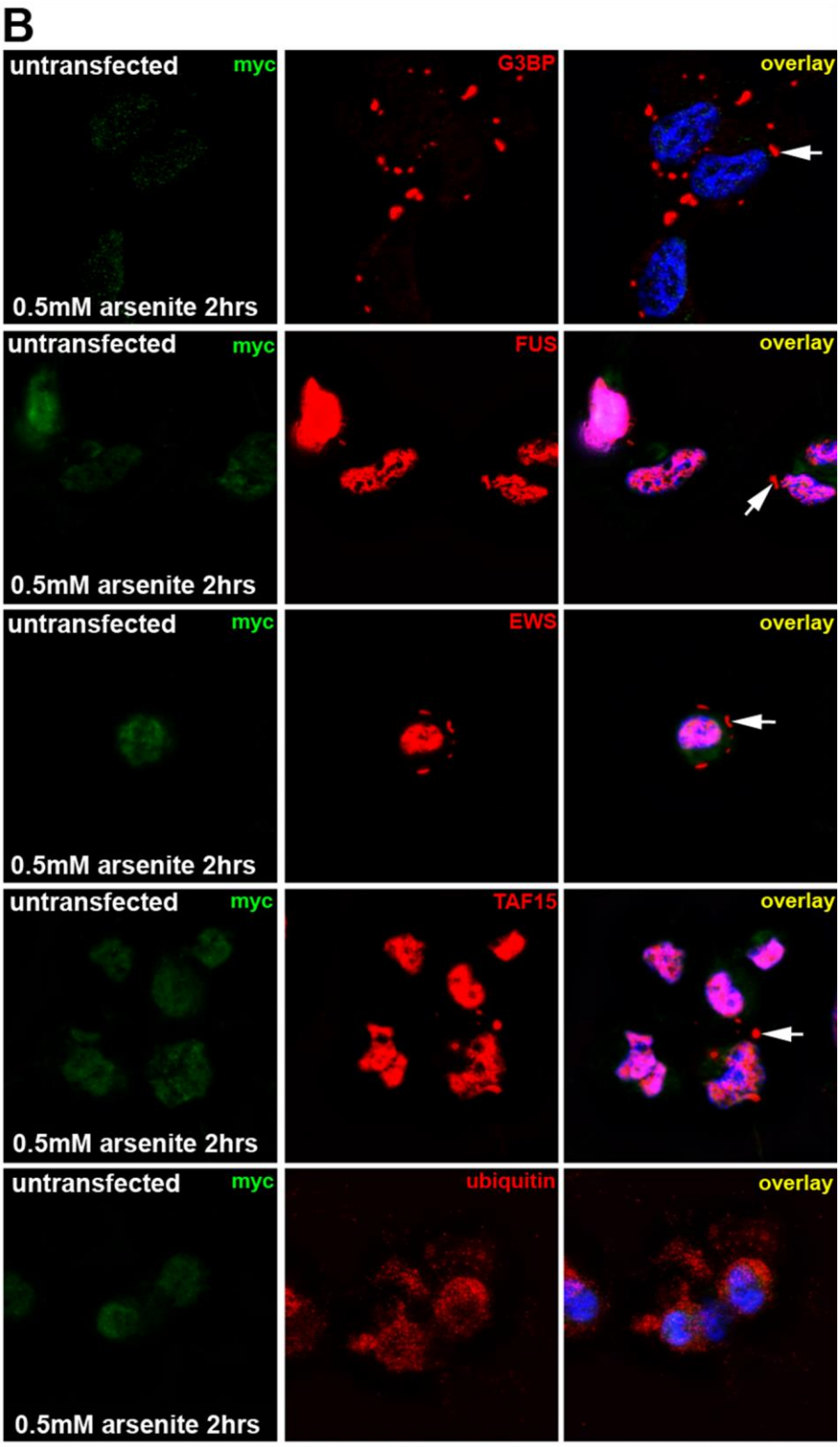
B
untransfected
myc
G3BP
overlay
0.5mM arsenite 2hrs
untransfected
myc
FUS
overlay
0.5mM arsenite 2hrs
untransfected
myc
EWS
overlay
0.5mM arsenite 2hrs
untransfected
myc
TAF15
overlay
0.5mM arsenite 2hrs
untransfected
myc
ubiquitin
overlay
0.5mM arsenite 2hrs

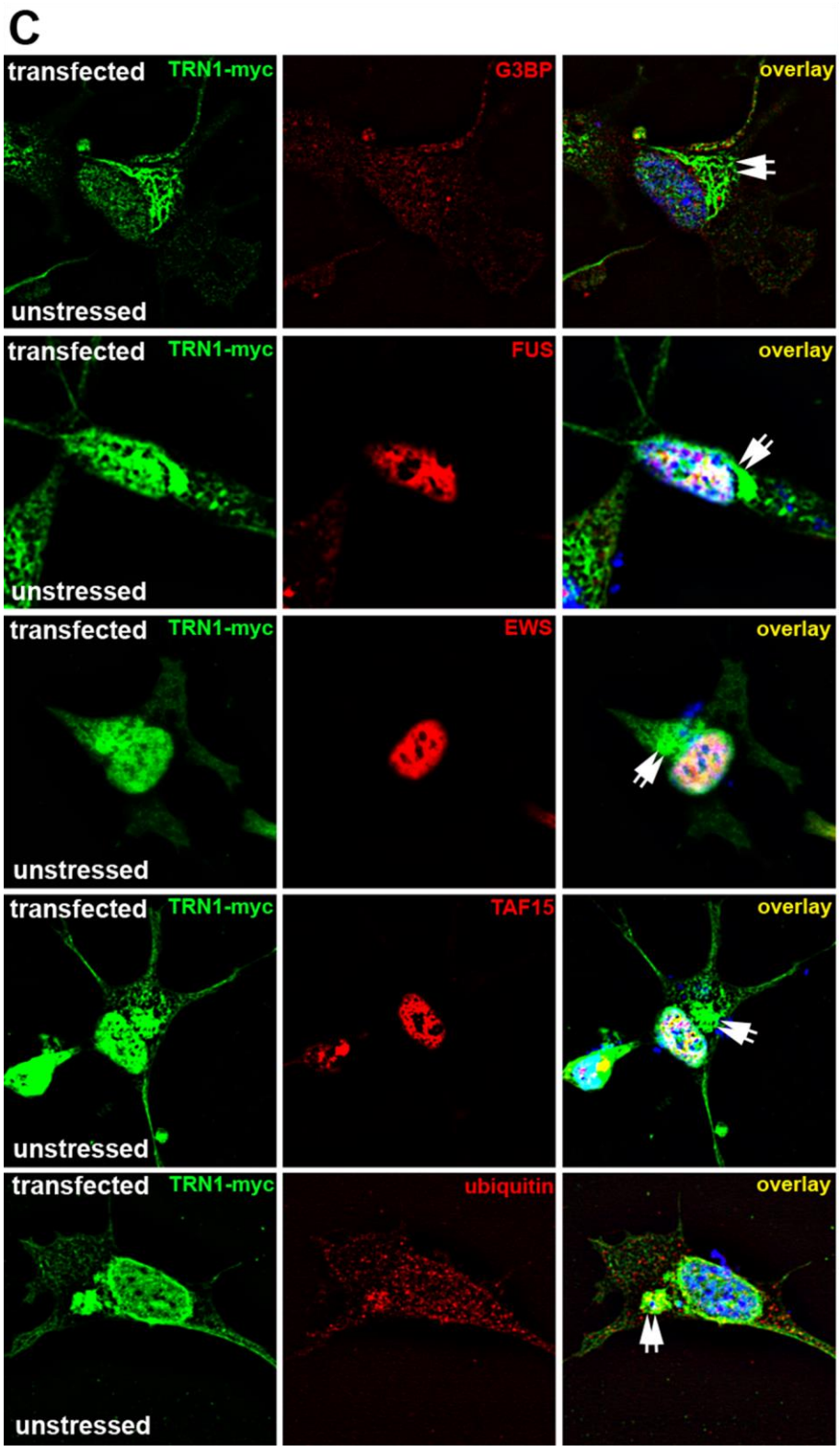
C
transfected
TRN1-myc
G3BP
overlay
unstressed
transfected
TRN1-myc
FUS
overlay
unstressed
transfected
TRN1-myc
EWS
overlay
unstressed
transfected
TRN1-myc
TAF15
overlay
unstressed
transfected
TRN1-myc
ubiquitin
overlay
unstressed

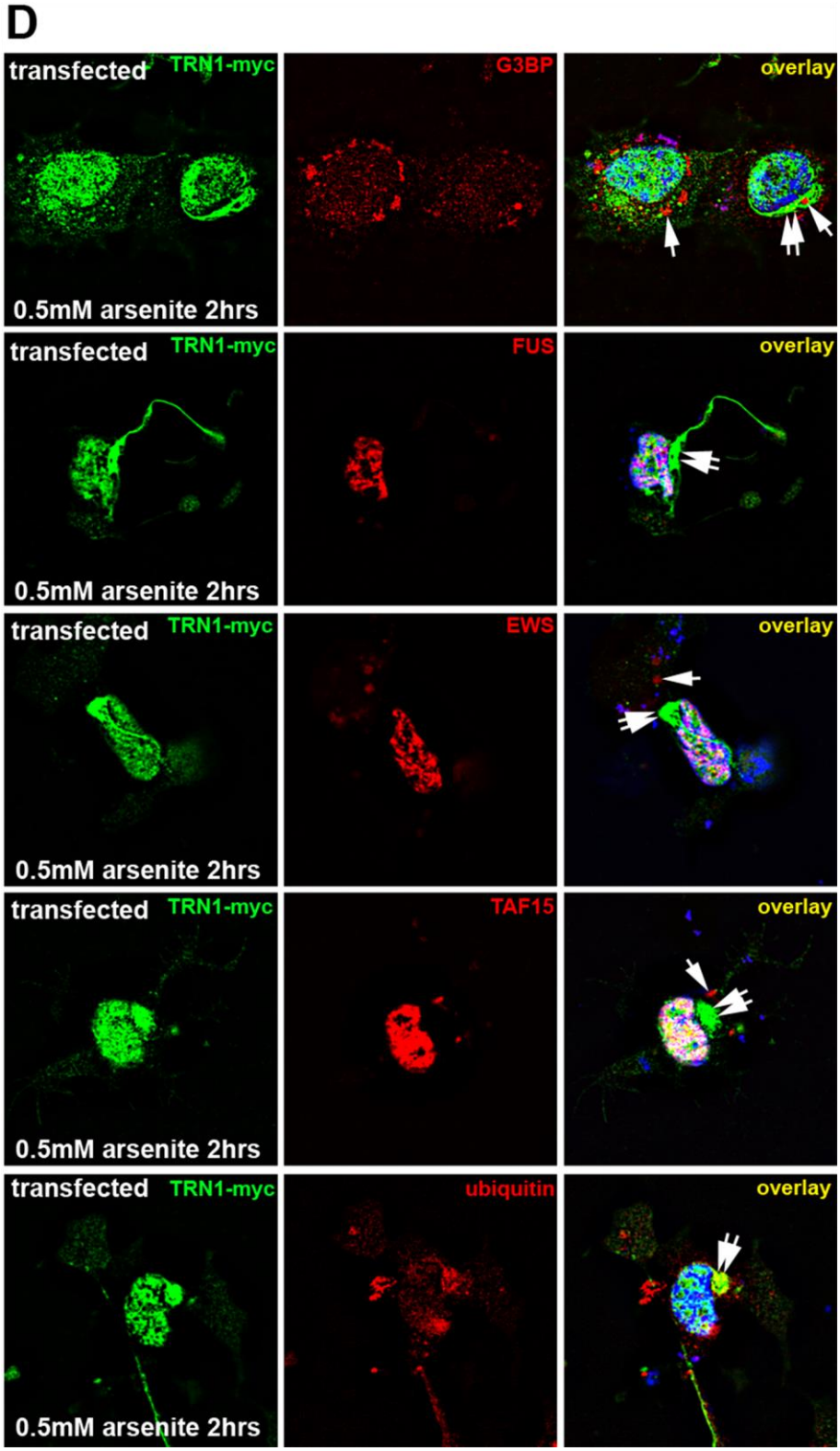

Figure 4.27. Transfection with TRN1-myc plasmid DNA produces additional cytoplasmic staining that is unrelated to stress granules. Anti-myc antibody shows minimal background staining in unstressed (A) or stressed cells (B arrows). Unstressed transfected cells show cytoplasmic –myc staining negative for the FET proteins and weakly ubiquitin positive(C double arrows). 0.5mM arsenite for 2 hours produces stress granules (D arrows) separate from the –myc staining (D double arrows). Scale bar in A represents 5µm. N=3

4.20 Thioflavin S staining of TRN1-myc transfected cells is inconclusive

One of the characteristic hallmarks of many neurodegenerative diseases is the formation of β-sheet enriched protein aggregates. These can be detected with Thioflavin S thanks to its ability to incorporate into this secondary structure and undergo a red shift in florescence. Unusually, FTLD-FUS inclusions are not thioflavin S positive and are therefore unlikely to contain proteins enriched for β-sheet structures. To investigate the nature of the additional cytoplasmic –myc staining SH-SY5Y cells were transfected as before and stained with thioflavin S. Unfortunately, lipofectamine produced false positives which preclude any meaningful interpretation of the transfected cells (Figure 4.27).

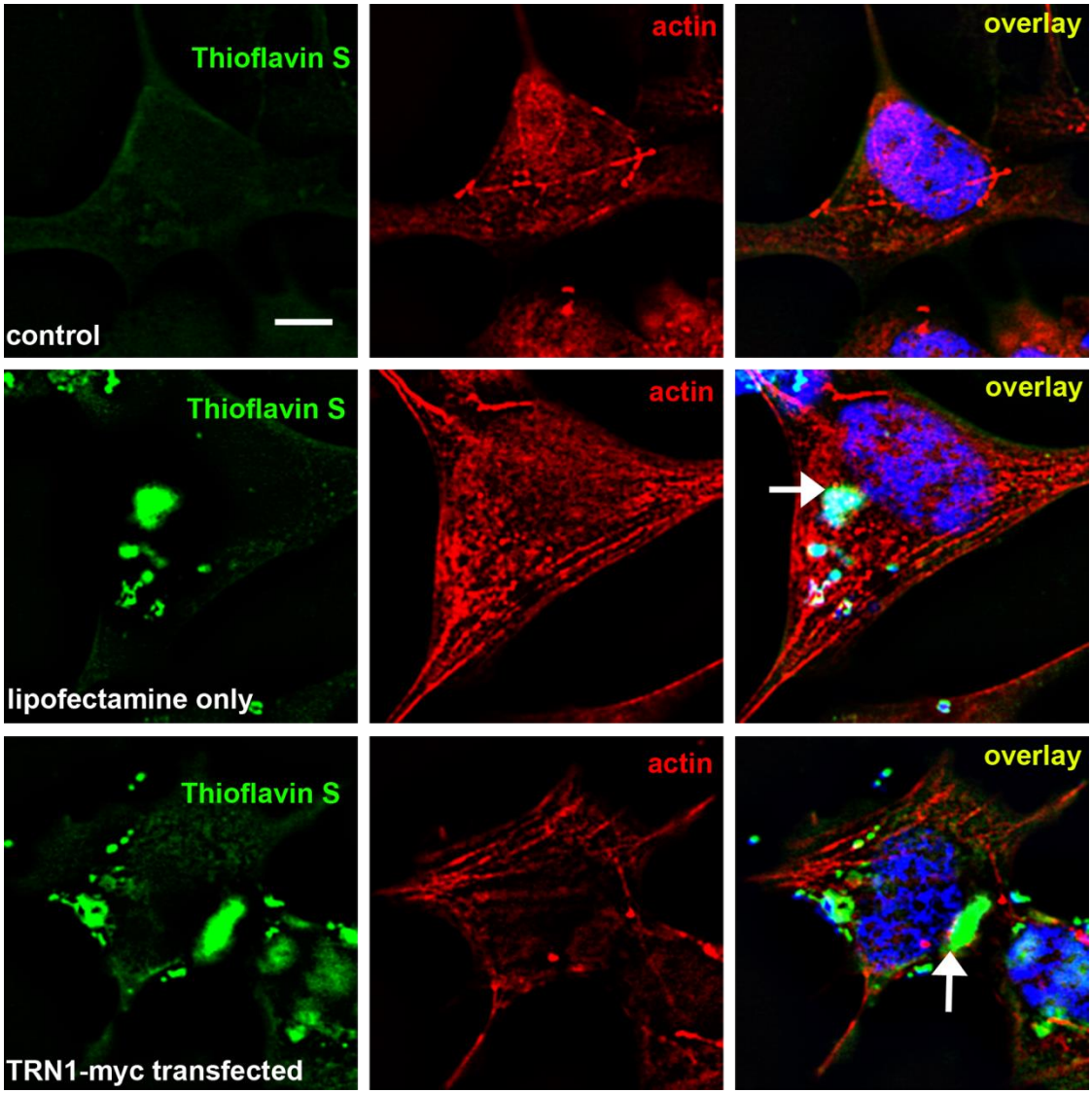

Figure 4.28. Lipofectamine 2000 produces false positive thioflavin S staining. Control SH-SY5Y cells are thioflavin negative, but lipofectamine2000 appears to produce false positive thioflavin S foci (arrows). Scale bar represents 5μm. N=3

4.21 Discussion

These data demonstrate the nuclear importer TRN1 is radically re-localised to cytoplasmic stress granules in response to various stressors and incubation periods. The FET proteins are less amenable to stress granule re-localisation, but this can be increased by prolonging the incubation with stressors at lower concentrations. Recovery in fresh media produces TRN1 positive, G3BP negative foci. These are variably positive for the FET proteins and strongly positive for ubiquitin. These foci showed some co-localisation with DCP1a, suggesting a link to P-bodies and mRNA degradation factors. Oxidative stress over 2 hours will increase the levels of urea soluble (RIPA insoluble) TRN1. This result does not hold true for FUS which remains resolutely unaffected in terms of solubility. The change in TRN1 insolubility is not due to incorporation into stress granules because blocking stress granule formation with emetine in arsenite stressed cells did not rescue the increase in urea soluble TRN1 levels. The incorporation of FET proteins into stress granules does not appear to be mediated by TRN1. Unfortunately, over expression of TRN1 did not provide viable data because immunocytochemistry was hampered by artefacts, which could not be resolved due to lack of the appropriate empty vector.

One of the central findings of this investigation is that the nuclear importer TRN1 readily re-localises to stress granules in SH-SY5Y cells. Previously, it has been shown that members of the importin family, including TRN1 re-localise to eIF4A positive stress granules under arsenite treatment in HeLa and HEK293 cells (Chang and Tarn, 2009). In this study a cell line with a neuron-like background (SH-SY5Y) was exposed to various stressors and the properties of endogenous TRN1 and the FET proteins were followed by sequential solubility extraction and immunofluorescence. This investigation shows that TRN1 re-localises to G3BP positive stress granules, and that a fraction of FUS and TAF15 also re-localises to these TRN1 positive foci. EWS re-localises very strongly under oxidative stress which agrees with previous reports (Andersson et al., 2008a). However,

other authors have struggled to detect EWS in stress granules (Blechingberg et al., 2012b), though this may be due to the different antibodies used in these studies. The choice of antibodies for the cellular studies presented here was always rooted in their ability to detect pathology in FTLD-FUS tissue. It is possible that only certain epitopes are exposed for detection with antibodies depending on how the protein is folded. Additionally, this may change if the protein is post-translationally modified either as a result of different stressors (oxidative or osmotic) or incorporation into stress granules. Examples of which include the fragile X mental retardation protein which is methylated when found in stress granules (Xie and Denman, 2011). Interestingly, the aforementioned study struggled to detect a EWS-GFP fusion protein in stress granules despite being able to detect the endogenous form (Andersson et al., 2008a). This may suggest that incorporation of a tag at the N terminal may alter protein translocation in response under oxidative stress.

In contrast to the effect of oxidative stress on EWS, more prominent re-localisation of FUS was observed under the osmotic stressor sorbitol. This has been replicated to a greater extent in other cell lines (Sama et al., 2013). Whilst some re-localisation was seen after arsenite exposure, the majority of FUS remained nuclear, which agrees with previous reports that have not detected FUS in stress granules (Gal et al., 2011, Bosco et al., 2010). Most authors report TAF15 is easily detectable in stress granules induced by arsenite or heat shock but those reports are from HeLa or HT22 cell lines (Andersson et al., 2008a, Marko et al., 2012). Since neuronal cells have a different mRNA profile, and TAF15 is a RNA binding protein, different linages might explain why detection at the 2 hour time point in SH-SY5Y was muted. It is interesting to note that the number of TRN1 positive stress granules also positive for TAF15 increased when cells were exposed to a lower concentration of stressor over a 24 hour period. It may be that in this particular cell line the recruitment of TAF15 to stress granules is slower than other proteins, or that a particular set of conditions or modifications that occur after prolonged stress are

required. For instance, a reduction in methylation status is associated with TAF15 positive stress granules (Jobert et al., 2009a). Given that one of the hallmarks of FTLD-FUS inclusions is the incorporation of ubiquitin and the proteasomal marker p62, the ubiquitin status of TRN1 positive stress granules and post-stress granule foci was investigated. The incorporation of ubiquitin after recovery in fresh media would seem to support a stress granule-inclusion precursor hypothesis but ubiquitin and ubiquitin associated proteins in stress granules is not unheard of (Athanasopoulos et al., 2010). Additionally, double staining of these TRN1 positive foci after 6 hours recovery with DCP1a suggests they are P-bodies and linked to mRNA processes like de-capping and degradation. P-bodies, unlike stress granules are constitutive, but they do respond to stimuli that effect mRNA translation and decay. However, they are highly related to stress granules and are often found adjacent to one another. They can pass mRNA between one another for processing and they also share a number of protein components such as RNA-associated protein 55 (Rap55), tristetraprolin (TTP), and TRN1 (Buchan and Parker, 2009, Chang and Tarn, 2009). Since P-body markers are not found within the inclusions of FTLD-FUS it would seem unlikely that the TRN1 positive P-bodies seen here represent early inclusions.

To further substantiate the nature of the stress granules and foci observed after acute and prolonged stresses together with recovery in fresh media, we pre-treated the cells with emetine. Emetine is a well-characterized pharmacological compound known to bind to the 40S subunit of the ribosome, stabilize the polysome, and promote disassembly of stress granules. The observation that emetine pre-treatment prevents the detection of cytoplasmic foci under all of the treatment conditions investigated here suggests that the foci observed are indeed bona fide stress granules, but additionally it suggests that the formation of these foci is also dependent on ribosomal disassembly induced by translation interruption in response to stress, and assembly of mRNA factors linked to stress granules. The absence of stress granules or other foci after emetine pre-treatment

was accompanied by a pronounced cytoplasmic redistribution of TRN1 to the cytoplasm. One possible explanation is that TRN1 may require stress granules or a component of stress granules for re-nucleation in the context of cellular stress. It has been previously shown by FRET analysis of TRN1 in early stress granules that it is not statically sequestered away, but instead can shuttle in and out of stress granules (Chang and Tarn, 2009). The same has been shown for the highly related protein importin α, once again through FRET photobleaching of an arsenite induced stress granule (Fujimura et al., 2010). It is possible that one of TRN1's roles in the integrated stress response is to interact with an unidentified protein present in the stress granules which targets it back to the nucleus. One possibility is the Ran protein, which has been shown to be present in stress granules (Fujimura et al., 2010), and is an important co-factor for nuclear shuttling.

Aside from cytoplasmic re-localisation, the production of insoluble protein species is a distinctive biochemical marker for FTLD (Neumann et al., 2006, Neumann et al., 2009a, Brelstaff et al., 2011). The results show that acute exposure to oxidative stress increased the insolubility of TRN1, but the osmotic stressor sorbitol did not produce a significant change in the insolubility of TRN1. This difference suggests there is a biochemical or cellular consequence of oxidative stress on TRN1 that reduces protein solubility. Given that urea soluble (highly insoluble) TRN1 is a characteristic of FTLD-FUS (Brelstaff et al., 2011), these data support the hypothesis that the FTLD-FUS brain is subject to oxidative stress. To compare and contrast the response of FUS with another mRNA binding protein the blots were stripped and re-probed for TDP43. TDP43 is deeply involved in FTLD as the sole primary marker of pathology in FTLD-TDP, and only is occasionally reported in stress granules much like FUS (Liu-Yesucevitz et al., 2010, Colombrita et al., 2009). In contrast to FUS, not only was the urea fraction of TDP43 increased over time, but this also corresponded to a concomitant decrease in the RIPA fraction. This finding has been subsequently recapitulated in published data using Cos7 cells and a reduced incubation

time and concentration of arsenite (Cohen et al., 2012). Those authors speculated that this shift in solubility is due to disulphide cysteine cross linking at C173-C175 induced by oxidative stress. Furthermore, osmotic stress appeared to produce the same pattern whereas previously this stressor had no effect on TRN1 or FUS. At the time of writing this effect of sorbitol stress on TDP 43 solubility is a novel finding and may suggest a convergent pathway of multiple stress types on TDP 43. Densitometric quantification and analysis is preferable to qualitative assessment but the presence of multiple higher molecular weight bands merging with the 43kDa signal precluded this. It is possible that these bands represent pathologically relavent post-transcriptional modifications such as phosphorylation, which is a known alteration of TDP 43 (Neumann et al., 2006). However, to clearify this issue would require phosphotase treatment to investigate whether the bands disappear.

Given the dual observation of strong re-localisation to stress granules and increasing levels of insoluble protein a causal relationship between the two was investigated. Emetine blockade of stress granule formation does not prevent the rise in insoluble TRN1 levels in response to 2 hours 0.5mM arsenite stress despite TRN1 strongly re-localising to stress granules and previous authors stating these foci represent insoluble aggregates (Kedersha and Anderson, 2007, Wolozin, 2012). The inference of this is that the biochemical consequence of oxidative stress on TRN1 occurs in the absence of stress granules.

Despite the fact that TRN1 is a functional binding partner of the FET proteins and readily re-localises to stress granules, it is not responsible for the re-localisation of FET proteins to said foci. Knockdown of TRN1 and TRN2 by siRNA re-localises the FET proteins to the cytoplasm and subsequent 0.5mM arsenite stress for 2 hours significantly increases stress granule FET positivity. This would seem to argue that the importin protein TRN1 (or TRN2) is not required for stress granule incorporation. Other studies into the recruitment of FUS and the other FET proteins into stress granules have strongly

implicated their zinc finger, glycine-rich domain and RRM which would seem to underscore the importance of RNA binding rather than TRN1 binding in stress granule recruitment (Bentmann et al., 2012, Marko et al., 2012). Over expression of wild type TRN1 produced morphologically heterogeneous cytoplasmic staining additional to the normal nuclear localisation. This cytoplasmic staining was likely artifactual despite a passing similarity to the inclusions of FTLD-FUS. Neither the FET proteins nor stress granule markers co-localise with this staining suggesting it may be an artefact of over expression rather than unique inclusion formation. These data also contrasts with previously published reports describing co-localisation of over expressed GFP-TRN1 with stress granules (Chang and Tarn, 2009). Whether or not the additional cytoplasmic TRN1 staining represents an artefact or genuine inclusion formation, further characterisation is warranted. To elicudate the presence of this additional, often aggregation like, myc-TRN1 staining an empty vector should have been used as an overexpression control. This would allow the clarification of whether what is observed is just an artifact of overexpressing any protein or something specific to TRN1. However this was not possible here due to finantial and time constraints. Unfortunately, thioflavin S staining proved inconclusive because cells treated with only lipofectamine2000 gave a false positive result.

In summary TRN1 positive stress granules are variably positive for the FET proteins, and G3BP negative TRN1 foci seen after recovery periods are likely to be P-bodies. The insolubility of TRN1 increases under oxidative stress but this does not require stress granule formation. Furthermore, TRN1 (and TRN2) is not responsible for FET protein incorporation into stress granules. Finally, over expression of TRN1 in SH-SY5Y cells produces unusual cytoplasmic staining. One final caveat to this work it that this SH-SY5Y line was not differentiated with retinoic acid into a more quiescent neuron like phenotype. The main reason for this is that retinoic acid treatment has been shown to alter the expression levels of the FET proteins (Andersson et al., 2008a) and it was

therefore decided that this variable should be avoided. Further investigations into a separate cell model are explored in the next chapter.

Chapter Five: Validation of stress granule findings in rat hippocampal primary neurons (Results III)

5.1 Introduction

It is widely accepted that oxidative stress has a major role in the neurodegeneration behind the myriad of dementias and movement disorders afflicting millions. Neurons are particularly susceptible to stress and oxidative damage by virtue of their high oxygen consumption, lower anti-oxidant enzyme activity in the aged brain, and elevated concentrations of poly unsaturated fatty acids in their cell membranes (Raichle and Gusnard, 2002, Marcus et al., 1998). Given these unique properties, models of oxidative stress driven neurodegeneration constructed in transformed cells must be ported to more relevant ex vivo models before meaningful inferences are made regarding pathogenesis.

Confirmation of data derived from transformed cell lines in primary cultures is a common feature of published research into neurodegeneration. For instance, the cytoplasmic re-localisation and subsequent aggregation into stress granules of ALS-associated mutant FUS was confirmed in e19 cortical and hippocampal neurons (Dormann et al., 2010). Furthermore, because the movement and dynamics of stress granules are dependent on cytoskeletal elements, primary neurons have been utilised to study this in highly polarised cytoskeletal dependant morphology (Tsai et al., 2009).

Hippocampal pyramidal cells are the most widely used thanks to their distinctive and defined morphology. A single axon sprouting from the soma, dendritic arborisation including apical and basilar dendrites all highly branch and peppered with dendritic spines form a distinctive silhouette. Hippocampal pyramidal neurons develop at

embryonic day 15, meaning when the tissue is typically harvested at embryonic day 18, the generation of pyramidal neurons is essentially complete. Harvesting at this stage has the added advantage of easily removable membranes, tissue amenable to dissociation, and minimal glial contamination.

5.2 Hypothesis

TRN1 and the FET proteins re-localise to stress granules in rat hippocampal primary neurons upon arsenite stress & the biochemistry of TRN1 will shift towards the insoluble fraction.

5.3 Mature hippocampal neurons are differentiated over five days

To confirm that the dissection technique and culturing practices produced viable cells that differentiated into the morphologically characteristic profile of hippocampal neurons phase contrast microscopy was used to follow their *in vitro* differentiation. Three hours after plating cells had attached to the poly-$_D$-lysine coated coverslips and lamellipodia were visible (Figure 5.1 A). Three days into differentiation the neurons had sprouted an axon and simple dendritic processes (Figure 5.1 B) corresponding to the 'Axonal outgrowth phase' depicted in Figure 2. By day five, complex arborisation of the dendrites was obvious meaning the cell has fully matured and likely begun to form synapses with other cells (Figure 5.1 C). All subsequent experiments would take place on day five unless otherwise stated.

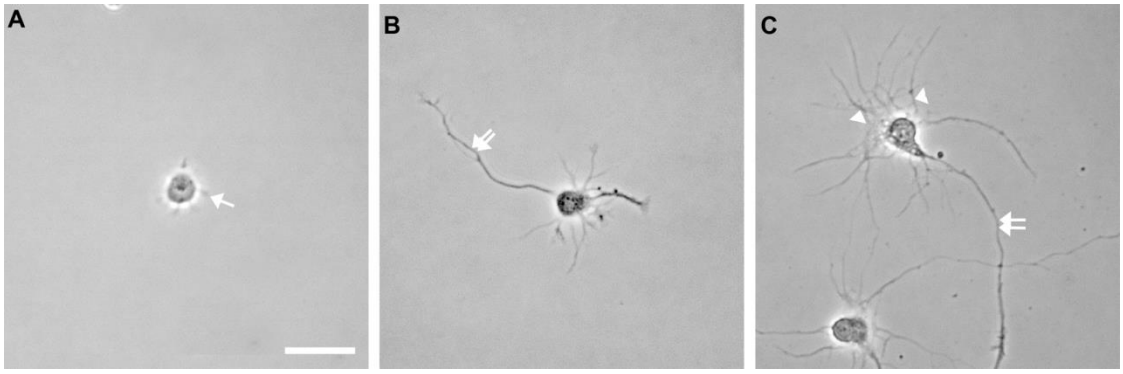

Figure 5.1. Cells differentiate into mature hippocampal neurons by day five in vitro. Phase contrast microscopy shows three hours after dissociation and plating the cells have adhered to the coverslip and minute lamellipodia are visible (A arrow). Three days into differentiation and a single axon has extended from the cell body (B double arrow). Five days into differentiation and the neuron has full differentiated showing a single axon (C double arrow), and extensive complex dendritic arborisation (C arrow heads). Scale bar in A represents 25µm. N=3

5.4 Antibody characterisation on rat primary neuron lysate

All previous experiments in this thesis have utilised antibodies raised against human peptides to visualise human tissue and cells. To ensure they recognise the same conserved proteins in rat neurons western blotting of cell lysate was undertaken, and the bands compared to expected molecular weight listed at Ensembl database (http://www.ensembl.org/Rattus_norvegicus). All but two of the antibodies available recognised a band of the appropriate molecular weight (Figure 5.2 asterisks). Mouse anti-TRN1 (abcam ab10303) failed to recognise the appropriate band at approximately 102kD, instead recognising a smaller band at approximately 80kD. Mouse anti-G3BP only recognised very weak bands at approximately 100 and 40kD, neither near the correct molecular weight.

Both species of FUS antibody recognised the appropriate expected band at approximately 74kD. Despite the predicted molecular weight of murine FUS being approximately 52kD, higher than expected bands on immunoblots are commonly seen in human lysate (Figure 4.2). Both species of TAF15 antibody recognised the appropriate band at 58kD for murine TAF15. Whilst several extra bands were highlighted by the mouse anti-EWS antibody the most prominent band was at the correct molecular weight of 68kD. The stress granule markers rabbit anti-G3BP and mouse anti-TIA-1 recognised bands at the expected size of 52 and 41kD respectively.

For the subsequent experiments rabbit anti-TRN1 (abcam ab67352) and the appropriate co-stain antibody raised in mouse were used.

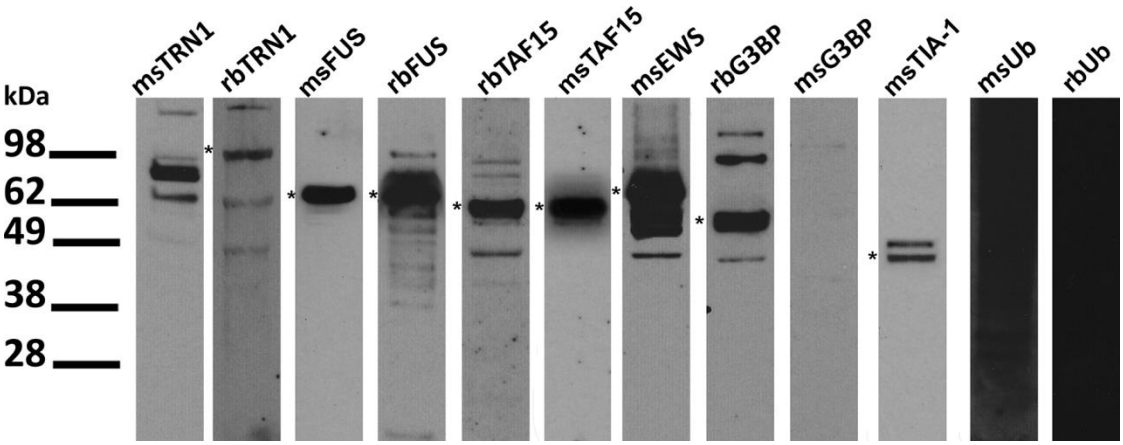

Figure 5.2. Most antibodies detect bands of correct corresponding molecular weight in rat neuron lysate. Bands of correct molecular weight for the protein to which an antibody is raised are indicated with an asterisk (*). Mouse anti-TRN1 (msTRN1) and mouse anti-G3BP (msG3BP) fail to recognise the correct bands. Both species of ubiquitin antibody (msUb and rbUb) produce the expected ubiquitin-smear. Protein load was 5µg in all lanes.

5.5 TRN1 and the FET proteins re-localise to stress granules in primary neurons

The re-localisation of normally nuclear proteins to cytoplasmic stress granules is described for SH-SY5Y cells in the preceding chapter. Since this re-localisation has been suggested to be crucial for the development of cytoplasmic aggregates central to the development of FTLD-FUS, primary neurons were investigated to see whether this re-localisation under arsenite stress was an isolated phenomenon of transformed cell lines or whether it replicated in primary neurons. Confocal microscopy shows unstressed control primary hippocampal neurons have strongly nuclear TRN1, TIA-1 and FET proteins (Figure 5.3 A). Actin staining reveals well defined projecting axons and complex dendritic arborisation typical of healthy hippocampal neurons. However, after 2 hours of 0.5mM arsenite stress immunocytochemistry shows TRN1 has partially re-localised to cytoplasmic foci that strongly co-localise with the stress granule marker TIA-1. The re-localisation is not complete because there is retention of the original nuclear TRN1 stain. The same is true of FUS, EWS and TAF15 which appear to partially re-localise to cytoplasmic TRN1 stress granule foci (Figure 5.3 B). Actin staining reveals loss of morphological polarisation, axon retraction and loss of dendritic complexity. Quantificantion of co-localisation with TRN1 foci shows complete agreement between the number of TRN1 foci also positive for TIA-1 indicating they are all stress granules. Co-localisation of all the FET proteins with TRN1 stress granule foci is seen (≥90% in all instances) (Figure 5.3 C).

Figure 5.3 continued overleaf

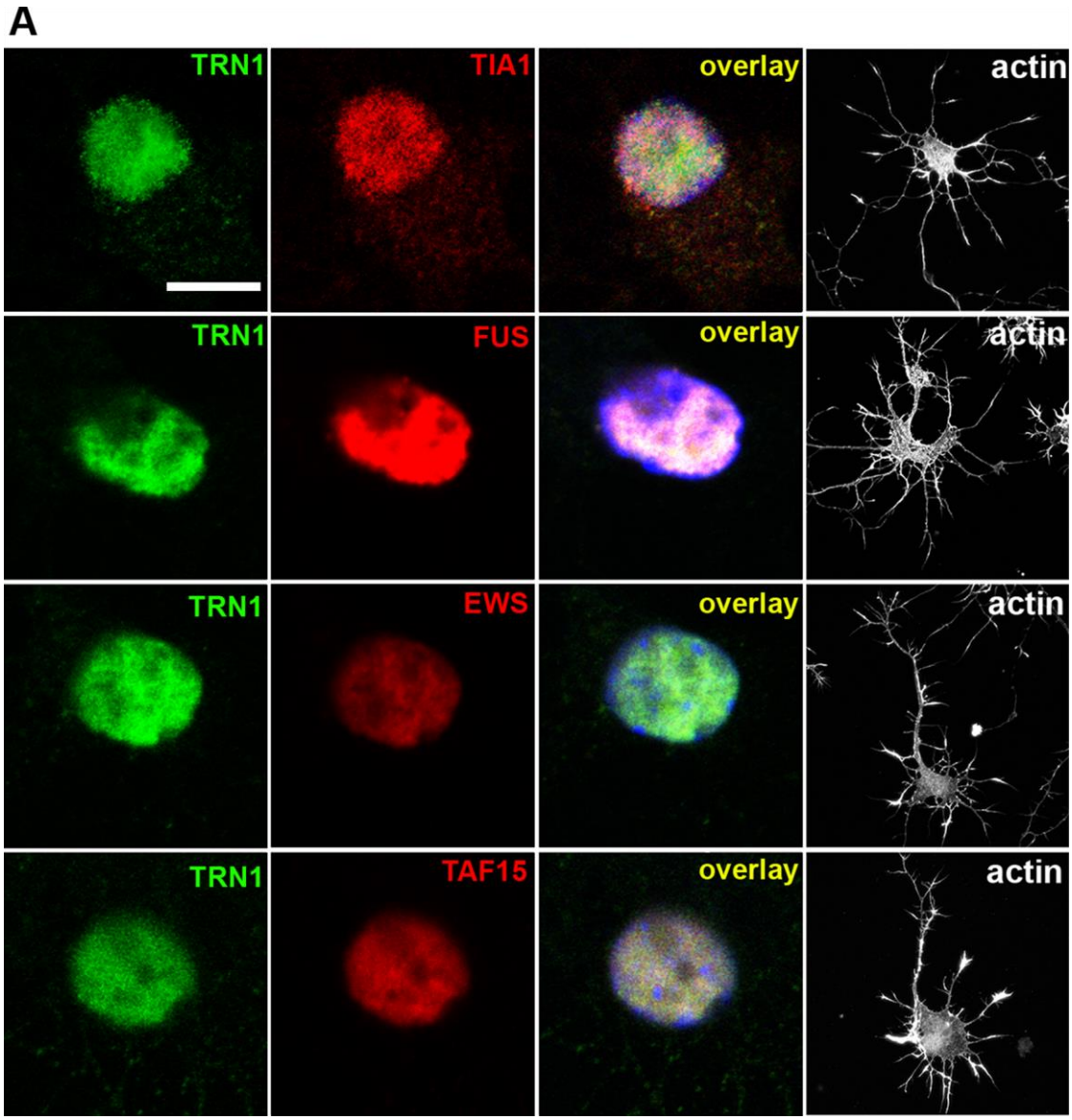

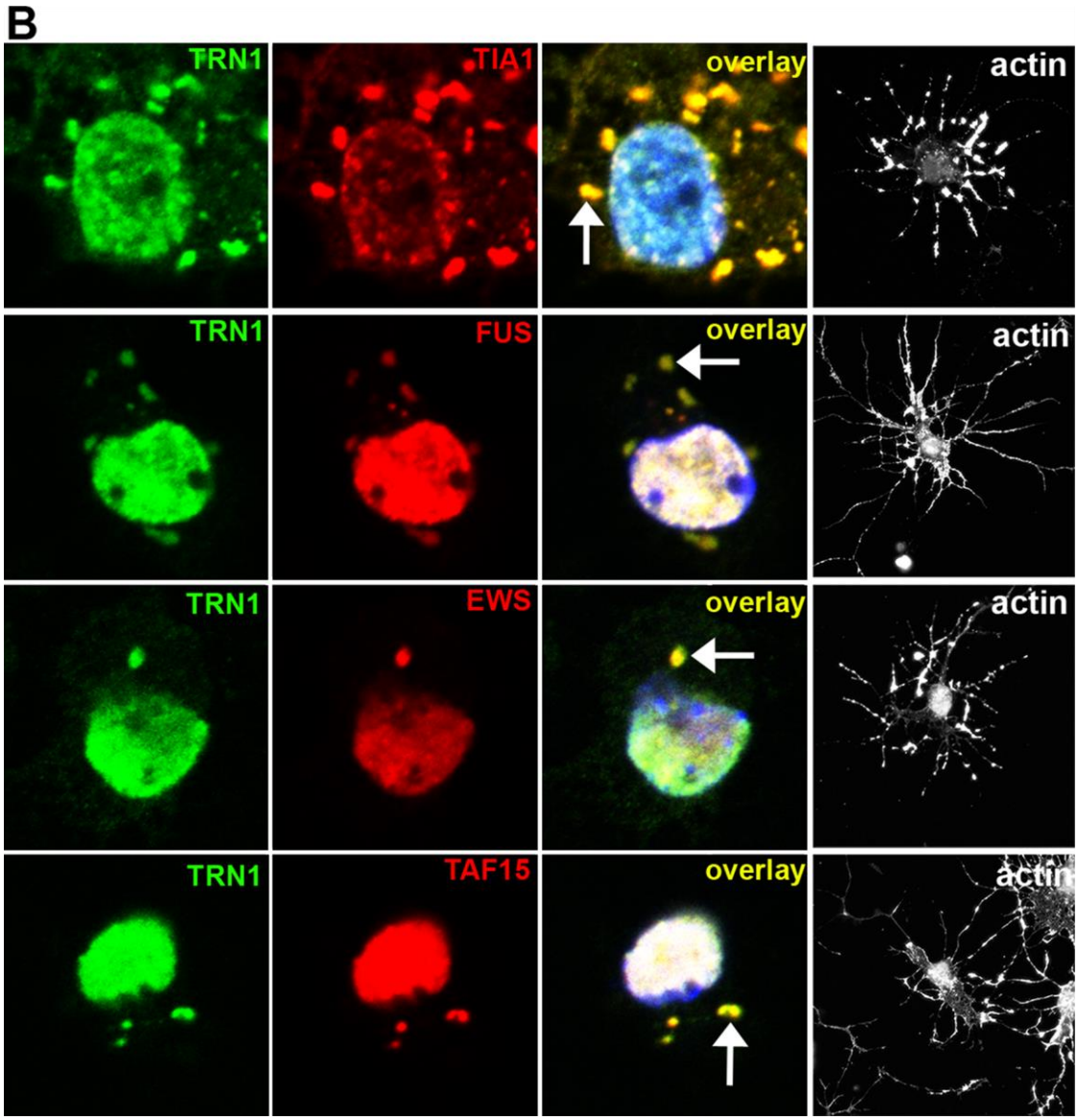

Figure 5.3. The nuclear protein TRN1 and the FET proteins partially re-localise to cytoplasmic stress granules. TRN1, the FET proteins and the stress granule marker TIA-1 are nuclear in unstressed primary rat neurons (A). After 2hrs of 0.5mM arsenite stress TRN1 is present in cytoplasmic stress granules (TIA-1 positive) whilst also retaining some nuclear staining. The FET proteins also partially re-localise to these TRN1 positive stress granules (B). Quantification of numbers of TRN1 foci also positive for co-stain shows strong co-localisation of TIA-1, FUS, EWS and TAF15 in the TRN1 foci (C). Scale bar in A represents 20μm and 10μm in insets. Overlay includes blue nuclear DAPI stain. N=3.

5.6 Arsenite stress shifts TRN1 to the insoluble fraction in rat primary neurons

Given that oxidative stress produces a significant increase in urea soluble TRN1, primary rat neurons were stressed to investigate whether this recapitulated. Untreated control cells show strongly detectable TRN1 in the RIPA soluble fraction and only small amounts detectable in the insoluble urea fraction. However, after 2 hours of 0.5mM arsenite stress no RIPA soluble TRN1 is detectable whilst the urea soluble fraction has increased markedly (Figure 5.4 A). Densitometric quantification and analysis by Mann-Whitney U test reveals the loss of RIPA soluble TRN1 is highly significant (**$p<0.01$). Additionally, the increase in urea soluble TRN1 is also significant (*$p<0.05$) (Figure 5.4 B). Adjustment to loading control was possible only in the RIPA fraction, not the urea fraction because there is no reliable control. Protein assay of all samples ensured equal loading across all lanes, including the urea fraction.

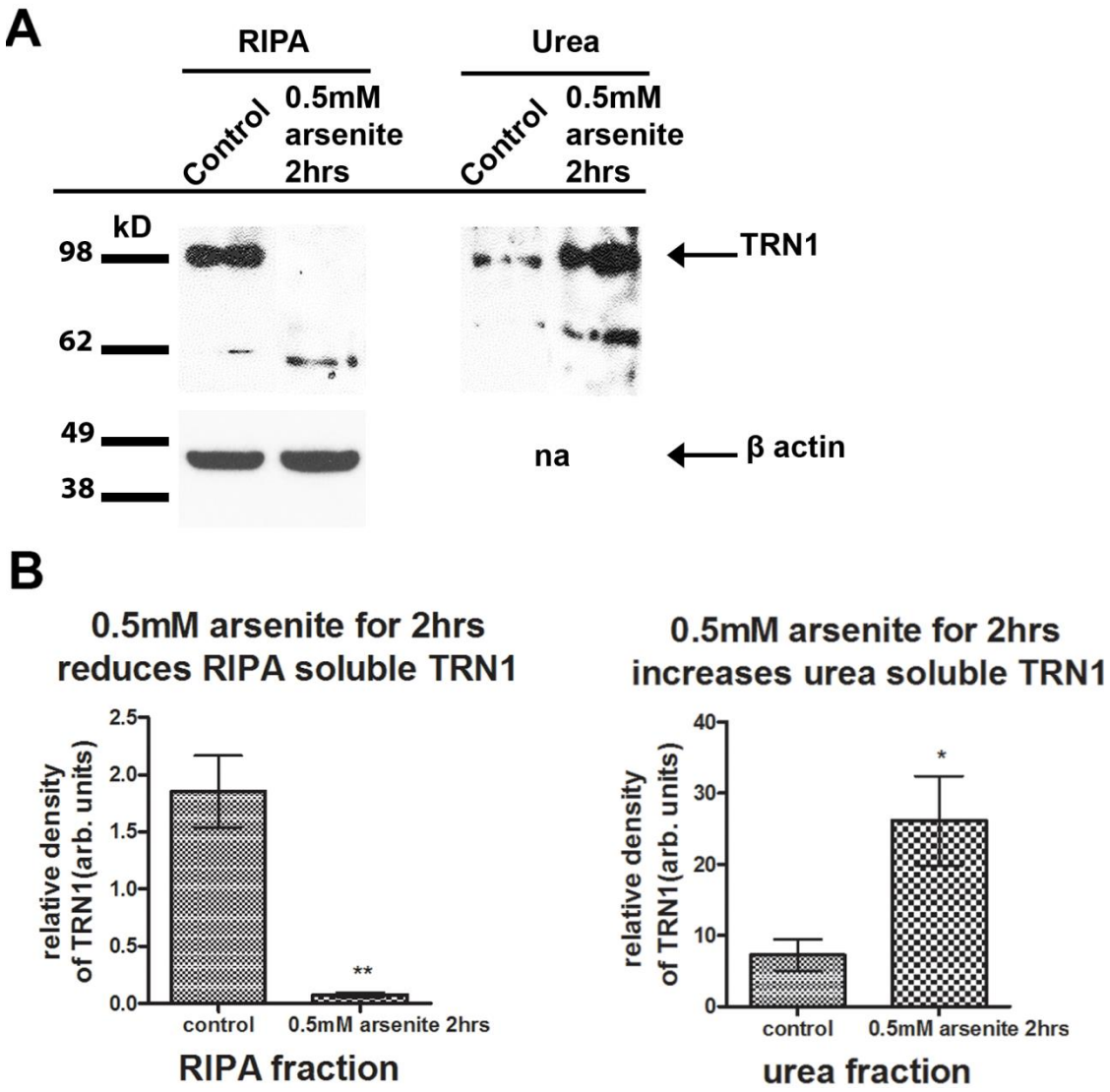

Figure 5.4. Arsenite exposure shifts the biochemistry of TRN1 towards the insoluble fraction. Unstressed control cells show strong RIPA soluble and weak urea soluble TRN1. However, after 2hrs 0.5mM arsenite stress TRN1 has left the soluble RIPA fraction accompanied by an increase in urea fraction of TRN1 (A). Quantification with densitometry and analysis with Mann-Whitney U test shows the loss of RIPA soluble TRN1 is highly significant (**$p<0.01$), and the increase in urea soluble TRN1 is also significant (*$p<0.05$) (B). Immunoblot representative of three independent experiments. Protein loading was 5 µg in all lanes. Loading control for RIPA fraction was β actin but no loading control is available for urea fractions (na). Error bars SEM.

5.7 Prolonged arsenite stress produced the same immunocytochemical pattern as acute stress, but recovery in fresh media produced TIA-1 negative foci.

Previous investigations in this thesis using SH-SY5Y cells have shown that prolonged stress followed by recovery in fresh media led to stress granule marker negative TRN1 and FET protein positive foci. To investigate whether this held true in primary neurons, cells were incubated with 0.5mM arsenite for 24 hours and then either fixed for immunocytochemistry or allowed to recover in fresh media for 6 hours. Widefield microscopy shows TRN1, TIA-1 and the FET proteins are strongly nuclear with some background FITC staining (Figure 5.5 A). However, after 24 hours of 0.5mM arsenite TRN1 has re-localised to cytoplasmic stress granules (TIA-1 positive). This re-localisation is variable; in some instances it appears complete whilst in other cases there is some retention of the original nuclear stain (Figure 5.5 B). The FET proteins, FUS, EWS and TAF15 all strongly co-localise with these cytoplasmic TRN1 stress granule foci but similarly to TRN1 there is occasional retention of the nuclear stain (Figure 5.5 B). Quantification of TRN1 foci shows that in almost all instances TRN1 foci are also positive for TIA-1, and the FET proteins (C). This good co-localisation is a continuation of the pattern observed at 2 hours, but after 6 hours of recovery in fresh media the pattern changes. The TRN1 foci no longer co-localise with TIA-1 which has instead returned to the nucleus (Figure 5.5 D). However, strong co-localisation was still evident between TRN1 foci and the FET proteins. Quantification of TRN1 foci shows that in almost all instances after recovery, TRN1 foci are not positive for TIA-1, but remain strongly positive for the FET proteins (D). Statistical analysis of all the count data via one-way ANOVA with bonferroni correction reveals this is the only significant change in co-localisation with TRN1 foci ($p<0.001$).

Figure 5.5 continued overleaf

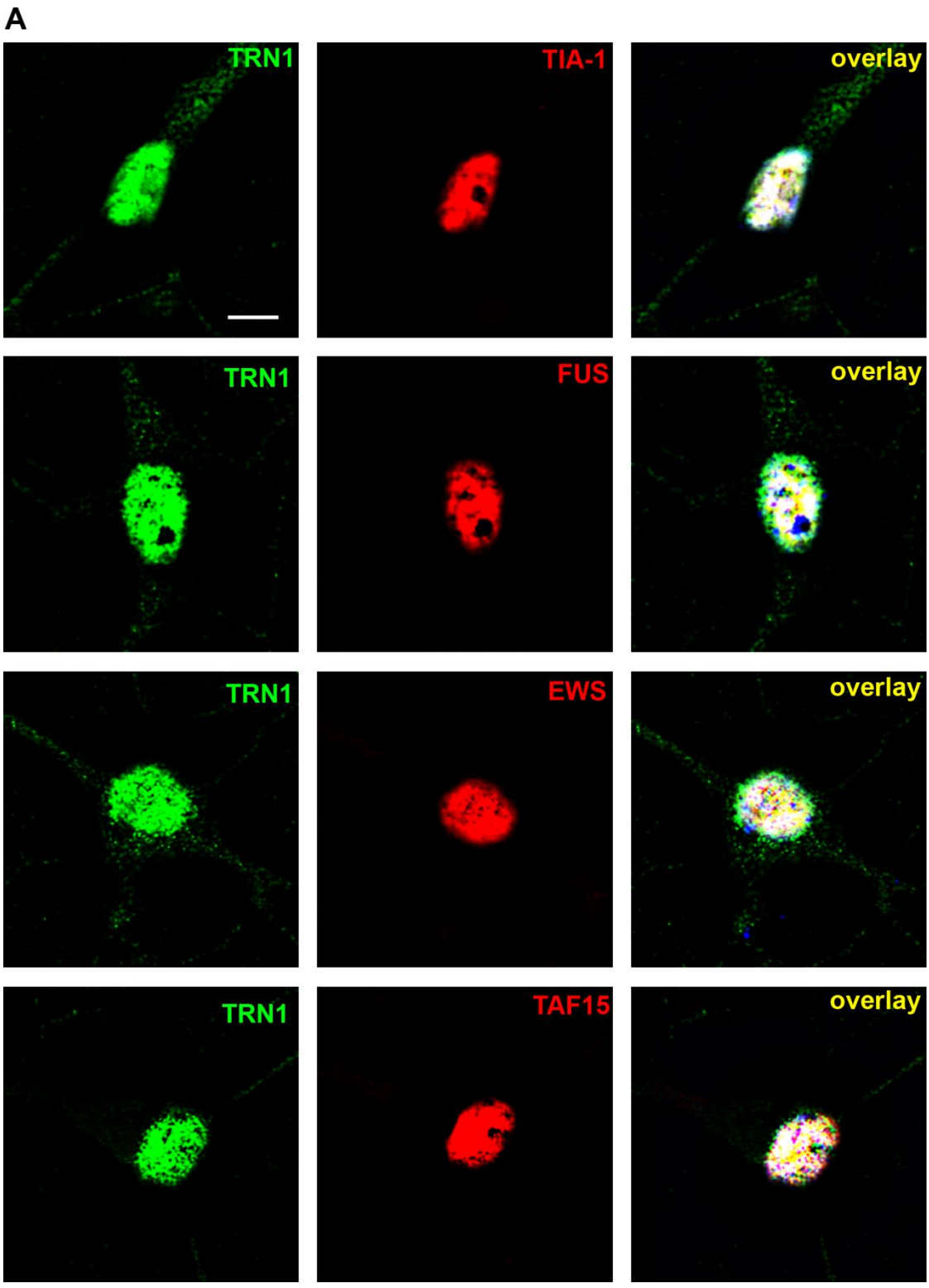

B

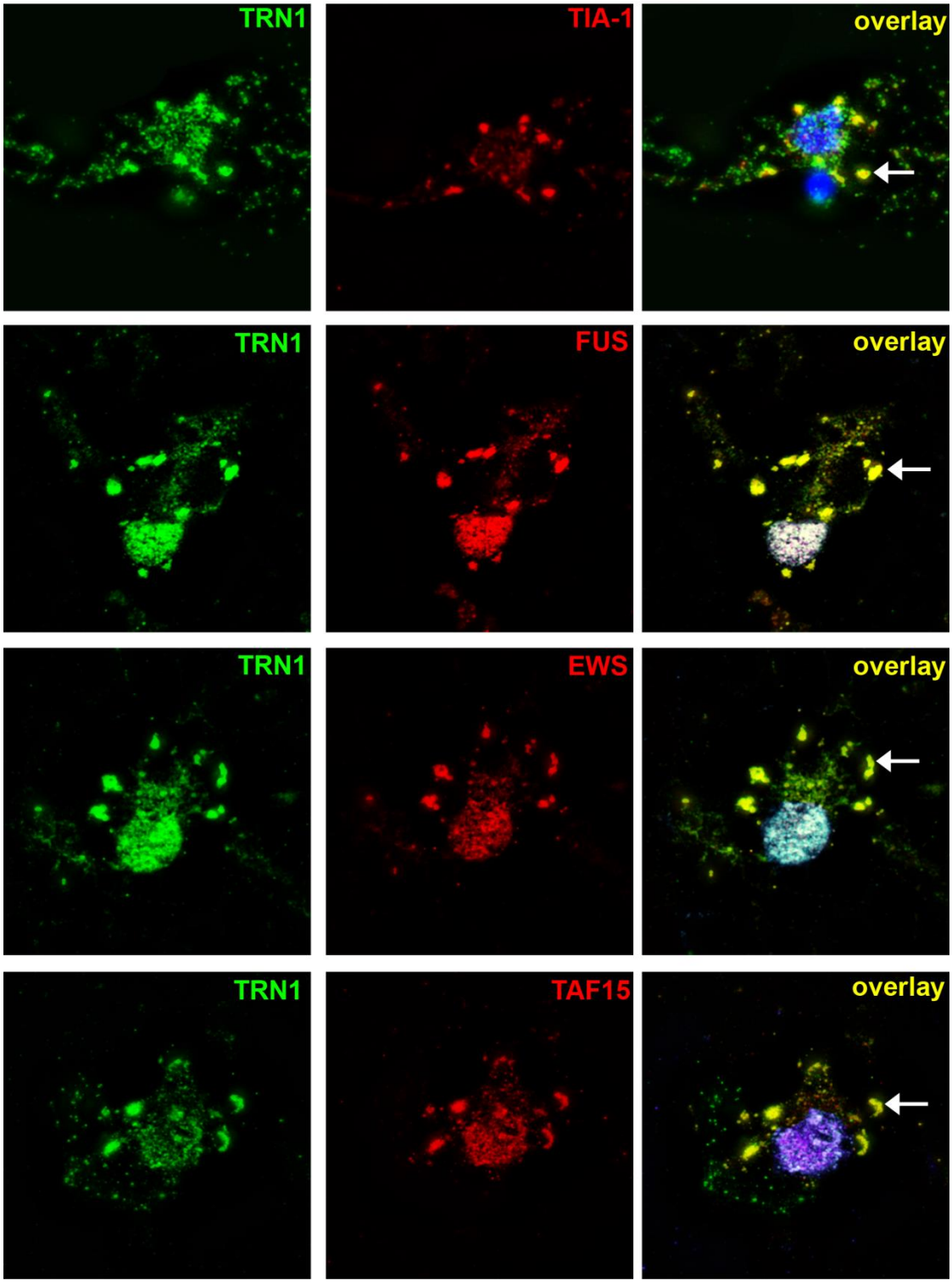

C

Percentage of TRN1 foci also positive for co-stain

TIA-1	FUS	EWS	TAF15
99.31% ±0.49SEM	98.67% ±0.74SEM	99.58% ±0.23SEM	98.80% ±0.59SEM

D

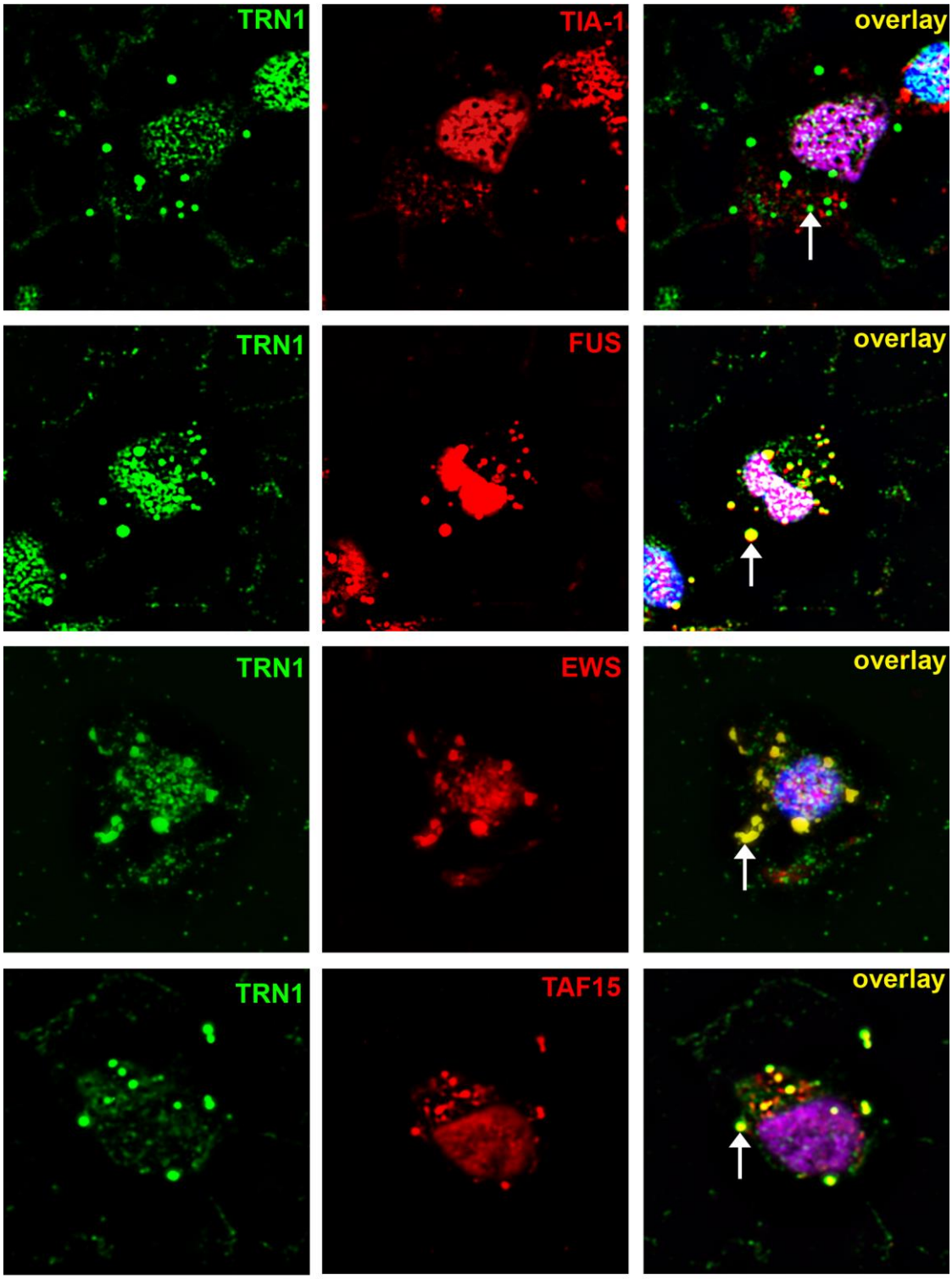

E

Percentage of TRN1 foci also positive for co-stain

TIA-1	FUS	EWS	TAF15
7.46% ±0.98SEM	98.79% ±0.63SEM	99.38% ±0.35SEM	97.63% ±1.13SEM

Figure 5.5. Prolonged 0.5mM arsenite stress over 24hrs re-localises TRN1 and the FET proteins to stress granules, but recovery in fresh media shows TIA-1 negative foci. Unstressed control cells show nuclear TRN1, TIA-1 and FET proteins (A). Prolonged 0.5mM arsenite stress after 24hrs produces TRN1 cytoplasmic foci co-localising with the stress granule marker TIA-1. The FET proteins FUS, EWS, and TAF15 also co-localise with TRN1 in these foci (B arrows). Quantification of numbers of TRN1 foci also positive for co-stain shows strong co-localisation of TIA-1, FUS, EWS and TAF15 in the TRN1 foci (C). Recovery in fresh media produced a different staining pattern showing predominantly TIA-1 negative TRN1 foci which nevertheless remained positive for the FET proteins (D arrows). Quantification of numbers of TRN1 foci also positive for co-stain shows negligible co-localisation with TIA-1 but good co-localisation with FUS, EWS and TAF15 (E). Scale bar in A represents 15μm. Overlay includes blue nuclear DAPI stain. N=3

5.8 Reduction of TIA-1 positivity is statistically significant

Due to the statistically significant reduction in G3BP staining seen after recovery in SH-SY5Y cells, the same investigation was mounted for primary neurons. Analysis by ANOVA and Bonferoni post-test indicates the reduction of TIA-1 positivity in TRN1 foci is significant ($p<0.001$). It would appear that a large proportion of TRN1 foci seen after 6hrs of recovery in fresh media are not stress granule marker positive.

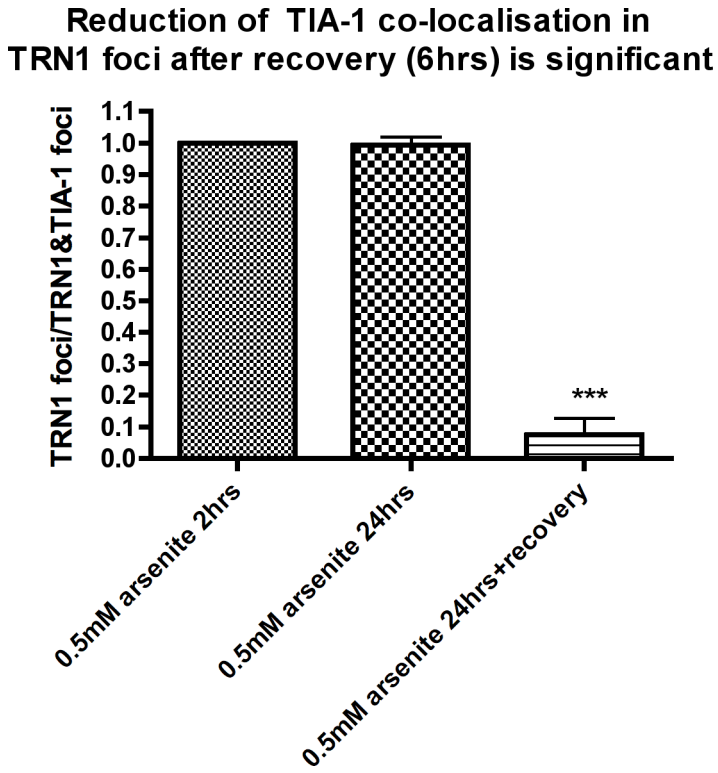

Figure 5.6. Statistical analysis reveals loss of TIA-1 positivity in TRN1 foci after recovery is significant. The proportion of TRN1 foci also positive for TIA-1 is significantly lower ($p<0.001$) after recovery in fresh media. Analysis by ANOVA.

5.9 Pre-treatment with the stress granule blocker Emetine prevents the formation of stress granules and therefore the re-localisation of TRN1 and the FET proteins

To confirm that the foci observed in rat primary neurons are indeed stress granules, primary neurons were pre-treated with 16.4μM emetine before being stressed with 0.5mM arsenite for 2 or 24 hours. The resulting lack of stress granules (TIA-1 or TRN1 positive cytoplasmic foci) at 2hours suggests that the previously observed foci were indeed stress granules, and that cytoplasmic foci formation might require stress granule formation (Figure 5.6 B). Interestingly, in contrast to SH-SY5Y cells TRN1 was not re-localised to the cytoplasm. Nor were any of the FET proteins. Emetine treatment alone did not affect the immunocytochemical staining pattern of TRN1, TIA-1, or the FET proteins which remained predominantly nuclear (Figure 5.6 A). Incubation with 0.5mM arsenite for 24 hours after pre-treatment resulted in cell detachment from the coverslip. This detachment is likely due to cell death.

Figure 5.6 continued overleaf

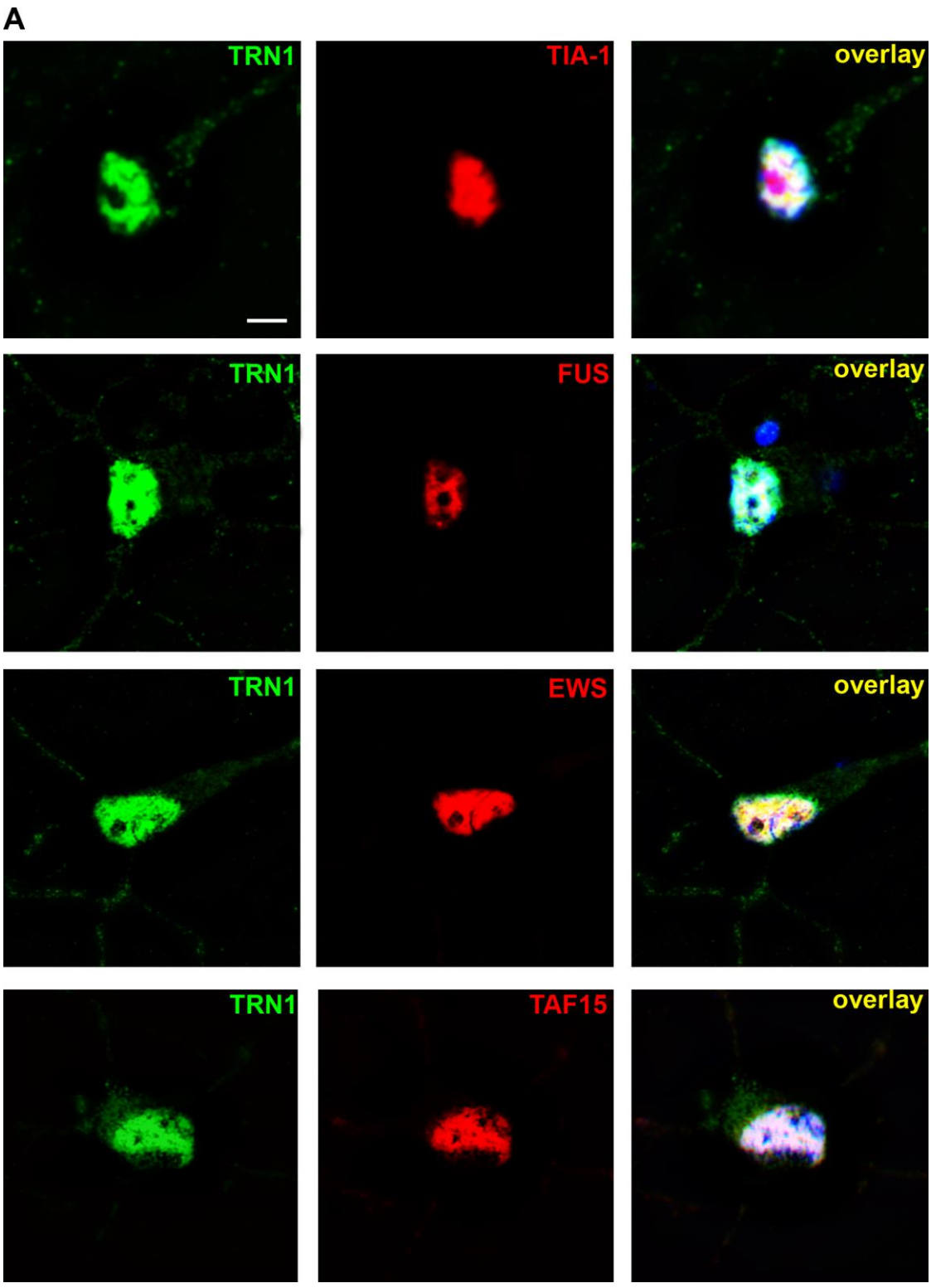

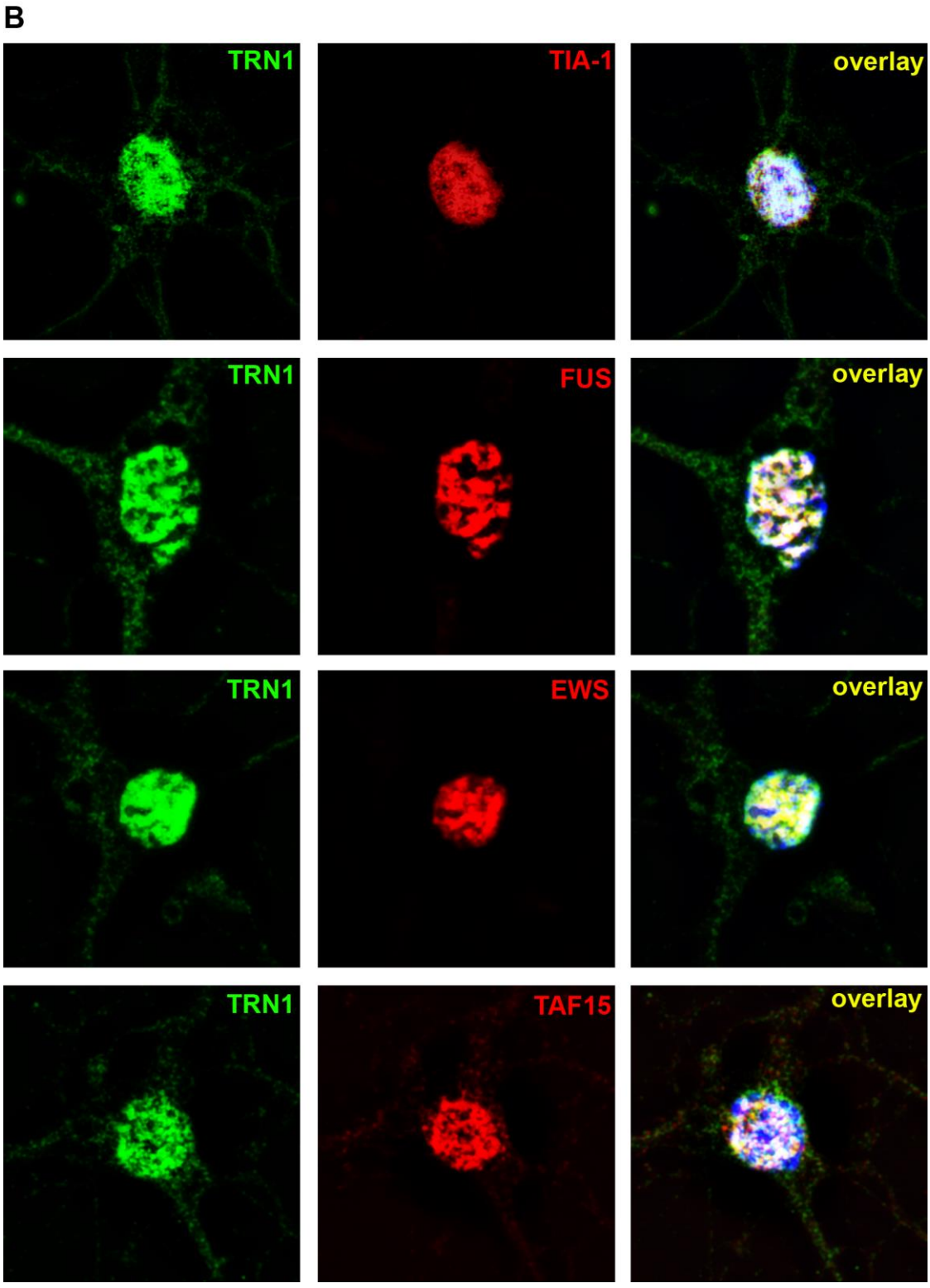

Figure 5.7. Pre-treatment with the stress granule blocker emetine prevents the formation of stress granules. Emetine pre-treatment alone does not affect the nuclear localisation of TRN1, TIA-1 or the FET proteins (A). Pre-treatment with emetine before 2hrs of 0.5mM arsenite stress prevents the formation of stress granules (TIA-1 or TRN1 positive cytoplasmic foci) (B). Scale bar in A represents 15μm. Overlay includes blue nuclear DAPI stain. N=3

5.10 Discussion

These data indicate western blotting of primary cell lysates shows the polyclonal anti-TRN1 antibody and monoclonal FUS, EWS, TAF15 and TIA-1 recognise bands at the correct predicted size for their corresponding protein. Immunocytochemistry of unstressed control neurons reveals nuclear TRN1, FET protein and TIA-1 consistent with previous results from SH-SY5Y data and published descriptions (Tsai et al., 2009, Dormann et al., 2010, Blechingberg et al., 2012a). For the first time this work follows the response of TRN1 and the FET proteins to 2 hours of 0.5mM arsenite, and shows partial re-localisation from the nucleus to cytoplasmic TRN1 positive stress granule foci. Biochemical analysis of TRN1 solubility reveals a clear shift towards the insoluble fraction in response to this oxidative insult. Prolonging the incubation with arsenite for 24 hours recapitulates the immunocytochemical pattern seen at 2 hours, but when neurons are allowed to recover in fresh media TRN1 positive TIA-1 negative foci predominate. Unlike SH-SY5Y cells these foci are all strongly positive for the FET proteins. Finally, emetine pre-treatment prevents the formation of stress granules in primary neurons and therefore the re-localisation of TRN1, and the FET proteins.
It is perhaps unsurprising that TRN1 and the FET proteins are detectable in rat hippocampal neurons given the high degree of conservation across species (Blechingberg et al., 2012a, Burd and Dreyfuss, 1994). These evolutionarily conserved proteins likely serve important functions and may also require a conserved TRN1 to maintain their localisation (http://www.ncbi.nlm.nih.gov/gene/309126). Small differences are noted between the molecular weight of human and murine proteins. For example human FUS is composed of 526 amino acids while rat FUS has 518 producing a protein that is nonetheless 97% identical (Altschul et al., 1997).

Immunocytochemistry of rat hippocampal neurons shows the nuclear staining of TRN1 and the FET proteins replicates from transformed SH-SY5Y cells. Little published data is currently available to contrast these data with, but what is known is that other importins

are predominately nuclear in rat neurons (Kortvely et al., 2005), and overexpressed wild type FUS is also nuclear (Dormann et al., 2010). Perhaps most importantly there is no published description of TRN1 and the FET proteins in neurons subjected to oxidative stress. Arsenite at 0.5mM is commonly used to elicit stress granules formation and as a model of oxidative stress in primary neurons (Tsai et al., 2009, Kunde et al., 2011). Despite their reduced robustness compared to immortalised cell lines these data show they are able to survive for at least 24 hours in 0.5mM arsenite. Immunocytochemistry reveals the formation of cytoplasmic stress granules demarcated by the presence of TIA-1, a commonly used marker of stress granules in primary neurons (Tsai et al., 2009). These are strongly positive for TRN1 which agrees with data gathered from the SH-SY5Y line describing strong and robust co-localisation of TRN1 with stress granules. However, unlike neuroblastoma lines the re-localisation of TRN1 was less pronounced because a considerable proportion remained nuclear. The same was true of EWS which retained its nuclear character whilst also being found in TRN1 positive stress granules. Unlike SH-SY5Y cells TAF15 and FUS were readily found within the TRN1 positive stress granules of rat primary neurons after 2 hours of 0.5mM arsenite. Once again this was in addition to their nuclear stain, indicating partial incomplete re-localisation.

Sequential solubility fractionation after 2 hours 0.5mM arsenite stress showed a pronounced effect of oxidative stress on the solubility of TRN1. Immunoblotting of RIPA soluble and urea soluble fractions revealed unstressed control primary neurons have a predominantly soluble pool of TRN1. However, this is undetectable after 2 hours of arsenite stress. In parallel to this there was a significant increase in the urea soluble fraction of TRN1. This suggests a shift in solubility towards an insoluble likely aggregated form of TRN1. In comparison to data collected form SH-SY5Y cells, this shift is far more pronounced. A significant increase in urea soluble TRN1 is seen in both cell cultures but the RIPA soluble fraction does not diminish in SH-SY5Y cells. The presence of TRN1 in the urea fraction is an important characteristic of FTLD-FUS (Brelstaff et al., 2011), but

presumably the loss of soluble TRN1 would also have a similar affect to removal by siRNA (Figure 4.24). This may explain the higher proportion of FUS, EWS, and TAF15 positive stress granules.

Prolonged incubation with 0.5mM arsenite over 24 hours recapitulates the findings at two hours with an abundance of TRN1 positive stress granules also positive for the FET proteins. However, after a 6 hour recovery period the staining profile has changed in a similar fashion to that seen in SH-SY5Y cells. Only 7.46% of TRN1 positive cytoplasmic foci seen at this time point are also TIA-1 positive and therefore stress granules. Furthermore, these TRN1 foci are strongly positive for all the FET proteins. These foci co-localised with the P-body marker DCP1a in SH-SY5Y cells but it remains to be seen if the same phenomenon is occurring here. At the time of writing there are no published descriptions of stress granules dissociation or P-body transformation in primary neurons but given the importance of cytoplasmic TRN1 and FET protein aggregation to FTLD-FUS this is likely to change.

Finally, emetine pre-treatment successfully prevented the formation of stress granules as illustrated by the lack of TIA-1 positive foci. Moreover, the lack of stress granules corresponded to a lack of TRN1 and FET protein re-localisation. This contrasts at least in part with the data from SH-SY5Y cells in that TRN1 did not re-localise to a diffuse cytoplasmic pattern. This may mean the response of human and rat TRN1 in the face of oxidative stress and emetine pre-treatment is different. Then again the observed difference may be due the immortalised or primary nature of the cells. Other transportins and importins have been implicated in controlling the cell cycle (Roscioli et al., 2012) (Lau et al., 2009). No data is available for the effect of emetine at 24 hours because this resulted in complete cell death. This observation may indicate that the formation of stress granules, at least in the short term is anti-apoptotic. Previous publications regarding the role of stress granules as an adaptive survival response might support this (Takahashi et al., 2013).

Chapter Six: Discussion

6.1 Introduction

Epidemiological studies suggest that FTD is the second most common cause of dementia in individuals under 65, just behind Alzheimer's disease (Onyike and Diehl-Schmid, 2013). Despite the first descriptions of FTD patients and FTLD pathology dating back over a hundred years (Pick, 1892), it was not until recently that a full appreciation of the various subtypes and idiosyncrasies has developed. In 1994 two research groups based in Lund and Manchester proposed clinical and neuropathological criteria for the diagnosis of FTD (1994). The implication of the RNA binding proteins TDP43 and later FUS (Neumann et al., 2009a) has further diversified an already heterogeneous disease. More than anything the renaissance of FTLD research has asked more questions than it has delivered answers. All the while no cure or effective disease modifying treatment is available, leaving patients and their families with cold comfort.

TRN1 and defects in nuclear import were first implicated by investigations focused on ALS-FUS, namely the unusual clustering of causative mutations in the NLS of FUS (Dormann et al., 2010). It was deduced that these would retard the binding to TRN1 and therefore affect nuclear localisation. Given the well documented and widely accepted link between FTLD and ALS the finger of suspicion pointed squarely at TRN1 in FTLD-FUS. The discovery of abundant TRN1 pathology co-localising with FUS in FTLD-FUS (Brelstaff et al., 2011), shortly followed by two more TRN1 cargos (Neumann et al., 2011) compounds the case for a TRN1 centric pathology.

It was noted relatively early on that cytoplasmic diffuse FUS is toxic (Ju et al., 2011), but FTLD-FUS is characterised by inclusion bodies. Consequentially, an appropriate model must include a paradigm of aggregation and inclusion formation. The FET proteins are all heavily involved in RNA binding which when combined with the observation of stress

granule markers in the inclusions begins to suggest these temporary RNA/protein foci as accomplices to aggregation. The data presented herein aligns with mounting publications suggesting that aberrant stress granule persistence may seed aggregate formation, or at the very least sequester FET proteins away from basal functions such as chaperoning mRNA (Fujii and Takumi, 2005).

The absence of causative mutations in the aggregating proteins distinguishes FTLD-FUS from ALS-FUS. Moreover, this is doubly important because many more proteins are aggregating compared with ALS-FUS, including TRN1, EWS and TAF15. This thesis investigated the pathology of banked FTLD-FUS brains in terms of immunohistochemistry, and biochemistry of TRN1. Additionally it details the response of TRN1 to oxidative stress and described for the first time the propensity of this protein to change localisation and solubility in a manner akin to FTLD-FUS. Whilst this work explores the role of TRN1 it remains to be seen whether stress granules are definitive aggregate precursors, or even whether aggregates themselves are toxic or protective. The loss of nuclear FET protein likely has a myriad of consequences, defining which if any represents a single disease causing event is not attempted here due to time constraints. However, such an investigation is crucial if disease modifying treatments are to be designed.

6.2 Summary

In summary, the immunohistochemical staining profile of TRN1 in healthy control brain and spinal cord is nuclear. However, in FTLD-FUS it re-localises to neuronal cytoplasmic and intranuclear inclusions to co-localise with FUS, EWS and TAF15. TRN1 pathology is unique to FTLD-FUS with the one exception of NIIBD, but because only one case of this extremely rare disease was available little can be concluded. Importantly, whilst FUS was strongly detected in the poly glutamine inclusions of Huntington's disease and spinocerebellar ataxia, TRN1 was absent. Biochemical solubility fractionation of healthy

control and FTLD-FUS frontal cortex reveals highly insoluble likely highly aggregated TRN1 in diseased brain. The inclusion of TRN1 appears to be specific in that no other importins are incorporated into the inclusions of FTLD-FUS. Variable positivity of NUP98 and hnRNP A1 suggest the disease does not encompass FET proteins exclusively. Cellular studies in SH-SY5Y cells have shown TRN1 strongly re-localises to stress granules under oxidative and osmotic stress, but only increases in insolubility under the former. Low levels of FET protein positivity in said stress granules can be increased by prolonging the exposure to stress at lower concentrations. FUS does not change its solubility profile like TRN1. Recovery in stressor free fresh media changes the biology of TRN1 cytoplasmic foci by incorporating ubiquitin and DCP1a and defining them as P-bodies. Importantly, stress granules are not responsible for the increase in TRN1 insolubility suggesting an unidentified event outside of stress granules. Moreover, TRN1 is not culpable for FET protein inclusion in stress granules but it remains to be seen if FET proteins are responsible for TRN1 inclusion. Many of these findings hold true in primary neurons. Strong TRN1 stress granule incorporation is accompanied by near complete positivity for all the FET proteins. Additionally, TRN1 increases in terms of insolubility in response to arsenite stress. Recovery in fresh media recapitulates the loss of stress granule markers seen in SH-SY5Y cells but it remains to be seen if the foci have developed the characteristics of P-bodies.

6.3 Suggested model

From these data the following model of FTLD-FUS pathogenesis is suggested (Figure 6.1). Healthy neurons maintain a predominantly nuclear TRN1 and FET protein allowing them to splice appropriate mRNA whilst low levels in the cytoplasm still allow chaperoning of mRNA to dendrites for translation. As the neuron ages oxidative insult becomes more problematic, or an as yet unidentified change hampers TRN1 driven import. The result is the formation of cytoplasmic stress granules, and a shift towards insolubility of TRN1. The chronic nature of the stress means more and more FET protein is incorporated into

these foci. A change in protein characteristics, perhaps due to their prionoid properties, prevents the dissociation of these TRN1-FET foci after stress granule dissolution. Over time and continued oxidative stress these stress granule foci coalesce into a permanent inclusion body. Either this inclusion creates a toxic weight on the cell, or sequestration of proteins into this inclusion creates a loss of function in a vital cellular process such as splicing of tau and cytoskeleton maintenance (Orozco and Edbauer, 2013). The result is an overwhelming cellular challenge that leads to loss of neuronal function and eventual cell death. The evidence for which is the spongiosis and massive inclusion burden seen in FTLD-FUS.

6.4 Limitations

Whilst this work contributes to the sum knowledge of the field it does not presume to hold all the answers to pathogenesis. Many questions still remain, some could be answered easily, others would require a great deal more time and resources. For example, the insolubility status of EWS and TAF15 in FTLD-FUS and cells exposed to oxidative stress remains unknown. Whilst other authors have reported a shift in insolubility, this is yet to be confirmed in the QSBB collection (Neumann et al., 2011). This thesis focused on FTLD-FUS but it would be interesting to see if EWS and TAF15 also appear in the poly-glutamine inclusions of Huntington's disease alongside FUS. Given their high degree of homology this might be expected but if not the sole inclusion of FUS would highlight a unique property in the FET family. The seeding of stress granules occurs via the prionoid domains of TIA-1 and other proteins, the incorporation of FET proteins is likely via their RNA binding domains, but little is known about the incorporation of TRN1. It would be informative to investigate whether it is recruited via its binding to FET proteins or some other method. A tripartite knockdown of FUS, EWS and TAF15 followed by arsenite stress may shed some light on TRN1 recruitment. However there are other proteins imported by TRN1 that also re-localise to stress granules, such as hnRNP A1. To avoid these confounding proteins the use of a global NLS-

competitor peptide like M9 (Nakielny et al., 1996), would prevent or reduce TRN1 binding. Subsequent treatment with arsenite might reveal a reduced TRN1 presence in stress granules. Now that is it clear that FUS, EWS and TAF15 are recruited to stress granules in neurons, investigations should now focus on what if any folding, dimerization, or post-transcriptional changes occur in these foci. This may yield clues as to why these foci appear to be resilient to stress granule dissolution. In this vein it is still uncertain whether inclusion bodies represent protective or toxic phenomena. There is evidence that loss of FUS increases the inclusion of exon 10 in tau mRNA leading to an increase in 4R tau (Orozco and Edbauer, 2013). In such a morphologically complex cell type loss of cytoskeletal control could have profound consequences. On the other hand, virtually all neurodegenerative diseases have some form of aggregate pathology despite a multitude of different mutations with different actions, suggesting that neurodegeneration is inexorably linked to aggregates. Finally, broader questions still remain to be answered. The QSBB collection of FTLD-FUS includes a mother and son pair who both developed the disease, with such a strong familial link why has a causative mutation yet to be found? Perhaps broader and more complex defects in an individual's response to a lifetime's exposure to oxidative stress are to blame.

The discovery of TRN1 aggregating alongside a whole family of cargos has dramatically changed the landscape of FTLD-FUS research. Whilst a definitive pathogenic pathway has yet to be proven it has opened many new avenues of research. Undoubtedly one of these will spawn new drug targets and the promise of disease modifying treatments in the near future.

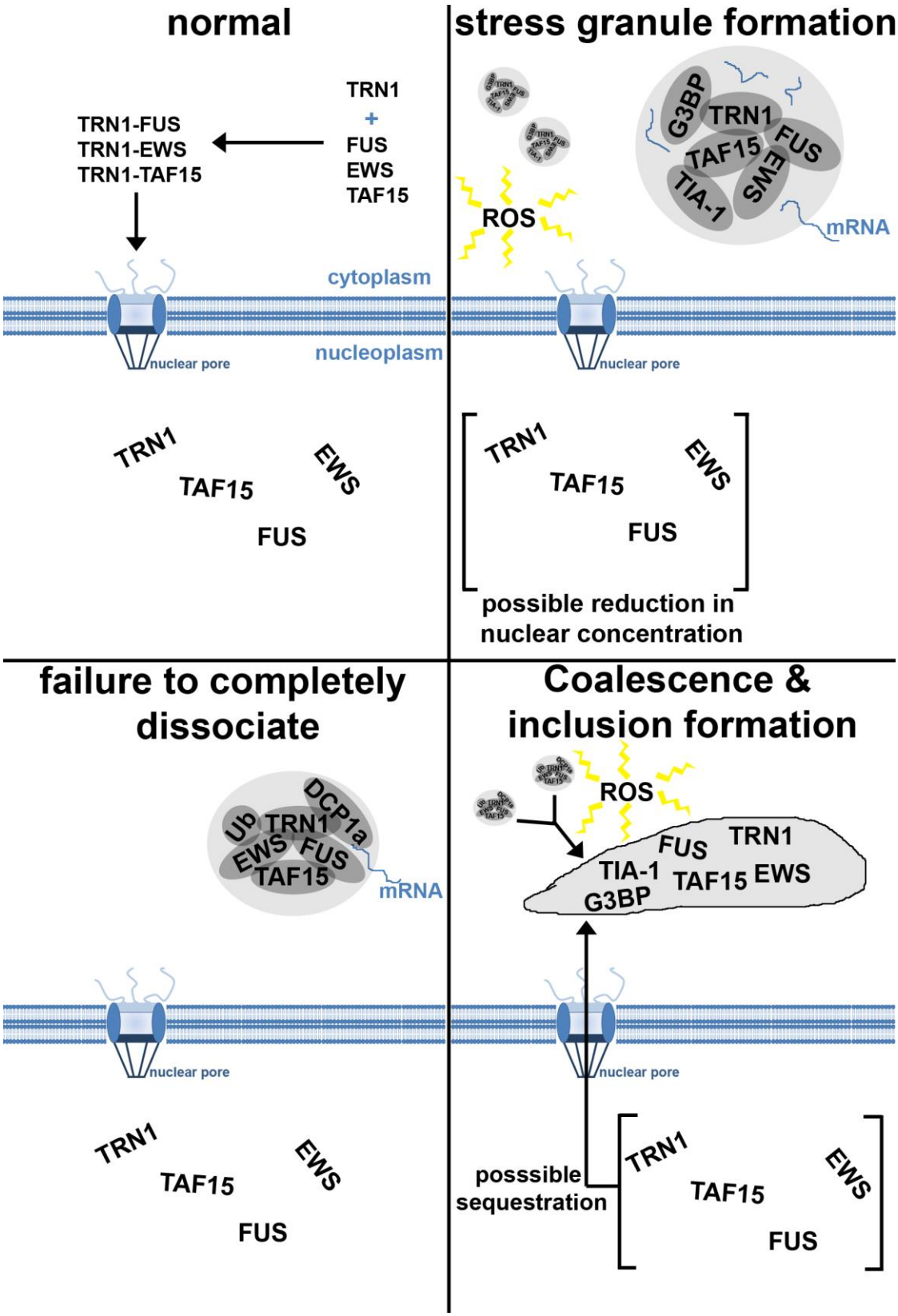

Figure 6.1. Possible progression of disease pathology in FTLD-FUS. In healthy normal neurons the importer TRN1 activity translocates the FET proteins FUS, EWS and TAF15 back into the nucleus (top left). In response to reactive oxygen species (ROS) a proportion of TRN1, FUS, EWS and TAF15 re-localise to stress granules and TRN1 becomes more insoluble (top right). These cytoplasmic foci do not dissociate after stress granule dissolution and incorporate ubiquitin (bottom left). Over time and chronic

oxidative stress, stress granules coalesce and take on inclusion morphology as permanent features (bottom right).

References

(1994) Clinical and neuropathological criteria for frontotemporal dementia. The Lund and Manchester Groups. *J Neurol Neurosurg Psychiatry,* 57**,** 416-8.

ABERNATHY, C. O., LIU, Y. P., LONGFELLOW, D., APOSHIAN, H. V., BECK, B., FOWLER, B., GOYER, R., MENZER, R., ROSSMAN, T., THOMPSON, C. & WAALKES, M. (1999) Arsenic: health effects, mechanisms of actions, and research issues. *Environ Health Perspect,* 107**,** 593-7.

ALBERTI, S., HALFMANN, R., KING, O., KAPILA, A. & LINDQUIST, S. (2009) A systematic survey identifies prions and illuminates sequence features of prionogenic proteins. *Cell,* 137**,** 146-58.

ALTSCHUL, S. F., MADDEN, T. L., SCHAFFER, A. A., ZHANG, J., ZHANG, Z., MILLER, W. & LIPMAN, D. J. (1997) Gapped BLAST and PSI-BLAST: a new generation of protein database search programs. *Nucleic Acids Res,* 25**,** 3389-402.

ANDERSSON, M. K., STAHLBERG, A., ARVIDSSON, Y., OLOFSSON, A., SEMB, H., STENMAN, G., NILSSON, O. & AMAN, P. (2008a) The multifunctional FUS, EWS and TAF15 proto-oncoproteins show cell type-specific expression patterns and involvement in cell spreading and stress response. *BMC Cell Biol,* 9**,** 37.

ANDERSSON, M. K., STAHLBERG, A., ARVIDSSON, Y., OLOFSSON, A., SEMB, H., STENMAN, G., NILSSON, O. & AMAN, P. (2008b) The multifunctional FUS, EWS and TAF15 proto-oncoproteins show cell type-specific expression patterns and involvement in cell spreading and stress response. *BMC.Cell Biol,* 9**,** 37.

ANDRADE, M. A. & BORK, P. (1995) HEAT repeats in the Huntington's disease protein. *Nat Genet,* 11**,** 115-6.

ANVAR, S. Y., RAZ, Y., VERWAY, N., VAN DER SLUIJS, B., VENEMA, A., GOEMAN, J. J., VISSING, J., VAN DER MAAREL, S. M., T HOEN, P. A., VAN ENGELEN, B. G. & RAZ, V. (2013) A decline in PABPN1 induces progressive muscle weakness in oculopharyngeal muscle dystrophy and in muscle aging. *Aging (Albany NY),* 5**,** 412-26.

ARAI, T., HASEGAWA, M., AKIYAMA, H., IKEDA, K., NONAKA, T., MORI, H., MANN, D., TSUCHIYA, K., YOSHIDA, M., HASHIZUME, Y. & ODA, T. (2006) TDP-43 is a component of ubiquitin-positive tau-negative inclusions in frontotemporal lobar degeneration and amyotrophic lateral sclerosis. *Biochem Biophys Res Commun,* 351**,** 602-11.

ARNOLD, S. E., HYMAN, B. T. & VAN HOESEN, G. W. (1994) Neuropathologic changes of the temporal pole in Alzheimer's disease and Pick's disease. *Arch Neurol,* 51**,** 145-50.

ATHANASOPOULOS, V., BARKER, A., YU, D., TAN, A. H., SRIVASTAVA, M., CONTRERAS, N., WANG, J., LAM, K. P., BROWN, S. H., GOODNOW, C. C., DIXON, N. E., LEEDMAN, P. J., SAINT, R. & VINUESA, C. G. (2010) The

ROQUIN family of proteins localizes to stress granules via the ROQ domain and binds target mRNAs. *FEBS J,* 277**,** 2109-27.
AYALA, Y. M., ZAGO, P., D'AMBROGIO, A., XU, Y. F., PETRUCELLI, L., BURATTI, E. & BARALLE, F. E. (2008) Structural determinants of the cellular localization and shuttling of TDP-43. *J Cell Sci,* 121**,** 3778-85.
BAKER, M., MACKENZIE, I. R., PICKERING-BROWN, S. M., GASS, J., RADEMAKERS, R., LINDHOLM, C., SNOWDEN, J., ADAMSON, J., SADOVNICK, A. D., ROLLINSON, S., CANNON, A., DWOSH, E., NEARY, D., MELQUIST, S., RICHARDSON, A., DICKSON, D., BERGER, Z., ERIKSEN, J., ROBINSON, T., ZEHR, C., DICKEY, C. A., CROOK, R., MCGOWAN, E., MANN, D., BOEVE, B., FELDMAN, H. & HUTTON, M. (2006) Mutations in progranulin cause tau-negative frontotemporal dementia linked to chromosome 17. *Nature,* 442**,** 916-9.
BARR, D. P. & MASON, R. P. (1995) Mechanism of radical production from the reaction of cytochrome c with organic hydroperoxides. An ESR spin trapping investigation. *J Biol Chem,* 270**,** 12709-16.
BARROW, C. J., YASUDA, A., KENNY, P. T. & ZAGORSKI, M. G. (1992) Solution conformations and aggregational properties of synthetic amyloid beta-peptides of Alzheimer's disease. Analysis of circular dichroism spectra. *J Mol Biol,* 225**,** 1075-93.
BATHGATE, D., SNOWDEN, J. S., VARMA, A., BLACKSHAW, A. & NEARY, D. (2001) Behaviour in frontotemporal dementia, Alzheimer's disease and vascular dementia. *Acta Neurol Scand,* 103**,** 367-78.
BAUMER, D., HILTON, D., PAINE, S. M., TURNER, M. R., LOWE, J., TALBOT, K. & ANSORGE, O. (2010) Juvenile ALS with basophilic inclusions is a FUS proteinopathy with FUS mutations. *Neurology,* 75**,** 611-8.
BELZIL, V. V., DAOUD, H., ST-ONGE, J., DESJARLAIS, A., BOUCHARD, J. P., DUPRE, N., LACOMBLEZ, L., SALACHAS, F., PRADAT, P. F., MEININGER, V., CAMU, W., DION, P. A. & ROULEAU, G. A. (2011a) Identification of novel FUS mutations in sporadic cases of amyotrophic lateral sclerosis. *Amyotroph Lateral Scler,* 12**,** 113-7.
BELZIL, V. V., LANGLAIS, J. S., DAOUD, H., DION, P. A., BRAIS, B. & ROULEAU, G. A. (2012) Novel FUS deletion in a patient with juvenile amyotrophic lateral sclerosis. *Arch Neurol,* 69**,** 653-6.
BELZIL, V. V., ST-ONGE, J., DAOUD, H., DESJARLAIS, A., BOUCHARD, J. P., DUPRE, N., CAMU, W., DION, P. A. & ROULEAU, G. A. (2011b) Identification of a FUS splicing mutation in a large family with amyotrophic lateral sclerosis. *J Hum Genet,* 56**,** 247-9.
BELZIL, V. V., VALDMANIS, P. N., DION, P. A., DAOUD, H., KABASHI, E., NOREAU, A., GAUTHIER, J., HINCE, P., DESJARLAIS, A., BOUCHARD, J. P., LACOMBLEZ, L., SALACHAS, F., PRADAT, P. F., CAMU, W., MEININGER, V., DUPRE, N. & ROULEAU, G. A. (2009) Mutations in FUS cause FALS and SALS in French and French Canadian populations. *Neurology,* 73**,** 1176-9.
BENAJIBA, L., LE BER, I., CAMUZAT, A., LACOSTE, M., THOMAS-ANTERION, C., COURATIER, P., LEGALLIC, S., SALACHAS, F., HANNEQUIN, D., DECOUSUS, M., LACOMBLEZ, L., GUEDJ, E., GOLFIER, V., CAMU, W., DUBOIS, B., CAMPION, D., MEININGER, V. & BRICE, A. (2009) TARDBP mutations in motoneuron disease with frontotemporal lobar degeneration. *Ann Neurol,* 65**,** 470-3.

BENTMANN, E., NEUMANN, M., TAHIROVIC, S., RODDE, R., DORMANN, D. & HAASS, C. (2012) Requirements for stress granule recruitment of fused in sarcoma (FUS) and TAR DNA-binding protein of 43 kDa (TDP-43). *J Biol Chem,* 287**,** 23079-94.

BERTOLOTTI, A., LUTZ, Y., HEARD, D. J., CHAMBON, P. & TORA, L. (1996) hTAF(II)68, a novel RNA/ssDNA-binding protein with homology to the pro-oncoproteins TLS/FUS and EWS is associated with both TFIID and RNA polymerase II. *EMBO J,* 15**,** 5022-31.

BERTOLOTTI, A., MELOT, T., ACKER, J., VIGNERON, M., DELATTRE, O. & TORA, L. (1998) EWS, but not EWS-FLI-1, is associated with both TFIID and RNA polymerase II: interactions between two members of the TET family, EWS and hTAFII68, and subunits of TFIID and RNA polymerase II complexes. *Mol Cell Biol,* 18**,** 1489-97.

BIGIO, E. H., WU, J. Y., DENG, H. X., BIT-IVAN, E. N., MAO, Q., GANTI, R., PETERSON, M., SIDDIQUE, N., GEULA, C., SIDDIQUE, T. & MESULAM, M. (2013) Inclusions in frontotemporal lobar degeneration with TDP-43 proteinopathy (FTLD-TDP) and amyotrophic lateral sclerosis (ALS), but not FTLD with FUS proteinopathy (FTLD-FUS), have properties of amyloid. *Acta Neuropathol,* 125**,** 463-5.

BLAIR, I. P., WILLIAMS, K. L., WARRAICH, S. T., DURNALL, J. C., THOENG, A. D., MANAVIS, J., BLUMBERGS, P. C., VUCIC, S., KIERNAN, M. C. & NICHOLSON, G. A. (2010) FUS mutations in amyotrophic lateral sclerosis: clinical, pathological, neurophysiological and genetic analysis. *J Neurol Neurosurg Psychiatry,* 81**,** 639-45.

BLECHINGBERG, J., HOLM, I. E. & NIELSEN, A. L. (2012a) Characterization and expression analysis in the developing embryonic brain of the porcine FET family: FUS, EWS, and TAF15. *Gene,* 493**,** 27-35.

BLECHINGBERG, J., LUO, Y., BOLUND, L., DAMGAARD, C. K. & NIELSEN, A. L. (2012b) Gene expression responses to FUS, EWS, and TAF15 reduction and stress granule sequestration analyses identifies FET-protein non-redundant functions. *PLoS One,* 7**,** e46251.

BOL, G. M., RAMAN, V., VAN DER GROEP, P., VERMEULEN, J. F., PATEL, A. H., VAN DER WALL, E. & VAN DIEST, P. J. (2013) Expression of the RNA helicase DDX3 and the hypoxia response in breast cancer. *PLoS One,* 8**,** e63548.

BONIFACI, N., MOROIANU, J., RADU, A. & BLOBEL, G. (1997) Karyopherin beta2 mediates nuclear import of a mRNA binding protein. *Proc Natl Acad Sci U S A,* 94**,** 5055-60.

BORCHELT, D. R., DAVIS, J., FISCHER, M., LEE, M. K., SLUNT, H. H., RATOVITSKY, T., REGARD, J., COPELAND, N. G., JENKINS, N. A., SISODIA, S. S. & PRICE, D. L. (1996) A vector for expressing foreign genes in the brains and hearts of transgenic mice. *Genet Anal,* 13**,** 159-63.

BORRONI, B., ARCHETTI, S., DEL BO, R., PAPETTI, A., BURATTI, E., BONVICINI, C., AGOSTI, C., COSSEDDU, M., TURLA, M., DI LORENZO, D., PIETRO COMI, G., GENNARELLI, M. & PADOVANI, A. (2010) TARDBP mutations in frontotemporal lobar degeneration: frequency, clinical features, and disease course. *Rejuvenation Res,* 13**,** 509-17.

BOSCO, D. A., LEMAY, N., KO, H. K., ZHOU, H., BURKE, C., KWIATKOWSKI, T. J., JR., SAPP, P., MCKENNA-YASEK, D., BROWN, R. H., JR. & HAYWARD, L. J. (2010)

Mutant FUS proteins that cause amyotrophic lateral sclerosis incorporate into stress granules. *Hum Mol Genet,* 19**,** 4160-75.
BRANDMEIR, N. J., GESER, F., KWONG, L. K., ZIMMERMAN, E., QIAN, J., LEE, V. M. & TROJANOWSKI, J. Q. (2008) Severe subcortical TDP-43 pathology in sporadic frontotemporal lobar degeneration with motor neuron disease. *Acta Neuropathol,* 115**,** 123-31.
BRASS, A. L., DYKXHOORN, D. M., BENITA, Y., YAN, N., ENGELMAN, A., XAVIER, R. J., LIEBERMAN, J. & ELLEDGE, S. J. (2008) Identification of host proteins required for HIV infection through a functional genomic screen. *Science,* 319**,** 921-6.
BRELSTAFF, J., LASHLEY, T., HOLTON, J. L., LEES, A. J., ROSSOR, M. N., BANDOPADHYAY, R. & REVESZ, T. (2011) Transportin1: a marker of FTLD-FUS. *Acta Neuropathol,* 122**,** 591-600.
BUCHAN, J. R. & PARKER, R. (2009) Eukaryotic stress granules: the ins and outs of translation. *Mol Cell,* 36**,** 932-41.
BURATTI, E., DORK, T., ZUCCATO, E., PAGANI, F., ROMANO, M. & BARALLE, F. E. (2001) Nuclear factor TDP-43 and SR proteins promote in vitro and in vivo CFTR exon 9 skipping. *EMBO J,* 20**,** 1774-84.
BURD, C. G. & DREYFUSS, G. (1994) Conserved structures and diversity of functions of RNA-binding proteins. *Science,* 265**,** 615-21.
CAIRNS, N. J., BIGIO, E. H., MACKENZIE, I. R., NEUMANN, M., LEE, V. M., HATANPAA, K. J., WHITE, C. L., 3RD, SCHNEIDER, J. A., GRINBERG, L. T., HALLIDAY, G., DUYCKAERTS, C., LOWE, J. S., HOLM, I. E., TOLNAY, M., OKAMOTO, K., YOKOO, H., MURAYAMA, S., WOULFE, J., MUNOZ, D. G., DICKSON, D. W., INCE, P. G., TROJANOWSKI, J. Q. & MANN, D. M. (2007) Neuropathologic diagnostic and nosologic criteria for frontotemporal lobar degeneration: consensus of the Consortium for Frontotemporal Lobar Degeneration. *Acta Neuropathol,* 114**,** 5-22.
CHANG, W. L. & TARN, W. Y. (2009) A role for transportin in deposition of TTP to cytoplasmic RNA granules and mRNA decay. *Nucleic Acids Res,* 37**,** 6600-12.
CHIO, A., RESTAGNO, G., BRUNETTI, M., OSSOLA, I., CALVO, A., MORA, G., SABATELLI, M., MONSURRO, M. R., BATTISTINI, S., MANDRIOLI, J., SALVI, F., SPATARO, R., SCHYMICK, J., TRAYNOR, B. J. & LA BELLA, V. (2009) Two Italian kindreds with familial amyotrophic lateral sclerosis due to FUS mutation. *Neurobiol Aging,* 30**,** 1272-5.
CIRONI, L., RIGGI, N., PROVERO, P., WOLF, N., SUVA, M. L., SUVA, D., KINDLER, V. & STAMENKOVIC, I. (2008) IGF1 is a common target gene of Ewing's sarcoma fusion proteins in mesenchymal progenitor cells. *PLoS One,* 3**,** e2634.
CLEVELAND, D. W., HWO, S. Y. & KIRSCHNER, M. W. (1977) Purification of tau, a microtubule-associated protein that induces assembly of microtubules from purified tubulin. *J Mol Biol,* 116**,** 207-25.
COHEN, T. J., HWANG, A. W., UNGER, T., TROJANOWSKI, J. Q. & LEE, V. M. (2012) Redox signalling directly regulates TDP-43 via cysteine oxidation and disulphide cross-linking. *EMBO J,* 31**,** 1241-52.
COLOMBRITA, C., ZENNARO, E., FALLINI, C., WEBER, M., SOMMACAL, A., BURATTI, E., SILANI, V. & RATTI, A. (2009) TDP-43 is recruited to stress granules in conditions of oxidative insult. *J Neurochem,* 111**,** 1051-61.

CONTE, A., LATTANTE, S., ZOLLINO, M., MARANGI, G., LUIGETTI, M., DEL GRANDE, A., SERVIDEI, S., TROMBETTA, F. & SABATELLI, M. (2012) P525L FUS mutation is consistently associated with a severe form of juvenile amyotrophic lateral sclerosis. *Neuromuscul Disord,* 22**,** 73-5.

CONWAY, K. A., LEE, S. J., ROCHET, J. C., DING, T. T., WILLIAMSON, R. E. & LANSBURY, P. T., JR. (2000) Acceleration of oligomerization, not fibrillization, is a shared property of both alpha-synuclein mutations linked to early-onset Parkinson's disease: implications for pathogenesis and therapy. *Proc Natl Acad Sci U S A,* 97**,** 571-6.

COOK, C., GENDRON, T. F., SCHEFFEL, K., CARLOMAGNO, Y., DUNMORE, J., DETURE, M. & PETRUCELLI, L. (2012) Loss of HDAC6, a novel CHIP substrate, alleviates abnormal tau accumulation. *Hum Mol Genet,* 21**,** 2936-45.

CORRADO, L., DEL BO, R., CASTELLOTTI, B., RATTI, A., CEREDA, C., PENCO, S., SORARU, G., CARLOMAGNO, Y., GHEZZI, S., PENSATO, V., COLOMBRITA, C., GAGLIARDI, S., COZZI, L., ORSETTI, V., MANCUSO, M., SICILIANO, G., MAZZINI, L., COMI, G. P., GELLERA, C., CERONI, M., D'ALFONSO, S. & SILANI, V. (2010) Mutations of FUS gene in sporadic amyotrophic lateral sclerosis. *J Med Genet,* 47**,** 190-4.

COUGOT, N., BABAJKO, S. & SERAPHIN, B. (2004) Cytoplasmic foci are sites of mRNA decay in human cells. *J Cell Biol,* 165**,** 31-40.

COUTHOUIS, J., HART, M. P., SHORTER, J., DEJESUS-HERNANDEZ, M., ERION, R., ORISTANO, R., LIU, A. X., RAMOS, D., JETHAVA, N., HOSANGADI, D., EPSTEIN, J., CHIANG, A., DIAZ, Z., NAKAYA, T., IBRAHIM, F., KIM, H. J., SOLSKI, J. A., WILLIAMS, K. L., MOJSILOVIC-PETROVIC, J., INGRE, C., BOYLAN, K., GRAFF-RADFORD, N. R., DICKSON, D. W., CLAY-FALCONE, D., ELMAN, L., MCCLUSKEY, L., GREENE, R., KALB, R. G., LEE, V. M., TROJANOWSKI, J. Q., LUDOLPH, A., ROBBERECHT, W., ANDERSEN, P. M., NICHOLSON, G. A., BLAIR, I. P., KING, O. D., BONINI, N. M., VAN DEERLIN, V., RADEMAKERS, R., MOURELATOS, Z. & GITLER, A. D. (2011) A yeast functional screen predicts new candidate ALS disease genes. *Proc Natl Acad Sci U S A,* 108**,** 20881-90.

CROZAT, A., AMAN, P., MANDAHL, N. & RON, D. (1993) Fusion of CHOP to a novel RNA-binding protein in human myxoid liposarcoma. *Nature,* 363**,** 640-4.

CRUTS, M., GIJSELINCK, I., VAN DER ZEE, J., ENGELBORGHS, S., WILS, H., PIRICI, D., RADEMAKERS, R., VANDENBERGHE, R., DERMAUT, B., MARTIN, J. J., VAN DUIJN, C., PEETERS, K., SCIOT, R., SANTENS, P., DE POOTER, T., MATTHEIJSSENS, M., VAN DEN BROECK, M., CUIJT, I., VENNEKENS, K., DE DEYN, P. P., KUMAR-SINGH, S. & VAN BROECKHOVEN, C. (2006) Null mutations in progranulin cause ubiquitin-positive frontotemporal dementia linked to chromosome 17q21. *Nature,* 442**,** 920-4.

DAUPHINOT, L., DE OLIVEIRA, C., MELOT, T., SEVENET, N., THOMAS, V., WEISSMAN, B. E. & DELATTRE, O. (2001) Analysis of the expression of cell cycle regulators in Ewing cell lines: EWS-FLI-1 modulates p57KIP2and c-Myc expression. *Oncogene,* 20**,** 3258-65.

DAVIDSON, W. S., JONAS, A., CLAYTON, D. F. & GEORGE, J. M. (1998) Stabilization of alpha-synuclein secondary structure upon binding to synthetic membranes. *J Biol Chem,* 273**,** 9443-9.

DAVIDSON, Y., KELLEY, T., MACKENZIE, I. R., PICKERING-BROWN, S., DU PLESSIS, D., NEARY, D., SNOWDEN, J. S. & MANN, D. M. (2007) Ubiquitinated pathological lesions in frontotemporal lobar degeneration contain the TAR DNA-binding protein, TDP-43. *Acta Neuropathol,* 113**,** 521-33.

DAVIDSON, Y. S., ROBINSON, A. C., HU, Q., MISHRA, M., BABORIE, A., JAROS, E., PERRY, R. H., CAIRNS, N. J., RICHARDSON, A., GERHARD, A., NEARY, D., SNOWDEN, J. S., BIGIO, E. H. & MANN, D. M. (2012) Nuclear Carrier and RNA Binding Proteins in Frontotemporal Lobar Degeneration associated with Fused in Sarcoma (FUS) pathological changes. *Neuropathol Appl Neurobiol*.

DE STROOPER, B., SIMONS, M., MULTHAUP, G., VAN LEUVEN, F., BEYREUTHER, K. & DOTTI, C. G. (1995) Production of intracellular amyloid-containing fragments in hippocampal neurons expressing human amyloid precursor protein and protection against amyloidogenesis by subtle amino acid substitutions in the rodent sequence. *EMBO J,* 14**,** 4932-8.

DEJESUS-HERNANDEZ, M., KOCERHA, J., FINCH, N., CROOK, R., BAKER, M., DESARO, P., JOHNSTON, A., RUTHERFORD, N., WOJTAS, A., KENNELLY, K., WSZOLEK, Z. K., GRAFF-RADFORD, N., BOYLAN, K. & RADEMAKERS, R. (2010) De novo truncating FUS gene mutation as a cause of sporadic amyotrophic lateral sclerosis. *Hum Mutat,* 31**,** E1377-89.

DEJESUS-HERNANDEZ, M., MACKENZIE, I. R., BOEVE, B. F., BOXER, A. L., BAKER, M., RUTHERFORD, N. J., NICHOLSON, A. M., FINCH, N. A., FLYNN, H., ADAMSON, J., KOURI, N., WOJTAS, A., SENGDY, P., HSIUNG, G. Y., KARYDAS, A., SEELEY, W. W., JOSEPHS, K. A., COPPOLA, G., GESCHWIND, D. H., WSZOLEK, Z. K., FELDMAN, H., KNOPMAN, D. S., PETERSEN, R. C., MILLER, B. L., DICKSON, D. W., BOYLAN, K. B., GRAFF-RADFORD, N. R. & RADEMAKERS, R. (2011) Expanded GGGGCC Hexanucleotide Repeat in Noncoding Region of C9ORF72 Causes Chromosome 9p-Linked FTD and ALS. *Neuron,* 72**,** 245-56.

DELACOURTE, A. (2008) Tau, a biological marker of neurodegenerative diseases. *Handb Clin Neurol,* 89**,** 161-72.

DENNING, D. P., PATEL, S. S., UVERSKY, V., FINK, A. L. & REXACH, M. (2003) Disorder in the nuclear pore complex: the FG repeat regions of nucleoporins are natively unfolded. *Proc Natl Acad Sci U S A,* 100**,** 2450-5.

DEWEY, C. M., CENIK, B., SEPHTON, C. F., DRIES, D. R., MAYER, P., 3RD, GOOD, S. K., JOHNSON, B. A., HERZ, J. & YU, G. (2011) TDP-43 is directed to stress granules by sorbitol, a novel physiological osmotic and oxidative stressor. *Mol Cell Biol,* 31**,** 1098-108.

DOI, H., KOYANO, S., SUZUKI, Y., NUKINA, N. & KUROIWA, Y. (2010) The RNA-binding protein FUS/TLS is a common aggregate-interacting protein in polyglutamine diseases. *Neurosci Res,* 66**,** 131-3.

DORMANN, D., MADL, T., VALORI, C. F., BENTMANN, E., TAHIROVIC, S., ABOU-AJRAM, C., KREMMER, E., ANSORGE, O., MACKENZIE, I. R., NEUMANN, M. & HAASS, C. (2012) Arginine methylation next to the PY-NLS modulates Transportin binding and nuclear import of FUS. *EMBO J,* 31**,** 4258-75.

DORMANN, D., RODDE, R., EDBAUER, D., BENTMANN, E., FISCHER, I., HRUSCHA, A., THAN, M. E., MACKENZIE, I. R., CAPELL, A., SCHMID, B., NEUMANN, M. & HAASS, C. (2010) ALS-associated fused in sarcoma (FUS) mutations disrupt Transportin-mediated nuclear import. *EMBO J,* 29**,** 2841-57.

DOWNING, J. R., HEAD, D. R., PARHAM, D. M., DOUGLASS, E. C., HULSHOF, M. G., LINK, M. P., MOTRONI, T. A., GRIER, H. E., CURCIO-BRINT, A. M. & SHAPIRO, D. N. (1993) Detection of the (11;22)(q24;q12) translocation of Ewing's sarcoma and peripheral neuroectodermal tumor by reverse transcription polymerase chain reaction. *Am J Pathol,* 143**,** 1294-300.

DUTERTRE, M., SANCHEZ, G., DE CIAN, M. C., BARBIER, J., DARDENNE, E., GRATADOU, L., DUJARDIN, G., LE JOSSIC-CORCOS, C., CORCOS, L. & AUBOEUF, D. (2010) Cotranscriptional exon skipping in the genotoxic stress response. *Nat Struct Mol Biol,* 17**,** 1358-66.

FERRANTE, R. J., BROWNE, S. E., SHINOBU, L. A., BOWLING, A. C., BAIK, M. J., MACGARVEY, U., KOWALL, N. W., BROWN, R. H., JR. & BEAL, M. F. (1997) Evidence of increased oxidative damage in both sporadic and familial amyotrophic lateral sclerosis. *J Neurochem,* 69**,** 2064-74.

FINCH, N., BAKER, M., CROOK, R., SWANSON, K., KUNTZ, K., SURTEES, R., BISCEGLIO, G., ROVELET-LECRUX, A., BOEVE, B., PETERSEN, R. C., DICKSON, D. W., YOUNKIN, S. G., DERAMECOURT, V., CROOK, J., GRAFF-RADFORD, N. R. & RADEMAKERS, R. (2009) Plasma progranulin levels predict progranulin mutation status in frontotemporal dementia patients and asymptomatic family members. *Brain,* 132**,** 583-91.

FRASER, P. E., DUFFY, L. K., O'MALLEY, M. B., NGUYEN, J., INOUYE, H. & KIRSCHNER, D. A. (1991) Morphology and antibody recognition of synthetic beta-amyloid peptides. *J Neurosci Res,* 28**,** 474-85.

FUJII, R., OKABE, S., URUSHIDO, T., INOUE, K., YOSHIMURA, A., TACHIBANA, T., NISHIKAWA, T., HICKS, G. G. & TAKUMI, T. (2005) The RNA binding protein TLS is translocated to dendritic spines by mGluR5 activation and regulates spine morphology. *Curr Biol,* 15**,** 587-93.

FUJII, R. & TAKUMI, T. (2005) TLS facilitates transport of mRNA encoding an actin-stabilizing protein to dendritic spines. *J Cell Sci,* 118**,** 5755-65.

FUJIMURA, K., SUZUKI, T., YASUDA, Y., MURATA, M., KATAHIRA, J. & YONEDA, Y. (2010) Identification of importin alpha1 as a novel constituent of RNA stress granules. *Biochim Biophys Acta,* 1803**,** 865-71.

FUJITA, K., ITO, H., NAKANO, S., KINOSHITA, Y., WATE, R. & KUSAKA, H. (2008) Immunohistochemical identification of messenger RNA-related proteins in basophilic inclusions of adult-onset atypical motor neuron disease. *Acta Neuropathol,* 116**,** 439-45.

FUKUMA, M., OKITA, H., HATA, J. & UMEZAWA, A. (2003) Upregulation of Id2, an oncogenic helix-loop-helix protein, is mediated by the chimeric EWS/ets protein in Ewing sarcoma. *Oncogene,* 22**,** 1-9.

GAL, J., ZHANG, J., KWINTER, D. M., ZHAI, J., JIA, H., JIA, J. & ZHU, H. (2011) Nuclear localization sequence of FUS and induction of stress granules by ALS mutants. *Neurobiol Aging,* 32**,** 2323 e27-40.

GARCIA-ARAGONCILLO, E., CARRILLO, J., LALLI, E., AGRA, N., GOMEZ-LOPEZ, G., PESTANA, A. & ALONSO, J. (2008) DAX1, a direct target of EWS/FLI1 oncoprotein, is a principal regulator of cell-cycle progression in Ewing's tumor cells. *Oncogene,* 27**,** 6034-43.

GEORGE, J. M., JIN, H., WOODS, W. S. & CLAYTON, D. F. (1995) Characterization of a novel protein regulated during the critical period for song learning in the zebra finch. *Neuron,* 15**,** 361-72.

GESER, F., MARTINEZ-LAGE, M., ROBINSON, J., URYU, K., NEUMANN, M., BRANDMEIR, N. J., XIE, S. X., KWONG, L. K., ELMAN, L., MCCLUSKEY, L., CLARK, C. M., MALUNDA, J., MILLER, B. L., ZIMMERMAN, E. A., QIAN, J., VAN DEERLIN, V., GROSSMAN, M., LEE, V. M. & TROJANOWSKI, J. Q. (2009) Clinical and pathological continuum of multisystem TDP-43 proteinopathies. *Arch Neurol,* 66**,** 180-9.

GILKS, N., KEDERSHA, N., AYODELE, M., SHEN, L., STOECKLIN, G., DEMBER, L. M. & ANDERSON, P. (2004) Stress granule assembly is mediated by prion-like aggregation of TIA-1. *Mol Biol Cell,* 15**,** 5383-98.

GIORDANA, M. T., FERRERO, P., GRIFONI, S., PELLERINO, A., NALDI, A. & MONTUSCHI, A. (2011) Dementia and cognitive impairment in amyotrophic lateral sclerosis: a review. *Neurol Sci,* 32**,** 9-16.

GIORDANA, M. T., PICCININI, M., GRIFONI, S., DE MARCO, G., VERCELLINO, M., MAGISTRELLO, M., PELLERINO, A., BUCCINNA, B., LUPINO, E. & RINAUDO, M. T. (2010) TDP-43 redistribution is an early event in sporadic amyotrophic lateral sclerosis. *Brain Pathol,* 20**,** 351-60.

GITCHO, M. A., BIGIO, E. H., MISHRA, M., JOHNSON, N., WEINTRAUB, S., MESULAM, M., RADEMAKERS, R., CHAKRAVERTY, S., CRUCHAGA, C., MORRIS, J. C., GOATE, A. M. & CAIRNS, N. J. (2009) TARDBP 3'-UTR variant in autopsy-confirmed frontotemporal lobar degeneration with TDP-43 proteinopathy. *Acta Neuropathol,* 118**,** 633-45.

GLASSER, M. F. & RILLING, J. K. (2008) DTI tractography of the human brain's language pathways. *Cereb Cortex,* 18**,** 2471-82.

GOEDERT, M. (2004) Tau protein and neurodegeneration. *Semin Cell Dev Biol,* 15**,** 45-9.

GOEDERT, M. & SPILLANTINI, M. G. (2006) A century of Alzheimer's disease. *Science,* 314**,** 777-81.

GOEDERT, M., SPILLANTINI, M. G., JAKES, R., RUTHERFORD, D. & CROWTHER, R. A. (1989a) Multiple isoforms of human microtubule-associated protein tau: sequences and localization in neurofibrillary tangles of Alzheimer's disease. *Neuron,* 3**,** 519-26.

GOEDERT, M., SPILLANTINI, M. G., POTIER, M. C., ULRICH, J. & CROWTHER, R. A. (1989b) Cloning and sequencing of the cDNA encoding an isoform of microtubule-associated protein tau containing four tandem repeats: differential expression of tau protein mRNAs in human brain. *EMBO J,* 8**,** 393-9.

GROEN, E. J., VAN ES, M. A., VAN VUGHT, P. W., SPLIET, W. G., VAN ENGELEN-LEE, J., DE VISSER, M., WOKKE, J. H., SCHELHAAS, H. J., OPHOFF, R. A., FUMOTO, K., PASTERKAMP, R. J., DOOIJES, D., CUPPEN, E., VELDINK, J. H. & VAN DEN BERG, L. H. (2010) FUS mutations in familial amyotrophic lateral sclerosis in the Netherlands. *Arch Neurol,* 67**,** 224-30.

GUIPAUD, O., GUILLONNEAU, F., LABAS, V., PRASEUTH, D., ROSSIER, J., LOPEZ, B. & BERTRAND, P. (2006) An in vitro enzymatic assay coupled to proteomics analysis reveals a new DNA processing activity for Ewing sarcoma and TAF(II)68 proteins. *Proteomics,* 6**,** 5962-72.

HAHM, K. B., CHO, K., LEE, C., IM, Y. H., CHANG, J., CHOI, S. G., SORENSEN, P. H., THIELE, C. J. & KIM, S. J. (1999) Repression of the gene encoding the TGF-beta type II receptor is a major target of the EWS-FLI1 oncoprotein. *Nat Genet,* 23**,** 222-7.

HARA, M., MINAMI, M., KAMEI, S., SUZUKI, N., KATO, M. & AOKI, M. (2012) Lower motor neuron disease caused by a novel FUS/TLS gene frameshift mutation. *J Neurol,* 259**,** 2237-9.
HARDY, J. (2005) Expression of normal sequence pathogenic proteins for neurodegenerative disease contributes to disease risk: 'permissive templating' as a general mechanism underlying neurodegeneration. *Biochem Soc Trans,* 33**,** 578-81.
HARDY, J. & ALLSOP, D. (1991) Amyloid deposition as the central event in the aetiology of Alzheimer's disease. *Trends Pharmacol Sci,* 12**,** 383-8.
HASEGAWA, M., ARAI, T., NONAKA, T., KAMETANI, F., YOSHIDA, M., HASHIZUME, Y., BEACH, T. G., BURATTI, E., BARALLE, F., MORITA, M., NAKANO, I., ODA, T., TSUCHIYA, K. & AKIYAMA, H. (2008) Phosphorylated TDP-43 in frontotemporal lobar degeneration and amyotrophic lateral sclerosis. *Ann Neurol,* 64**,** 60-70.
HATANPAA, K. J., BIGIO, E. H., CAIRNS, N. J., WOMACK, K. B., WEINTRAUB, S., MORRIS, J. C., FOONG, C., XIAO, G., HLADIK, C., MANTANONA, T. Y. & WHITE, C. L., 3RD (2008) TAR DNA-binding protein 43 immunohistochemistry reveals extensive neuritic pathology in FTLD-U: a midwest-southwest consortium for FTLD study. *J Neuropathol Exp Neurol,* 67**,** 271-9.
HE, Z., ISMAIL, A., KRIAZHEV, L., SADVAKASSOVA, G. & BATEMAN, A. (2002) Progranulin (PC-cell-derived growth factor/acrogranin) regulates invasion and cell survival. *Cancer Res,* 62**,** 5590-6.
HERRERO-MARTIN, D., OSUNA, D., ORDONEZ, J. L., SEVILLANO, V., MARTINS, A. S., MACKINTOSH, C., CAMPOS, M., MADOZ-GURPIDE, J., OTERO-MOTTA, A. P., CABALLERO, G., AMARAL, A. T., WAI, D. H., BRAUN, Y., EISENACHER, M., SCHAEFER, K. L., POREMBA, C. & DE ALAVA, E. (2009) Stable interference of EWS-FLI1 in an Ewing sarcoma cell line impairs IGF-1/IGF-1R signalling and reveals TOPK as a new target. *Br J Cancer,* 101**,** 80-90.
HEWITT, C., KIRBY, J., HIGHLEY, J. R., HARTLEY, J. A., HIBBERD, R., HOLLINGER, H. C., WILLIAMS, T. L., INCE, P. G., MCDERMOTT, C. J. & SHAW, P. J. (2010) Novel FUS/TLS mutations and pathology in familial and sporadic amyotrophic lateral sclerosis. *Arch Neurol,* 67**,** 455-61.
HEYD, F. & LYNCH, K. W. (2011) Degrade, move, regroup: signaling control of splicing proteins. *Trends Biochem Sci,* 36**,** 397-404.
HOLUND, B., CLAUSEN, P. P. & CLEMMENSEN, I. (1981) The influence of fixation and tissue preparation on the immunohistochemical demonstration of fibronectin in human tissue. *Histochemistry,* 72**,** 291-9.
HU, F., PADUKKAVIDANA, T., VAEGTER, C. B., BRADY, O. A., ZHENG, Y., MACKENZIE, I. R., FELDMAN, H. H., NYKJAER, A. & STRITTMATTER, S. M. (2010) Sortilin-mediated endocytosis determines levels of the frontotemporal dementia protein, progranulin. *Neuron,* 68**,** 654-67.
HUANG, C., ZHOU, H., TONG, J., CHEN, H., LIU, Y. J., WANG, D., WEI, X. & XIA, X. G. (2011) FUS transgenic rats develop the phenotypes of amyotrophic lateral sclerosis and frontotemporal lobar degeneration. *PLoS Genet,* 7**,** e1002011.
HUTTON, M., LENDON, C. L., RIZZU, P., BAKER, M., FROELICH, S., HOULDEN, H., PICKERING-BROWN, S., CHAKRAVERTY, S., ISAACS, A., GROVER, A., HACKETT, J., ADAMSON, J., LINCOLN, S., DICKSON, D., DAVIES, P., PETERSEN, R. C., STEVENS, M., DE GRAAFF, E., WAUTERS, E., VAN BAREN,

J., HILLEBRAND, M., JOOSSE, M., KWON, J. M., NOWOTNY, P., CHE, L. K., NORTON, J., MORRIS, J. C., REED, L. A., TROJANOWSKI, J., BASUN, H., LANNFELT, L., NEYSTAT, M., FAHN, S., DARK, F., TANNENBERG, T., DODD, P. R., HAYWARD, N., KWOK, J. B., SCHOFIELD, P. R., ANDREADIS, A., SNOWDEN, J., CRAUFURD, D., NEARY, D., OWEN, F., OOSTRA, B. A., HARDY, J., GOATE, A., VAN SWIETEN, J., MANN, D., LYNCH, T. & HEUTINK, P. (1998) Association of missense and 5'-splice-site mutations in tau with the inherited dementia FTDP-17. *Nature,* 393**,** 702-5.

IBRAHIM, F., MARAGKAKIS, M., ALEXIOU, P., MARONSKI, M. A., DICHTER, M. A. & MOURELATOS, Z. (2013) Identification of in vivo, conserved, TAF15 RNA binding sites reveals the impact of TAF15 on the neuronal transcriptome. *Cell Rep,* 3**,** 301-8.

IGAZ, L. M., KWONG, L. K., LEE, E. B., CHEN-PLOTKIN, A., SWANSON, E., UNGER, T., MALUNDA, J., XU, Y., WINTON, M. J., TROJANOWSKI, J. Q. & LEE, V. M. (2011) Dysregulation of the ALS-associated gene TDP-43 leads to neuronal death and degeneration in mice. *J Clin Invest,* 121**,** 726-38.

IGAZ, L. M., KWONG, L. K., XU, Y., TRUAX, A. C., URYU, K., NEUMANN, M., CLARK, C. M., ELMAN, L. B., MILLER, B. L., GROSSMAN, M., MCCLUSKEY, L. F., TROJANOWSKI, J. Q. & LEE, V. M. (2008) Enrichment of C-terminal fragments in TAR DNA-binding protein-43 cytoplasmic inclusions in brain but not in spinal cord of frontotemporal lobar degeneration and amyotrophic lateral sclerosis. *Am J Pathol,* 173**,** 182-94.

IMASAKI, T., SHIMIZU, T., HASHIMOTO, H., HIDAKA, Y., KOSE, S., IMAMOTO, N., YAMADA, M. & SATO, M. (2007) Structural basis for substrate recognition and dissociation by human transportin 1. *Mol Cell,* 28**,** 57-67.

INGELFINGER, D., ARNDT-JOVIN, D. J., LUHRMANN, R. & ACHSEL, T. (2002) The human LSm1-7 proteins colocalize with the mRNA-degrading enzymes Dcp1/2 and Xrnl in distinct cytoplasmic foci. *RNA,* 8**,** 1489-501.

INUKAI, Y., NONAKA, T., ARAI, T., YOSHIDA, M., HASHIZUME, Y., BEACH, T. G., BURATTI, E., BARALLE, F. E., AKIYAMA, H., HISANAGA, S. & HASEGAWA, M. (2008) Abnormal phosphorylation of Ser409/410 of TDP-43 in FTLD-U and ALS. *FEBS Lett,* 582**,** 2899-904.

JAKES, R., SPILLANTINI, M. G. & GOEDERT, M. (1994) Identification of two distinct synucleins from human brain. *FEBS Lett,* 345**,** 27-32.

JANKNECHT, R. (2005) EWS-ETS oncoproteins: the linchpins of Ewing tumors. *Gene,* 363**,** 1-14.

JENSEN, P. H., SORENSEN, E. S., PETERSEN, T. E., GLIEMANN, J. & RASMUSSEN, L. K. (1995) Residues in the synuclein consensus motif of the alpha-synuclein fragment, NAC, participate in transglutaminase-catalysed cross-linking to Alzheimer-disease amyloid beta A4 peptide. *Biochem J,* 310 (Pt 1)**,** 91-4.

JIANG, H. Y., WEK, S. A., MCGRATH, B. C., SCHEUNER, D., KAUFMAN, R. J., CAVENER, D. R. & WEK, R. C. (2003) Phosphorylation of the alpha subunit of eukaryotic initiation factor 2 is required for activation of NF-kappaB in response to diverse cellular stresses. *Mol Cell Biol,* 23**,** 5651-63.

JOBERT, L., ARGENTINI, M. & TORA, L. (2009a) PRMT1 mediated methylation of TAF15 is required for its positive gene regulatory function. *Exp Cell Res,* 315**,** 1273-86.

JOBERT, L., PINZON, N., VAN HERREWEGHE, E., JADY, B. E., GUIALIS, A., KISS, T. & TORA, L. (2009b) Human U1 snRNA forms a new chromatin-associated snRNP with TAF15. *EMBO Rep,* 10**,** 494-500.

JOHNSON, B. S., MCCAFFERY, J. M., LINDQUIST, S. & GITLER, A. D. (2008) A yeast TDP-43 proteinopathy model: Exploring the molecular determinants of TDP-43 aggregation and cellular toxicity. *Proc Natl Acad Sci U S A,* 105**,** 6439-44.

JOHNSON, B. S., SNEAD, D., LEE, J. J., MCCAFFERY, J. M., SHORTER, J. & GITLER, A. D. (2009) TDP-43 is intrinsically aggregation-prone, and amyotrophic lateral sclerosis-linked mutations accelerate aggregation and increase toxicity. *J Biol Chem,* 284**,** 20329-39.

JOSEPHS, K. A. (2011) Neuronal intranuclear inclusion disease: no longer a pain in the butt. *Neurology,* 76**,** 1368-9.

JOSEPHS, K. A., HOLTON, J. L., ROSSOR, M. N., BRAENDGAARD, H., OZAWA, T., FOX, N. C., PETERSEN, R. C., PEARL, G. S., GANGULY, M., ROSA, P., LAURSEN, H., PARISI, J. E., WALDEMAR, G., QUINN, N. P., DICKSON, D. W. & REVESZ, T. (2003a) Neurofilament inclusion body disease: a new proteinopathy? *Brain,* 126**,** 2291-303.

JOSEPHS, K. A., HOLTON, J. L., ROSSOR, M. N., BRAENDGAARD, H., OZAWA, T., FOX, N. C., PETERSEN, R. C., PEARL, G. S., GANGULY, M., ROSA, P., LAURSEN, H., PARISI, J. E., WALDEMAR, G., QUINN, N. P., DICKSON, D. W. & REVESZ, T. (2003b) Neurofilament inclusion body disease: a new proteinopathy? *Brain,* 126**,** 2291-2303.

JU, S., TARDIFF, D. F., HAN, H., DIVYA, K., ZHONG, Q., MAQUAT, L. E., BOSCO, D. A., HAYWARD, L. J., BROWN, R. H., JR., LINDQUIST, S., RINGE, D. & PETSKO, G. A. (2011) A yeast model of FUS/TLS-dependent cytotoxicity. *PLoS Biol,* 9**,** e1001052.

KAUER, M., BAN, J., KOFLER, R., WALKER, B., DAVIS, S., MELTZER, P. & KOVAR, H. (2009) A molecular function map of Ewing's sarcoma. *PLoS One,* 4**,** e5415.

KEDERSHA, N. & ANDERSON, P. (2007) Mammalian stress granules and processing bodies. *Methods Enzymol,* 431**,** 61-81.

KEDERSHA, N., CHO, M. R., LI, W., YACONO, P. W., CHEN, S., GILKS, N., GOLAN, D. E. & ANDERSON, P. (2000) Dynamic shuttling of TIA-1 accompanies the recruitment of mRNA to mammalian stress granules. *J Cell Biol,* 151**,** 1257-68.

KEDERSHA, N. L., GUPTA, M., LI, W., MILLER, I. & ANDERSON, P. (1999) RNA-binding proteins TIA-1 and TIAR link the phosphorylation of eIF-2 alpha to the assembly of mammalian stress granules. *J Cell Biol,* 147**,** 1431-42.

KIKUCHI, R., MURAKAMI, M., SOBUE, S., IWASAKI, T., HAGIWARA, K., TAKAGI, A., KOJIMA, T., ASANO, H., SUZUKI, M., BANNO, Y., NOZAWA, Y. & MURATE, T. (2007) Ewing's sarcoma fusion protein, EWS/Fli-1 and Fli-1 protein induce PLD2 but not PLD1 gene expression by binding to an ETS domain of 5' promoter. *Oncogene,* 26**,** 1802-10.

KIM, H. J., KIM, N. C., WANG, Y. D., SCARBOROUGH, E. A., MOORE, J., DIAZ, Z., MACLEA, K. S., FREIBAUM, B., LI, S., MOLLIEX, A., KANAGARAJ, A. P., CARTER, R., BOYLAN, K. B., WOJTAS, A. M., RADEMAKERS, R., PINKUS, J. L., GREENBERG, S. A., TROJANOWSKI, J. Q., TRAYNOR, B. J., SMITH, B. N., TOPP, S., GKAZI, A. S., MILLER, J., SHAW, C. E., KOTTLORS, M., KIRSCHNER, J., PESTRONK, A., LI, Y. R., FORD, A. F., GITLER, A. D., BENATAR, M., KING, O.

D., KIMONIS, V. E., ROSS, E. D., WEIHL, C. C., SHORTER, J. & TAYLOR, J. P. (2013) Mutations in prion-like domains in hnRNPA2B1 and hnRNPA1 cause multisystem proteinopathy and ALS. *Nature,* 495**,** 467-73.
KIM, H. S., KUWANO, Y., ZHAN, M., PULLMANN, R., JR., MAZAN-MAMCZARZ, K., LI, H., KEDERSHA, N., ANDERSON, P., WILCE, M. C., GOROSPE, M. & WILCE, J. A. (2007) Elucidation of a C-rich signature motif in target mRNAs of RNA-binding protein TIAR. *Mol Cell Biol,* 27**,** 6806-17.
KIM, J. (1997) Evidence that the precursor protein of non-A beta component of Alzheimer's disease amyloid (NACP) has an extended structure primarily composed of random-coil. *Mol Cells,* 7**,** 78-83.
KIMONIS, V. E., FULCHIERO, E., VESA, J. & WATTS, G. (2008) VCP disease associated with myopathy, Paget disease of bone and frontotemporal dementia: review of a unique disorder. *Biochim Biophys Acta,* 1782**,** 744-8.
KING, O. D., GITLER, A. D. & SHORTER, J. (2012) The tip of the iceberg: RNA-binding proteins with prion-like domains in neurodegenerative disease. *Brain Res,* 1462**,** 61-80.
KINO, Y., WASHIZU, C., AQUILANTI, E., OKUNO, M., KUROSAWA, M., YAMADA, M., DOI, H. & NUKINA, N. (2011) Intracellular localization and splicing regulation of FUS/TLS are variably affected by amyotrophic lateral sclerosis-linked mutations. *Nucleic Acids Res,* 39**,** 2781-98.
KIPPS, C. M., KNIBB, J. A., PATTERSON, K. & HODGES, J. R. (2008) Neuropsychology of frontotemporal dementia. *Handb Clin Neurol,* 88**,** 527-48.
KIPPS, C. M., NESTOR, P. J., ACOSTA-CABRONERO, J., ARNOLD, R. & HODGES, J. R. (2009) Understanding social dysfunction in the behavioural variant of frontotemporal dementia: the role of emotion and sarcasm processing. *Brain,* 132**,** 592-603.
KONIG, R., ZHOU, Y., ELLEDER, D., DIAMOND, T. L., BONAMY, G. M., IRELAN, J. T., CHIANG, C. Y., TU, B. P., DE JESUS, P. D., LILLEY, C. E., SEIDEL, S., OPALUCH, A. M., CALDWELL, J. S., WEITZMAN, M. D., KUHEN, K. L., BANDYOPADHYAY, S., IDEKER, T., ORTH, A. P., MIRAGLIA, L. J., BUSHMAN, F. D., YOUNG, J. A. & CHANDA, S. K. (2008) Global analysis of host-pathogen interactions that regulate early-stage HIV-1 replication. *Cell,* 135**,** 49-60.
KORTVELY, E., BURKOVICS, P., VARSZEGI, S. & GULYA, K. (2005) Cloning and characterization of rat importin 9: implication for its neuronal function. *Brain Res Mol Brain Res,* 139**,** 103-14.
KRICHEVSKY, A. M. & KOSIK, K. S. (2001) Neuronal RNA granules: a link between RNA localization and stimulation-dependent translation. *Neuron,* 32**,** 683-96.
KRUMAN, I., BRUCE-KELLER, A. J., BREDESEN, D., WAEG, G. & MATTSON, M. P. (1997) Evidence that 4-hydroxynonenal mediates oxidative stress-induced neuronal apoptosis. *J Neurosci,* 17**,** 5089-100.
KUNDE, S. A., MUSANTE, L., GRIMME, A., FISCHER, U., MULLER, E., WANKER, E. E. & KALSCHEUER, V. M. (2011) The X-chromosome-linked intellectual disability protein PQBP1 is a component of neuronal RNA granules and regulates the appearance of stress granules. *Hum Mol Genet,* 20**,** 4916-31.
KURODA, M., SOK, J., WEBB, L., BAECHTOLD, H., URANO, F., YIN, Y., CHUNG, P., DE ROOIJ, D. G., AKHMEDOV, A., ASHLEY, T. & RON, D. (2000) Male sterility and enhanced radiation sensitivity in TLS(-/-) mice. *EMBO J,* 19**,** 453-62.

KUROSAKI, T., GOJOBORI, J. & UEDA, S. (2012) Comparative genetics of the poly-Q tract of ataxin-1 and its binding protein PQBP-1. *Biochem Genet,* 50**,** 309-17.

KWEK, K. Y., MURPHY, S., FURGER, A., THOMAS, B., O'GORMAN, W., KIMURA, H., PROUDFOOT, N. J. & AKOULITCHEV, A. (2002) U1 snRNA associates with TFIIH and regulates transcriptional initiation. *Nat Struct Biol,* 9**,** 800-5.

KWIATKOWSKI, T. J., JR., BOSCO, D. A., LECLERC, A. L., TAMRAZIAN, E., VANDERBURG, C. R., RUSS, C., DAVIS, A., GILCHRIST, J., KASARSKIS, E. J., MUNSAT, T., VALDMANIS, P., ROULEAU, G. A., HOSLER, B. A., CORTELLI, P., DE JONG, P. J., YOSHINAGA, Y., HAINES, J. L., PERICAK-VANCE, M. A., YAN, J., TICOZZI, N., SIDDIQUE, T., KENNA-YASEK, D., SAPP, P. C., HORVITZ, H. R., LANDERS, J. E. & BROWN, R. H., JR. (2009a) Mutations in the FUS/TLS gene on chromosome 16 cause familial amyotrophic lateral sclerosis. *Science,* 323**,** 1205-1208.

KWIATKOWSKI, T. J., JR., BOSCO, D. A., LECLERC, A. L., TAMRAZIAN, E., VANDERBURG, C. R., RUSS, C., DAVIS, A., GILCHRIST, J., KASARSKIS, E. J., MUNSAT, T., VALDMANIS, P., ROULEAU, G. A., HOSLER, B. A., CORTELLI, P., DE JONG, P. J., YOSHINAGA, Y., HAINES, J. L., PERICAK-VANCE, M. A., YAN, J., TICOZZI, N., SIDDIQUE, T., MCKENNA-YASEK, D., SAPP, P. C., HORVITZ, H. R., LANDERS, J. E. & BROWN, R. H., JR. (2009b) Mutations in the FUS/TLS gene on chromosome 16 cause familial amyotrophic lateral sclerosis. *Science,* 323**,** 1205-8.

KWON, M. J., BAEK, W., KI, C. S., KIM, H. Y., KOH, S. H., KIM, J. W. & KIM, S. H. (2012) Screening of the SOD1, FUS, TARDBP, ANG, and OPTN mutations in Korean patients with familial and sporadic ALS. *Neurobiol Aging,* 33**,** 1017 e17-23.

KWON, S., ZHANG, Y. & MATTHIAS, P. (2007) The deacetylase HDAC6 is a novel critical component of stress granules involved in the stress response. *Genes Dev,* 21**,** 3381-94.

LAGIER-TOURENNE, C., POLYMENIDOU, M. & CLEVELAND, D. W. (2010) TDP-43 and FUS/TLS: emerging roles in RNA processing and neurodegeneration. *Hum Mol Genet,* 19**,** R46-R64.

LAGUINGE, L., BAJENOVA, O., BOWDEN, E., SAYYAH, J., THOMAS, P. & JUHL, H. (2005) Surface expression and CEA binding of hnRNP M4 protein in HT29 colon cancer cells. *Anticancer Res,* 25**,** 23-31.

LAI, M. C., WANG, S. W., CHENG, L., TARN, W. Y., TSAI, S. J. & SUN, H. S. (2013) Human DDX3 interacts with the HIV-1 Tat protein to facilitate viral mRNA translation. *PLoS One,* 8**,** e68665.

LAI, S. L., ABRAMZON, Y., SCHYMICK, J. C., STEPHAN, D. A., DUNCKLEY, T., DILLMAN, A., COOKSON, M., CALVO, A., BATTISTINI, S., GIANNINI, F., CAPONNETTO, C., MANCARDI, G. L., SPATARO, R., MONSURRO, M. R., TEDESCHI, G., MARINOU, K., SABATELLI, M., CONTE, A., MANDRIOLI, J., SOLA, P., SALVI, F., BARTOLOMEI, I., LOMBARDO, F., MORA, G., RESTAGNO, G., CHIO, A. & TRAYNOR, B. J. (2011) FUS mutations in sporadic amyotrophic lateral sclerosis. *Neurobiol Aging,* 32**,** 550 e1-4.

LASHLEY, T., ROHRER, J. D., BANDOPADHYAY, R., FRY, C., AHMED, Z., ISAACS, A. M., BRELSTAFF, J. H., BORRONI, B., WARREN, J. D., TROAKES, C., KING, A., AL-SARAJ, S., NEWCOMBE, J., QUINN, N., OSTERGAARD, K., SCHRODER, H. D., BOJSEN-MOLLER, M., BRAENDGAARD, H., FOX, N. C., ROSSOR, M. N.,

LEES, A. J., HOLTON, J. L. & REVESZ, T. (2011) A comparative clinical, pathological, biochemical and genetic study of fused in sarcoma proteinopathies. *Brain,* 134**,** 2548-64.
LAU, C. K., DELMAR, V. A., CHAN, R. C., PHUNG, Q., BERNIS, C., FICHTMAN, B., RASALA, B. A. & FORBES, D. J. (2009) Transportin regulates major mitotic assembly events: from spindle to nuclear pore assembly. *Mol Biol Cell,* 20**,** 4043-58.
LEE, B. J., CANSIZOGLU, A. E., SUEL, K. E., LOUIS, T. H., ZHANG, Z. & CHOOK, Y. M. (2006) Rules for nuclear localization sequence recognition by karyopherin beta 2. *Cell,* 126**,** 543-58.
LEE, N., PIMIENTA, G. & STEITZ, J. A. (2012) AUF1/hnRNP D is a novel protein partner of the EBER1 noncoding RNA of Epstein-Barr virus. *RNA,* 18**,** 2073-82.
LEE, V. M., GOEDERT, M. & TROJANOWSKI, J. Q. (2001) Neurodegenerative tauopathies. *Annu Rev Neurosci,* 24**,** 1121-59.
LERGA, A., HALLIER, M., DELVA, L., ORVAIN, C., GALLAIS, I., MARIE, J. & MOREAU-GACHELIN, F. (2001) Identification of an RNA binding specificity for the potential splicing factor TLS. *J Biol Chem,* 276**,** 6807-16.
LI, H., WATFORD, W., LI, C., PARMELEE, A., BRYANT, M. A., DENG, C., O'SHEA, J. & LEE, S. B. (2007) Ewing sarcoma gene EWS is essential for meiosis and B lymphocyte development. *J Clin Invest,* 117**,** 1314-23.
LI, J. Y., ENGLUND, E., HOLTON, J. L., SOULET, D., HAGELL, P., LEES, A. J., LASHLEY, T., QUINN, N. P., REHNCRONA, S., BJORKLUND, A., WIDNER, H., REVESZ, T., LINDVALL, O. & BRUNDIN, P. (2008) Lewy bodies in grafted neurons in subjects with Parkinson's disease suggest host-to-graft disease propagation. *Nat Med,* 14**,** 501-3.
LIAO, W. T., LIU, J. L., WANG, Z. G., CUI, Y. M., SHI, L., LI, T. T., ZHAO, X. H., CHEN, X. T., DING, Y. Q. & SONG, L. B. (2013) High expression level and nuclear localization of Sam68 are associated with progression and poor prognosis in colorectal cancer. *BMC Gastroenterol,* 13**,** 126.
LIEBMAN, S. W. & SHERMAN, F. (1979) Extrachromosomal psi+ determinant suppresses nonsense mutations in yeast. *J Bacteriol,* 139**,** 1068-71.
LIN, P. P., WANG, Y. & LOZANO, G. (2011) Mesenchymal Stem Cells and the Origin of Ewing's Sarcoma. *Sarcoma,* 2011.
LIU, Y., MIMURO, M., YOSHIDA, M., HASHIZUME, Y., NIWA, H., MIYAO, S., UJIHIRA, N. & AKATSU, H. (2008) Inclusion-positive cell types in adult-onset intranuclear inclusion body disease: implications for clinical diagnosis. *Acta Neuropathol,* 116**,** 615-23.
LIU-YESUCEVITZ, L., BASSELL, G. J., GITLER, A. D., HART, A. C., KLANN, E., RICHTER, J. D., WARREN, S. T. & WOLOZIN, B. (2011) Local RNA translation at the synapse and in disease. *J Neurosci,* 31**,** 16086-93.
LIU-YESUCEVITZ, L., BILGUTAY, A., ZHANG, Y. J., VANDERWEYDE, T., CITRO, A., MEHTA, T., ZAARUR, N., MCKEE, A., BOWSER, R., SHERMAN, M., PETRUCELLI, L. & WOLOZIN, B. (2010) Tar DNA binding protein-43 (TDP-43) associates with stress granules: analysis of cultured cells and pathological brain tissue. *PLoS One,* 5**,** e13250.
LOPEZ DE SILANES, I., GALBAN, S., MARTINDALE, J. L., YANG, X., MAZAN-MAMCZARZ, K., INDIG, F. E., FALCO, G., ZHAN, M. & GOROSPE, M. (2005)

Identification and functional outcome of mRNAs associated with RNA-binding protein TIA-1. *Mol Cell Biol,* 25**,** 9520-31.
LOPEZ DE SILANES, I., ZHAN, M., LAL, A., YANG, X. & GOROSPE, M. (2004) Identification of a target RNA motif for RNA-binding protein HuR. *Proc Natl Acad Sci U S A,* 101**,** 2987-92.
LU, R. & SERRERO, G. (2001) Mediation of estrogen mitogenic effect in human breast cancer MCF-7 cells by PC-cell-derived growth factor (PCDGF/granulin precursor). *Proc Natl Acad Sci U S A,* 98**,** 142-7.
LYNN, S., SHIUNG, J. N., GURR, J. R. & JAN, K. Y. (1998) Arsenite stimulates poly(ADP-ribosylation) by generation of nitric oxide. *Free Radic Biol Med,* 24**,** 442-9.
MACARA, I. G. (2001) Transport into and out of the nucleus. *Microbiol Mol Biol Rev,* 65**,** 570-94.
MACIEJCZYK, A., SZELACHOWSKA, J., EKIERT, M., MATKOWSKI, R., HALON, A., LAGE, H. & SUROWIAK, P. (2012) Elevated nuclear YB1 expression is associated with poor survival of patients with early breast cancer. *Anticancer Res,* 32**,** 3177-84.
MACKENZIE, I. R., BABORIE, A., PICKERING-BROWN, S., DU PLESSIS, D., JAROS, E., PERRY, R. H., NEARY, D., SNOWDEN, J. S. & MANN, D. M. (2006) Heterogeneity of ubiquitin pathology in frontotemporal lobar degeneration: classification and relation to clinical phenotype. *Acta Neuropathol,* 112**,** 539-49.
MACKENZIE, I. R., NEUMANN, M., BIGIO, E. H., CAIRNS, N. J., ALAFUZOFF, I., KRIL, J., KOVACS, G. G., GHETTI, B., HALLIDAY, G., HOLM, I. E., INCE, P. G., KAMPHORST, W., REVESZ, T., ROZEMULLER, A. J., KUMAR-SINGH, S., AKIYAMA, H., BABORIE, A., SPINA, S., DICKSON, D. W., TROJANOWSKI, J. Q. & MANN, D. M. (2009) Nomenclature for neuropathologic subtypes of frontotemporal lobar degeneration: consensus recommendations. *Acta Neuropathol,* 117**,** 15-8.
MACKENZIE, I. R., NEUMANN, M., BIGIO, E. H., CAIRNS, N. J., ALAFUZOFF, I., KRIL, J., KOVACS, G. G., GHETTI, B., HALLIDAY, G., HOLM, I. E., INCE, P. G., KAMPHORST, W., REVESZ, T., ROZEMULLER, A. J., KUMAR-SINGH, S., AKIYAMA, H., BABORIE, A., SPINA, S., DICKSON, D. W., TROJANOWSKI, J. Q. & MANN, D. M. (2010a) Nomenclature and nosology for neuropathologic subtypes of frontotemporal lobar degeneration: an update. *Acta Neuropathol,* 119**,** 1-4.
MACKENZIE, I. R., RADEMAKERS, R. & NEUMANN, M. (2010b) TDP-43 and FUS in amyotrophic lateral sclerosis and frontotemporal dementia. *Lancet Neurol,* 9**,** 995-1007.
MANNING-BOG, A. B., MCCORMACK, A. L., LI, J., UVERSKY, V. N., FINK, A. L. & DI MONTE, D. A. (2002) The herbicide paraquat causes up-regulation and aggregation of alpha-synuclein in mice: paraquat and alpha-synuclein. *J Biol Chem,* 277**,** 1641-4.
MARCUS, D. L., THOMAS, C., RODRIGUEZ, C., SIMBERKOFF, K., TSAI, J. S., STRAFACI, J. A. & FREEDMAN, M. L. (1998) Increased peroxidation and reduced antioxidant enzyme activity in Alzheimer's disease. *Exp Neurol,* 150**,** 40-4.

MARKO, M., VLASSIS, A., GUIALIS, A. & LEICHTER, M. (2012) Domains involved in TAF15 subcellular localisation: dependence on cell type and ongoing transcription. *Gene,* 506**,** 331-8.
MARTINEZ, A., CARMONA, M., PORTERO-OTIN, M., NAUDI, A., PAMPLONA, R. & FERRER, I. (2008) Type-dependent oxidative damage in frontotemporal lobar degeneration: cortical astrocytes are targets of oxidative damage. *J Neuropathol Exp Neurol,* 67**,** 1122-36.
MASISON, D. C. & WICKNER, R. B. (1995) Prion-inducing domain of yeast Ure2p and protease resistance of Ure2p in prion-containing cells. *Science,* 270**,** 93-5.
MASUDA-SUZUKAKE, M., NONAKA, T., HOSOKAWA, M., OIKAWA, T., ARAI, T., AKIYAMA, H., MANN, D. M. & HASEGAWA, M. (2013) Prion-like spreading of pathological alpha-synuclein in brain. *Brain,* 136**,** 1128-38.
MATSUKI, H., TAKAHASHI, M., HIGUCHI, M., MAKOKHA, G. N., OIE, M. & FUJII, M. (2013) Both G3BP1 and G3BP2 contribute to stress granule formation. *Genes Cells,* 18**,** 135-46.
MILLECAMPS, S., SALACHAS, F., CAZENEUVE, C., GORDON, P., BRICKA, B., CAMUZAT, A., GUILLOT-NOEL, L., RUSSAOUEN, O., BRUNETEAU, G., PRADAT, P. F., LE FORESTIER, N., VANDENBERGHE, N., DANEL-BRUNAUD, V., GUY, N., THAUVIN-ROBINET, C., LACOMBLEZ, L., COURATIER, P., HANNEQUIN, D., SEILHEAN, D., LE BER, I., CORCIA, P., CAMU, W., BRICE, A., ROULEAU, G., LEGUERN, E. & MEININGER, V. (2010) SOD1, ANG, VAPB, TARDBP, and FUS mutations in familial amyotrophic lateral sclerosis: genotype-phenotype correlations. *J Med Genet,* 47**,** 554-60.
MITCHELL, J. C., MCGOLDRICK, P., VANCE, C., HORTOBAGYI, T., SREEDHARAN, J., ROGELJ, B., TUDOR, E. L., SMITH, B. N., KLASEN, C., MILLER, C. C., COOPER, J. D., GREENSMITH, L. & SHAW, C. E. (2013) Overexpression of human wild-type FUS causes progressive motor neuron degeneration in an age- and dose-dependent fashion. *Acta Neuropathol,* 125**,** 273-88.
MONAMI, G., GONZALEZ, E. M., HELLMAN, M., GOMELLA, L. G., BAFFA, R., IOZZO, R. V. & MORRIONE, A. (2006) Proepithelin promotes migration and invasion of 5637 bladder cancer cells through the activation of ERK1/2 and the formation of a paxillin/FAK/ERK complex. *Cancer Res,* 66**,** 7103-10.
MORENO, J. A., RADFORD, H., PERETTI, D., STEINERT, J. R., VERITY, N., MARTIN, M. G., HALLIDAY, M., MORGAN, J., DINSDALE, D., ORTORI, C. A., BARRETT, D. A., TSAYTLER, P., BERTOLOTTI, A., WILLIS, A. E., BUSHELL, M. & MALLUCCI, G. R. (2012) Sustained translational repression by eIF2alpha-P mediates prion neurodegeneration. *Nature,* 485**,** 507-11.
MUNOZ, D. G., NEUMANN, M., KUSAKA, H., YOKOTA, O., ISHIHARA, K., TERADA, S., KURODA, S. & MACKENZIE, I. R. (2009) FUS pathology in basophilic inclusion body disease. *Acta Neuropathol,* 118**,** 617-27.
MUNOZ-GARCIA, D. & LUDWIN, S. K. (1984) Classic and generalized variants of Pick's disease: a clinicopathological, ultrastructural, and immunocytochemical comparative study. *Ann Neurol,* 16**,** 467-80.
NAGAYAMA, S., MINATO-HASHIBA, N., NAKATA, M., KAITO, M., NAKANISHI, M., TANAKA, K., ARAI, M., AKIYAMA, H. & MATSUI, M. (2012) Novel FUS mutation in patients with sporadic amyotrophic lateral sclerosis and corticobasal degeneration. *J Clin Neurosci,* 19**,** 1738-9.

NAKATANI, F., TANAKA, K., SAKIMURA, R., MATSUMOTO, Y., MATSUNOBU, T., LI, X., HANADA, M., OKADA, T. & IWAMOTO, Y. (2003) Identification of p21WAF1/CIP1 as a direct target of EWS-Fli1 oncogenic fusion protein. *J Biol Chem,* 278**,** 15105-15.

NAKIELNY, S., SIOMI, M. C., SIOMI, H., MICHAEL, W. M., POLLARD, V. & DREYFUSS, G. (1996) Transportin: nuclear transport receptor of a novel nuclear protein import pathway. *Exp Cell Res,* 229**,** 261-6.

NEUMANN, M., BENTMANN, E., DORMANN, D., JAWAID, A., DEJESUS-HERNANDEZ, M., ANSORGE, O., ROEBER, S., KRETZSCHMAR, H. A., MUNOZ, D. G., KUSAKA, H., YOKOTA, O., ANG, L. C., BILBAO, J., RADEMAKERS, R., HAASS, C. & MACKENZIE, I. R. (2011) FET proteins TAF15 and EWS are selective markers that distinguish FTLD with FUS pathology from amyotrophic lateral sclerosis with FUS mutations. *Brain,* 134**,** 2595-609.

NEUMANN, M., KWONG, L. K., TRUAX, A. C., VANMASSENHOVE, B., KRETZSCHMAR, H. A., VAN DEERLIN, V. M., CLARK, C. M., GROSSMAN, M., MILLER, B. L., TROJANOWSKI, J. Q. & LEE, V. M. (2007) TDP-43-positive white matter pathology in frontotemporal lobar degeneration with ubiquitin-positive inclusions. *J Neuropathol Exp Neurol,* 66**,** 177-83.

NEUMANN, M., RADEMAKERS, R., ROEBER, S., BAKER, M., KRETZSCHMAR, H. A. & MACKENZIE, I. R. (2009a) A new subtype of frontotemporal lobar degeneration with FUS pathology. *Brain,* 132**,** 2922-31.

NEUMANN, M., RADEMAKERS, R., ROEBER, S., BAKER, M., KRETZSCHMAR, H. A. & MACKENZIE, I. R. (2009b) A new subtype of frontotemporal lobar degeneration with FUS pathology. *Brain,* 132**,** 2922-2931.

NEUMANN, M., ROEBER, S., KRETZSCHMAR, H. A., RADEMAKERS, R., BAKER, M. & MACKENZIE, I. R. (2009c) Abundant FUS-immunoreactive pathology in neuronal intermediate filament inclusion disease. *Acta Neuropathol,* 118**,** 605-16.

NEUMANN, M., ROEBER, S., KRETZSCHMAR, H. A., RADEMAKERS, R., BAKER, M. & MACKENZIE, I. R. (2009d) Abundant FUS-immunoreactive pathology in neuronal intermediate filament inclusion disease. *Acta Neuropathol,* 118**,** 605-616.

NEUMANN, M., SAMPATHU, D. M., KWONG, L. K., TRUAX, A. C., MICSENYI, M. C., CHOU, T. T., BRUCE, J., SCHUCK, T., GROSSMAN, M., CLARK, C. M., MCCLUSKEY, L. F., MILLER, B. L., MASLIAH, E., MACKENZIE, I. R., FELDMAN, H., FEIDEN, W., KRETZSCHMAR, H. A., TROJANOWSKI, J. Q. & LEE, V. M. (2006) Ubiquitinated TDP-43 in frontotemporal lobar degeneration and amyotrophic lateral sclerosis. *Science,* 314**,** 130-3.

NEUMANN, M., VALORI, C. F., ANSORGE, O., KRETZSCHMAR, H. A., MUNOZ, D. G., KUSAKA, H., YOKOTA, O., ISHIHARA, K., ANG, L. C., BILBAO, J. M. & MACKENZIE, I. R. (2012) Transportin 1 accumulates specifically with FET proteins but no other transportin cargos in FTLD-FUS and is absent in FUS inclusions in ALS with FUS mutations. *Acta Neuropathol,* 124**,** 705-16.

NISHIMURA, A. L., ZUPUNSKI, V., TROAKES, C., KATHE, C., FRATTA, P., HOWELL, M., GALLO, J. M., HORTOBAGYI, T., SHAW, C. E. & ROGELJ, B. (2010) Nuclear import impairment causes cytoplasmic trans-activation response DNA-binding protein accumulation and is associated with frontotemporal lobar degeneration. *Brain,* 133**,** 1763-71.

NUKINA, N. (2010a) FUS/TLS as a polyglutamine aggregate interacting protein. *Rinsho Shinkeigaku,* 50**,** 945-7.
NUKINA, N. (2010b) [FUS/TLS as a polyglutamine aggregate interacting protein]. *Rinsho Shinkeigaku,* 50**,** 945-7.
NYQUIST, K. B., THORSEN, J., ZELLER, B., HAALAND, A., TROEN, G., HEIM, S. & MICCI, F. (2011) Identification of the TAF15-ZNF384 fusion gene in two new cases of acute lymphoblastic leukemia with a t(12;17)(p13;q12). *Cancer Genet,* 204**,** 147-52.
OCWIEJA, K. E., BRADY, T. L., RONEN, K., HUEGEL, A., ROTH, S. L., SCHALLER, T., JAMES, L. C., TOWERS, G. J., YOUNG, J. A., CHANDA, S. K., KONIG, R., MALANI, N., BERRY, C. C. & BUSHMAN, F. D. (2011) HIV integration targeting: a pathway involving Transportin-3 and the nuclear pore protein RanBP2. *PLoS Pathog,* 7**,** e1001313.
ONYIKE, C. U. & DIEHL-SCHMID, J. (2013) The epidemiology of frontotemporal dementia. *Int Rev Psychiatry,* 25**,** 130-7.
OROZCO, D. & EDBAUER, D. (2013) FUS-mediated alternative splicing in the nervous system: consequences for ALS and FTLD. *J Mol Med (Berl)*.
OROZCO, D., TAHIROVIC, S., RENTZSCH, K., SCHWENK, B. M., HAASS, C. & EDBAUER, D. (2012) Loss of fused in sarcoma (FUS) promotes pathological Tau splicing. *EMBO Rep,* 13**,** 759-64.
OTEIZA, P. I., UCHITEL, O. D., CARRASQUEDO, F., DUBROVSKI, A. L., ROMA, J. C. & FRAGA, C. G. (1997) Evaluation of antioxidants, protein, and lipid oxidation products in blood from sporadic amyotrophic lateral sclerosis patients. *Neurochem Res,* 22**,** 535-9.
OU, S. H., WU, F., HARRICH, D., GARCIA-MARTINEZ, L. F. & GAYNOR, R. B. (1995) Cloning and characterization of a novel cellular protein, TDP-43, that binds to human immunodeficiency virus type 1 TAR DNA sequence motifs. *J Virol,* 69**,** 3584-96.
PAGE, T., GITCHO, M. A., MOSAHEB, S., CARTER, D., CHAKRAVERTY, S., PERRY, R. H., BIGIO, E. H., GEARING, M., FERRER, I., GOATE, A. M., CAIRNS, N. J. & THORPE, J. R. (2011) FUS immunogold labeling TEM analysis of the neuronal cytoplasmic inclusions of neuronal intermediate filament inclusion disease: a frontotemporal lobar degeneration with FUS proteinopathy. *J Mol Neurosci,* 45**,** 409-21.
PARKER, R. & SHETH, U. (2007) P bodies and the control of mRNA translation and degradation. *Mol Cell,* 25**,** 635-46.
PARONETTO, M. P., MINANA, B. & VALCARCEL, J. (2011) The Ewing sarcoma protein regulates DNA damage-induced alternative splicing. *Mol Cell,* 43**,** 353-68.
PATINO, M. M., LIU, J. J., GLOVER, J. R. & LINDQUIST, S. (1996) Support for the prion hypothesis for inheritance of a phenotypic trait in yeast. *Science,* 273**,** 622-6.
PHILLIPS, K., KEDERSHA, N., SHEN, L., BLACKSHEAR, P. J. & ANDERSON, P. (2004) Arthritis suppressor genes TIA-1 and TTP dampen the expression of tumor necrosis factor alpha, cyclooxygenase 2, and inflammatory arthritis. *Proc Natl Acad Sci U S A,* 101**,** 2011-6.
PICK, A. (1892) Uber die Beziehungen der senilen Hiratropie zur Aphasie. *Pragen Medizinischen Wochenschrift,* 17**,** 165-7.

PINOL-ROMA, S. & DREYFUSS, G. (1993) hnRNP proteins: localization and transport between the nucleus and the cytoplasm. *Trends Cell Biol,* 3**,** 151-5.
POORKAJ, P., BIRD, T. D., WIJSMAN, E., NEMENS, E., GARRUTO, R. M., ANDERSON, L., ANDREADIS, A., WIEDERHOLT, W. C., RASKIND, M. & SCHELLENBERG, G. D. (1998) Tau is a candidate gene for chromosome 17 frontotemporal dementia. *Ann Neurol,* 43**,** 815-25.
PRIEUR, A., TIRODE, F., COHEN, P. & DELATTRE, O. (2004) EWS/FLI-1 silencing and gene profiling of Ewing cells reveal downstream oncogenic pathways and a crucial role for repression of insulin-like growth factor binding protein 3. *Mol Cell Biol,* 24**,** 7275-83.
PUCHTLER, H. & MELOAN, S. N. (1985) On the chemistry of formaldehyde fixation and its effects on immunohistochemical reactions. *Histochemistry,* 82**,** 201-4.
RADEMAKERS, R., STEWART, H., DEJESUS-HERNANDEZ, M., KRIEGER, C., GRAFF-RADFORD, N., FABROS, M., BRIEMBERG, H., CASHMAN, N., EISEN, A. & MACKENZIE, I. R. (2010) Fus gene mutations in familial and sporadic amyotrophic lateral sclerosis. *Muscle Nerve,* 42**,** 170-6.
RAICHLE, M. E. & GUSNARD, D. A. (2002) Appraising the brain's energy budget. *Proc Natl Acad Sci U S A,* 99**,** 10237-9.
REBANE, A., AAB, A. & STEITZ, J. A. (2004) Transportins 1 and 2 are redundant nuclear import factors for hnRNP A1 and HuR. *RNA,* 10**,** 590-9.
RENTON, A. E., MAJOUNIE, E., WAITE, A., SIMON-SANCHEZ, J., ROLLINSON, S., GIBBS, J. R., SCHYMICK, J. C., LAAKSOVIRTA, H., VAN SWIETEN, J. C., MYLLYKANGAS, L., KALIMO, H., PAETAU, A., ABRAMZON, Y., REMES, A. M., KAGANOVICH, A., SCHOLZ, S. W., DUCKWORTH, J., DING, J., HARMER, D. W., HERNANDEZ, D. G., JOHNSON, J. O., MOK, K., RYTEN, M., TRABZUNI, D., GUERREIRO, R. J., ORRELL, R. W., NEAL, J., MURRAY, A., PEARSON, J., JANSEN, I. E., SONDERVAN, D., SEELAAR, H., BLAKE, D., YOUNG, K., HALLIWELL, N., CALLISTER, J. B., TOULSON, G., RICHARDSON, A., GERHARD, A., SNOWDEN, J., MANN, D., NEARY, D., NALLS, M. A., PEURALINNA, T., JANSSON, L., ISOVIITA, V. M., KAIVORINNE, A. L., HOLTTA-VUORI, M., IKONEN, E., SULKAVA, R., BENATAR, M., WUU, J., CHIO, A., RESTAGNO, G., BORGHERO, G., SABATELLI, M., HECKERMAN, D., ROGAEVA, E., ZINMAN, L., ROTHSTEIN, J. D., SENDTNER, M., DREPPER, C., EICHLER, E. E., ALKAN, C., ABDULLAEV, Z., PACK, S. D., DUTRA, A., PAK, E., HARDY, J., SINGLETON, A., WILLIAMS, N. M., HEUTINK, P., PICKERING-BROWN, S., MORRIS, H. R., TIENARI, P. J. & TRAYNOR, B. J. (2011) A Hexanucleotide Repeat Expansion in C9ORF72 Is the Cause of Chromosome 9p21-Linked ALS-FTD. *Neuron,* 72**,** 257-68.
RICHTER, G. H., PLEHM, S., FASAN, A., ROSSLER, S., UNLAND, R., BENNANI-BAITI, I. M., HOTFILDER, M., LOWEL, D., VON LUETTICHAU, I., MOSSBRUGGER, I., QUINTANILLA-MARTINEZ, L., KOVAR, H., STAEGE, M. S., MULLER-TIDOW, C. & BURDACH, S. (2009) EZH2 is a mediator of EWS/FLI1 driven tumor growth and metastasis blocking endothelial and neuro-ectodermal differentiation. *Proc Natl Acad Sci U S A,* 106**,** 5324-9.
RIGGI, N., SUVA, M. L., DE VITO, C., PROVERO, P., STEHLE, J. C., BAUMER, K., CIRONI, L., JANISZEWSKA, M., PETRICEVIC, T., SUVA, D., TERCIER, S., JOSEPH, J. M., GUILLOU, L. & STAMENKOVIC, I. (2010) EWS-FLI-1

modulates miRNA145 and SOX2 expression to initiate mesenchymal stem cell reprogramming toward Ewing sarcoma cancer stem cells. *Genes Dev,* 24**,** 916-32.
ROBERTSON, J., BILBAO, J., ZINMAN, L., HAZRATI, L. N., TOKUHIRO, S., SATO, C., MORENO, D., STROME, R., MACKENZIE, I. R. & ROGAEVA, E. (2011) A novel double mutation in FUS gene causing sporadic ALS. *Neurobiol Aging,* 32**,** 553 e27-30.
RODRIGUEZ-GALINDO, C., SPUNT, S. L. & PAPPO, A. S. (2003) Treatment of Ewing sarcoma family of tumors: current status and outlook for the future. *Med Pediatr Oncol,* 40**,** 276-87.
ROSCIOLI, E., DI FRANCESCO, L., BOLOGNESI, A., GIUBETTINI, M., ORLANDO, S., HAREL, A., SCHININA, M. E. & LAVIA, P. (2012) Importin-beta negatively regulates multiple aspects of mitosis including RANGAP1 recruitment to kinetochores. *J Cell Biol,* 196**,** 435-50.
SAMA, R. R., WARD, C. L., KAUSHANSKY, L. J., LEMAY, N., ISHIGAKI, S., URANO, F. & BOSCO, D. A. (2013) FUS/TLS assembles into stress granules and is a prosurvival factor during hyperosmolar stress. *J Cell Physiol*.
SAMPATHU, D. M., NEUMANN, M., KWONG, L. K., CHOU, T. T., MICSENYI, M., TRUAX, A., BRUCE, J., GROSSMAN, M., TROJANOWSKI, J. Q. & LEE, V. M. (2006) Pathological heterogeneity of frontotemporal lobar degeneration with ubiquitin-positive inclusions delineated by ubiquitin immunohistochemistry and novel monoclonal antibodies. *Am J Pathol,* 169**,** 1343-52.
SCHLENK, D., WOLFORD, L., CHELIUS, M., STEEVENS, J. & CHAN, K. M. (1997) Effect of arsenite, arsenate, and the herbicide monosodium methyl arsonate (MSMA) on hepatic metallothionein expression and lipid peroxidation in channel catfish. *Comp Biochem Physiol C Pharmacol Toxicol Endocrinol,* 118**,** 177-83.
SCHNELLMANN, R. G. (1988) Mechanisms of t-butyl hydroperoxide-induced toxicity to rabbit renal proximal tubules. *Am J Physiol,* 255**,** C28-33.
SCHWARTZ, J. C., EBMEIER, C. C., PODELL, E. R., HEIMILLER, J., TAATJES, D. J. & CECH, T. R. (2012) FUS binds the CTD of RNA polymerase II and regulates its phosphorylation at Ser2. *Genes Dev,* 26**,** 2690-5.
SELKOE, D. J. (1996) Amyloid beta-protein and the genetics of Alzheimer's disease. *J Biol Chem,* 271**,** 18295-8.
SERPELL, L. C., BERRIMAN, J., JAKES, R., GOEDERT, M. & CROWTHER, R. A. (2000) Fiber diffraction of synthetic alpha-synuclein filaments shows amyloid-like cross-beta conformation. *Proc Natl Acad Sci U S A,* 97**,** 4897-902.
SERPELL, L. C., SUNDE, M., FRASER, P. E., LUTHER, P. K., MORRIS, E. P., SANGREN, O., LUNDGREN, E. & BLAKE, C. C. (1995) Examination of the structure of the transthyretin amyloid fibril by image reconstruction from electron micrographs. *J Mol Biol,* 254**,** 113-8.
SHEN, C. L. & MURPHY, R. M. (1995) Solvent effects on self-assembly of beta-amyloid peptide. *Biophys J,* 69**,** 640-51.
SHIBATA, N., NAGAI, R., UCHIDA, K., HORIUCHI, S., YAMADA, S., HIRANO, A., KAWAGUCHI, M., YAMAMOTO, T., SASAKI, S. & KOBAYASHI, M. (2001) Morphological evidence for lipid peroxidation and protein glycoxidation in spinal cords from sporadic amyotrophic lateral sclerosis patients. *Brain Res,* 917**,** 97-104.

SHIH, J. W., WANG, W. T., TSAI, T. Y., KUO, C. Y., LI, H. K. & WU LEE, Y. H. (2012) Critical roles of RNA helicase DDX3 and its interactions with eIF4E/PABP1 in stress granule assembly and stress response. *Biochem J,* 441**,** 119-29.
SILIGAN, C., BAN, J., BACHMAIER, R., SPAHN, L., KREPPEL, M., SCHAEFER, K. L., POREMBA, C., ARYEE, D. N. & KOVAR, H. (2005) EWS-FLI1 target genes recovered from Ewing's sarcoma chromatin. *Oncogene,* 24**,** 2512-24.
SILLARS-HARDEBOL, A. H., CARVALHO, B., BELIEN, J. A., DE WIT, M., DELIS-VAN DIEMEN, P. M., TIJSSEN, M., VAN DE WIEL, M. A., PONTEN, F., MEIJER, G. A. & FIJNEMAN, R. J. (2012) CSE1L, DIDO1 and RBM39 in colorectal adenoma to carcinoma progression. *Cell Oncol (Dordr),* 35**,** 293-300.
SMITH, R., OWEN, L. A., TREM, D. J., WONG, J. S., WHANGBO, J. S., GOLUB, T. R. & LESSNICK, S. L. (2006) Expression profiling of EWS/FLI identifies NKX2.2 as a critical target gene in Ewing's sarcoma. *Cancer Cell,* 9**,** 405-16.
SOLLAZZO, M. R., BENASSI, M. S., MAGAGNOLI, G., GAMBERI, G., MOLENDINI, L., RAGAZZINI, P., MERLI, M., FERRARI, C., BALLADELLI, A. & PICCI, P. (1999) Increased c-myc oncogene expression in Ewing's sarcoma: correlation with Ki67 proliferation index. *Tumori,* 85**,** 167-73.
SPILLANTINI, M. G., CROWTHER, R. A., JAKES, R., CAIRNS, N. J., LANTOS, P. L. & GOEDERT, M. (1998a) Filamentous alpha-synuclein inclusions link multiple system atrophy with Parkinson's disease and dementia with Lewy bodies. *Neurosci Lett,* 251**,** 205-8.
SPILLANTINI, M. G., MURRELL, J. R., GOEDERT, M., FARLOW, M. R., KLUG, A. & GHETTI, B. (1998b) Mutation in the tau gene in familial multiple system tauopathy with presenile dementia. *Proc Natl Acad Sci U S A,* 95**,** 7737-41.
STRONG, M. J., VOLKENING, K., HAMMOND, R., YANG, W., STRONG, W., LEYSTRA-LANTZ, C. & SHOESMITH, C. (2007) TDP43 is a human low molecular weight neurofilament (hNFL) mRNA-binding protein. *Mol Cell Neurosci,* 35**,** 320-7.
SUN, Z., DIAZ, Z., FANG, X., HART, M. P., CHESI, A., SHORTER, J. & GITLER, A. D. (2011) Molecular determinants and genetic modifiers of aggregation and toxicity for the ALS disease protein FUS/TLS. *PLoS Biol,* 9**,** e1000614.
SUZUKI, M., IIJIMA, M., NISHIMURA, A., TOMOZOE, Y., KAMEI, D. & YAMADA, M. (2005) Two separate regions essential for nuclear import of the hnRNP D nucleocytoplasmic shuttling sequence. *FEBS J,* 272**,** 3975-87.
SUZUKI, N., AOKI, M., WARITA, H., KATO, M., MIZUNO, H., SHIMAKURA, N., AKIYAMA, T., FURUYA, H., HOKONOHARA, T., IWAKI, A., TOGASHI, S., KONNO, H. & ITOYAMA, Y. (2010) FALS with FUS mutation in Japan, with early onset, rapid progress and basophilic inclusion. *J Hum Genet,* 55**,** 252-4.
TAKAHASHI, M., HIGUCHI, M., MATSUKI, H., YOSHITA, M., OHSAWA, T., OIE, M. & FUJII, M. (2013) Stress granules inhibit apoptosis by reducing reactive oxygen species production. *Mol Cell Biol,* 33**,** 815-29.
TALBOT, K. & ANSORGE, O. (2006) Recent advances in the genetics of amyotrophic lateral sclerosis and frontotemporal dementia: common pathways in neurodegenerative disease. *Hum Mol Genet,* 15 Spec No 2**,** R182-7.
TAN, A. Y. & MANLEY, J. L. (2010) TLS inhibits RNA polymerase III transcription. *Mol Cell Biol,* 30**,** 186-96.

TICOZZI, N., LECLERC, A. L., VAN BLITTERSWIJK, M., KEAGLE, P., MCKENNA-YASEK, D. M., SAPP, P. C., SILANI, V., WILLS, A. M., BROWN, R. H., JR. & LANDERS, J. E. (2011) Mutational analysis of TARDBP in neurodegenerative diseases. *Neurobiol Aging,* 32**,** 2096-9.

TICOZZI, N., SILANI, V., LECLERC, A. L., KEAGLE, P., GELLERA, C., RATTI, A., TARONI, F., KWIATKOWSKI, T. J., JR., MCKENNA-YASEK, D. M., SAPP, P. C., BROWN, R. H., JR. & LANDERS, J. E. (2009) Analysis of FUS gene mutation in familial amyotrophic lateral sclerosis within an Italian cohort. *Neurology,* 73**,** 1180-5.

TOLNAY, M. & PROBST, A. (2003) The neuropathological spectrum of neurodegenerative tauopathies. *IUBMB Life,* 55**,** 299-305.

TOOMBS, J. A., MCCARTY, B. R. & ROSS, E. D. (2010) Compositional determinants of prion formation in yeast. *Mol Cell Biol,* 30**,** 319-32.

TOURRIERE, H., GALLOUZI, I. E., CHEBLI, K., CAPONY, J. P., MOUAIKEL, J., VAN DER GEER, P. & TAZI, J. (2001) RasGAP-associated endoribonuclease G3Bp: selective RNA degradation and phosphorylation-dependent localization. *Mol Cell Biol,* 21**,** 7747-60.

TSAI, C. P., SOONG, B. W., LIN, K. P., TU, P. H., LIN, J. L. & LEE, Y. C. (2011) FUS, TARDBP, and SOD1 mutations in a Taiwanese cohort with familial ALS. *Neurobiol Aging,* 32**,** 553 e13-21.

TSAI, N. P., TSUI, Y. C. & WEI, L. N. (2009) Dynein motor contributes to stress granule dynamics in primary neurons. *Neuroscience,* 159**,** 647-56.

UCHIDA, K. (2003) 4-Hydroxy-2-nonenal: a product and mediator of oxidative stress. *Prog Lipid Res,* 42**,** 318-43.

VAHTER, M., CONCHA, G., NERMELL, B., NILSSON, R., DULOUT, F. & NATARAJAN, A. T. (1995) A unique metabolism of inorganic arsenic in native Andean women. *Eur J Pharmacol,* 293**,** 455-62.

VAN BLITTERSWIJK, M., VAN ES, M. A., HENNEKAM, E. A., DOOIJES, D., VAN RHEENEN, W., MEDIC, J., BOURQUE, P. R., SCHELHAAS, H. J., VAN DER KOOI, A. J., DE VISSER, M., DE BAKKER, P. I., VELDINK, J. H. & VAN DEN BERG, L. H. (2012) Evidence for an oligogenic basis of amyotrophic lateral sclerosis. *Hum Mol Genet,* 21**,** 3776-84.

VAN DAMME, P., VAN HOECKE, A., LAMBRECHTS, D., VANACKER, P., BOGAERT, E., VAN SWIETEN, J., CARMELIET, P., VAN DEN BOSCH, L. & ROBBERECHT, W. (2008) Progranulin functions as a neurotrophic factor to regulate neurite outgrowth and enhance neuronal survival. *J Cell Biol,* 181**,** 37-41.

VAN DEERLIN, V. M., LEVERENZ, J. B., BEKRIS, L. M., BIRD, T. D., YUAN, W., ELMAN, L. B., CLAY, D., WOOD, E. M., CHEN-PLOTKIN, A. S., MARTINEZ-LAGE, M., STEINBART, E., MCCLUSKEY, L., GROSSMAN, M., NEUMANN, M., WU, I. L., YANG, W. S., KALB, R., GALASKO, D. R., MONTINE, T. J., TROJANOWSKI, J. Q., LEE, V. M., SCHELLENBERG, G. D. & YU, C. E. (2008) TARDBP mutations in amyotrophic lateral sclerosis with TDP-43 neuropathology: a genetic and histopathological analysis. *Lancet Neurol,* 7**,** 409-16.

VAN DUUREN, B. L., LANGSETH, L., ORRIS, L., TEEBOR, G., NELSON, N. & KUSCHNER, M. (1966) Carcinogenicity of epoxides, lactones, and peroxy compounds. IV. Tumor response in epithelial and connective tissue in mice and rats. *J Natl Cancer Inst,* 37**,** 825-38.

VANCE, C., ROGELJ, B., HORTOBAGYI, T., DE VOS, K. J., NISHIMURA, A. L., SREEDHARAN, J., HU, X., SMITH, B., RUDDY, D., WRIGHT, P., GANESALINGAM, J., WILLIAMS, K. L., TRIPATHI, V., AL-SARAJ, S., AL-CHALABI, A., LEIGH, P. N., BLAIR, I. P., NICHOLSON, G., DE BELLEROCHE, J., GALLO, J. M., MILLER, C. C. & SHAW, C. E. (2009a) Mutations in FUS, an RNA processing protein, cause familial amyotrophic lateral sclerosis type 6. *Science,* 323**,** 1208-11.

VANCE, C., ROGELJ, B., HORTOBAGYI, T., DE VOS, K. J., NISHIMURA, A. L., SREEDHARAN, J., HU, X., SMITH, B., RUDDY, D., WRIGHT, P., GANESALINGAM, J., WILLIAMS, K. L., TRIPATHI, V., AL-SARAJ, S., AL-CHALABI, A., LEIGH, P. N., BLAIR, I. P., NICHOLSON, G., DE, B. J., GALLO, J. M., MILLER, C. C. & SHAW, C. E. (2009b) Mutations in FUS, an RNA processing protein, cause familial amyotrophic lateral sclerosis type 6. *Science,* 323**,** 1208-1211.

VANDERWEYDE, T., YU, H., VARNUM, M., LIU-YESUCEVITZ, L., CITRO, A., IKEZU, T., DUFF, K. & WOLOZIN, B. (2012) Contrasting pathology of the stress granule proteins TIA-1 and G3BP in tauopathies. *J Neurosci,* 32**,** 8270-83.

WAIBEL, S., NEUMANN, M., RABE, M., MEYER, T. & LUDOLPH, A. C. (2010) Novel missense and truncating mutations in FUS/TLS in familial ALS. *Neurology,* 75**,** 815-7.

WANG, H. Y., WANG, I. F., BOSE, J. & SHEN, C. K. (2004) Structural diversity and functional implications of the eukaryotic TDP gene family. *Genomics,* 83**,** 130-9.

WANG, I. F., WU, L. S., CHANG, H. Y. & SHEN, C. K. (2008) TDP-43, the signature protein of FTLD-U, is a neuronal activity-responsive factor. *J Neurochem,* 105**,** 797-806.

WANG, J., LI, D., WANG, B. & WU, Y. (2013) Predictive and prognostic significance of cytoplasmic expression of ELAV-like protein HuR in invasive breast cancer treated with neoadjuvant chemotherapy. *Breast Cancer Res Treat*.

WANG, T. S., SHU, Y. F., LIU, Y. C., JAN, K. Y. & HUANG, H. (1997) Glutathione peroxidase and catalase modulate the genotoxicity of arsenite. *Toxicology,* 121**,** 229-37.

WANG, X., XU, X., ZHU, S., XIAO, Z., MA, Z., LI, Y. & WANG, Y. (2011) Molecular dynamics simulation of conformational heterogeneity in transportin 1. *Proteins*.

WATTS, G. D., WYMER, J., KOVACH, M. J., MEHTA, S. G., MUMM, S., DARVISH, D., PESTRONK, A., WHYTE, M. P. & KIMONIS, V. E. (2004) Inclusion body myopathy associated with Paget disease of bone and frontotemporal dementia is caused by mutant valosin-containing protein. *Nat Genet,* 36**,** 377-81.

WEINGARTEN, M. D., LOCKWOOD, A. H., HWO, S. Y. & KIRSCHNER, M. W. (1975) A protein factor essential for microtubule assembly. *Proc Natl Acad Sci U S A,* 72**,** 1858-62.

WEIS, K. (2003) Regulating access to the genome: nucleocytoplasmic transport throughout the cell cycle. *Cell,* 112**,** 441-51.

WILHELMSEN, K. C., LYNCH, T., PAVLOU, E., HIGGINS, M. & NYGAARD, T. G. (1994) Localization of disinhibition-dementia-parkinsonism-amyotrophy complex to 17q21-22. *Am J Hum Genet,* 55**,** 1159-65.

WINTON, M. J., IGAZ, L. M., WONG, M. M., KWONG, L. K., TROJANOWSKI, J. Q. & LEE, V. M. (2008) Disturbance of nuclear and cytoplasmic TAR DNA-binding protein (TDP-43) induces disease-like redistribution, sequestration, and aggregate formation. *J Biol Chem,* 283**,** 13302-9.
WOLOZIN, B. (2012) Regulated protein aggregation: stress granules and neurodegeneration. *Mol Neurodegener,* 7**,** 56.
WOOD, S. J., WYPYCH, J., STEAVENSON, S., LOUIS, J. C., CITRON, M. & BIERE, A. L. (1999) alpha-synuclein fibrillogenesis is nucleation-dependent. Implications for the pathogenesis of Parkinson's disease. *J Biol Chem,* 274**,** 19509-12.
XIE, W. & DENMAN, R. B. (2011) Protein methylation and stress granules: posttranslational remodeler or innocent bystander? *Mol Biol Int,* 2011**,** 137459.
XU, L. & MASSAGUE, J. (2004) Nucleocytoplasmic shuttling of signal transducers. *Nat Rev Mol Cell Biol,* 5**,** 209-19.
YAMASHITA, S., MORI, A., SAKAGUCHI, H., SUGA, T., ISHIHARA, D., UEDA, A., YAMASHITA, T., MAEDA, Y., UCHINO, M. & HIRANO, T. (2012) Sporadic juvenile amyotrophic lateral sclerosis caused by mutant FUS/TLS: possible association of mental retardation with this mutation. *J Neurol,* 259**,** 1039-44.
YAN, J., DENG, H. X., SIDDIQUE, N., FECTO, F., CHEN, W., YANG, Y., LIU, E., DONKERVOORT, S., ZHENG, J. G., SHI, Y., AHMETI, K. B., BROOKS, B., ENGEL, W. K. & SIDDIQUE, T. (2010) Frameshift and novel mutations in FUS in familial amyotrophic lateral sclerosis and ALS/dementia. *Neurology,* 75**,** 807-14.
YORK, A. & FODOR, E. (2013) Biogenesis, assembly and export of viral messenger ribonucleoproteins in the influenza A virus infected cell. *RNA Biol,* 10.
YOUNES, M. & WESS, A. (1990) The role of iron in t-butyl hydroperoxide-induced lipid peroxidation and hepatotoxicity in rats. *J Appl Toxicol,* 10**,** 313-7.
ZAKARYAN, R. P. & GEHRING, H. (2006) Identification and characterization of the nuclear localization/retention signal in the EWS proto-oncoprotein. *J Mol Biol,* 363**,** 27-38.
ZANOCCO-MARANI, T., BATEMAN, A., ROMANO, G., VALENTINIS, B., HE, Z. H. & BASERGA, R. (1999) Biological activities and signaling pathways of the granulin/epithelin precursor. *Cancer Res,* 59**,** 5331-40.
ZARKOVIC, N. (2003) 4-hydroxynonenal as a bioactive marker of pathophysiological processes. *Mol Aspects Med,* 24**,** 281-91.
ZHANG, D., PALEY, A. J. & CHILDS, G. (1998) The transcriptional repressor ZFM1 interacts with and modulates the ability of EWS to activate transcription. *J Biol Chem,* 273**,** 18086-91.
ZHOU, H., XU, M., HUANG, Q., GATES, A. T., ZHANG, X. D., CASTLE, J. C., STEC, E., FERRER, M., STRULOVICI, B., HAZUDA, D. J. & ESPESETH, A. S. (2008) Genome-scale RNAi screen for host factors required for HIV replication. *Cell Host Microbe,* 4**,** 495-504.
ZHOU, Z. J., DAI, Z., ZHOU, S. L., FU, X. T., ZHAO, Y. M., SHI, Y. H., ZHOU, J. & FAN, J. (2013) Overexpression of HnRNP A1 promotes tumor invasion through regulating CD44v6 and indicates poor prognosis for hepatocellular carcinoma. *Int J Cancer,* 132**,** 1080-9.

ZINSZNER, H., SOK, J., IMMANUEL, D., YIN, Y. & RON, D. (1997) TLS (FUS) binds RNA in vivo and engages in nucleo-cytoplasmic shuttling. *J Cell Sci,* 110 (Pt 15)**,** 1741-50.

ZOU, Z. Y., CUI, L. Y., SUN, Q., LI, X. G., LIU, M. S., XU, Y., ZHOU, Y. & YANG, X. Z. (2013) De novo FUS gene mutations are associated with juvenile-onset sporadic amyotrophic lateral sclerosis in China. *Neurobiol Aging,* 34**,** 1312 e1-8.

ZURLA, C., LIFLAND, A. W. & SANTANGELO, P. J. (2011) Characterizing mRNA interactions with RNA granules during translation initiation inhibition. *PLoS One,* 6**,** e19727.

ZWERNER, J. P., JOO, J., WARNER, K. L., CHRISTENSEN, L., HU-LIESKOVAN, S., TRICHE, T. J. & MAY, W. A. (2008) The EWS/FLI1 oncogenic transcription factor deregulates GLI1. *Oncogene,* 27**,** 3282-91.

Appendix 1.1

ALS-associate mutations in FUS				
DNA mutation	**Protein change**	**Protein Domain**	**Cognitive involvement**	**Reported Paper**
c.52 C>T	P18S	SYGQ rich	None	(Belzil et al., 2011a)
c.170-172delCTT	S57del	SYGQ rich	None	(Belzil et al., 2009)
c.287-291 delCCTACinsAT	S96del	SYGQ rich	Mental retardation	(Yan et al., 2010)
c.344 G>A	S115N	SYGQ rich	None	(van Blitterswijk et al., 2012)
c.430-447delGGAAAGCTAT	G144Y149del	G rich	None	(Belzil et al., 2011b)
c.467 G>A	G156E	G rich	Dementia	(Ticozzi et al., 2009)
c.518-523delGAGGTG	G174-G175del	G rich	schizophrenia , FTD	(Kwiatkowski et al., 2009b)
c.559 G>A	G187S	G rich	None	(Rademakers et al., 2010)
c.571 G>A	G191S	G rich	None	(Corrado et al., 2010)
c.616 G>A	G206S	G rich	FTD	(Yan et al., 2010)
c.646 C>T	R216C	G rich	None	(Corrado et al., 2010)
c.674 G>T	G225V	G rich	None	(Corrado et al., 2010)
c.681-684delGGC	G230delG	G rich	None	(Kwon et al., 2012)
c.688 G>T	G230C	G rich	None	(Corrado et al., 2010)
c.700 C>T	R234C	G rich	None	(Corrado et al., 2010)
c.701 G>T	R234L	G rich	None	(Ticozzi et al., 2009)
c.730 C>T	R244C	G rich	None	(Kwiatkowski et al., 2009b)
c.1196 G>T	G399V	ZnF	None	(Kwon et al., 2012)
c.1204-1232 delinsGGAGGTGGAGG	S402-P411delinsGGGG	ZnF	None	(DeJesus-Hernandez et al., 2010)
c.1385 C>T	S462F	ZnF	None	(Groen et al., 2010)
c.1392G>T	M464I	ZnF	None	(Nagayama et

				al., 2012)
c.1394-1541delCTACCGGGGCCGCGGCGGGGACCGTGGGGCTTCCGAGGG	G466VfsX14	RGG rich	None	(DeJesus-Hernandez et al., 2010)
c.1420-1421insGT	G472VfsX57	RGG rich	None	(Hara et al., 2012)
c.1449-1488del	Y485AfsX514	RGG rich	n.a.	(Yan et al., 2010)
c.1459 C>T	R487C	RGG rich	None	(van Blitterswijk et al., 2012)
c.1475delG	G492EfsX527	NLS	Mental retardation	(Yamashita et al., 2012)
c.1483delC	R495EfsX527	NLS	None	(Yan et al., 2010)
c.1483 C>T	R495X	NLS	None	(Bosco et al., 2010)
c.1484delG	R495QfsX527	NLS	None	(Belzil et al., 2012)
c.1485delA	G497AfsX527	NLS	Learning disabilities	(Yan et al., 2010)
c.1506 dupA	R502fsX15	NLS	None	(Belzil et al., 2011b)
c.1507-1508delAG	G503WfsX12	NLS	None	(Kwon et al., 2012)
c.1509-1510delAG	G504WfsX12	NLS	Learning disabilities	(Zou et al., 2013)
c.1520 G>A	G507D	NLS	None	(Hewitt et al., 2010)
c.1527-1528insTGCC	K510WfsX517	NLS	None	(Yan et al., 2010)
c.1528 A>G	K510E	NLS	None	(Suzuki et al., 2010)
c.1529 A>G	K510R	NLS	None	(Waibel et al., 2010)
c.1537 T>C	S513P	NLS	None	(Suzuki et al., 2010)
c.1540 A>G	R514G	NLS	None	(Vance et al., 2009a)
c.1542 G>C	R514Sa	NLS	None	(Chio et al., 2009)
c.1543 G>T	G515C	NLS	None	(Kwiatkowski et al., 2009b)
c.1547 A>T	E516Va	NLS	None	(Robertson et al., 2011)
c.1549 C>G	H517D	NLS	None	(Tsai et al., 2011)
c.1550 A>C	H517P	NLS	None	(Suzuki et al., 2010)

c.1551 C>G	H517Q	NLS	None	(Kwiatkowski et al., 2009b)
c.1552 A>G	R518G	NLS	None	(Lai et al., 2011)
c.1553 G>A	R518K	NLS	None	(Kwiatkowski et al., 2009b)
c.1554-1557delACAG	R518del	NLS	None	(Baumer et al., 2010)
c.1555 C>T	Q519X	NLS	None	(Belzil et al., 2011b)
c.1561 C>T	R521C	NLS	Parkinsonism and dementia	(Belzil et al., 2009)
c.1561 C>G	R521G	NLS	None	(Ticozzi et al., 2009)
c.1561 C>A	R521S	NLS	None	(Millecamps et al., 2010)
c.1562 G>A	R521H	NLS	FTD	(Blair et al., 2010)
c.1562 G>T	R521L	NLS	None	(Conte et al., 2012)
c.1564 A>G	R522G	NLS	None	(Kwiatkowski et al., 2009b)
c.1570 A>T	R524W	NLS	None	(Hewitt et al., 2010)
c.1571 G>C	R524T	NLS	None	(Kwiatkowski et al., 2009b)
c.1572 G>C	R524S	NLS	None	(Kwiatkowski et al., 2009b)
c.1574 C>T	P525L	NLS	None	(Baumer et al., 2010)
c.1581delA	X527YextX	NLS	None	(Kwon et al., 2012)
Nucleotide numbering=cDNA numbering . Reference sequence is NM_004960.3.				
del=deletion ins=insertion fs=frameshift ext=extention dup=duplication n.a.=not applicable				

Appendix 1.1. Table of ALS-associated FUS mutations

Appendix 1.2

TRN1 cargos	Associated disease	Reference
FUS	FTLD-FUS / ALS-FUS	(Neumann et al., 2009a, Neumann et al., 2009c, Vance et al., 2009a)
EWS	FTLD-FUS	(Neumann et al., 2011)
TAF15	FTLD-FUS	(Neumann et al., 2011)
hnRNP A1	Inclusion body myopathy associated with Paget disease of bone / FTLD-TDP / ALS-TDP43 / Cancer	(Kim et al., 2013, Zhou et al., 2013)
hnRNP A0	none	
hnRNP A2/B1	inclusion body myopathy associated with Paget disease of bone / FTLD-TDP / ALS-TDP43	(Kim et al., 2013)
hnRNP M3/M4	Cancer	(Laguinge et al., 2005)
hnRNP D	Viral infection	(Lee et al., 2012)
hnRNP H1	none	
PQBP-1	PolyQ expansion	(Kurosaki et al., 2012)
SAM68	Cancer	(Liao et al., 2013)
SLM-2	none	
HEX1M1	none	
RBM39	Cancer	(Sillars-Hardebol et al., 2012)
HuR	Cancer	(Wang et al., 2013)
PABPN1	Muscular dystrophy	(Anvar et al., 2013)
YB1	Cancer	(Maciejczyk et al., 2012)
DDX3	Cancer / viral infection	(Bol et al., 2013, Lai et al., 2013)
NXF1	Viral infection	(York and Fodor, 2013)